PHARMACOLOGIC TARGETING OF THE CB2 CANNABINOID RECEPTOR FOR

APPLICATION IN CENTRALLY-MEDIATED CHRONIC PAIN

by

Dana Marie Lambert

B.Sc.(Pharm), The University of British Columbia, 2010

A THESIS SUBMITTED IN PARTIAL FULFILLMENT OF

THE REQUIREMENTS FOR THE DEGREE OF

DOCTOR OF PHILOSOPHY

in

THE FACULTY OF GRADUATE AND POSTDOCTORAL STUDIES

(Pharmaceutical Sciences)

THE UNIVERSITY OF BRITISH COLUMBIA

(Vancouver)

January 2019

The following individuals certify that they have read, and recommend to the Faculty of Graduate and Postdoctoral Studies for acceptance, the dissertation entitled:

Pharmacologic Targeting of the CB2 Cannabinoid Receptor for Application in Centrally-Mediated Chronic Pain

submitted by   Dana Lambert   in partial fulfillment of the requirements for

the degree of   Doctor of Philosophy

in   Pharmaceutical Sciences

Examining Committee:

Prof. Urs Häfeli, Pharmaceutical Sciences
Supervisor

Prof. Ujendra Kumar, Pharmaceutical Sciences
Supervisory Committee Member

Prof. Lynn Raymond, Psychiatry (Neurological Sciences)
University Examiner

Prof. Sastry Bhagavatula, Anesthesiology, Pharmacology and Therapeutics
University Examiner

Prof. Ronald Tuma, Physiology, Temple University
External Examiner

Additional Supervisory Committee Members:

Prof. John McNeill, Pharmaceutical Sciences
Supervisory Committee Member

Prof. Michael Negraeff, Vancouver Coastal Health
Supervisory Committee Member

Abstract

Cannabis preparations have been used for millennia for the treatment of pain and various ailments. However, psychotropic effects, mediated by the CB1 cannabinoid receptor in the central nervous system (CNS), limit their therapeutic use. Research to date suggests that selective activation of the CB2 cannabinoid receptor promotes analgesia without the occurrence of psychotropic effects. Cannabinoids, the principal active compounds in *Cannabis sativa,* lack the ability to selectively activate CB2. Glial cells of the CNS are known to play an important role in mediating certain forms of chronic pain through pro-inflammatory activity. Furthermore, CB2 receptors expressed by glia are now recognized as a potential therapeutic target for such disease states; however, the contribution of glial cell-mediated neuro-inflammation to the pathophysiology of chronic widespread musculoskeletal pain (CWP) disorders, such as fibromyalgia syndrome, remains unclear.

An immunohistology investigation within the acidic saline model of CWP revealed significant up-regulation of Iba-1 and GFAP in the lumbar spinal cord, suggesting that gliosis may potentially mediate hyperalgesia in CWP disorders. Although further investigations are required, these data support that targeting of cannabinoid receptors expressed by glia may be a potentially viable approach for addressing CWP.

To target cannabinoid receptors expressed by glia while minimizing the potential for CB1-associated CNS effects, compounds with selective CB2 agonist activity were designed, guided by CB2 molecular docking studies *in silico*, and synthesized for further investigation. β-caryophyllene, a naturally occurring sesquiterpene, along with two novel compounds, DML-3 and DML-4, were found to be full agonists at CB2 with 109, > 40 and $>10,000$ –fold selectivity over CB1, respectively. Furthermore, all three compounds significantly reduced activation of

NF-κB, ERK1/2 and PI3K in U87MG astrocytes. Significant reductions in astrocyte IL-6 and IL-8 secretion occurred following treatment with β-caryophyllene (1 µM) and DML-4 (25 µM), with minor, non-significant reductions observed following treatment with DML-3 (25 µM). Based on the pharmacologic properties determined, each compound may be a potential candidate for therapeutically targeting pro-inflammatory glial cell activity. Further suggested investigations include quantification of β-arrestin recruitment, screening for off-target effects, testing for efficacy in research models of CWP, followed by *in vivo* pharmacokinetic and toxicological profiling.

Lay Summary

This research investigation aimed to determine whether specialized immune cells present in the brain and spinal cord may contribute to pain in individuals who experience chronic widespread musculoskeletal pain disorders, such as fibromyalgia. Although further studies are required in order to draw firm conclusions, the present investigation provided evidence that increased activity of these specialized immune cells in the spinal cord may contribute to chronic widespread musculoskeletal pain.

In addition, this research investigation aimed to develop novel drug candidates which may be effective in treating the pain-causing activity of immune cells by working through the endocannabinoid system. This investigation also aimed to determine whether a naturally occurring medicinal compound called β-caryophyllene may be capable of exerting the same effects. Two novel drug candidates along with β-caryophyllene were found to act on the endocannabinoid system and diminish some of the known effects of immune cells associated with pain.

Preface

I designed, conducted and interpreted the research experiments included in this dissertation. My supervisor, Dr. Urs Häfeli, provided advising in the execution of these experiments and in the preparation of this dissertation. Contributions from collaborators are as follows:

Chapter 2

Dr. Kathleen Sluka provided the experimental protocol for the acidic saline research model and advised on spinal cord regions to be included in the investigation. Dr. Ujendra Kumar advised on the immunohistology investigation. Drs. Peter Soja and Ramakrishna Tadavarty advised on conducting mechanical hyperalgesia testing. Dr. Laura Mowbray, Stephanie Laprise and Micky Burgess assisted with transcardiac perfusion and laminectomy. Histology data acquisition and quantitative analysis was performed at the Fred Hutchinson Cancer Research Center, Seattle, WA, U.S.A. under the guidance of Kimberley Melton, Technical Lead Digital Pathology, in the Department of Experimental Histopathology. Undergraduate research students Nicole Sarden and Connor McIntyre assisted with immunohistochemistry and animal monitoring. I completed the majority of the immunohistochemistry and animal monitoring without assistance. I conducted all behavioral hyperalgesia assessments on my own.

Chapter 3

Dr. Cristina Rodríguez developed the molecular CB2 homology model and carried out ligand docking experiments. Dr. Katayoun Saatchi synthesized and chemically analyzed the CB2 agonists DML-3 and DML-4. Dr. Ujendra Kumar provided CB1-transfected HEK293 cells. Dr. Rishi Somvanshi provided advising on conducting *in vitro* assays.

Chapter 4

Dr. Ujendra Kumar provided advising on cell proliferation and viability assays and western blotting experiments. Connor McIntyre, an undergraduate research student, assisted with cell viability and proliferation assays in HEK293 and THP1 cells. I conducted the majority of the cell viability, proliferation and death assays unassisted. Use of the Micolux beta counter for the radio-ligand displacement assay was provided by the Bally Laboratory at the British Columbia Cancer Research Centre (BCCRC).

At the time of writing, modified versions of some sections have been published:

Chapter 2: Lambert DM, Kumar U and Häfeli UO. (2018). *Up-regulation of Iba-1 and GFAP in the acidic saline model of chronic widespread musculoskeletal pain: a pilot study examining the relationship between gliosis and hyperalgesia.* J Neurosci Neuropharm **4**, 121-130.

Before publication of this dissertation, modified versions of some sections will be submitted as manuscripts:

Chapter 3: Lambert DM, Rodríguez C and Häfeli UO. *β-caryophyllene: Selectivity as a CB2 cannabinoid receptor agonist, key receptor-ligand interactions and in vitro cytotoxicity.*

Chapters 3 and 4: Lambert DM, Rodríguez C, Saatchi K and Häfeli UO. *Development of novel selective CB2 cannabinoid receptor agonists, DML-3 and DML-4, for therapeutic application in gliosis.*

All studies requiring the utilization of animals and biohazards were reviewed and approved by the Animal Care Committee and the Biosafety Committee at UBC, respectively. The following two certificates were granted: A14-0334 and B14-0187.

Table of Contents

List of Tables

List of Figures

List of Abbreviations

2D	Two-dimensional
2AG	2-Arachadonyl glycerol
3D	Three-dimensional
A2a	Adenosine receptor type 2a
ADO	Adenosine
ATP	Adenosine tri-phosphate
AMPA	α-Amino-3-hydroxy-5-methyl-4-isoxazolepropionic acid
AS	Acidic saline
ASIC	Acid-sensing ion channel
BDNF	Brain-derived neurotrophic factor
cAMP	Cyclic adenosine mono-phosphate
CB	Cannabinoid
CB1	Cannabinoid receptor type 1
CB2	Cannabinoid receptor type 2
CBD	Cannabidiol
CCL2	C-C motif chemokine ligand 2
c-Myc	C gene of myc proto-oncogene family
CGRP	Calcitonin gene-related peptide
CHO	Chinese hamster ovary
cLogP	Calculated LogP
CNS	Central nervous system
COX-2	Cyclo-oxygenase-2 enzyme

CSF	Cerebrospinal fluid
CWP	Chronic widespread pain
DA	Dopamine
DAMP	Danger-associated molecular patterns
DMEM	Dulbecco's modified eagle medium
DMSO	Dimethyl sulfoxide
DRASIC	Dorsal root acid sensing ion channel (also known as ASIC3)
ELISA	Enzyme linked immunosorbent assay
ERK1/2	Extracellular signal-related kinases 1/2
FAAH	Fatty acid amide hydrolase
FBS	Fetal bovine serum
FM	Fibromyalgia syndrome
GDP	Guanosine diphosphate
GFAP	Glial fibrillary acidic protein
GI	Gastro-intestinal
Glu	Glutamate
Gly	Glycine
GPCR	G-protein coupled receptor
GTP	Guanosine triphosphate
GTPγS	Guanosine 5'-O-[gamma-thio]triphosphate
His	Histamine
HEK-293	Human embryonic kidney cell line 293
HRP	Horseradish peroxidase

hTERT	Human telomerase reverse transcriptase
Iba-1	Ionized calcium binding adapter molecule 1
IgE	Immunoglobulin E
IL	Interleukin
IM	Intramuscular
i.pl.	Intraplantar
iNOS	Inducible nitric oxide synthase
IUPAC	International union of pure and applied chemistry
LPS	Lipopolysaccharide
LogP	Logarithm of octanol-water partition co-efficient
MAPK	p38 Mitogen activated protein kinase
MDEG	Mammalian degenerin cation channel receptor
mGlu	Metabotropic glutamate receptor
mRNA	Messenger ribonucleic acid
MTP	Myofascial trigger point
MRI	Magnetic resonance imaging
NA	Noradrenaline
NF-κB	Nuclear transcription factor kappa B
NGC	Nucleus reticularis gigantocellularis
NGF	Nerve growth factor
NMDA	N-methyl-D-aspartate
NMR	Nuclear Magnetic Resonance
NR2B	N-methyl-D-aspartate receptor subunit 2B

NO	Nitric oxide
NPY	Neuropeptide Y
NSAID	Non-steroidal anti-inflammatory drug
OD	Optical Density
PAF	Platelet activating factor
PBS	Phosphate-buffered saline
PG	Prostaglandin
PGE_2	Prostaglandin-E_2
PGG_2	Prostglandin-G_2
PI3K	Phosphatidylinositol-4,5-bisphosphate 3-kinase
PKA	Protein kinase A
PKC	Protein kinase C
PPAR	Peroxisome proliferator-activated receptor
PPARγ	Peroxisome proliferator-activated receptor gamma
PVDF	Polyvinylidene fluoride
PXR	Purinergic receptor
RIPA	Radio immunoprecipitation assay
RPMI	Roswell park memorial institute medium
RVM	Rostroventral medulla
SD	Standard deviation
SE	Standard error
Ser	Serine
STT	Spinothalamic tract

SOM	Somatostatin
SP	Substance P
TBS	Tris-buffered saline
TBST	Tris-buffered saline with 0.1% v/v Tween20$^{®}$
THCA	Δ^9-Tetrahydrocannabinolic acid
THC	Δ^9-Tetrahydrocannabinol
THP-1	Human leukemic monocyte cell line, type THP-1
TMH	Transmembrane helix
TNF	Tumor necrosis factor
TPSA	Topological polar surface area
TREK-1	Tandem p-domain weak inward rectifying K^+(TWIK)-related K^+ channel 1
TRP	Transient receptor potential cation channel receptor
Trp	Tryptophan
TRPV	Transient receptor potential cation channel subfamily vanilloid
TRPM	Transient receptor potential cation channel subfamily menthol
UBC	University of British Columbia
USA	United States of America
VBC	Ventrobasal complex of the thalamus

List of Symbols

©	Copyright
°C	Degrees Celsius
=	Equal
>	Greater than
<	Less than
μ	Micro-
%	Percent
±	Plus-minus
®	Registered trademark
Å	Angstrom
A	Alanine
C	Carbon
C	Cysteine
c	Centi-
Ca	Calcium
Cl	Chlorine
Co	Cobalt
D	Aspartic acid
Da	Dalton
EC_{50}	Half maximal effective concentration
F	Fluorine
F	Phenylalanine

g	Gram
Gα	G-protein, alpha subunit
Gβ/γ	G-protein, beta/gamma subunits
$G_{i/o}$	G-protein, inhibitory subtype
G_s	G-protein, stimulatory subtype
H	Histidine
H	Hydrogen
Hz	Hertz
h	Hour
I	Isoleucine
IC_{50}	Half maximal inhibitory concentration
K	Lysine
K	Potassium
k	Kilo-
K_D	Equilibrium dissociation constant of a protein-ligand complex
K_i	Equilibrium dissociation constant of a protein-ligand complex
L	Leucine
L	Litre
L[n]	Lumbar spinal cord, n^{th} vertebral level
M	Mega-
M	Methionine
M	Molar
m	Metre

m	Milli-
Mg	Magnesium
min	Minute
mol	Mole
N	Asparagine
N	Nitrogen
n	Nano-
P	Proline
p	Pico-
S	Serine
S	Sulphur
s	Second
T	Threonine
T[n]	Thoracic spinal cord, n^{th} vertebral level
V	Valine
V	Volt
v/v	Percentage in terms of volume
W	Tryptophan
w/w	Percentage in terms of weight

Glossary

Afferent: conducting or conducted inward or toward something (for nerves, the central nervous system; for blood vessels, the organ supplied).

Agonist: a substance that initiates a physiological response when combined with a receptor.

Antagonist: a substance that interferes with or inhibits the physiologic action of another.

Algogenic: pain-producing. Also known as algesiogenic.

Allodynia: refers to central pain sensitization (increased response of neurons) following normally non-painful, often repetitive, stimulation. Allodynia can lead to the triggering of a pain response from stimuli which do not normally provoke pain.

Dorsal Root Ganglion: (also known as a posterior root ganglion) is a cluster of nerve cell bodies (a ganglion) in a dorsal root of a spinal nerve. The dorsal root ganglia contain the cell bodies of sensory neurons (afferent).

Fos: (also known as c-Fos) is an intracellular protein often transcribed in response to neuronal cell firing.

Gliosis: a nonspecific reactive change of glial cells in response to damage or insult to the central nervous system. In most cases, gliosis involves the proliferation or hypertrophy of several different types of glial cells, including astrocytes and microglia.

Hyperalgesia: 'hyper' from Greek huper (over), '-algesia' from Greek algos (pain), is an increased sensitivity to pain from a noxious stimulus, which may be caused by damage to, or sensitization of, nociceptors or peripheral nerves.

Neuraxis: referring to the axis or direction of the central nervous system.

Nociceptive: relating to or denoting pain arising from the stimulation of nerve cells.

Nociceptor: a sensory neuron that responds to damaging or potentially damaging stimuli by sending "possible threat" signals to the spinal cord and the brain.

Noxious: harmful, poisonous, or very unpleasant.

Schwann cell: any of the cells in the peripheral nervous system that produce the myelin sheath around neuronal axons.

Acknowledgements

I offer my enduring gratitude to my supervisor, Dr. Urs Häfeli, for the opportunity to engage in this research, and for the tremendous support throughout every step of the journey.

I thank my research committee, including Dr. Marc Levine (Chair), Dr. Thomas Chang and Dr. Peter Soja (Interim Chairs), Dr. Ujendra Kumar, Dr. John McNeill and Dr. Michael Negraeff for the excellent guidance, advising, teaching, and critical feedback which have contributed greatly to this dissertation.

I owe particular thanks to Dr. Ujendra Kumar and Dr. Rishi Somvanshi who have provided their guidance and advising continuously throughout my time as a graduate student. Were it not for their help, I would not have completed my research investigations.

I thank Dr. Katayoun Saatchi for continuously providing support and encouragement, for ensuring that I always had the materials required for my research, for ensuring the lab operated in a safe manner, and for synthesizing and chemically characterizing the CB2 agonist compounds.

I thank Dr. Cristina Rodríguez for committing incredible expertise and endless hours for the development of the CB2 homology model and ligand docking studies. I am indebted for the immense contribution this has made to the research investigation.

I thank Dr. Kathleen Sluka for encouraging me to carry out the immunohistology investigation and for providing guidance on the experimental protocol.

I am grateful to Kimberly Melton and Christopher Rogers at the Fred Hutchinson Cancer Research Center for their expert technical assistance which allowed me to collect and analyze histology data.

I am also grateful for the assistance of Dr. Laura Mowbray, Stephanie Laprise and Micky Burgess which allowed for successful collection of all CNS tissue samples for immunohistology.

I offer my sincerest thanks to two undergraduate students, Connor McIntyre and Nicole Sarden, whose assistance in the lab was tremendously helpful.

I am grateful to all of the Häfeli Lab members, past and present, for their support: Dr. Thomas Schneider, Dr. Gernot Marten, Dr. Mehrdad Bokharaei, Dr. Veronika Schmitt, Dr. José Carlos De La Vega, Dr. Guillaume Amouroux, Dr. Stoyan Karagiozov, Zeynab Nosrati, Lennart Bohrmann, Lovelyn Charles, Christian Buchwalder, Tullio Esposito, Jason Asnis, Tanya Saxena, Jenna Neufeld-Peters, Marta Bergamo, Jeppe Harboe and Monica Agnoletti.

I would also like to sincerely thank the faculty members and graduate students who provided assistance to me: Dr. Peter Soja, Dr. Ramakrishna Tadavarty, John Jackson, Dr. Bahira Hussein, Dr. Seungil Paik, Dr. Shenglong Zhou and Nathaniel Lal.

I am especially and deeply grateful for the unwavering, heart-felt support of my best friend and other half, John Thompson.

I am grateful for the moral support from my parents, Marcel and Linda Lambert, and brother Kevin Lambert, throughout my journey in graduate school.

Special thanks are owed to my grandmothers, who both encouraged me to follow my dreams and helped cultivate my respect for plant medicine.

This dissertation is dedicated to my grandmothers, Margaret and Hermance.

Chapter 1: Introduction

1.1   Theories and Concepts in Human Pain Perception

1.1.1   Definition & Purpose

Pain is defined by the International Association for the Study of Pain as an unpleasant sensory and emotional experience associated with actual or potential tissue damage, or described in terms of such damage [1]. Although considered unpleasant, the experience of pain has served humans throughout evolutionary history by helping to ensure protection and survival [2,3]. Perhaps the most valuable function of pain is to signal injury, thereby prompting withdrawal from the causative activity and pursuit of treatment. An additional function of pain is to prompt rest, thereby allowing the body's healing processes to be carried out more effectively. Memories of a past pain experience may also serve us by signaling avoidance of a potentially dangerous situation.

1.1.2   Acute Versus Chronic Pain

The mechanisms responsible for the perception of acute pain that occurs in response to a brief noxious stimulus have been extensively studied and are generally well understood. Not surprisingly then, modern medical treatment of acute pain is well established, generally effective and reasonably safe with currently available pharmacotherapies and non-pharmacologic measures. In such circumstances, the duration of pain perception is directly related, firstly, to the duration of the noxious stimulus, and secondly, if applicable, to the duration of tissue damage, with cessation of pain perception upon tissue healing. Chronic pain, on the other hand, is pain perception that persists beyond normal tissue healing time [4] and therefore the protection and

survival benefits conferred by acute pain are no longer applicable. Clinically, chronic pain is classified as pain which persists or recurs for 3 to 6 months or longer [5].

Chronic pain is considered to be a significant global disease burden, affecting an estimated 20% of the global population [6,7]. It is one of the most frequent reasons for physician visits, a leading reason for taking prescribed medication, and a major cause of disability [8,9]. There are a multitude and diversity of chronic pain conditions which are categorized according to clinical diagnostic criteria. However, the individual experience of pain, regardless of the specific diagnosis, is unique since it is the cumulative result of a complex interplay of patient-specific factors such as neurologic sensations, psychological and emotional functions, as well as physiologic contributors such as hormones. Despite tremendous advances in medicine and health care in recent history, chronic pain is still considered, in general, difficult to treat by health care providers today.

1.1.3   Theories of Pain Perception

Indeed, the science of pain perception is intricate and multifarious, and has evolved considerably over the past centuries. Figure 1.1 illustrates schematically the four predominant early models of pain mechanisms. Specificity theory, the earliest of which, was proposed by the seventeenth century philosopher Rene Descartes and suggested that pain perception was the direct result of sensory neurologic projection of some form of peripheral injury to the brain [10]. According to Descartes, both large and small nerve fibers sensed peripheral injury and were the only contributors to pain perception [2]. The pain experience was therefore thought to be directly proportional to the peripheral injury or pathology and determined purely by the anatomical structure of the nervous system, as it was understood at the time. Under this theory, individuals

2
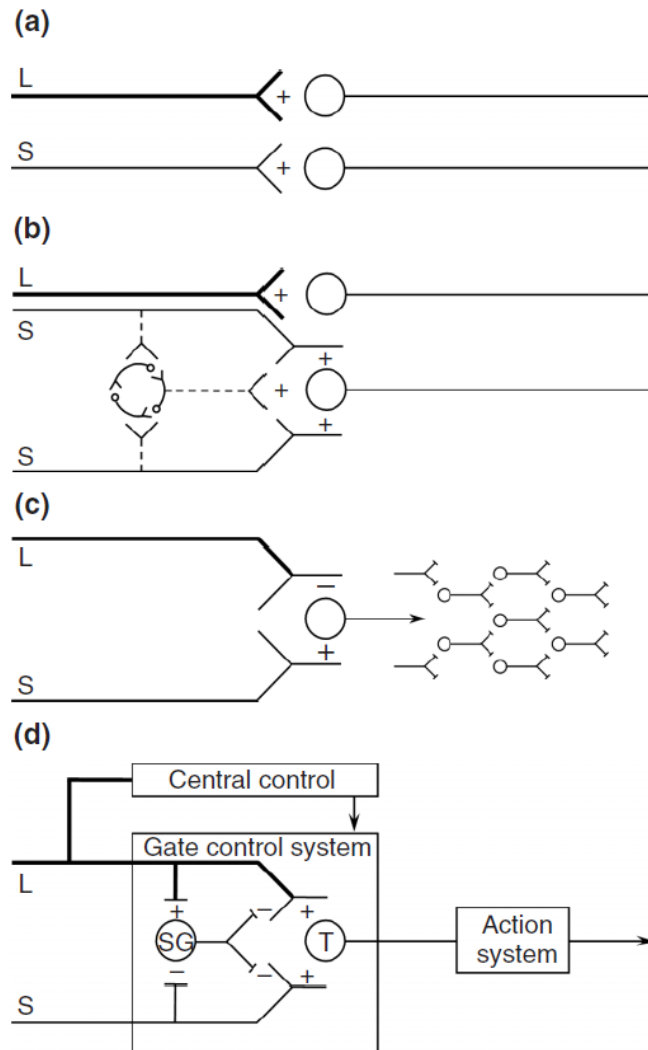
Figure 1.1. Schematic illustration of early pain model mechanisms.
(a) Specificity theory is depicted in which large (L) and small (S) fibers are thought to transmit touch and pain impulses, respectively, in distinct, direct, and specific pathways to touch and pain centers in the brain. (b) Summation theory [11], shown by small fiber convergence onto a spinal cord dorsal horn cell is depicted along with the model of reverberatory circuits [12] showing a central network of spinal cord cells projecting to a higher CNS cell. Touch is depicted to be transmitted to the CNS separately by larger fibers. (c) Sensory interaction theory [13] is shown by a multi-synaptic afferent system in which small fibers excite (+) and large fibers inhibit (-) central transmission neurons. These fibers then project to the spinal cord. (d) Gate control theory [14] is depicted by large and small fibers projecting to the substantia gelatinosa (SG) and first central transmission (T) cells. The line running from the large fiber system to the central control mechanisms represents a central control trigger which acts upon the gate control system. Central transmission cells project to the action system. This figure was published in Pain Research and Therapy: Proceedings of the VIth World Congress on Pain, Melzack, R., The gate control theory 25 years later: New perspectives on phantom limb pain, pages 9-21 [11]. Reproduced with permission, Copyright Elsevier, 1991.

claiming to perceive pain in the absence of identifiable injury were considered to have psychiatric illness, rather than a medical condition with a physiologic basis [2]. Specificity theory influenced health care providers until as recently as the 1950's [2].

There were subsequently several efforts to bring a new theory forward and these are known, collectively, as pattern theory. Pattern theory is comprised of summation theory, proposed by Goldscheider [12], and reverberatory systems theory proposed by Livingston [13] (both are depicted in Figure 1.1 (b)) as well as sensory interaction theory proposed by Noorenbos (depicted in Figure 1.1 (c)) [14]. The various forms of pattern theory each suggest that the brain plays a passive role in pain perception by acting simply as a receiver of the pain signal.

In 1965, Melzack and Wall proposed the gate control theory of pain [15], depicted in Figure 1.1 (d). According to this theory, sensory nerve fibers relay pain signals to spinal cord transmission (T) cells, and these inputs can be modified by a gating mechanism within the spinal cord dorsal horn [15]. Additionally, the brain is capable of sending signals to the spinal cord (descending input) to modulate the gating mechanism [15]. This was the first theory to identify, firstly, that pain inputs could be modified within the spinal cord dorsal horn, and secondly, that the brain plays a dynamic role in perceiving and responding to pain signals. This theory was further expanded by Melzack and Casey in 1968 as it was proposed that sensory-discriminative, motivational-affective and cognitive-evaluative systems within the brain also contribute to the overall subjective pain experience [16]. Ten years later, the theory was again built upon as Melzack and Loeser identified that phantom body pain in paraplegic patients could be generated by brain mechanisms in the absence of a spinal cord gate, through a so-called central pattern generating mechanism [17].

Thirty-six years after his initial gate control theory publication, Ronald Melzack published "Pain and the Neuromatrix in the Brain" [3], describing the neuromatrix model of pain, depicted in Figure 1.2.
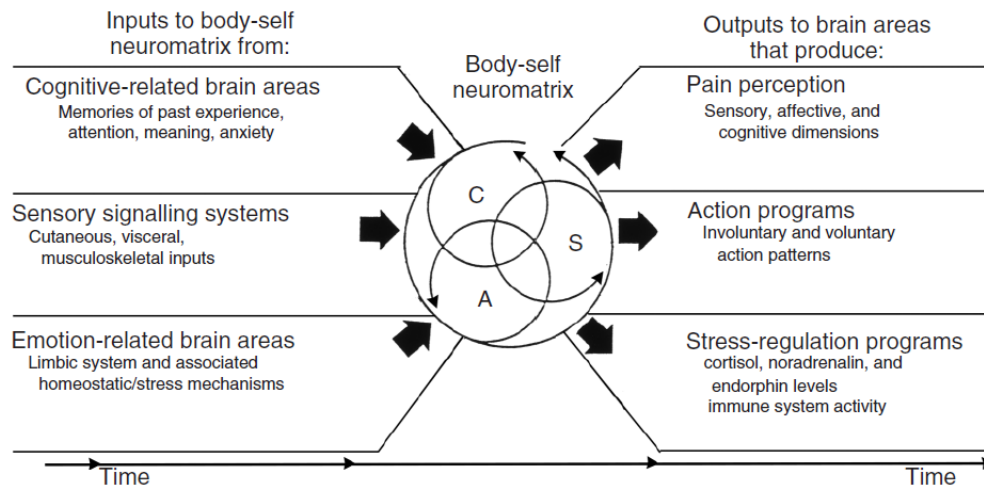
Figure 1.2. Schematic illustration of the neuromatrix model of pain.
The body-self neuromatrix is shown to be comprised of sensory (S), affective (A), and cognitive modules (C). It receives input from cognitive and emotional brain areas as well as sensory systems. The patterns of output are shown as multi-dimensional facets of the pain experience as well as behavioral and homeostatic responses. Reproduced with permission from the American Dental Education Association [3]. Copyright Melzack, R., 2001.

Gate control theory identified many new concepts, around which, a great deal of new details have been discovered through scientific research. The basic aspects of gate control theory have stood the test of time as research continues to support the overall concepts. The neuromatrix model does not replace or discard the concepts illustrated by gate control theory, but rather provides a new framework with which to examine the subjective pain experience, particularly within the context of chronic pain syndromes with little or no discernible injury or physical pathology. The theory proposes that pain perception is not simply a nociceptive phenomenon governed only by the parts of the nervous system dedicated to sensing and responding to noxious input, but rather a multidimensional experience which is generated by a widely distributed neural

5

network, termed the body-self neuromatrix [3]. According to this model, the pain experience generated by the neuromatrix arises from the unique "neurosignature" produced from multiple converging inputs, with the peripheral sensory nervous system comprising only one of these [3]. In addition to sensory nervous system inputs, the neuromatrix model asserts that cognitive as well as emotional brain processes also contribute to pain perception [3]. Furthermore, the pain perception experience itself can produce output signals to other brain areas which influence affective and cognitive patterns as well as our actions and behavior patterns [3]. Another important output area affected by the pain perception of the neuromatrix includes the body's chemical, immune, and hormonal stress-regulation programs [3]. The model recognizes that the body-self neuromatrix is not the only thing which sends signals to and influences these brain areas; however, this is the first theory to recognize the effect of pain perception on these neurological processes [3].

1.2 Sensory Mechanisms of Pain

1.2.1 Spinothalamic Tract

With respect to peripheral tissues of the body, all are innervated by sensory nerve fibers which are capable of sensing injury and inflammation. With the exception of craniofacial tissue, all peripheral sensory inputs from the neck to the toes are received by the spinal cord [18]. Sensory inputs signaling pain reach the dorsal horn region of the spinal cord and are directed to the ventrobasal complex (VBC) of the thalamus. From here, the pain signal is sent to the somatosensory cortex of the brain, allowing for the nociceptive sensation to be perceived. These pathways form the basic architecture of the spinothalamic tract, depicted in Figure 1.3.

1.2.2   Nociceptors: Sensory Afferent Neurons

Based upon the works of Erlanger and Gasser [19-21], peripheral nerves are classified as A, B and C fibers, based on their conduction velocity. The A fibers have the fastest conduction velocity, due to the fact that they are myelinated by Schwann cells, while C fibers have the slowest conduction velocity and are unmyelinated. Different nerve subtypes act to sense different types of stimuli. For example, Aβ fibers are capable of sensing touch, pressure and joint rotation while Aδ fibers sense touch, temperature, pressure and various chemical stimuli [18]. In general, the two types of nerve fibers responsible for sensing noxious stimuli are Aδ and C fibers [18]. For this reason, these two types of nerve fibers are also known as nociceptors.

Nociceptors innervate the various tissues and organs of the body. Noxious signals from the periphery are initially transduced by nociceptors and relayed to the spinal cord. These sensory afferent nerves have cell bodies located in the dorsal root ganglia which span the spinal cord roots from the cervical to the sacral level [18]. The efferent terminals of these fibers are located within the spinal cord dorsal horn region.

1.2.3   Spinoparabrachial Pathway

In addition to the spinothalamic tract, afferent noxious input is also relayed to the brain via the spinoparabrachial pathway. From the dorsal horn, spinal cord neurons project noxious input to the parabrachial nucleus of the brainstem. This region has connections to the ventral medialhippocampus and the central nucleus of the amygdala which play a role in mediating the emotional and affective response to pain [22].
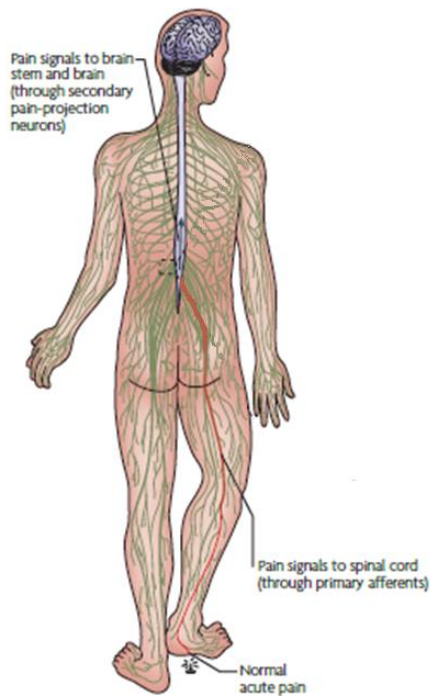
A   B
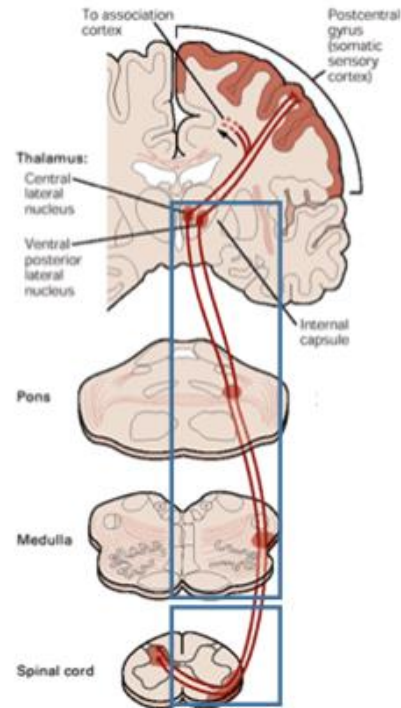
Figure 1.3. Schematic illustration of the spinothalamic tract.
(A) Nociceptive signal from the foot is transmitted to the spinal cord through a sensory afferent neuron.
The signal is then relayed upwards to the brainstem and brain. (B) A more detailed look of the spinal cord
and brain regions of the spinothalamic tract shows that, in the spinal cord, the nociceptive signal is
received in the dorsal horn region. A spinal cord projection neuron, passing through the ventral white
matter on the opposite side and through the medulla and pons, sends the nociceptive signal to the
thalamus VBC, comprised of the central lateral and ventral posterior lateral nuclei. The signal is then
relayed to the somatosensory cortex of the postcentral gyrus. This figure was published online [23].
Copyright Physiopedia, 2018.

1.2.4   Descending Modulation

Noxious signals sent to supraspinal centers are integrated in the periaqueductal gray of

the midbrain [24]. Here, the nucleus raphe magnus sends descending input down the spinal cord

which acts to modulate the ascending sensory afferent input. The periaqueductal gray is capable

of both facilitating and inhibiting sensory afferent input [22].

1.2.5   Signal Transduction Mechanisms and Pain Classification

Pain can be classified according to the mechanism through which the noxious stimulus is transduced. There are three main types of noxious stimuli, each of which are sensed by nociceptors through distinct signal transduction mechanisms, giving rise to three distinct categories of pain. These are described below.

1.2.5.1   Nociceptive

Nociceptive pain occurs in response to stimuli which cause actual or potential tissue damage. It occurs through the direct activation of peripheral nociceptor sensory fibers under normal physiologic conditions. Nociceptors express various types of receptors and/or ion channels which transduce signals from distinct noxious inputs or stimuli, thereby allowing the nociceptor to send an action potential via the spinothalamic tract in response to a noxious stimulus. In the absence of pre-existing injury or inflammation, these signal transduction mechanisms are considered to be high-threshold [24]. For example, intense mechanical stimuli such as pinch, pressure and indentation of the skin, intense heat such as contact of the skin with a flame, or certain algesic substances such as acid, capsaicin and mustard oil would be capable of producing nociceptive pain [18,24]. As depicted in Figure 1.4 (a), various TRP receptors, expressed on nociceptive nerve terminals in the skin, are capable of sensing heat (> 45°C) as well as certain chemicals such as capsaicin. The TRP receptors are non-selective cation channels, which, when activated by stimuli, open, thereby allowing influx of cations into the nerve, leading to de-polarization of the net intracellular electrical charge. If the action potential threshold is reached (approximately -55 mV), the nerve's sodium channels will open, causing the neuron to fire, thereby relaying the noxious signal to the CNS. Additional examples of nociceptive pain
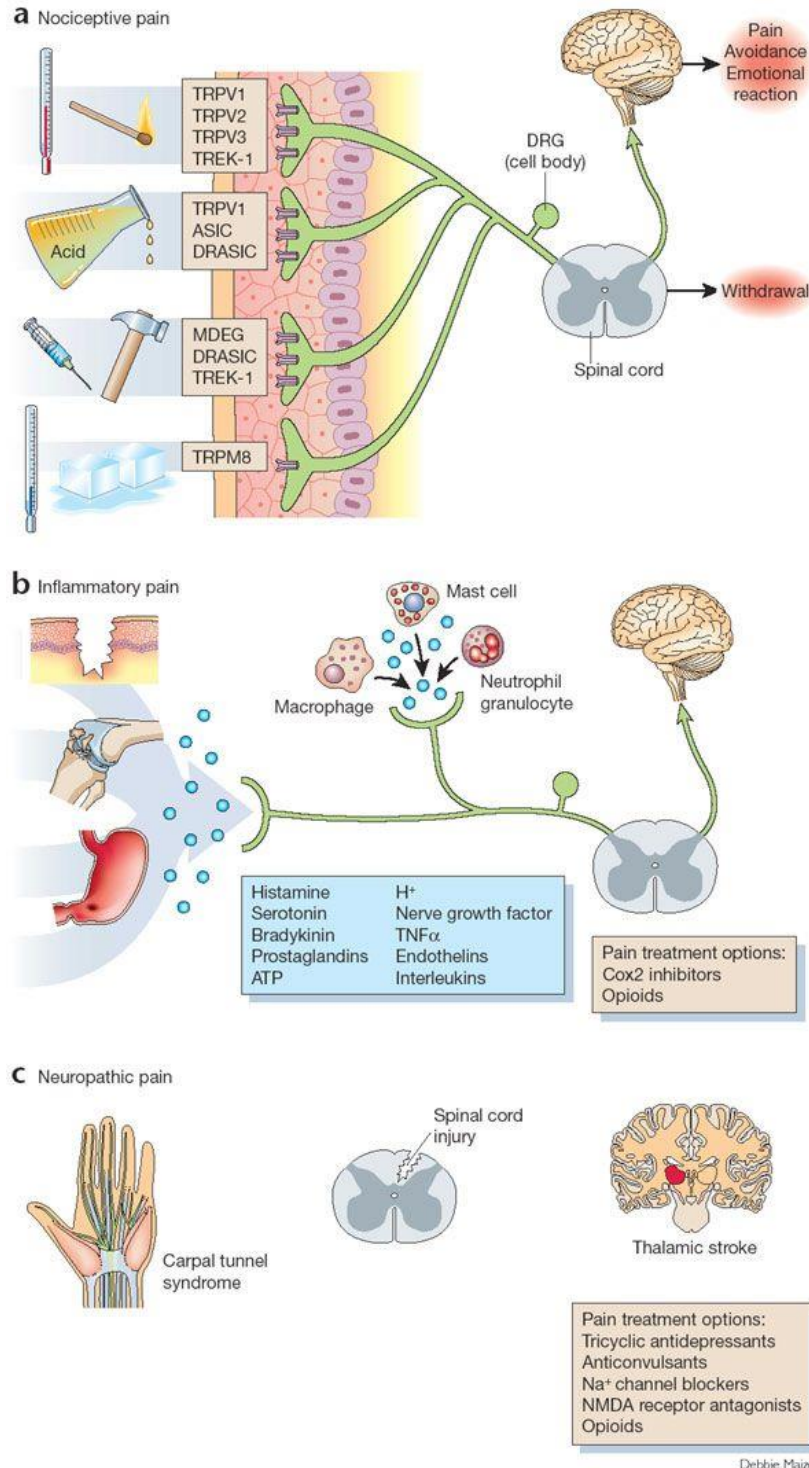
Figure 1.4. Noxious signal transduction mechanisms.
(a) Nociceptive pain signal transduction pathways may involve stimulation of sensory nerve receptors through mechanical, chemical or thermal stimuli. (b) Inflammatory pain results from the release of chemical mediators from injured tissue or inflammatory cells, thereby sensitizing peripheral neurons. (c) Neuropathic pain can result from nerve damage and/or trauma peripherally, within the spinal cord or brain. Reprinted with permission [24]. Copyright Springer Nature, 2002.

signal transduction in Figure 1.4 (a) include the ASIC channels sensing algesic chemicals such as low pH, menthol and mustard oil, the MDEG, DRASIC and TREK-1 receptors sensing intense mechanical pressure, and TRPM8 channels sensing very low temperatures [24].

1.2.5.2 Inflammatory

In response to tissue damage and/or inflammation, the functioning of nociceptors becomes altered, which may result in the experience of inflammatory pain. In such cases, chemical mediators are released either by injured tissue, inflammatory cells or tumor cells which act to directly activate nociceptors or sensitize them [24]. These inflammatory chemicals may include, for example, cytokines, prostaglandins, or bradykinin, as depicted in Figure 1.4 (b). These substances bind to GPCRs expressed by sensory nerve fibers and, in turn, increase the activity of intracellular kinases PKA and PKC. This results in increased phosphorylation of membrane-bound receptors and ion channels, such as TRPV1, which causes their threshold of activation to become reduced. De-polarization of the sensory nerve fibers then happens more readily in response to stimuli, a state known as 'peripheral sensitization'. Therefore, inflammatory pain is associated with peripheral sensitization and hyperalgesia of the affected tissue. In addition to pain, other signs which may be associated with a localized inflammatory response may include redness, swelling and heat. In response to an acute injury, such as a torn ligament, inflammatory pain will generally occur over the duration of the injury and end upon tissue healing. In cases of chronic inflammatory disease, however, inflammatory pain may be present on a chronic and/or recurring basis. Examples of such cases may include rheumatoid arthritis and inflammatory bowel disease.

1.2.5.3 Neuropathic

Neuropathic pain occurs specifically in response to damage of nerve tissue itself. Changes to both the injured nerve in the periphery and within pain-processing regions of the CNS can occur in such cases, leading to both peripheral and central sensitization, hyperalgesia and allodynia. Some of the key changes implicated in neuropathic pain include increased transcription or altered trafficking of sodium channels and reduced transcription of potassium channels [24], increasing the excitability of sensory neurons and resulting in peripheral sensitization. Within the CNS, biochemical changes within the dorsal horn region such as phosphorylation of NMDA and TRPV1 receptors work to enhance nociceptive signal transmission, contributing to central pain sensitization. Clinically, patients may experience hyperalgesia, allodynia, as well as spontaneously-evoked pain sensations. As depicted in Figure 1.4 (c), injury to nerve tissue may occur in the periphery, for example, by damage to sensory nerves caused by swelling of the carpal tunnel. Nerve tissue damage may also occur within the CNS, for example, via traumatic spinal cord injury or ischemic stroke. The experience of neuropathic pain is commonly described as sharp, burning, shooting, electrical or shock-like sensations. Although healing of nerve tissue injury followed by the absence of neuropathic pain may occur, many cases of neuropathic pain are chronic.

1.3 Pathophysiology of Chronic Pain

Normally, nociceptive input from the periphery is delivered to the dorsal horn of the spinal cord by thinly myelinated and non-myelinated sensory afferent neurons known as Aδ and C fibers, respectively. During this process, excitatory neurotransmitters such as substance P and glutamate are released in the dorsal horn from the terminals of the Aδ and C neurons. Glutamate

leads to short term activation of both the AMPA and kainate ionotropic glutamate receptors on dorsal horn pain projection neurons [25]. These signals are relayed to the brain via the spino-thalamic tract and allow for perception of the intensity, duration, and time of onset of the noxious stimulus [25]. Under these circumstances, the function of spinal cord glial cells remains unchanged and NMDA ionotropic glutamate receptors are not activated as they remain plugged by Mg^{2+} [26]. In situations in which inflammation or tissue damage is prolonged, ongoing excitation of afferent nociceptive neurons can occur, sending repeated noxious signals into the dorsal horn. Prolonged and repetitive nociceptive signaling can lead to several well-characterized changes within the spinal cord. These changes ultimately result in a shift within the dorsal horn from a normal state to a pain-facilitating state, referred to as 'central sensitization' (specific mechanisms discussed in Section 1.3.2). When pain persists for greater than 3 months following an injury, it is considered chronic and no longer conducive to protection and healing. An important system involved in the development and maintenance of some forms of chronic pain is now understood to be the neuronal-glial network of the spinal cord dorsal horn [27-29].

1.3.1   Spinal Cord Glial Cells

Glial cells are the most abundant cell type in the CNS and are capable of influencing neuronal signaling, particularly within the context of chronic pain. The concept of the tripartite synapse posits that pre-and post-synaptic nerve terminals as well as glial cells mediate synaptic transmission within the CNS through reciprocal communication [30,31]. Being cells of the immune system, glia are capable of mounting inflammatory responses. As evidence to date

suggests, glia-mediated neuro-inflammation within the dorsal horn of the spinal cord has important consequences for the spinothalamic pain sensing system.

1.3.1.1   Microglia

Microglia, a type of glial cell, are residents of the brain, spinal cord, and retina [32]. They are similar to peripheral cells of macrophage lineage in terms of their phenotype, function and morphology [32]. Microglia express a variety of cell surface receptors including ionotropic glutamate receptors (AMPA and NMDA), metabotropic glutamate receptors (mGluR), toll-like receptors (TLRs), NK1R (neurokinin-1/substance P receptor), purinergic receptors (PXRs), among others, allowing the cells to sense and respond to a number of different environmental stimuli [33]. In this manner, these cells are thought to play a role in host defense and tissue repair in the CNS via migration, proliferation, phagocytosis, antigen processing, and cytolytic functions [25]. These activities normally occur in response to pathogenic proteins and/or toxic cell debris produced during infection or injury [25]. Activated microglia are capable of releasing a variety of pro-inflammatory and neuroactive substances including interleukins, TNF, prostaglandins, excitatory amino acids (*i.e.*, glutamate and/or aspartate), NO, BDNF and NGF.

Previous research has found that microglial activation and localization within the dorsal horn occurs in certain models of pain in animals (reviewed in [33]). It is now understood that microglia are capable of modulating neuronal signaling and facilitating central sensitization through a phenomenon called neuro-inflammation (specific mechanisms discussed in Section 1.3.2)

1.3.1.2   Astrocytes

Astrocytes are a second type of glial cell within the CNS, and, like microglia, are also capable of mediating the innate immune response and modulating neuronal signaling within the spinal cord [34]. They are derived from the neuroectoderm during embryonic development and remain residents of the CNS throughout their lifespan. Unlike microglia, astrocytes are non-migratory and form elaborate networks via cell-cell gap junction linkages with other astrocytes [34]. Astrocytes express an array of functional neurotransmitter receptors which facilitate cellular activation in response to substance P, glutamate, and ATP. In states of hyperalgesia and allodynia, astrocytes may become 'reactive' leading to increased transcription and synthesis of inflammatory factors such as IL-1β, TNFα, PGE$_2$, CCL2 and NO (reviewed in [34]).
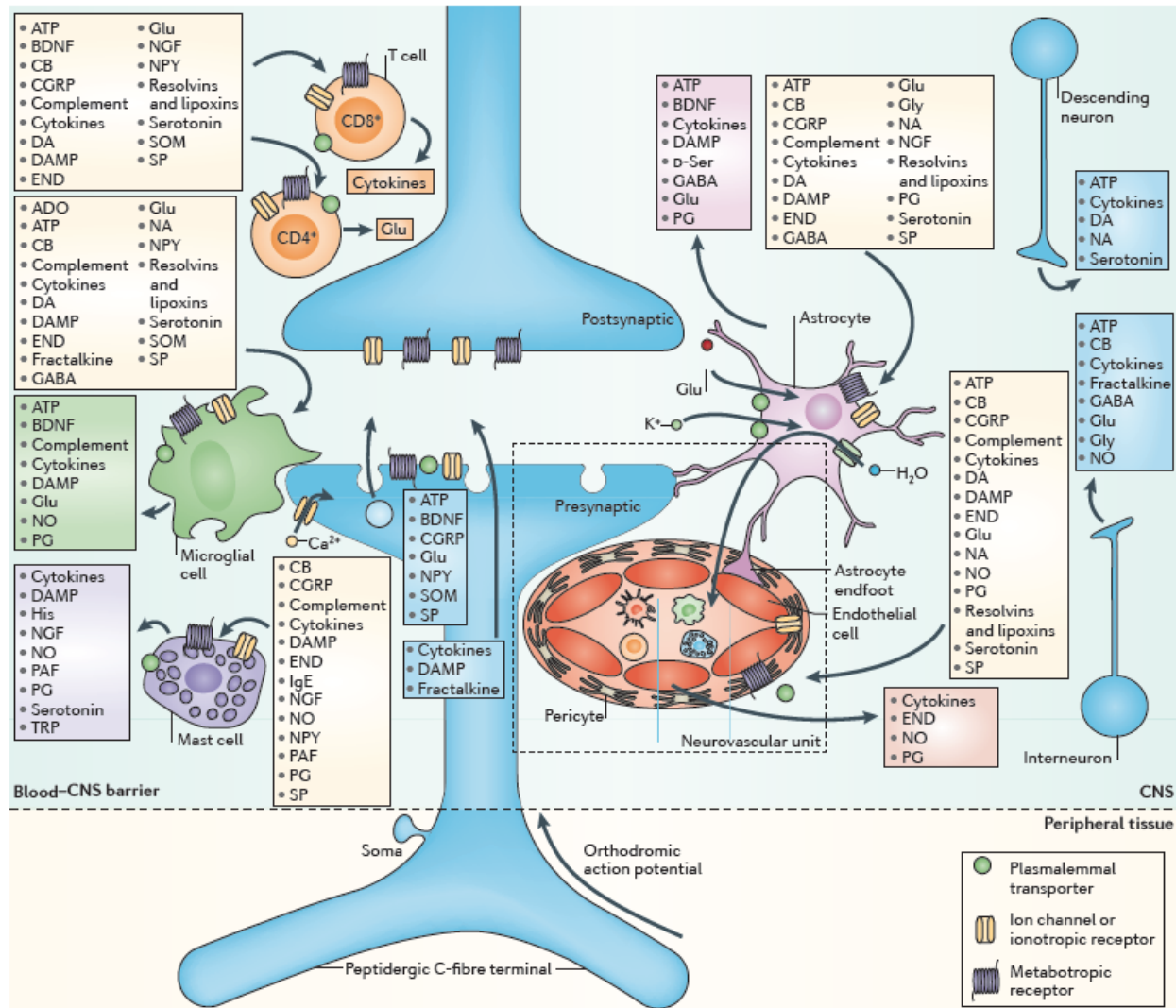
Figure 1.5. Dorsal horn neuro-inflammation.
Depicted here are the cell types and biochemical mediators thought to contribute to neurogenic neuro-inflammation within the spinal cord. In this example, persistent neuronal activity from a peripheral injury promotes release of neurotransmitters and neuropeptides (light blue boxes) from the afferent C-fibre presynaptic terminal. This induces a complex cascade of interacting responses from immune cells (microglia and astrocytes), neuronal vasculature, and higher-order neurons (descending and interneurons). Mast cells, perivascular macrophages and T cells may also release pro-inflammatory mediators to further enhance the response. Substances released by each cell type are listed in boxes colored according to the respective cell type. Key substances which act on each cell type are listed in light yellow boxes. These biochemical mediators normally maintain a net balance between pro- and anti-inflammatory signaling. However, ongoing noxious afferent input can drive a net pro-inflammatory environment, resulting in neuro-inflammation. Neuro-inflammation can ultimately amplify neuronal signals within the spino-thalamic pain pathway and drive hallmark features of chronic pain such as hyperalgesia and allodynia. Abbreviations in this figure are defined in the List of Abbreviations. Reprinted with permission [35]. Copyright Springer Nature, 2014.

16

1.3.2 Mechanisms of Spinal Cord Neuro-Inflammation

Currently, there are postulated biochemical mechanisms through which neuro-inflammation of the spinal cord may develop. Figure 1.5 depicts this phenomenon within the context of chronic neuropathic pain following peripheral nerve injury.

NMDA receptors are expressed by both spinal cord neurons and glial cells and can become activated in response to elevated synaptic glutamate concentrations, ongoing afferent signaling, and sustained depolarization of pain projection neurons [25]. NMDA receptor activation results in the influx of Ca^{2+} and other cations, thus favoring cell depolarization and firing of neurons and pro-inflammatory cytokine production in glia. NR2B is one subunit comprising the tetrameric NMDA receptor in the spinal cord. Increased activity of intracellular protein kinase A (PKA) (*i.e,.* in response to inflammatory stimuli such as CGRP or PGE_2) can result in NR2B phosphorylation which increases NMDA Ca^{2+} permeability [26]. PKA activation is increased by increased intracellular cAMP concentration and its activity has been shown to play a critical role in maintaining central pain sensitization [36,37]. CGRP is found in the terminals of nociceptive C and Aδ fibers and when released, acts on CGRP receptors in the dorsal horn of the spinal cord [38,39]. CGRP release is induced in diseases such as arthritis and is strongly associated with central sensitization [39]. CGRP is known to increase PKA activity and enhance NMDA Ca^{2+} permeability [40]. In glia, Ca^{2+} influx triggers p38 mitogen activated protein kinase (MAPK) activation, causing production and secretion of inflammatory mediators such as IL-1β, TNFα, IL-6, PGE_2, BDNF, and activation of nuclear transcription factor kappa-B (NF-κB) which induces further synthesis of pro-inflammatory molecules [25]. IL-1β, TNFα and IL-6 have been shown to increase neuro-excitatory synaptic transmission and potentiate currents via AMPA and NMDA glutamate receptors in spinal cord sections. BDNF impairs inhibition and

17

enhances excitability of pain projection neurons in the dorsal horn by altering chloride

homeostasis [41,42]. In neurons, Ca^{2+} influx triggers synthesis of NO and PGE_2 which can

directly activate microglia and astrocytes, further driving synthesis and secretion of

inflammatory mediators. Peripheral nerve injury is known to induce monocyte chemoattractant

protein-1 (also known as MCP-1) secretion in the dorsal horn of the spinal cord as well as

microglial activation [43,44]. TNFα can also induce marked production of CCL2 by astrocytes

[45]. CCL2 is known to rapidly induce central sensitization by increasing NMDA receptor

activity in dorsal horn neurons [27,45], likely via the cAMP-PKA pathway**.** In addition, neuron-

derived ATP is known to stimulate microglia via the P2X4 receptor which induces cellular

secretion of ATP and BDNF [41,42,46]. Furthermore, the presence of inflammatory mediators

can increase expression of TRPV1 channels, leading to increased neuronal sensitivity [41].

TRPV1 receptors are ligand-gated cation channels expressed on nociceptive neurons and play an

important role in mediating inflammatory and thermal nociception [47,48]. When activated, the

channel opens generating an influx of cations which increases the probability of the membrane

voltage reaching the threshold for action potential firing. In response to inflammatory molecules

(ex. PGE_2 or ATP), the TRPV1 receptor becomes phosphorylated by either PKA or PKC which

causes the channel to open more readily in response to stimuli [48-55]. Thus, the increased

expression and phosphorylation of TRPV1 receptors on neuronal fibers within the dorsal horn

could considerably amplify noxious input in the presence of inflammatory ligands.

1.4 Pharmacologic Management of Chronic Pain

Various pharmacologic options exist for the treatment of chronic pain conditions. Pharmacologic agents with a Health Canada-approved indication for the treatment of one or more forms of chronic pain are listed in Table 1.1, grouped according to drug class. Importantly, each drug class is associated with several characteristic adverse effects, also included in Table 1.1, which commonly limit the ability of these agents to provide adequate pain therapy. All approved treatment indications and common adverse effects listed in Table 1.1 were obtained from The Canadian Pharmacists Association's RxTx database [56]. Recommended therapeutic choices for the most common types of chronic pain, including neuropathic pain and chronic joint pain, are described here. Therapeutic choices for fibromyalgia treatment are specifically discussed in Section 1.5. Discussion of pharmacotherapy for additional chronic pain states is outside the scope of this dissertation.

With respect to treatment of chronic neuropathic pain conditions, the Canadian Pain Society recommends that gabapentinoids, tricyclic anti-depressants and serotonin-norepinephrine re-uptake inhibitors be used as first-line agents [57]. In moderate to severe pain not responsive to treatment with first-line agents, tramadol and other controlled-release opioids are recommended as second-line options [57]. Cannabinoids are considered to be third-line treatment options in the event an adequate response is not obtained from first or second-line agents [57]. Fourth-line agents include methadone and selected anti-convulsants [57]. In selected chronic neuropathic pain conditions, evidence exists to support the use of combination therapy with multiple specific agents in the event that first-line treatments fail [57].

For the treatment of pain in chronic joint disorders such as arthritis, acetaminophen and NSAIDs, used either topically or orally, are considered first-line options [58]. Topical capsaicin

derivatives may also provide benefit either as first-line treatment or as an adjunctive therapy [58]. Serotonin-norepinephrine re-uptake inhibitors are recommended for patients with concomitant depression and/or neuropathic pain [58]. Opioids are recommended in moderate to severe cases not adequately controlled using NSAIDs [58].

Despite published treatment guidelines and the approved indications for chronic pain treatment, systematic reviews of randomized controlled trials consistently report that the efficacy of pharmacologic agents for chronic pain treatment is generally low or modest [57,59-62]. Some scholars feel this is due to the fact that the currently available pharmacologic agents were not designed to address the underlying pathophysiology, coupled with the fact that their mechanisms are generally non-specific [24]. In addition, the therapeutic mechanisms of many agents result in unwanted side-effects, commonly limiting patients' willingness to adhere to treatment and/or presenting serious safety issues warranting discontinuation. For example, gabapentinoids act on voltage-gated calcium channels in the CNS, contributing to an overall, non-specific decrease in neurotransmission. The side effect profile, listed in Table 1.1, illustrates some of the common clinical consequences of this non-specific action. A recent Cochrane Database Systematic Review of chronic neuropathic pain treatment concluded that "[o]ver half of those treated with gabapentin will not have worthwhile pain relief but may experience adverse events" [61]. As a second example, opioid analgesics are relied upon for treatment of chronic pain that is moderate to severe and/or non-responsive to first-line options. However, these agents often fail to provide clinically meaningful benefit and commonly cause adverse effects. As concluded by a recent Cochrane Review, "[n]o convincing, unbiased evidence suggests that oxycodone (as oxycodone CR) is of value in treating people with painful diabetic neuropathy or postherpetic neuralgia.

There is no evidence at all for other neuropathic pain conditions, or for fibromyalgia. Adverse events typical of opioids appear to be common." [62].

Clearly, improved pharmacotherapies are required for chronic pain treatment. Because chronic pain is considered heterogeneous in terms of its etiological factors and mechanisms, it has been asserted that future pharmacotherapies should not aim to address pain as an overall symptom, but rather aim to target the underlying neurobiological mechanisms responsible [24].

Table 1.1. Pharmaceutical agents indicated for chronic pain treatment.

Drug Class	Drug	Brand Name(s)	Route of Administration / Dosage Format	Approved Chronic Pain Indication(s)	Adverse Effects and Limitations
Anti-Convulsant	Carbamazepine	Tegretol®	Oral / Tablet, Suspension	Trigeminal neuralgia	Hypersensitivity reactions, ataxia, dizziness, somnolence, hypotension, sedation, blurred vision, hyponatremia, leucopenia, skin rashes and dermatitis
Cannabinoids	Nabiximols (Δ^9-THC and CBD)	Sativex®	Buccal / Oromucosal Spray	Spasticity and neuropathic pain in multiple sclerosis; adjunctive analgesic in advanced cancer	Psychotropic effects, psychological dependence, mood changes, decrease in cognitive performance, dizziness, fainting, tachycardia, postural hypotension
Capsaicin Derivatives	Capsaicin	Capzacin HP®	Topical / Cream	Pain syndromes	Arthralgia, local pain, burning, stinging, erythema
	Zucapsaicin	Zostrix®, Rub A535®		Osteoarthritis of the knee	
Centrally-Acting Analgesic	Acetaminophen	Tylenol®	Oral / Tablet	Temporary relief of mild to moderate pain in arthritis, myalgia, neuralgia, low back pain, musculoskeletal pain, dysmenorrhea	Hepatotoxicity associated with overdose and alcoholism

Gabapentin-oids	Gabapentin	Neurontin®	Oral / Capsule, Tablet	Chronic low back pain, trigeminal neuralgia, chronic peripheral neuropathic pain	Renal failure, blurred vision, angioedema, edema, dizziness, somnolence, discontinuation symptoms, constipation, GI obstruction, weight gain
	Pregabalin	Lyrica®	Oral / Capsule	Fibromyalgia, diabetic peripheral neuropathy, postherpetic neuralgia, neuropathic pain associated with spinal cord injury	
NSAID	Ibuprofen	Advil®	Oral / Tablet, Gelcap, Suspension	Osteoarthritis, juvenile rheumatoid arthritis, dysmenorrhea	Cardiovascular related events (heart attack, stroke, thrombosis), peptic/duodenal ulceration, GI perforation, GI bleeding, renal impairment, hypertension, edema, hematuria, cystitis
	Naproxen	Naprosyn®	Oral, Rectal / Tablet, Suspension, Suppository	Osteoarthritis, juvenile rheumatoid arthritis, dysmenorrhea, low back pain	
	Diclofenac	Arthrotec®, Pennsaid®	Oral, Topical, Rectal / Tablet, Powder, Gel, Suppository	Osteoarthritis, rheumatoid arthritis	
	Indometha-cin	Indocin®	Oral, Rectal / Tablet, Suppository	Osteoarthritis, rheumatoid arthritis, ankylosing spondylitis	
	Meloxicam	Mobicox®	Oral / Tablet	Osteoarthritis, rheumatoid arthritis	
	Celecoxib	Celebrex®	Oral / Capsule	Osteoarthritis, rheumatoid arthritis, ankylosing spondylitis	
	Diflunisal	Dolobid®	Oral / Tablet	Osteoarthritis, rheumatoid arthritis	

	Etodolac	Lodine®	Oral / Capsule	Osteoarthritis, rheumatoid arthritis
	Flurbiprofen	Ansaid®	Oral / Tablet	Osteoarthritis, rheumatoid arthritis, ankylosing spondylitis
	Ketoprofen	Orudis®	Oral / Capsule	Osteoarthritis, rheumatoid arthritis, ankylosing spondylitis
	Piroxicam	Feldene®	Oral / Capsule	Osteoarthritis, rheumatoid arthritis, ankylosing spondylitis
	Tiaprofenic acid	Surgam®	Oral / Tablet	Osteoarthritis, rheumatoid arthritis
Opioid	Codeine	Codeine Contin®, Tylenol #3®	Oral / Tablet	Mild-moderate chronic pain and cancer pain
	Oxycodone	Oxy.IR®, OxyNEO®, Percocet®	Oral / Tablet	Moderate-severe chronic pain and cancer pain
	Tramadol	Zytram®, Tramacet®	Oral / Tablet	Moderate-severe chronic pain and cancer pain
	Hydromorph-one	Dilaudid, Hydromorph Contin®	Oral / Tablet, Capsule	Moderate-severe chronic pain and cancer pain
	Fentanyl	Duragesic®	Topical / Patch	Severe chronic pain and cancer pain
	Morphine	M-Eslon®, MS.IR®	Oral / Tablet, Capsule	Severe chronic pain and cancer pain
	Methadone	Not applicable	Oral / Solution	(Without Health Canada Approval) Chronic pain and cancer pain

Physiological tolerance, psychological dependence, addiction, fatal overdosing, withdrawal syndrome, hyperalgesia, CNS depression, constipation, sedation, dizziness, hypotension, respiratory depression, anorexia, hyperhidrosis, hallucinations, confusion, delirium

	Tapentadol	Nucynta®	Oral / Tablet	(Without Health Canada Approval) Diabetic neuropathy	
Serotonin-Norepineph-rine Re-Uptake Inhibitor	Duloxetine	Cymbalta®	Oral / Capsule	Fibromyalgia, diabetic peripheral neuropathy, chronic low back pain, osteoarthritis of the knee	Hypertension, hepatotoxicity, discontinuation symptoms, decreased glycemic control, abnormal bleeding, hyponatremia, seizures, sedation, sexual dysfunction, serotonin syndrome
Tricyclic Antidepressant	Amitriptyline	Elavil®	Oral / Tablet	(Without Health Canada Approval) Fibromyalgia, neuropathic pain, chronic neck pain	Dry mouth, blurred vision, constipation, tachycardia, delirium, sedation, weight gain, orthostatic hypotension, seizures, sexual dysfunction

1.5   Fibromyalgia Syndrome: A Chronic Widespread Musculoskeletal Pain Disorder

Fibromyalgia (FM) is a syndrome characterized by chronic widespread myofascial pain and is associated with fatigue, cognitive difficulties and non-restorative sleep, along with the experience of a number of additional wide-ranging somatic symptoms such as frequent headaches, sinus problems, and muscle spasm [63,64]. FM is also associated with the presence of myofascial trigger points (MTPs) which are hyperirritable, palpable nodules within a muscle taut band (an endogenous localized contracture within the muscle without activation of the motor endplate) [65-67]. A Canadian study estimates the prevalence of FM to be 4.9% in women and 1.6% in men [68]. The estimated mean global prevalence of FM is 2.7% with the majority of affected individuals being women [69]. This medical condition represents a major global economic burden as FM patients frequently access health care services and experience reduced daily functioning and productivity [70].

1.5.1   Clinical Features and Diagnosis

The chronic widespread pain experienced by individuals with FM can present clinically as pain and/or tenderness in response to non-painful stimuli (known as allodynia) as well as increased subjective pain sensation in response to modestly painful stimuli (known as hyperalgesia). This pain may also be associated with stiffness, subjective weakness, and/or muscle fatigue.

Updated since 1990, the most recent diagnostic criteria for fibromyalgia published by the American College of Rheumatology in 2010 require that patients have had symptoms for at least three months and do not have another disorder which would explain their symptoms of pain [63]. Additionally, patients must have a widespread pain index (WPI) score and a symptom severity

(SS) score above a defined minimum level [63]. The WPI takes into account the number of

tender points or painful areas reported by the patient while the SS score is determined by taking

into account the number of somatic symptoms experienced as well as the severity of fatigue,

waking unrefreshed, and cognitive difficulty [63]. The common locations of tender points in FM

are shown in Figure 1.6 below.

Figure 1.6. Common locations of pain and/or tenderness in FM (yellow/red), referred to as tender points.
This figure was published online [71]. Copyright Peak Physical Therapy & Sports Rehabilitation, 2012.

1.5.2   Pathophysiology

Although the pathophysiology of FM remains to be fully elucidated, research to date

suggests that numerous sites along the pain neuraxis are involved. The underlying

pathophysiology is thought to involve peripheral and central sensitization coupled with

abnormalities in CNS pain processing [72-74].

Afferent nociceptive input from sensitized peripheral sites has been shown to play an important role in generating and maintaining central sensitization in FM [66,67,75-77]. Peripheral sensitization of afferent nociceptors may develop in focal regions of tissue abnormality, including MTPs, through an interplay of muscle ischemia, perpetual muscle contracture and locally released vasoactive and algogenic substances [78-80]. The expanded MTP hypothesis developed by Gerwin *et al.* outlines the formation of MTPs, asserting that hypo-perfusion and ischemia of a muscle region can lead to reduced pH, greatly increased acetylcholine concentrations within neuromuscular junctions, and release of cytokines, substance P, bradykinin, and CGRP [81]. It is now believed that MTPs result in a sensitized region in the periphery which deliver frequent and spontaneously evoked pain signals in FM (an 'afferent barrage' to the spinal cord), driving localized pain and tenderness as well as central sensitization, resulting in hyperalgesia and allodynia [65-67,79].

Another component of FM pathophysiology is thought to involve dysfunction of endogenous descending inhibitory systems, thereby enhancing the nociceptive sensitivity characteristic of FM. Opiate-mediated pain modulation in the brain appears to be abnormal in individuals with FM, as evidenced by a decrease in μ opioid receptor binding in the brain [82]. FM patients also have reduced cerebrospinal fluid (CSF) levels of dopamine [83], norepinephrine [83] and serotonin metabolites [84], which may also indicate reduced activity of descending inhibitory systems.

Importantly, studies have identified elevations in inflammatory biomarkers within both the periphery and CNS of FM patients, attesting the presence of inflammation in this disease state. Compared to healthy controls, significant elevations in glutamate, substance P, NGF, BDNF and IL-8 have been found in the CSF of FM patients [85-88]. As outlined above in

27

Section 1.3, each of these substances plays a role in enhancing nociceptive signaling, particularly within the spinal cord dorsal horn, via glial cell-mediated neuro-inflammation. Therefore, such processes may possibly contribute to the central sensitization present in FM. In addition, significant elevations in neuromuscular junction cytokine (TNFα and IL-1β) as well as serum cytokine and chemokine concentrations have been identified in FM patients [89-92]. The role of these inflammatory molecules in FM is not clear, however, increased IL-17A, a cytokine elevated in FM patients, has previously been associated with systemic autoimmune disease [93,94], anxiety [95], depression [95,96], and hyperalgesia [97].

1.5.3   Pharmacologic Treatment

Although a range of pharmacologic agents are prescribed for FM patients clinically, the only medications officially indicated for FM pain management are duloxetine (Cymbalta®) and pregabalin (Lyrica®) in Canada and the United States as well as milnacipran (Savella®) in the United States [59,60,98]. Classic analgesics such as acetaminophen, NSAIDs, and opiates typically provide modest or no benefit [99]. Opiates are generally considered to be potent analgesic drugs; however, current treatment guidelines recommend against the use of opiates for FM treatment [100,101] based on the notion that opiate drugs may exacerbate central pain sensitivity via provocation of inflammatory glial cell activity [102,103] and the absence of evidence demonstrating that any opiate drug provides analgesic benefit in FM [99,100,104].

Currently, no single indicated treatment can be expected to provide a high degree of benefit for FM patients nor does any single treatment reduce all the major symptoms of FM. Systematic meta-analyses reveal that the indicated drug treatments for FM provide modest reductions in pain and little benefit for other core disease symptoms [59,60]. For example, a

Cochrane Database Systematic Review reports that the majority of patients receiving SNRI (serotonin-norepinephrine re-uptake inhibitor) therapy with either duloxetine or milnacipran report less than 30% improvement in pain [59]. According to a separate Cochrane Review, the same is true for pregabalin in the treatment of FM [60]. Furthermore, SNRI treatment provided non-substantial or no benefit over placebo in improving fatigue, depression, anxiety, quality of life, cognitive disturbances, and sleep problems [59]. Also, one in every five FM patients receiving duloxetine or milnacipran discontinued treatment due to adverse effects [59].

1.6   Human Endocannabinoid System

In mammals, the endocannabinoid system consists of a group of lipid signaling molecules and the cannabinoid receptors through which they signal. Endocannabinoids are eicosanoids derived from lipid metabolites and include anandamide (AEA), palmitoylethanolamide (PEA), oleoylethanolamide (OEO), N-arachidonoyl dopamine (NADA) and 2-arachadonoyl glycerol (2AG) [105]. Endocannabinoids are generally synthesized on demand, in response to elevations in intracellular calcium [106]. The metabolic deactivation of the endocannabinoids occurs predominantly via two enzymes, fatty acid amide hydrolase (FAAH) and mono-acyl glycerol lipase (MAGL) [107,108]. The primary targets through which endocannabinoids signal are thought to be the metabotropic G protein-coupled receptors (GPCRs) designated as CB1 and CB2 [106]. Importantly, evidence suggests that endocannabinoid ligands are capable of signaling through additional receptors and biochemical pathways. These include the G protein-coupled receptor GPR55 [109], the peroxisome proliferator-activated receptor (PPAR) family [110], and several of the ionotropic transient receptor potential (TRP) channels [49,111-113]. Accordingly,

the endocannabinoid system has been implicated in modulation of a great number of physiologic processes. The role of the cannabinoid receptors CB1 and CB2 will be described further below.

1.6.1   CB1 Cannabinoid Receptor

The CB1 cannabinoid receptor is expressed primarily by central and peripheral neurons [106]. Within the brain, CB1 receptor expression is enriched in the cerebral cortex, hippocampus, basal ganglia and cerebellum [106]. Lower levels are present in the hypothalamus and spinal cord [106]. CB1 receptors are also expressed widely in peripheral nerves, particularly on sensory neurons and autonomic neurons [114]. CB1 expression has also been identified in the heart, gastrointestinal tract, kidney, liver, lung, muscle, spleen, testis and uterus [106,115]. On neurons, CB1 expression is mainly localized to the cell axon and nerve terminal (pre-synaptic bouton) [106,116]. Here, the general role of the CB1 receptor is thought to be maintaining homeostasis by preventing excessive neuronal activity [106,116]. Through $G_{i/o}$-mediated intracellular cascades, CB1 stimulation by agonists has been shown to inhibit N-type voltage-gated calcium channels in neurons [117,118] and inhibit the depolarization-evoked rise in intracellular calcium [119], thus working to prevent release of neurotransmitters from pre-synaptic terminals. *In vivo*, stimulation of pre-synaptic CB1 receptors is thought to occur in response to retrograde diffusion of endocannabinoids which have been synthesized and released from post-synaptic neurons in response to depolarization and calcium release [120,121]. Through retrograde signaling, the CB1 receptor is known to mediate suppression of neurotransmitter release from both excitatory and inhibitory nerves [106,122-124]. Other reported biochemical actions associated with CB1 stimulation include $G_{i/o}$-dependent activation of inwardly-rectifying potassium channels, and inhibition of L, P and Q-type voltage-gated calcium channels as well as

activation of MAPK (p42/44) and PI3K in CNS glial cells (reviewed in [106]). Through its

various functions, the CB1 receptor is thought to impact neural plasticity and regulate

phenomena such as pain perception, emotional memory, and adaptive learning [125]. It is also

thought to play a role in modulating other functions such as appetite [126-128], emesis, and

balance of autonomic nervous system tone [129]. Agonists of the CB1 receptor are also

responsible for inducing the so-called 'cannabinoid tetrad' effects characterized in wild-type

mice (*i.e.*, hypo-locomotion in an open field, catalepsy on a ring, tail flick latency, and

hypothermia) [130,131] and static ataxia in dogs [106]. In humans, undesirable effects of CB1

stimulation are generally recognized as alterations in cognition and memory, dysphoria/euphoria,

and sedation [106]. Targeting CB1 for therapeutic purposes such as pain treatment is therefore

limited by these undesirable effects.

1.6.2   CB2 Cannabinoid Receptor

The CB2 cannabinoid receptor is expressed most abundantly by peripheral cells of the

immune system including B and T cells, natural killer cells, monocytes, macrophages, and

neutrophils [132]. The CB2 receptor couples with $G\alpha_{i/o}$ receptor proteins and its stimulation via

agonist treatment inhibits adenylyl cyclase [133]. This results in reduced intracellular cAMP

concentrations, modulation of MAPK signaling pathways, and modulation of functionof certain

Ca^{2+} channels [133]. In contrast to CB1, the CB2 receptor is not capable of acting on inwardly-

rectifying potassium channels nor is it capable of inhibiting Q-type calcium channels [106].

Ligands of the CB2 receptor generally have suppressive effects on immune cells such as

modulation of B and T cell proliferation, reduction of inflammatory cytokine production, and

decreased chemotaxis and inflammatory cell migration [132]. More recently, low-level

expression of CB2 has been detected in a vast number of tissues, both centrally and peripherally. These include specific regions of the brain, spinal cord, dorsal root ganglia, enteric nervous system neurons, gastrointestinal epithelium, vascular smooth muscle and endothelium, myocardium, bone, pancreas, reproductive organs, and various human tumors [134].

CB2 activation is associated with broad-ranging anti-inflammatory and analgesic effects which have been studied vigorously *in vivo*. Activation of CB2 has shown benefit in models of acute and chronic inflammatory disease such as multiple sclerosis [135], ischemia-reperfusion injury [136], rheumatoid arthritis [137], ulcerative colitis [138], among many others. Activation of the CB2 receptor has been shown to play a role in reducing bone loss and osteoclastogenesis [139], protecting against atherosclerosis [140,141] and preventing bronchoconstriction of the airways [142] *in vivo*. In addition, a vast number of studies indicate that specific activation of the CB2 receptor via selective agonists (*i.e.*, ligands with low or negligible affinity for CB1) can mediate analgesia *in vivo* in models of nociceptive [143-145], inflammatory [146-150] and neuropathic pain [151-155]. The role of the CB2 receptor in chronic pain involving CNS neuro-inflammation will be discussed in Section 1.9.

1.7   Phytocannabinoids: Origins, Pharmacology and Current Role in Pain Treatment

Analogous to opium poppy preparations leading to the discovery of opioids and the human opioid receptors, Cannabis has led to the discovery of cannabinoids and the human cannabinoid receptors, CB1 and CB2. Species belonging to the Cannabaceae family, such as *Cannabis sativa*, are annual herbaceous plants which have been utilized for multiple purposes (*ex.*, medicinal, recreational, industrial fiber, seed oil, *etc.*) for thousands of years [156]. *Cannabis sativa* is known to produce approximately 120 different cannabinoids (specifically

referred to here as phytocannabinoids to distinguish their origin in the plant kingdom), which

have been grouped into eleven different categories, based on chemical similarity [156].

Phytocannabinoids all have a C_{21} structural backbone and belong to the terpenophenolic

chemical family [157]. Although the total cannabinoid content of herbal cannabis can range

considerably, the average is estimated to be approximately 24% (w/w) [157]. Among the

cannabinoids present, Δ^9-tetrahydrocannabinolic acid (THCA) is typically present in greatest

abundance [156]. Importantly, the non-acidic, de-carboxylated form of this molecule (*ex.*, Δ^9-

tetrahydrocannabinol [THC]), which is produced upon heating, is the phytocannabinoid

generally responsible for its pharmacologic activity [158]. The chemical de-carboxylation

reaction of THCA, producing THC, is depicted in Figure 1.6.

Δ^9-tetrahydrocannabinolic acid
(THCA)

Δ^9-tetrahydrocannabinol
(THC)
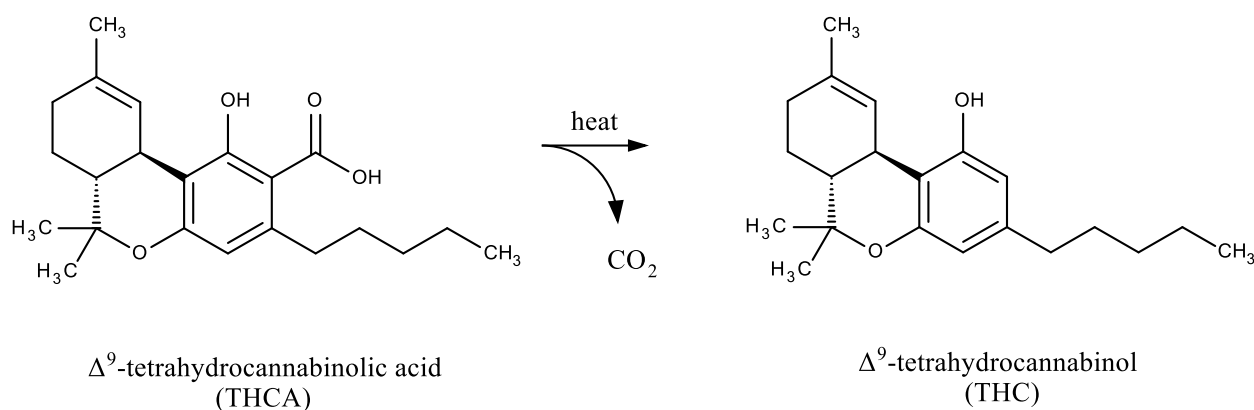
Figure 1.7. De-carboxylation of Δ^9-tetrahydrocannabinolic acid (THCA) to Δ^9-tetrahydrocannabinol (THC).

THC was chemically characterized and identified as the principal active compound

responsible for the psychotropic effects of Cannabis by Mechoulam and colleagues in 1963

[159]. THC binds to both the human CB1 and CB2 receptors with estimated K_i values of 5.05

and 3.13 nM, respectively [160]. THC also acts as a dual, non-selective agonist at both CB1 and

CB2 with estimated EC_{50} values of 6 and 0.4 nM, respectively [116]. Several THC-based and

THC analogue-based pharmaceutical agents including nabilone (Cesamet®, Valeant, Bridgewater, United States) and dronabinol (Marinol®, Solvay Pharmaceuticals, Brussels, Belgium) are available and have been utilized off-label for the treatment of several pain conditions (see Table 1.2) [161-165]. These treatments are not, however, considered first-line therapies, as discussed above in Section 1.4, and are commonly associated with adverse effects, largely owing to CB1 receptor stimulation (*ex.*, psychotropic effects, drowsiness, dizziness, decreased cognitive performance, *etc.*) [161-167].

The majority of all other phytocannabinoids studied display some degree of agonist activity at both CB1 and CB2 [157]. None have been found to act with greater potency, however, than THC [157]. In contrast, the pharmacologic activity of cannabidiol (CBD) is distinctly different. In some chemotypes of *Cannabis sativa*, CBD is present in approximately equal abundance as THC and, in some cases, is present as the predominant phytocannabinoid (*ex.*, 20% w/w) with only trace amounts of THC (*i.e.*, less than 1% w/w) [156]. In general, CBD is considered to be an antagonist at both CB1 and CB2 at the nanomolar range [168]. It has also been suspected of acting as an allosteric modulator of cannabinoid receptors [168,169]. In 2015, Laprairie and colleagues discovered that CBD negatively affects the ability of agonists to stimulate CB1 *in vitro* [170]. Furthermore, CBD treatment decreased CB1 receptor internalization in response to agonist treatment by decreasing arrestin-2 recruitment [170]. Recently, Martinez-Pinilla and colleagues at the University of Barcelona have demonstrated that the presence of CBD negatively impacts the ability of cannabinoid agonists to bind and stimulate the CB2 receptor at nanomolar concentrations, while at the same time, the half-life of the CB2-agonist complex is longer in the presence of CBD [171]. Interestingly, the ability of CBD to negatively modulate the effects of CB1 and CB2-selective agonists occurs at concentrations far

less than that required to displace dual CB1 and CB2 ligands from the orthosteric binding site, as determined by [^{3}H]CP55940 displacement assay [168,172]. For example, the K_i value at which CBD reduces CP-55,940 stimulation at CB2 (as measured by intracellular [^{35}S]GTPγS binding assay) was 65 nM whereas the K_i value at which CBD displaces [^{3}H]CP55940 binding at CB2 was 4.2 µM [168]. Collectively, these findings support the classification of CBD as a non-competitive allosteric modulator of both CB1 and CB2.

It is important to note that non-cannabinoid receptor-mediated effects of THC and CBD have been extensively reported (reviewed by Pertwee [173]). As brief examples, THC has been found to induce adipocyte differentiation as well as vascular smooth muscle relaxation via activation of PPARγ [174] while CBD has been found to exert analgesic activity via activation of TRPV1 and inhibition of FAAH [175].

The notion of phytocannabinoid synergy, also known as the 'entourage effect', asserts that the therapeutic benefits of Cannabis preparations are attributable to the combinatorial effect (or "synergy") of the multiple phytocannabinoids present, including the combination of THC and CBD [176]. Based on the pharmacological data, it has been postulated that administration of CBD along with THC may help to mitigate the undesirable CB1-mediated effects of THC alone [170]. Furthermore, CBD co-administration may reduce THC-induced tolerance and arrestin 2-mediated internalization of CB1 [170]. The data also suggest that CBD is capable of prolonging CB2-agonist complex stability which could potentially enhance the CB2-mediated benefits of THC [171]. Although clinical studies confirming the additive benefit and/or synergy of the THC and CBD combination are lacking, the Sativex® oromucosal spray (GW Pharmaceuticals, Salisbury, United Kingdom) is a phytocannabinoid extract-based product which contains THC

Table 2.2. Pharmaceutical agents targeting the endocannabinoid system for pain treatment.

Drug Class	Drug	Brand Name	Route of Administration / Dosage Format	Clinical Therapeutic Use	Adverse Effects and Limitations
Herbal Cannabis	Cured Cannabis flower	various	Intrapulmonary / Cigarette Oral / Capsule, Liquid Topical / Ointment	Available for various pain-related uses through Health Canada ACMPR program	Short term: confusion, sleepiness, fatigue, impairment in memory and concentration, anxiety, panic, paranoia, delusions, hallucinations, dizziness, fainting, tachycardia, postural hypotention. Long Term: Harm to memory, concentration, thinking, bronchitis and lung infections [175].
Phyto-cannabinoids	Dronabinol (Δ^9-THC)	Marinol®	Oral / Capsule	Non-Approved, off-label use for chronic non-cancer pain [163].	Psychotropic effects, psychological dependence, mood changes, decrease in cognitive performance, dizziness, fainting, tachycardia, postural hypotension [164,176].
	Nabiximols (Δ^9-THC and CBD)	Sativex®	Buccal / Oromucosal Spray	Health Canada Approved Use: Spasticity and neuropathic pain in multiple sclerosis; adjunctive analgesic in advanced cancer [176].	
Synthetic Phyto-cannabinoid Analogue	Nabilone (Δ^9-THC analogue)	Cesamet®	Oral / Capsule	Non-Approved, off-label use for chronic cancer and non-cancer pain [159-162].	Drowsiness, vertigo, psychological high, dry mouth, ataxia, blurred vision, sensation disturbance, headache, orthostatic hypotension, hallucinations [159,162].
Endo-cannabinoid Modulator	Acetaminophen	Tylenol®	Oral / Tablet, Suspension	Health Canada - Approved Uses: Temporary releif of mild to moderate pain in arthritis, myalgia, neuralgia, low back pain and musculoskeletal pain	Hepatotoxicity associated with overdose and alcoholism [177].

and CBD in an approximate ratio of 1:1 which has been approved as an adjunctive analgesic for cancer pain and for neuropathic pain and spasticity in multiple sclerosis (see Table 1.2) [178]. CB1-mediated adverse effects persist, however, with this formulation, limiting its therapeutic benefits (see Table 1.2) [178].

As listed in Table 1.2, acetaminophen is indeed a pharmaceutical analgesic agent which acts through the endocannabinoid system and therefore a brief discussion is included in this section. Acetaminophen was first synthesized by Morse in 1878 [180] and became widely used in North America beginning in the 1950's as an analgesic and anti-pyretic [181]. Its mechanism of action has been largely unclear, however, until recently. Acetaminophen likely works via several pharmacologic mechanisms, some of which are thought to involve the endocannabinoid system. The first analgesic mechanism of acetaminophen is thought to involve the inhibition of COX. This enzyme is known to catalyze the production of prostaglandins, thromboxanes and prostacyclins from a common precursor, arachidonic acid (AA). Prostaglandins are mediators of fever, pain and inflammation and therefore NSAIDs are effective analgesics and anti-pyretics since they inhibit COX activity both centrally and peripherally. In the case of acetaminophen, its major hepatic metabolite, para-aminophenol, is thought to reduce COX from the active oxidized form (Fe^{4+}) to the inactive reduced form (Fe^{3+}), primarily in the brain [182]. Since the synthesis of prostaglandins by COX is sensitive to the enzyme's oxidation state and the presence of peroxides, acetaminophen is likely not effective at inactivating COX at peripheral sites of inflammation because the presence of hydroperoxides such as PGG_2 and others will be increased in these regions [182]. Therefore, acetaminophen is thought to act on COX primarily in tissues with low oxidant status such as the brain and certain endothelial cells [181].

The endocannabinoid modulating effects of acetaminophen are thought to involve the metabolic conjugation of its metabolite, para-aminophenol, to arachidonic acid by FAAH to form a compound known as N-acylphenolamine (or AM404), with the greatest levels produced in the brain [183]. AM404 was reported by Beltramo and colleagues to inhibit cellular reuptake of anandamide (an endocannabinoid) and enhance its cannabinoid receptor-mediated analgesic effects *in vivo* [184]. Therefore, centrally-produced AM404 is thought to promote analgesia through indirectly enhancing cannabinoid receptor activation in the CNS. To support this finding, blockade of CB1 receptors has been shown to greatly inhibit the analgesic effect of acetaminophen in rats [185]. Additionally, AM404 has been found to activate both rat and human TRPV1 receptors at a 10 nM concentration [183,186,187]. It is therefore inferred that AM404 also acts on TRPV1 receptors of the CNS to mediate analgesia. Moreover, because FAAH is known to be co-localized with TRPV1 expression in primary sensory neurons [188], it is thought that the analgesic activity of AM404 at TRPV1 receptors may also take place in the periphery.

1.8   β-Caryophyllene: A Sesquiterpene With Selective CB2 Agonist Activity

1.8.1   Botanical Sources and Traditional Use

β-Caryophyllene is a small molecule (204.35 Da) produced in a variety of different botanicals including *Copaifera* spp. (copaiba balsam) [189], *Eugenia caryophyllata* (clove) [190], *Piper* spp. (black pepper) [191], *Oreganum* spp. (oregano) [192], *Cinnamomum zeylanicum* (cinnamon) [193] and *Cannabis sativa*[194]. Based on its chemical structure (see Figure 1.7), it is classified as a bicyclic sesquiterpene. β-caryophyllene has been identified as one of the principal constituents within the essential oil fraction of numerous botanicals which have a

history of traditional use in folk medicine. These include *Copaifera* spp. [195], *Cordia verbenacea* [196], *Croton campestris* [197], *Callistemon citrinus* [198], *Pinus heldreichii* [199], *Peperomia serpens* [200], *Ocimum micranthum* [201], *Mosla dianthera* [202], *Vitex agnus-castus* [203], *Senecio flammeus* [204], *Eremanthus erythropappus* [205], *Artemisia fukudo* [206] and *Saussurea lappa* [207]. Only botanicals in which β-caryophyllene has been identified as the most abundant or the principal active compound will be discussed here. Preparations of the trunk resin from *Copaifera* spp. (commonly known as "cobaiba oil"), found to contain β-caryophyllene as the most abundant compound, have been used traditionally in regions of Latin America for a vast number of medicinal uses, most commonly as an anti-inflammatory and anti-infective, since before the time of European colonization in the sixteenth century [195]. Today, commercial forms of cobaiba oil are marketed in several regions of South America, most abundantly in the Amazon region, where it is widely known as a medicinal plant [195]. In addition, β-caryophyllene is one of the principal active constituents of *Cordia verbenacea*, known as "erva baleeira" in Brazil [196,208]. Here, the aerial parts of the plant have been prepared as alcoholic extracts, teas and infusions and used in folk medicine both internally and topically as an anti-inflammatory, anti-rheumatic and analgesic [208,209]. *Croton campestris* is another botanical species used widely in folk medicine in Brazil for many wide-ranging ailments including pain, stroke, allergies, wounds, rheumatism and bronchitis [197,210]. β-caryophyllene is the most abundant and main active compound [197,210].
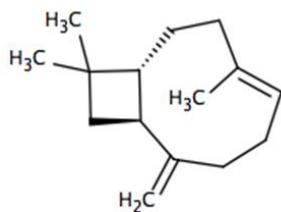
Figure 1.8. Chemical structure of β-caryophyllene.

1.8.2   Pharmacologic Properties

1.8.2.1   Selective CB2 Agonist

As demonstrated by Gertsch and colleagues, β-caryophyllene is an agonist of the CB2 cannabinoid receptor, binding with an apparent K_i of 155 nM in CB2-expressing HEK293 cells and inhibiting forskolin-induced cAMP production with an EC_{50} of 1.9 µM in CB2-expressing CHO cells [194]. Although Gertsch and colleagues demonstrated substantially lesser binding of β-caryophyllene in CB1-expressing HEK293 cells, neither binding affinity (K_i) nor agonist potency (EC_{50}) at CB1 were determined [194].

1.8.2.2   Anti-Inflammatory

As discussed in Section 1.6.2, pharmacologic activation of CB2 has been associated with anti-inflammatory effects via various CB2-mediated signaling cascades. Corroborating its pharmacologic activity as a CB2 agonist, β-caryophyllene has been found to mediate various anti-inflammatory effects *in vitro* and *in vivo*. Gertsch and colleagues demonstrated the ability of β-caryophyllene to reduce LPS-induced activation of MAPK (ERK1/2) in human peripheral monocytes and inhibit IL-1β and TNFα production in human whole blood samples at a 500 nM treatment concentration [194]. This treatment was not able, however, to inhibit IL-6 and IL-8

40

production in whole blood [194]. Fernandes and colleagues demonstrated that orally-administered β-caryophyllene reduced carrageenan-induced paw edema in rats at a 5 mg/kg dose [211]. At 50 mg/kg in this rat model, β-caryophyllene inhibited production of several carrageenan-induced pro-inflammatory mediators: TNFα, PGE_2, COX-2, and iNOS [211]. In mice, 50 mg/kg orally-administered β-caryophyllene reduced edema in response to hind paw injection of carrageenan, bradykinin, platelet activating factor and ovalbumin [211]. Furthermore, β-caryophyllene inhibited neutrophil migration and NF-kB activation in LPS-induced paw inflammation in rats [212]. In a study of CFA-induced arthritis in rats, orally administered β-caryophyllene at 100 and 300 mg/kg significantly reduced arthritis index scores and paw volume [213]. It was demonstrated to work through anti-inflammatory and anti-oxidant mechanisms which included decreasing serum NO and lipid peroxidation markers and increasing serum levels of the antioxidants glutathione and superoxide dismutase [213].

1.8.2.3   Anti-Cancer

In addition to the anti-inflammatory effects described above, β-caryophyllene has also been implicated in exerting pharmacologic effects relevant to cancer treatment and/or prevention. These effects include induction of glutathione-S-transferase activity in mice [190,214], prevention of mutagenic activity and DNA damage [214-216], prolonged survival of Ehrlich ascites tumor-bearing mice and enhancement of natural killer cell cytotoxicity [190], enhancement of paclitaxel-induced anti-proliferative effects in cancer cells by increasing intracellular drug accumulation [217] and direct cytotoxic effects in melanoma and renal adenocarcinoma cell lines equivalent to that of vinblastine [218].

1.8.2.4   Other

The pharmacologic effects of β-caryophyllene have also been studied in a diverse array of disease models *in vivo*. Specifically, the compound has been shown to exert beneficial effects in models of hepatic injury [219,220], alcoholic hepatitis [221], cisplatin-induced nephrotoxicity [222], ischemic stroke [223-225], seizure [226], colitis [219,227], Parkinson's disease [228,229], diabetes [230,231], Alzheimer's disease [232] Multiple Sclerosis [233,234], anxiety and depression [235], alcohol addiction [236], and endometriosis [237].

1.8.3   Evidence Suggesting Benefit for Pain Treatment

β-caryophyllene has been found to exert several effects which may be beneficial for the treatment of several types of pain including inflammatory, nociceptive and neuropathic forms. Although the mechanisms through which β-caryophyllene can confer analgesic effects may involve direct anti-inflammatory actions, as described above in Section 1.8.2.2, other analgesic properties have been reported which may or may not involve CB2-mediated effects. For example, Ghelardini and colleagues demonstrated local anesthetic effects of the compound, comparable to that of procaine [238]. In this investigation, β-caryophyllene significantly reduced the number of electrically-evoked hemidiaphragm contractions in rats in a dose-dependent manner, with contractions completely abolished at 4.9 µM [238]. Additionally, topical β-caryophyllene treatment greatly increased the number of stimuli required to induce eye closure in rabbits in a concentration-dependent pattern with a minimum effective concentration of 146.8 µM [238]. The mechanism of local anesthesia in this study was not investigated and therefore it is unknown whether the effects observed are CB2-mediated.

A study by Katsuyama and colleagues demonstrated that locally-administered β-caryophyllene significantly inhibited the behavioral pain response elicited by i.pl. injection of capsaicin in mice [239]. The effect was dose dependent and abolished by co-administration of the selective CB2 antagonist AM630, naloxone (a non-selective opioid receptor antagonist), the selective μ-opioid receptor antagonist β-funaltrexamine, and anti-sera against β-endorphin; however the analgesic effect of β-caryophyllene was not decreased by the selective CB1 antagonist AM251, nor by δ- or κ-opioid receptor selective antagonists [239]. An earlier study by the same research group demonstrated that locally-administered β-caryophyllene inhibited behavioral pain responses in the partial sciatic nerve ligation model of neuropathic pain in mice [240]. The effect was abolished by pre-treatment with a selective CB2 antagonist, AM630, but not by AM251, a selective CB1 antagonist [240]. Together, these findings suggest that β-caryophyllene works via peripheral CB2 receptors to evoke the release of β-endorphin to mediate analgesia [239]. This evidence is in parallel to that of Ibrahim and colleagues who demonstrated the ability of the selective CB2 agonist AM1241 to induce analgesia in rats via evoking release of β-endorphin in keratinocytes [145].

The effect of orally-administered β-caryophyllene has been studied in models of nociceptive, inflammatory and neuropathic pain *in vivo*. In the formalin test, a pain model characterized by both acute nociceptive and secondary inflammatory pain, both Klauke *et al*. and Paula-Feire *et al*. found that in mice, 5 mg/kg orally administered β-caryophyllene significantly reduced the secondary inflammatory pain response [241] while 10mg/kg also inhibited the acute nociceptive pain response [242]. Klauke and colleagues demonstrated that this effect was likely CB2-mediated as the analgesic effect was abolished in CB2 knockout mice and in mice pre-treated with a selective CB2 antagonist SR144528 [241]. Paula-Freire *et al*. also found 5 mg/kg

of orally administered β-caryophyllene significantly diminished thermal nociception, an effect which was abolished in the presence of the CB2-selective antagonist AM630 [242]. The effect of orally administered β-caryophyllene was also evaluated in models of neuropathic pain by both research groups. At 1 mg/kg, the compound greatly reduced mechanical hyperalgesia in the partial sciatic nerve ligation model [241]. The analgesic effect was absent in CB2 knockout mice [241]. In addition, the rise in expression of both microglia and astrocyte markers (Iba-1 and GFAP, respectively) in the spinal cord dorsal horn was significantly reduced by β-caryophyllene treatment [241]. In parallel to this finding, 5 mg/kg of the compound given orally significantly diminished both mechanical and thermal hyperalgesia in the chronic sciatic nerve constriction model in a CB2 antagonist-sensitive manner [242]. The analgesic effect of 5 mg/kg β-caryophyllene was approximately equal to 20 mg/kg pregabalin, the positive control treatment [194]. Furthermore, relative to the vehicle control, β-caryophyllene treatment was found to significantly reduce IL-1β production in the sciatic nerve [242]. In addition, Klauke and colleagues found an absence of CB1-mediated cannabinoid tetrad effects following both 1 and 10 mg/kg oral β-caryophyllene while Paula-Freire *et al*. found no change in motor coordination (rota-rod test) at each dosage of the compound tested, up to 80 mg/kg orally [242].

In the acidic saline model of chronic widespread musculoskeletal pain developed by Skuka and colleagues, 10 mg/kg orally administered β-caryophyllene was found to significantly reduce behavioral pain responses [243]. Also, 20 mg/kg of the compound reduced the number of Fos-positive neurons in the spinal cord dorsal horn, suggesting that β-caryophyllene may reduce neuronal firing frequency in this STT region [243].

Together, these findings suggest that β-caryophyllene is capable of acting as an analgesic in a variety of pain models, largely through CB2-mediated mechanisms.

1.9   Centrally-Expressed CB2 as a Pharmacologic Target for Chronic Pain Involving Neuro-Inflammation

In the CNS, CB2 is expressed by neurons, microglia and astrocytes [158,244-246]. Under pathological conditions, the expression of the CB2 receptor has been found to be markedly up-regulated. Clinically, abundant CB2 expression has been observed on microglia associated with brain and spinal cord lesions in patients with Huntington's disease [247], Alzheimer's disease [248-250], ALS and MS [251]. Increases in CB2 expression have also been observed in the brain following LPS administration [252], experimental autoimmune encephalitis [158] and middle cerebral artery occlusion [253] in animal models. CB2 expression has also been found to increase within the dorsal horn of the spinal cord in animal models of post-surgical hyperalgesia [254], arthritis [244], nerve injury [245] and spinal cord ligation [255]. For these reasons, CB2 has been considered a promising therapeutic target in conditions which involve neuro-inflammation of the CNS.

As discussed in Section 1.3, pathophysiologic changes in the spinal cord dorsal horn have been implicated in the development and maintenance of chronic pain through various mechanisms, collectively known as neuro-inflammation. These changes, largely driven by the cAMP-PKA pathway, involve increased proliferation and pro-inflammatory activity of astrocytes and microglia coupled with enhanced sensitivity and depolarization of STT neurons. Owing to its abundant expression in glia and neurons during inflammatory processes and its ability to signal via $G_{i/o}$ to downregulate the cAMP-PKA pathway, the CB2 receptor and its activation by ligands may therefore represent a pharmacologic pathway capable of mitigating CNS neuro-inflammation and counteracting the pathophysiologic processes at play in certain chronic pain

states. The following paragraphs will describe these pathophysiologic processes and discuss existing evidence which supports the role of the CB2 receptor in mitigating them.

Gliosis is a hallmark feature of neuro-inflammation and is characterized by enhanced proliferation and localization of glial cells within the dorsal horn region coupled with increased secretion of pro-inflammatory mediators. One of the critical intracellular drivers of glial cell proliferation and pro-inflammatory activity is nuclear transcription factor kappa-B (NF-κB) [256,257]. Via PKA phosphorylation of its p65 subunit, increased NF-κB activity in the spinal cord dorsal horn is associated with central pain sensitization via up-regulation of cytokine and pro-nociceptive peptide transcription [258]. Suppression of NF-κB has been shown to significantly reduce hyperalgesia and cytokine production in chronic pain models [259]. Previous studies have demonstrated the ability of JWH015, a selective CB2 agonist, to reduce microglial production of IL-1β, IL-6 and TNFα [260-262], which are transcriptional products promoted by NF-κB. In astrocytes, Sheng *et al*. demonstrated the ability of cannabinoid treatment to reduce production of TNFα and chemokines CCL2, CCL5, and CXCL 10 (also transcription products promoted by NF-κB) in a CB2 antagonist-sensitive manner [263]. Moreover, in a rat model of inflammatory arthritis, systemic administration of the CB2-selective agonist JWH133 prevented the model-induced increase in astrocyte immunofluorescence in the spinal cord, reduced the increase in dorsal horn neuron action potentials and prevented the increase in serum TNFα and IL-1β levels [244]. Furthermore, in a mouse model of diabetic neuropathy, CB2 agonist treatment given via intranasal or intraperitoneal administration attenuated the development of the neuropathic pain state and reduced the accumulation and activation of microglia within the spinal cord dorsal horn [264]. Additionally, the CB2-selective agonist JWH015, administered to rats via intrathecal injection, reduced tactile allodynia and

thermal hyperalgesia in a model of remifentanyl-induced post-operative hyperalgesia and significantly reduced both microglia and astrocyte immunofluorescence within the dorsal horn [254]. Dorsal horn levels of TNFα and IL-6 were also significantly reduced compared to vehicle-treated animals [254]. The effects were abolished upon pre-treatment with a CB2 antagonist.

Activation of the NMDA receptor in response to high glutamate levels in the dorsal horn is classically associated with central sensitization and increased pain perception [25]. We now know that phosphorylation of the NR2B subunit of NMDA by PKA is crucial in facilitating this process as it enhances NMDA receptor Ca^{2+} permeability [26]. In the post-operative hyperalgesia study described above, Sun and colleagues demonstrated that the reduction in behavioral pain response with JWH015 treatment was accompanied by significant reduction in immunofluorescence of phosphorylated NMDA NR2B in the dorsal horn of the spinal cord [254]. Also, in a model of bone cancer pain, Gu and colleagues demonstrated that JWH015 treatment significantly reduced NMDA NR2B mRNA in the spinal cord in addition to diminishing measures of behavioral hyperalgesia [265].

Cannabinoids may also reduce hyperalgesia associated with neuro-inflammation by de-sensitizing TRPV1 channels [112,266,267]. As discussed in Section 1.3, pro-inflammatory messengers can up-regulate the activity of kinases PKA and PKC. As discussed in Section 1.3 inflammation-induced activity of PKA and PKC can lead to phosphorylation of their intracellular targets. These include TRPV1 cation channels, which are expressed by both peripheral nociceptive C-fibers as well as STT neurons of the CNS [50,268]. The phosphorylation of TRPV1 by inflammation-induced post-translational modification is thought to induce receptor sensitization and play a critical role in mediating hyperalgesia in inflammatory pain models

[268,269]. The dual CB1 CB2 agonist WIN55,212-2 has been shown to de-phosphorylate

TRPV1 via calcineurin, reduce TRPV1 activation in response to capsaicin stimulation *in vitro*,

and reduce capsaicin-induced thermal hyperalgesia *in vivo* [112,266,267]. Therefore cannabinoid

ligands may also reduce hyperalgesia associated with neuro-inflammation by de-sensitizing

TRPV1 channels.

Stimulation of CB2 may therefore counteract important pro-nociceptive changes in the

dorsal horn, providing a potential means of mitigating chronic pain involving neuro-

inflammation.

1.10 Overview of the Dissertation

1.10.1 Research Aims

The general objective of this dissertation is to develop and evaluate selective small-molecule CB2R ligands for application in chronic pain involving reactive gliosis of the CNS. The main aims of the work described in this dissertation are:

Aim 1

To determine whether spino-thalamic tract gliosis is present in the acidic saline model of chronic widespread musculoskeletal pain and to characterize the relationship between behavioral pain response and glial cell expression.

Aim 2

To design, model and synthesize novel small molecules which act as CB2R-selective agonists and to evaluate their pharmacologic activity at human CB1 and CB2 cannabinoid receptors.

Aim 3

To evaluate the safety and potential therapeutic activity of the CB2R ligands by testing their effect on human cell proliferation, death, and mitochondrial respiration and by assessing their ability to exert anti-inflammatory and anti-proliferative effects in human glial cells.

The above aims are addressed in the following chapters:

Aim 1	Chapter 2: Involvement of Glia in a Research Model of Chronic Widespread Musculoskeletal Pain
Aim 2	Chapter 3: Development of Novel CB2-Selective Ligands and Assessment of Pharmacologic Activity at Cannabinoid Receptors
Aim 3	Chapter 4: Investigation of the Safety and Potential Therapeutic Activity of CB2R Ligands

Chapter 2: Involvement of Glia in a Research Model of Chronic Widespread Musculoskeletal Pain

2.1 Introduction

Glial cells of the CNS, including microglia and astrocytes, are known to exhibit functional and morphological changes in response to noxious stimuli and, through crosstalk with neurons, have been implicated in the development and maintenance of central sensitization and hyperalgesia [33,270]. These pathologic changes, known as gliosis, may include cell proliferation, migration, release of pro-inflammatory mediators (*i.e.*, cytokines, chemokines and neuropeptides) and enhancement of synaptic concentrations of excitatory amino acids (*i.e.*, aspartate and glutamate) [35,271]. Gliosis has been found to play a role in a variety of experimental pain models and clinical disease states and, as such, pharmacologic agents targeting activated glial cells have been investigated for potential therapeutic application both in research models [272-276] and clinical trials [277-283]. However, the contribution of gliosis to chronic widespread musculoskeletal pain disorders has not been clearly established.

Chronic widespread musculoskeletal pain is a cardinal feature of fibromyalgia syndrome (FMS), as discussed in Section 1.5. The underlying pathophysiology is thought to involve peripheral and central sensitization coupled with abnormalities in central nervous system (CNS) pain processing [72,73]. Clinical research has identified elevated cerebrospinal fluid (CSF) concentrations of glutamate, substance P, interleukin-8, brain-derived neurotrophic factor and nerve growth factor in FMS patients, suggesting that neuro-inflammatory processes may be at play within the CNS [85-88].

As outlined in Section 1.6, cannabinoids have an established clinical role in pain treatment and hold Health Canada-approved indications for treatment of neuropathic pain in MS as well as pain in advanced cancer [178]. Furthermore, the non-clinical evidence presented in section 1.9 points to analgesic activity of cannabinoid ligands specifically at the CB2 receptor in multiple pain research models, with an important mechanism being amelioration of glial cell-mediated neuro-inflammation within the CNS. We hypothesized that pharmacologic targeting of CB2 may potentially provide analgesic benefit for chronic widespread musculoskeletal pain, if indeed gliosis plays a role in the disease pathophysiology.

One of the few research models of chronic widespread musculoskeletal pain is the acidic saline (AS) model, developed by Sluka and colleagues [284]. In this model, two unilateral injections of acidic saline into the gastrocnemius muscle of male Sprague-Dawley rats, administered 5 days apart, produces bilateral hyperalgesia beginning 24 h following the second injection and persisting for 4-5 weeks [284] (See Figure 2.1). It is established that a portion of AS animals do not develop mechanical hyperalgesia and the rate of hyperalgesia response to the AS model in previous reports is widely varied [285-287].

Several factors involved in the development of hyperalgesia in the AS model have been previously identified. Firstly, excitatory amino acid transmission in the CNS has been found to play a critical role. Within the rostroventral medulla (RVM), enhancement of descending facilitative glutamatergic transmission has been shown to promote the development of hyperalgesia via NMDA glutamate receptors [288-290]. Within the lumbar spinal cord, increased concentrations of glutamate and aspartate have been detected in the dorsal horn 90 min following the second acidic saline injection [291,292]. The effect was abolished upon pre-treatment with $CoCl_2$, a non-specific calcium channel blocker, thereby demonstrating the involvement of

calcium-induced glutamate release immediately following the second injection [292]. At 1 week following the second injection, increases in glutamate, but not aspartate, were detected within the lumbar spinal cord dorsal horn [292] and blockade of both NMDA and non-NMDA glutamate receptors at this time point significantly diminished hyperalgesia responses [293]. As noted by the authors, astrocytes may contribute to the observed increases in dorsal horn glutamate by participation in calcium-induced vesicular release of excitatory amino acids, through glutamate-induced glutamate release upon AMPA and kainate glutamate receptor activation, and via pathological alterations in glutamate re-uptake capacity through the high affinity glutamate transporter GLT-1 [292].

The cAMP pathway in the lumbar spinal cord has also been examined and found to mediate the acute phase of hyperalgesia in the AS model, whereas modulation of the pathway had no effect on the pain response 1 week following the second injection [294]. Jasper *et al.* demonstrated that administration of the microglia inhibitor minocycline immediately prior to the first but not the second injection inhibited the development of hyperalgesia [286]. In contrast, Ledeboer *et al.* found no effect of various intrathecal treatments targeting glial cell activation (fluorocitrate, plasmid interleukin-10 DNA, and interleukin-1 receptor antagonist) administered 12-26 days following the second acidic saline injection [295]. The involvement of gliosis within this experimental model therefore remains inconclusive.
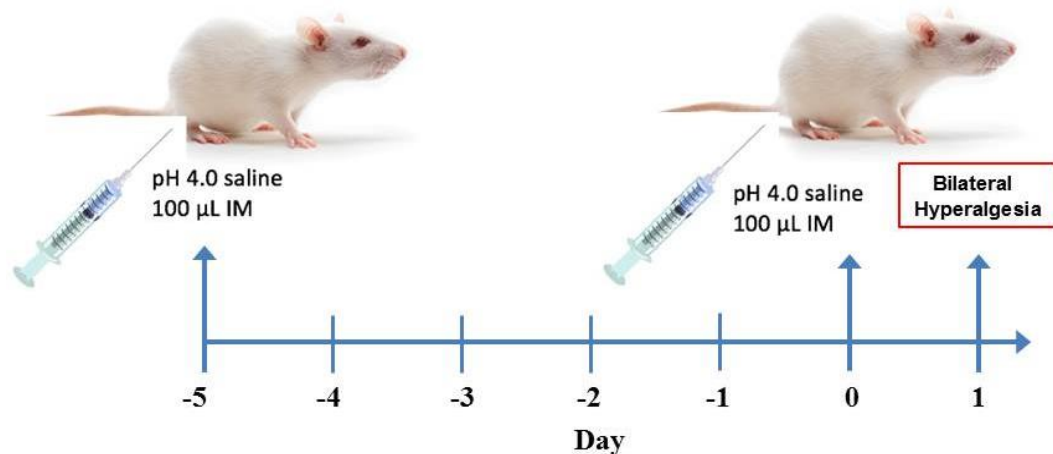
Figure 2.1. Schematic illustration of the acidic saline model of chronic widespread musculoskeletal pain. In the acidic saline model, two unilateral intramuscular (IM) injections of pH 4.0 saline are delivered to the gastrocnemius muscle, spaced apart by a five day interval. Twenty-four h following the second injection, animals are expected to develop bilateral hyperalgesia.

2.1.1   Specific Aims

The specific aim of the present investigation was to quantitatively compare the expression of Iba-1 and GFAP in the AS model with controls and to assess the relationship between Iba-1 and GFAP expression and mechanical hyperalgesia.

2.2   Materials and Methods

Monoclonal goat anti-GFAP, catalogue number sc-6171, was purchased from Santa Cruz Biotechnology, Dallas, USA. Monoclonal rabbit anti-Iba1 was purchased from Wako Chemicals, Richmond, VA, USA. Alexa Fluor® 647 donkey anti-rabbit IgG, catalogue number ab150075, and Alexa Fluor® 488 donkey anti-goat IgG, catalogue number ab150129 were purchased from Abcam, Cambridge, UK. Normal Donkey Serum, catalogue number D9663, was obtained from Millipore Sigma. Other reagents were obtained from different sources as indicated.

2.2.1 Animals and Experimental Grouping

The experimental protocol was approved by the University of British Columbia Animal Care Committee (protocol number A14-0334). Eight week-old male Sprague-Dawley rats (Charles River, Saint-Constant, QC, Canada) weighing 250 – 325 g at the time of the first acidic saline injection were used for the experiment. Animals were housed in an animal care facility having a 12 h dark (6:00 p.m. – 6:00 a.m.) and 12 h light cycle and allowed *ad libitum* access to standard rodent food and water. Prior to beginning the experiment, animals were acclimatized to the animal care facility for seven days. Pilot groups (n = 3) of AS model animals were sacrificed at each of four time points following induction of the AS model for CNS histology analysis. The control group consisted of n = 4 healthy animals sacrificed within the same time range as the AS model group. This study was repeated in a follow-up cohort of animals ("cohort 2") after cohort 1 data analysis revealed that only three animals in a single time point group showed a bilateral hyperalgesia response. In order to obtain histology data from hyperalgesia responder animals at different time points, nine cohort 2 animals were allocated to these time point groups, with n = 3 per group.

2.2.2 Acidic Saline Model

As per the previously published protocol, AS model animals received a 100 µL intramuscular injection of pH 4.0 saline into the right gastrocnemius muscle ("injection 1") and a second identical injection after a 5 day interval ("injection 2") [284]. To perform the injection, animals were placed in an anesthesia chamber and received a continuous flow of 4% isoflurane in oxygen (3 L/min). When the animal's righting reflex was lost and the respiratory rate reached approximately 68 breaths per min, the animal was removed from the chamber and given a

reduced level of isoflurane (2.5% in oxygen at 3 L/min) through a custom-made nose cone. The injection was administered via a 27 gauge needle and the animal was allowed to recover from anaesthesia in a recovery cage before being returned to its home cage. The injection was prepared by adjusting preservative-free 0.9% Sodium Chloride for Injection USP (No. 04888010, Hospira, Saint-Laurent, Canada) to pH 4.0 (+/- 0.1 pH) using 0.1N HCl with subsequent filtration through a 0.22 µm polyethersulfone membrane (Millipore, Burlington, USA).

2.2.3   Mechanical Hyperalgesia Assessment

Paw withdrawal threshold (PWT) measurements were conducted in a sensory testing room separate from the animal housing facility. Measurements were taken between 11:00 a.m. and 1:00 p.m. Prior to every PWT measurement, animals were allowed to acclimatize to the testing room in their home cage for 1 h, followed by a 10 min acclimatization period within the measurement stand (15 x 15 x 25 cm lucite cubicle with mesh flooring). Using an electronic von Frey meter with rigid tips (IITC Life Sciences, Woodland Hills, USA), gradually increasing force was applied to the plantar surface of the hindpaw until the animal exhibited a paw withdrawal response. The maximum force applied in grams was recorded. Three measurements were taken from each hindpaw with the mean of the three measurements reported as the paw withdrawal threshold. Prior to collecting experimental data, animals were taken through the measurement protocol on two separate occasions for training.

2.2.4   CNS Tissue Collection and Immunohistochemistry

Animals underwent transcardiac perfusion using approximately 100 mL heparinized 0.9% NaCl followed by approximately 100 mL 4% paraformaldehyde in phosphate-buffered

saline (PBS). The lumbar spinal cord was collected via laminectomy and the brain was dissected out and post-fixed for 3-5 h in 4% paraformaldehyde. After post-fixing, the tissues were transferred to 30% w/v sucrose aqueous solution and stored at 4°C until the time of sectioning. Thirty-five µm-thick free-floating vibratome sections were collected from the L5 and L6 spinal cord (transverse sections) and brain region passing through the thalamus (sagittal sections). Immunohistochemistry treatments took place in 24-well cell culture plates, all in PBS solutions. Sections underwent blocking in 5% v/v normal donkey serum (NDS) at room temperature for 1 h followed by overnight incubation in primary antibodies monoclonal goat anti-GFAP (1:1000) and monoclonal rabbit anti-Iba-1 (1:1000) prepared in 1% v/v NDS. Following three washes with 0.1% v/v Tween-20® in PBS (PBST), sections were incubated with Alexa Fluor® 647 donkey anti-rabbit IgG (1:1000) and Alexa Fluor® 488 donkey anti-goat IgG (1:1000) in 1% v/v NDS. Following three washes in TBST, tissue sections were mounted on poly-L-lysine coated microscope slides. Antibody concentration optimization and secondary antibody control tests were performed prior to the experiment.

2.2.5 Histology Imaging and Analysis

Histology images were acquired using an Aperio FL® digital pathology scanner (Leica Biosystems Buffalo Grove, IL, USA). All images were captured using identical, optimized settings. Spinal cord analysis was performed using Halo® software (Indica Labs, Albuquerque, NM, USA). For the analysis of microglia expression, the percent area of each tissue section having an immunofluorescence signal above a minimum threshold of 0.205 fluorescence units , was recorded. Astrocyte expression was analyzed using Halo® software to partition the superficial dorsal horn area into 2500 µm^2 square tiles within a manually selected sample region.

Thirty percent of the tiles were then randomly removed by the software in order to reduce selection bias of the sample region. Within the remaining 70% of tiles, the total number of cells was counted and then divided by the number of tiles, giving the average number of cells per 2500 μm^2 dorsal horn tissue. Five tissue sections each from the L5 and L6 lumbar spinal cord were analyzed per animal. Glial cell expression in the ventrobasal complex (VBC) of the thalamus was analyzed by counting the total number of cells within the VBC, bilaterally, within each tissue section. Five tissue sections were analyzed per animal.

2.2.6 Statistical Analysis

Statistical analyses were performed in R version 2.14.0 (R Foundation for Statistical Computing, Vienna, Austria). Paw withdrawal threshold data was analyzed by one-way ANOVA for differences between experimental days followed by Tukey's HSD test for post-hoc analysis. Following this analysis, an animal was considered to be a hyperalgesia responder if two criteria, similar to those published previously [286], were met, bilaterally. The first criterion required that the animal's PWT on day 1 and beyond was below 51.6 g. This value is the lower limit of the 95% confidence interval around the mean PWT in healthy control animals. The second criterion required that the animal's average PWT on day 1 and beyond decreased by at least 10 g, relative to its baseline PWT on day 0. For glial cell expression analysis, differences between the control and disease model groups were assessed using Welch's t-test for Iba-1 expression and the student's unpaired t-test for astrocyte cell count. Subgroup analysis was performed using one-way ANOVA followed by Dunnett's post-hoc test. For all statistical tests, p-values less than 0.05 were considered statistically significant.

2.3 Results

2.3.1 Incidence of Bilateral Hyperalgesia

Of the twenty-one animals subjected to the AS model protocol, a total of five were classified as bilateral hyperalgesia responders, according to our criteria, yielding a 23.8% response. Grouped according to the day of sacrifice following the second pH 4.0 injection, three animals in the Day 3 group and two animals in the Day 1 group met bilateral hyperalgesia responder criteria (Table 2.1). As shown in Figure 2.2, analysis of pooled data from bilateral hyperalgesia responder animals revealed significant reductions in both ipsilateral and contralateral hindpaw withdrawal thresholds, following the second pH 4.0 injection.

Table 2.1. Number of animals classified as bilateral hyperalgesia responders out of total animals per group.

Time Point Group	Cohort 1	Cohort 2
Day 1	0/3	2/3
Day 3	3/3	-
Day 7	0/3	0/3
Day 10	0/3	0/3

2.3.2 Increased Lumbar Spinal Cord Iba-1 and GFAP Expression, Dorsal Horn Localization and Morphological Changes

Overall, expression of both Iba-1 and GFAP appeared to be higher in AS animals relative to controls in both L5 and L6 spinal segments (Figure 2.3). Examination of immuno-staining revealed changes indicative of glial cell activation among AS animals, including increased cell

59

number and localization within the dorsal horn superficial laminae, larger and more densely

stained cell bodies, and increased number and length of cell processes.

A

Ipsilateral Hindpaw

B

Contralateral Hindpaw
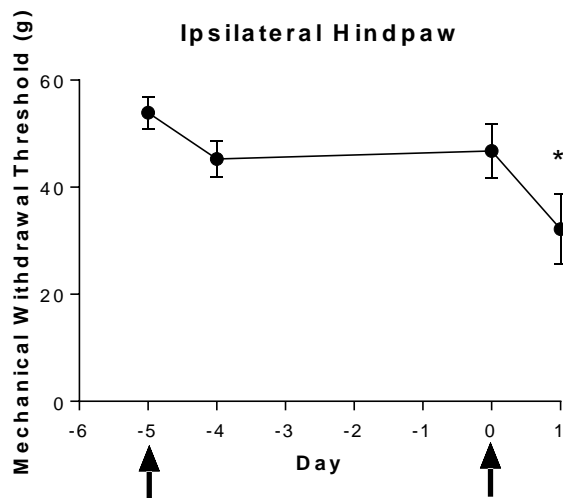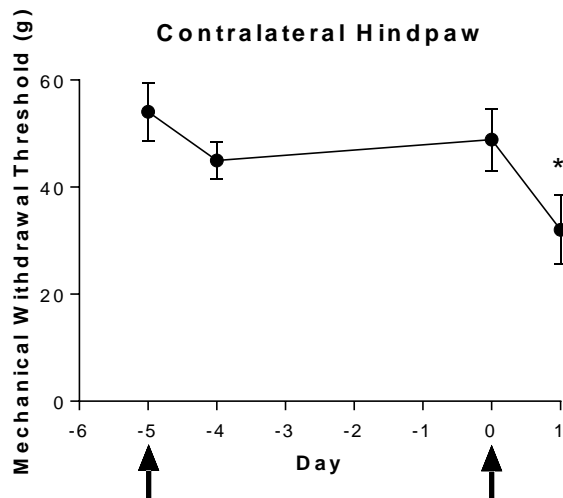
Figure 2.2. Pooled ipsilateral (A) and contralateral (B) hindpaw withdrawal thresholds from AS animals classified as bilateral hyperalgesia responders (n = 5).
Arrows indicate days of acidic saline injections. Mechanical withdrawal thresholds were assessed thirty min prior to injection on injection days. Data points represent mean ± SD. * = P < 0.05 vs. all other experimental days.
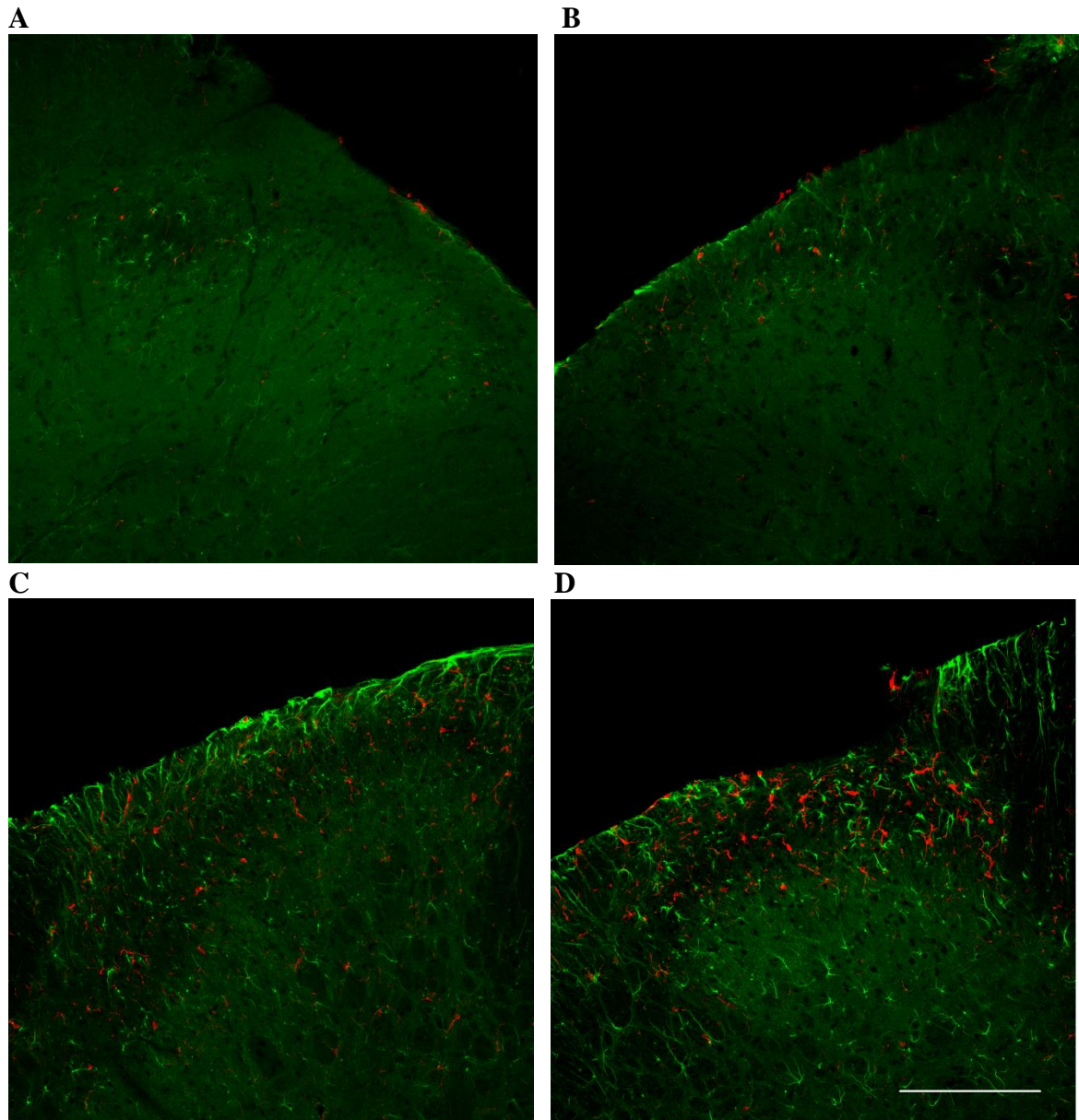
Figure 2.3. Representative confocal microscopy images of the dorsal horn region from control (A,B) and AS (C,D) animals showing Iba-1 (red) and GFAP (green) expression in L5 (A,C) and L6 (C,D) spinal segments. AS images shown were obtained from hyperalgesia responders in the Day 3 group. Scale bar = 200 µm.

2.3.3 Hyperalgesia-dependent Increase in Spinal Cord Iba-1 Expression

Quantitative analysis of spinal cord Iba-1 expression in cohort 1 animals revealed significant increases in AS animals relative to controls in both L5 and L6 spinal segments (Figure 2.4 A and D). Analysis of time point groups indicated that L5 Iba-1 expression was greatest and significantly different from controls on day 3, whereas the modest increases observed on days 1, 7 and 10 did not reach statistical significance (Figure 2.4 B). The significant increase in L5 Iba-1 expression detected on day 3 corresponds directly to bilateral hyperalgesia responder animals. Furthermore, analysis of L5 Iba-1 expression in AS animals grouped according to behavioural pain response revealed significant increases in hyperalgesia responders only (Figure 2.4 C). Comparatively, L6 Iba-1 expression was greatest and significantly different than controls on day 7 only, with non-significant increases observed on days 1, 3 and 10 (Figure 2.4 E). Although increases in L6 Iba-1 expression were observed in both responder and non-responder subgroups versus controls, neither increase reached statistical significance (Figure 2.4 F).
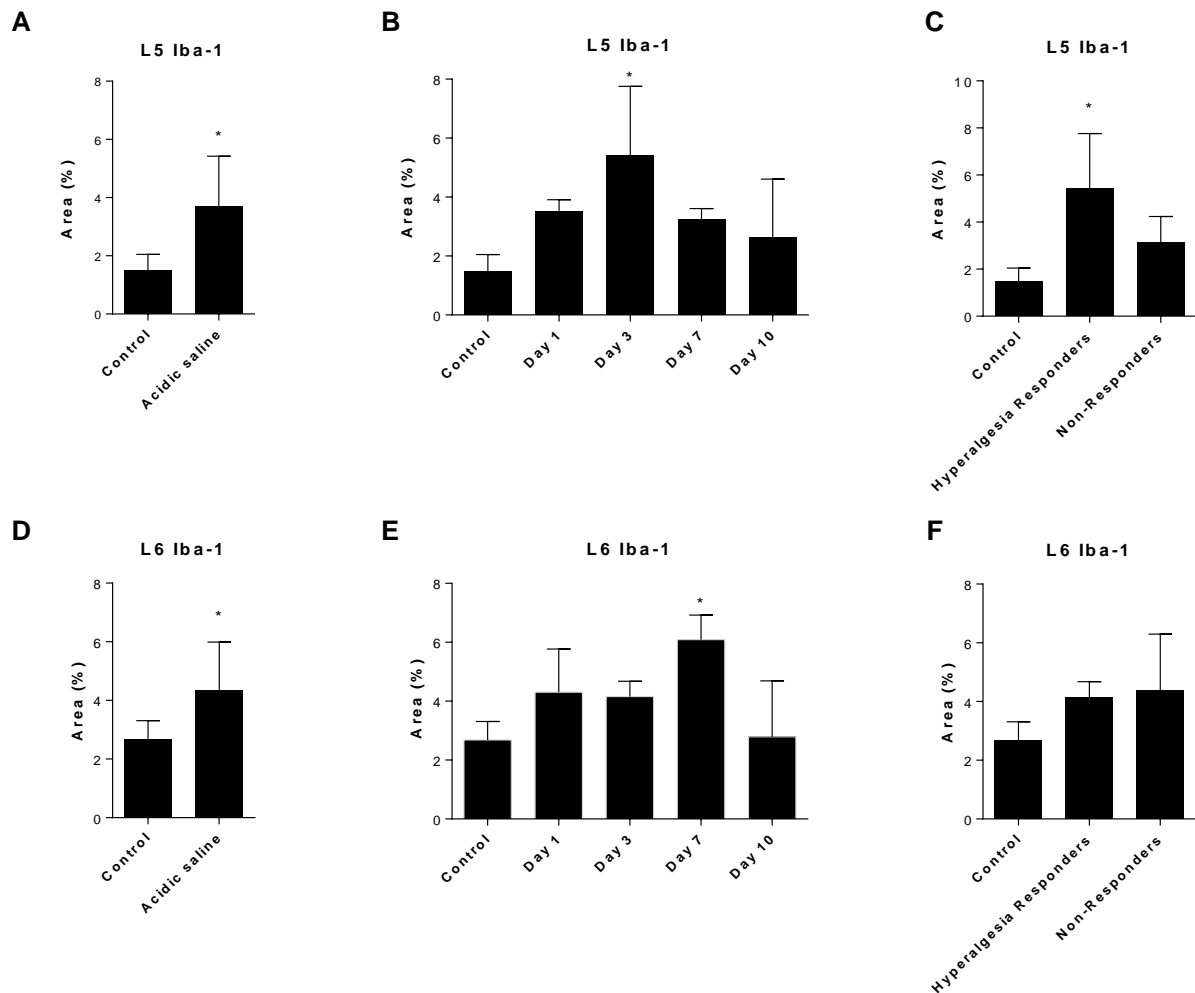
Figure 2.4. Percent tissue area positive for Iba-1 immunoreactivity in L5 (A – C) and L6 (D – F) spinal cord segments.
Iba-1area in control (n = 4) vs. cohort 1 AS animals (n = 12) (A,D). Iba-1 area in control (n = 4) vs. AS animals in time point groups (n = 3 per group) (B,E). Iba-1 area in control vs. AS hyperalgesia responders (n = 3) and non-responders (n = 9) (C,F). Data points represent mean ± SD. * = P < 0.05.

2.3.4 Increased GFAP Expression in Spinal Cord is Independent of Hyperalgesia Response

Significant increases in spinal cord GFAP expression were detected in AS animals, relative to controls, in both L5 and L6 segments (Figure 2.5 A and D). Significantly increased GFAP expression was apparent in both L5 and L6 as early as day 1 following the final pH 4.0 injection and subsequently in all other time point groups (Figure 2.5 B and E). GFAP expression reached the highest statistical significance on days 3 and 7 in both L5 and L6 segments. When analyzed as subgroups, both hyperalgesia responders and non-responder animals showed significantly higher astrocyte expression in the L5 and L6 spinal cord versus controls (Figure 2.5 C and F). Therefore, increases in GFAP expression occurred independently of hyperalgesia response in AS animals.
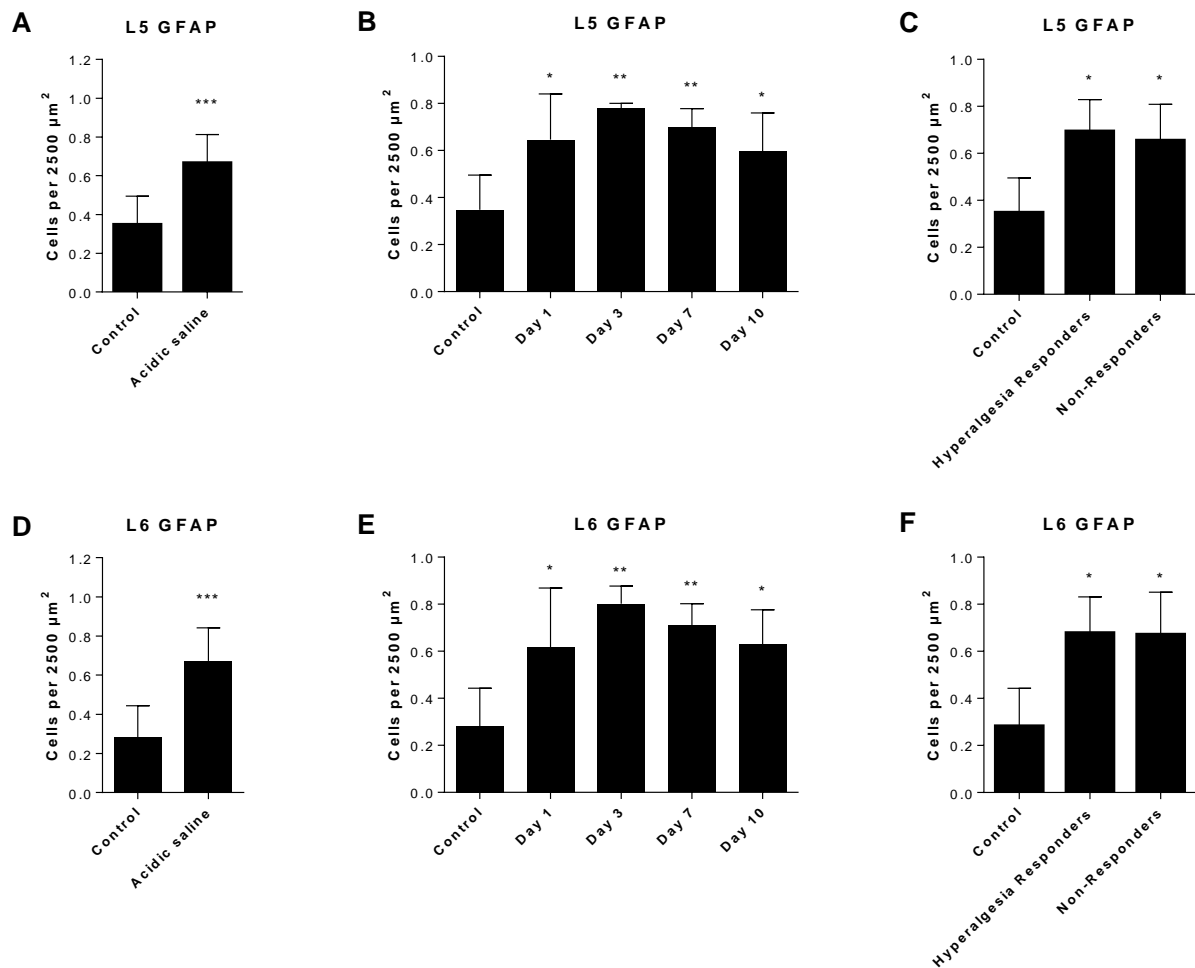
Figure 2.5. Mean dorsal horn astrocyte cell count from L5 (A – C) and L6 (D – F) spinal cord segments.
Cell count in control (n = 4) vs. all AS animals (n = 21) (A,D). Cell count in control (n = 4) vs. AS animals in time point groups (n = 3 – 6 per group) (B,E). Cell count in control versus AS hyperalgesia responders (n = 5) and non-responders (n = 16) (C,F). Data points represent mean ± SD. * = P < 0.05, ** = P < 0.01, *** = P < 0.001.

2.3.5 The Expression of Iba-1 and GFAP is Not Changed in the Thalamus Ventrobasal Complex
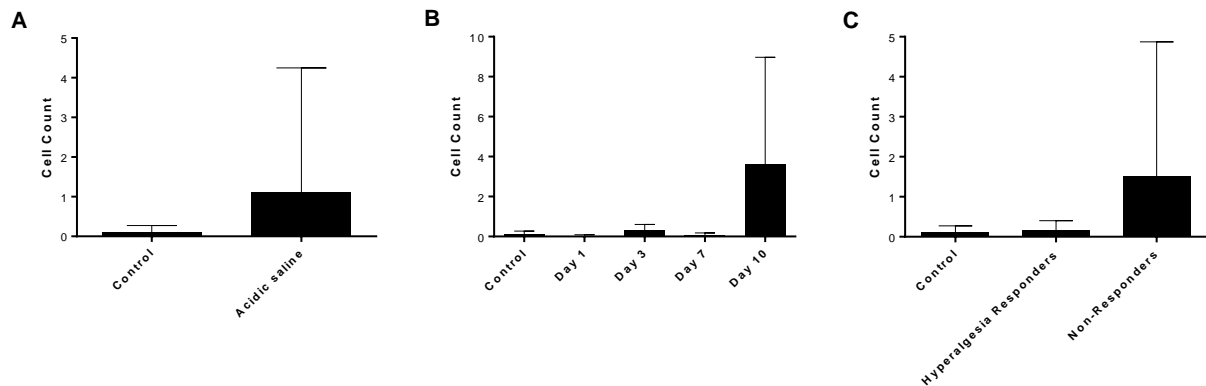
Figure 2.6. Mean VBC microglia cell count in control (n = 4) vs. all AS animals (n = 21) (A), in control (n = 4) vs. AS animals in time point groups (n = 3 – 6 per group) (B), in control versus AS hyperalgesia responders (n = 5) and non-responders (n = 16) (C).
Data points represent mean ± SD.

No differences in VBC expression of Iba-1 and GFAP were detected in AS animals compared to controls. Notably, two out of six animals in the Day 10 group were found to have a markedly increased microglia cell count, contributing to considerable variation in AS group overall (Figure 2.6 A and B). Iba-1 expression was otherwise generally low and appeared similar to that of controls. When assessed according to behavioural pain response, neither hyperalgesia responders nor non-responders had significantly different VBC expression of Iba-1 versus controls (Figure 2.6 C).

2.4 Discussion

Determining whether gliosis plays a role in chronic widespread musculoskeletal pain disorders is crucial in order to further our understanding of the underlying pathophysiology. In the present study we assessed the response of spinothalamic glial cells to repeated insults of low pH to skeletal muscle tissue using the acidic saline model of chronic widespread musculoskeletal pain and examined the relationship between the expression of glial cell markers and the behavioral pain response observed. Glial cells can have both pro- and anti-inflammatory functions, depending upon the nature of the stimulus prompting their activation. It is generally recognized that glial cell activation which occurs in response to nociceptive input to the CNS (*ex.*, ongoing release of SP, CGRP and glutamate) is pro-inflammatory. Although the activation pattern of glial cells can vary depending upon the specific injury or disease model, the presence of pro-inflammatory gliosis is usually characterized by up-regulation of glia-specific activation markers and distinct changes in morphological appearance [296]. Iba-1 and GFAP are well-validated markers of microglia and astrocyte activation, respectively [297-300]. We found evidence of increased expression of both Iba-1 and GFAP in the lumbar spinal cord dorsal horn and a correlation between L5 Iba-1 expression and the development of bilateral hyperalgesia. In agreement with published literature in which up-regulation of glial cell markers has been found within the lumbar spinal cord in other experimental pain models [244,254,301], the increased glial marker expression we observed appeared most apparent within the superficial laminae of the dorsal horn. Furthermore, morphological changes were observed including larger and more densely stained glial cell bodies as well as increased length and number of cell processes. Our findings therefore suggest that gliosis develops in the majority of rats within the lumbar enlargement (L5 and L6 segments) of the spinal cord in the acidic saline model of chronic

widespread musculoskeletal pain. To our knowledge, this is the first report describing that repeated insult of reduced pH to peripheral skeletal muscle tissue is sufficient to provoke a dorsal horn glial cell response.

The control of synaptic transmission in the CNS is thought to be tripartite, involving pre- and post-synaptic nerve terminals as well as glial cells [302]. The exaggerated excitatory amino acid transmission in response to the second pH 4.0 injection, as previously reported, is critically important to the development of hyperalgesia in the AS model as evidenced by the rise in lumbar dorsal horn glutamate and aspartate concentrations following the second, but not the first, acid injection as well as the ability of NMDA receptor blockade during the second, but not the first, injection to prevent the development of hyperalgesia [285,292,293]. Glutamatergic transmission is also involved in the maintenance phase of hyperalgesia in this model. Increased lumbar dorsal horn glutamate concentrations have been found at 1 week, with mechanical hyperalgesia diminished at this time point upon NMDA and non-NMDA ionotropic glutamate receptor blockade [292,293]. In parallel to these findings, our data demonstrate the presence of astrocyte activation in the lumbar spinal cord dorsal horn 24 h following the second acidic saline injection and thereafter on days 3, 7 and 10. These findings support the hypothesis of astrocyte involvement in the dysregulation of excitatory amino acid transmission which develops in this model. There may be several mechanisms through which this takes place.

Astrocytes in the dorsal horn surround glutamatergic synapses and normally maintain tight control of extracellular glutamate concentrations through glutamate re-uptake by Na^+-dependent low- and high-affinity glutamate transporters GLAST and GLT-1, respectively, thereby regulating the ability of glutamate to excite spinothalamic neurons. Handling of glutamate by astrocytes is, however, sensitive to a variety of extracellular signals, including

mediators secreted by microglia and neurons. In response to pro-inflammatory stimuli, glutamate transporters along with glutamate uptake capacity has been shown to decrease in astrocytes *in vitro* [303-305], while the expression and functional capacity of GLT-1 has been found to decrease significantly in chronic pain *in vivo* [276]. Furthermore, excessive spinal cord glutamate accumulation along with pain-related behaviours that are dependent upon ionotropic glutamate receptor activation have been invoked spontaneously *in vivo* upon blockade of high affinity glutamate transporters in the spinal cord [306]. Therefore, the ability of the second injection in the AS model to provoke rises in dorsal horn excitatory amino acid concentrations along with bilateral hyperalgesia could reflect a decrease in astrocyte-mediated glutamate clearance. Future studies could test this hypothesis by examining the cellular localization and magnitude of expression of glutamate transporters at different time points over the course of this model, specifically assessing differences before and after each acid injection.

Impaired glutamate uptake by astrocytes is not the only possible explanation for the exaggerated release of excitatory amino acids observed following the second injection. As previously demonstrated, cobalt chloride, a calcium channel antagonist capable of blocking synaptic voltage-gated calcium channels as well as NMDA and non-NMDA glutamate receptors, prevented the rise in dorsal horn excitatory amino acids following the second injection [292]. Indeed, the release of glutamate has been shown to occur through calcium-dependent vesicular release from both neurons and astrocytes [307-309]. Therefore, up-regulation of GFAP may point to an enhanced capacity for calcium-induced glutamate release from astrocytes in the lumbar dorsal horn following the second injection. Additionally, astrocytes express NMDA, AMPA and kainate ionotropic glutamate receptors as well as metabotropic glutamate receptors (*i.e.*, mGluR) [310,311]. Activation of these receptors has been shown to trigger further

glutamate release by astrocytes, with a rise in intracellular calcium found to be the common underlying intracellular mechanism [308,312-314]. Indeed, increased intracellular calcium concentrations in stimulated astrocytes have been directly associated with NMDA-mediated excitatory transmission in neurons [314-316]. Therefore, in cases of increased extracellular glutamate concentrations in the dorsal horn, for example, due to pro-inflammatory dysregulation of glutamate clearance or metabolism, excitatory synaptic transmission can be amplified further through glutamate-induced glutamate release from glia via AMPA, kainite, and/or mGlu receptor activation. The role of astrocytes in mediating excitatory synaptic communication is thus of critical importance. Taken together with previous findings, our data support the hypothesis that glial cells, in particular astrocytes, are involved in the pro-nociceptive changes in excitatory transmission that develop in the lumbar spinal cord in the AS model.

Enhancement of pain-like behaviours has been directly correlated with glial cell activation in previous studies [244,254,301,317,318]. Consistent with these observations, we found increased lumbar spinal cord expression of Iba-1 in bilateral hyperalgesia responder animals whereas no difference in Iba-1 expression was detected in non-responder animals versus controls. In contrast, however, increased lumbar GFAP expression was observed in both hyperalgesia responders and non-responders compared to healthy controls. Therefore, spinal cord glial cell activation is likely not the only pathophysiologic change required for a bilateral hyperalgesia response to develop in this animal model. Supporting this notion, previous studies have indicated that the second acidic saline injection in the AS model produces changes in the RVM (*i.e.*, increased release of excitatory neurotransmitters and reduced release of inhibitory neurotransmitters), and, that blockade of NMDA receptors within either the RVM or the nucleus reticularis gigantocellularis (NGC) is sufficient to abolish mechanical hyperalgesia [289,291].

Therefore, interplay between ascending nociceptive input from the spinal cord dorsal horn and descending excitatory facilitation from the RVM and NGC likely mediates the development of bilateral hyperalgesia in this model of musculoskeletal pain. Based on the results described here, it is expected that non-responder animals did not develop the same RVM changes in response to acidic saline injections, and therefore, despite the increased spinal cord GFAP expression detected, the absence of RVM hyper-excitation may have precluded the development of mechanical hyperalgesia in the non-responder subgroup.

Since the thalamus ventrobasal complex (VBC) is immediately afferent to the spinal cord dorsal horn along the ascending spinothalamic tract, examination of this region was included in the present investigation. Although no evidence of increased Iba-1 or GFAP expression in the VBC was found, the possibility of glial cell involvement here cannot be entirely discounted. Microglia activity within the VBC could potentially develop during a later time course within this model, given that a non-significant increase in Iba-1 expression was observed at day 10, the final time point of our study. Further data from an increased number of hyperalgesia responder animals captured from a broader range of time points is necessary to draw conclusions around thalamic gliosis in this animal model.

Despite the variable rates of bilateral hyperalgesia response reported in the AS model [285,286], the rate of response observed in our study was lower than expected. Interestingly, animals which developed hyperalgesia in our study were restricted to two of the four time point groups. In consideration of this observation, we note that the experimental protocol for each time point group was initiated on a different calendar day (*i.e.*, the experimental schedules for each group were stratified over the calendar). Therefore, environmental factors and/or stressors experienced (*ex.* cage cleaning by animal care staff on the day of an injection) could have

differed between groups. It has been previously demonstrated that environmental stress from confined restraint increases serum cortisol levels and increases pain-like behavioral responses (*i.e.*, reduced von Frey paw withdrawal thresholds), and, that sound stress enhances bradykinin-induced hyperalgesia in rats [301,319]. Therefore, variation in environmental factors across experimental groups may be responsible for the between-group differences in hyperalgesia response observed in our study.

Taken together with previous studies in this research model along with clinical evidence of elevated inflammatory CSF markers [85,88], our experimental findings support the need for further investigation into the role of gliosis in chronic widespread musculoskeletal pain. The present pilot study involved only immunohistological detection of glial cell activation. Further investigations in this model are therefore recommended to test for additional indicators of gliosis and CNS neuro-inflammation. These may include measurement of Iba-1 and GFAP mRNA levels, quantification of NF-κB expression and phosphorylation to the active state (p-NF-κB), expression and phosphorylation of the NMDA receptor subunit NR2B, as well as concentrations of cytokines such as IL-1β, IL-6 and TNFα. This area of investigation may also be further advanced through the use of imaging modalities to assess the location and magnitude of glial cell activation both in research models and human subjects. Such methods may include positron emission tomography (PET) to image tracers such as ^{18}F-PBR111 or ^{11}C-PBR28 which bind to translocator protein (TPSO) expressed by activated glial cells. For example, PET imaging studies with ^{11}C-PBR28 have detected increased thalamic glial cell activity in chronic low back pain as well as T11-T12 spinal cord neuro-inflammation in chronic lumbar radiculopathy [320,321]. Alternatively, the use of non-radioactive fluorinated TPSO ligands may allow for glial cell imaging through the use of ^{19}F-MRI [322,323]. Candidate ^{19}F-MRI tracers could include the high

affinity TPSO ligand FEDAA1106 or the fluorinated benzodiazepines SAS 643 and SAS 646 [324,325].

In conclusion, the evidence of glial cell involvement presented here supports the need for further investigation into the contribution of gliosis to the pathophysiology underlying chronic widespread musculoskeletal pain disorders. Additional investigations both in research models and human subjects are recommended to further advance the research findings of this pilot study.

Chapter 3: Development of Novel CB2-Selective Ligands and Assessment of Pharmacologic Activity at Cannabinoid Receptors

3.1 Introduction

Since the initial cloning of the CB1 receptor in 1991 by Matsuda et al. [326], followed by identification of the human CB2 receptor peptide sequence (Figure 3.1) in 1993 by Munro and colleagues [327], considerable research has enhanced our understanding of cannabinoid receptor functions and ligand binding properties. Like other members of the GPCR superfamily, both CB1 and CB2 cannabinoid receptors consist of a continuous peptide sequence comprised of seven trans-membrane peptide helices. The CB1 and CB2 receptors share 44% overall amino acid identity, which rises to 68% in transmembrane domains [327].
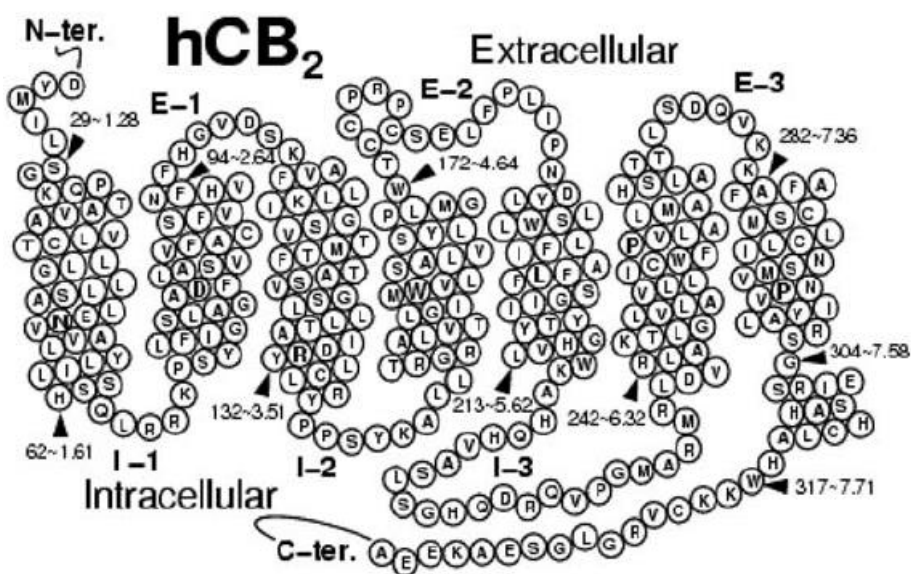
Figure 3.1. Peptide sequence and 2D receptor domain representation of the human cannabinoid receptor 2 (hCB2).
Beginning at the N-terminus (N-ter.) in the extracellular space, the hCB2 peptide chain forms seven trans-membrane helices linked by three intracellular (I-1 to I-3) and three extracellular (E-1 to E-3) loops. The C-terminus (C-ter.) is located within the intracellular space in close proximity to the intracellular loops. Amino acids are labelled according to IUPAC one-letter symbols [328] and are numbered according to their position in the peptide sequence, starting at the N-terminus. Reproduced from [327] permission pending.

As shown in the 'top-down' schematic view of the seven transmembrane GPCR helices (Figure 3.2), ligand binding can confer a conformational change in the receptor, resulting in specific interactions with G-protein subunits at the intracellular C-terminus. Ligands are considered to have agonist activity if the receptor binding interaction induces a conformational change such that exchange of GDP for GTP occurs at the intracellular $G\alpha$ subunit, resulting in release and down-stream activity of the $G\beta/\gamma$ subunits.
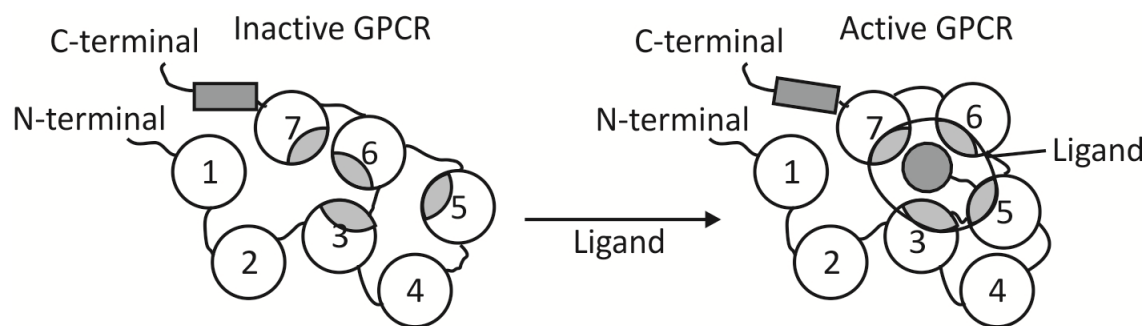
Figure 3.2. 'Top-down' schematic representation of the seven transmembrane domains (1-7) of an inactive GPCR (left) and active GPCR due to ligand binding (right).
Ligand binding induces a shift in the transmembrane domain conformation, thereby leading to receptor activation. The conformational shift induced by an agonist results in exchange of GDP for GTP at the $G\alpha$ subunit associated with the C-terminal (not shown).

Cannabinoid receptors generally couple to $G_{i/o}$ in a pertussis toxin-sensitive manner, although CB1 has been shown to couple to G_s under certain conditions [329-332]. Based on $G_{i/o}$ coupling, inhibition of adenylyl cyclase and reductions in intracellular cAMP concentration generally result in CB2-expressing cells upon agonist treatment. cAMP is a second-messenger formed by catalytic conversion of ATP by adenylyl cyclase which regulates the activity of several important intracellular signaling cascades and therefore plays a key role in GPCR-related signal transduction. Depending upon many factors including the particular cell type, degree of

cell surface CB2 expression and receptor coupling interactions, CB2 agonists have the ability to influence a variety of intracellular processes via the second messenger system. These may include cell proliferation, survival, and transcription of pro-inflammatory mediators. Specific effects of CB2 agonists on intracellular signaling cascades will be addressed in Chapter 4.

Cannabinoid receptors can be activated by plant-derived, synthetic, and endogenous cannabinoid ligands. These ligands are classified according to chemical structure into five diverse categories: the classical cannabinoids (Δ^9-THC, Δ^8-THC-dimethylheptyl (HU210)), non-classical cannabinoids (CP-55,940), indoles (WIN 55,212), eicosanoids/endogenous ligands (anandamide, 2-AG), and antagonist/inverse agonists (SR141716A, SR145528) [333-339]. Aside from the antagonist/inverse agonists, these compounds, depicted in Figure 3.3, are all dual agonists of both CB1 and CB2 cannabinoid receptors. Structure-activity relationship studies using these compounds have been fundamental to our understanding of the cannabinoid receptor active site and have also elucidated key differences between CB1 and CB2 receptor-ligand interactions.

Based on the early studies involving Δ^9-THC, its analogues, and non-classical cannabinoid compounds, it was originally thought that three structural properties were necessary in order for a ligand to bind within the cannabinoid receptor active site and act as an agonist: (1) the presence of a free phenolic hydroxyl group, (2) a suitable substituent at C9, preferably a hydroxyl group, and (3) a hydrophobic side chain [340-342]. This lead to the development of the non-classical, highly potent dual CB1-CB2 agonist CP-55,940 (Figure 3.3 C) [342].

A
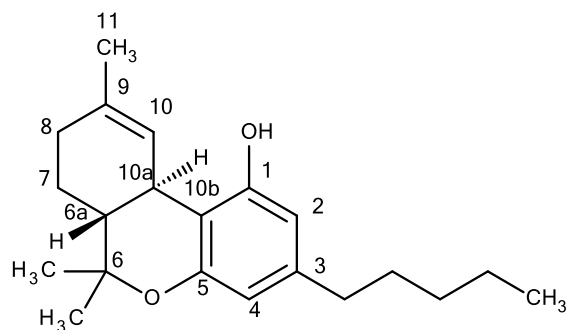
B
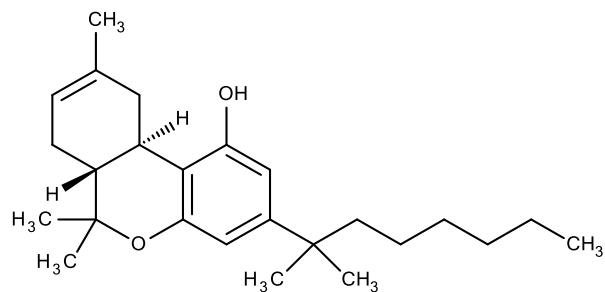
C
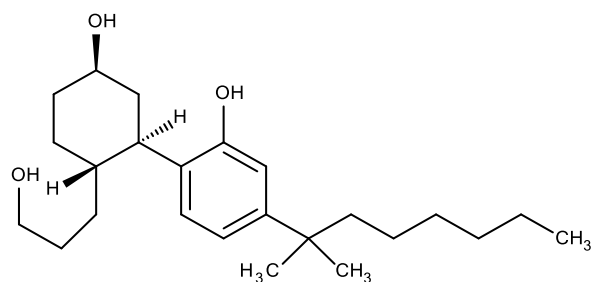
D
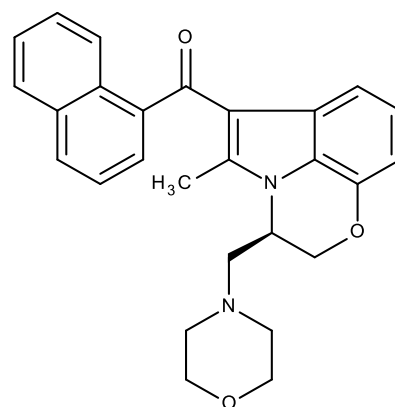
E
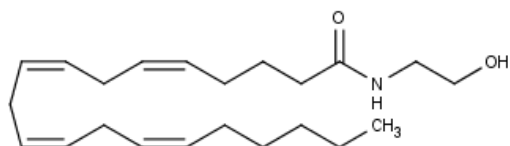
F
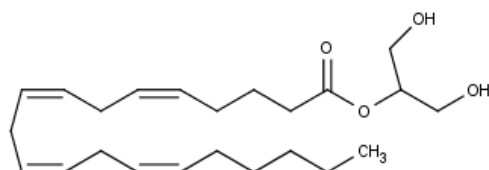
Figure 3.3. Dual CB1-CB2 receptor agonists Δ⁹-THC (A), Δ⁸-THC-dimethylheptyl (HU-210; B), CP-55,940 (C), WIN-55,212 (D), anandamide (E), and 2-arachadonoylglycerol (F).
Dibenzopyran numbering of the Δ⁹-THC cyclic backbone is shown in (A) for reference.

In CP-55,940, the phenolic hydroxyl at C1 as well as the C9 hydroxyl are thought to interact with a hydrophilic region of the cannabinoid receptor binding pocket. Specifically, H-bonding to a lysine residue in TMH 3, conserved in both CB1 and CB2 receptor subtypes, is thought to be a key interaction needed for ligand binding. Additionally, the hydrophobic side chain at C3 is thought to interact with a hydrophobic pocket formed by the hydrophobic cluster of amino acid residues in TMH 6 and 7. Further studies demonstrated that the phenolic hydroxyl group at C1 was not necessary for cannabinoid agonist activity, as long as another oxygen atom in the ligand is available for H-bonding to the TMH3 lysine residue [343]. Mutational studies then demonstrated that, although TMH3 lysine (K192) is critically important and necessary for classical and non-classical cannabinoid agonist binding to CB1, the agonist activity at CB2 could be maintained in the absence of the corresponding lysine residue, K109 [344]. Computational studies of the mutant CB2 receptor with alanine substituted in place of K109 suggested that a hydrogen bonding cluster comprised of serine (S112), threonine (T116) and asparagine (N295) interacted with the ligand hydroxyl groups, thereby compensating for the absence of K109 [344]. The discovery of a new class of cannabinoid agonists, aminoalkylindoles, occurred accidentally by the Sterling Research Group in 1991 during development of nonsteroidal anti-inflammatory drugs [345,346]. Previous studies with the aminoalkylindole WIN-55,212 have contributed significantly to our understanding of ligand interactions with cannabinoid receptors including pharmacophore properties conferring CB2-selectivity. These studies revealed that although the mode of binding of WIN-55,212 to cannabinoid receptors was distinct from classical and non-classical cannabinoids, its agonist activity was functionally equivalent to these compounds both *in vitro* and *in vivo*. Interestingly, binding of WIN-55,212 to TMH3 lysine was shown to be unnecessary for the receptor-ligand binding interaction, however, its binding within the active

site of both CB1 and CB2 receptors was sufficient to displace the binding of [³H]-CP-55,940, suggesting that it binds cannabinoid receptors through interactions distinct from classical and non-classical ligands, yet it binds within the same active site region [346-348].

Subsequently, WIN-55,212 was found to have modest (5 to 10 fold) selectivity for the CB2 receptor [349]. A study by Song and colleagues demonstrated that aromatic stacking (π-π) interactions between WIN-55,212 and TMH5 phenylalanine (F197) in the CB2 receptor are likely to be stronger than those occurring between the ligand and the equivalent residue in CB1 (V282), therefore the ability of a ligand to engage in π-π stacking interactions with F197 was found to be an important property conferring CB2-selectivity [350]. Furthermore, H-bonding interactions with S112 in TMH3 of CB2 were also shown to confer CB2-selectivity to aminoalkylindoles [351].

Further molecular modelling studies of CB2 receptor-ligand interactions revealed that several aromatic residues, exclusive to CB2, are capable of interacting with ligands via π-π stacking, thereby underscoring the importance of aromaticity in conferring ligand selectivity for CB2. Specifically, phenylalanine residues F87, F94, F97, F117 as well as tryptophan residues W258 and W194 have been found to engage in ligand binding interactions within the CB2 receptor active site [352-354]. Another key aromatic residue found to participate in receptor-ligand binding interactions is histidine 95 (H95) [355]. Furthermore, asparagine 188 (N188) and serine 285 (S285) were identified as additional hydrophilic residues capable of engaging in H-bond ligand interactions within the CB2 binding pocket [352,353,355]. Additionally, proline residues P178 and P187 have been found to line the CB2 binding pocket and engage in hydrophobic interactions with ligands [353].

Selectively targeting the CB2 receptor for potential therapeutic application in disease states including chronic pain is not a novel concept. Indeed, the CB2 receptor has been identified as a potential therapeutic target for a plethora of medical conditions, in addition to pain, some of which include autoimmune diseases, ischemia-reperfusion injury, endometriosis, and cancer [356,357]. Since the discovery of the aminoalylindoles' modest CB2-selectivity, considerable efforts, both in academia and industry, have resulted in the development of many novel small molecule ligands with selective CB2 agonist properties. Recently, Nettekoven and colleagues identified a hit cluster of compounds containing an adamantyl moiety upon high-throughput screening for compounds with selective CB2 agonist properties [358]. As noted by the authors, adamantane is a well-known chemical substituent present in approved drugs such as amantadine and vildagliptin, agents which are used clinically for peripheral and CNS-related pathologies. Further optimization of the initial hit cluster yielded compounds consisting of an adamantyl group connected via amide linkage to a bi-cyclic structure, shown in Figure 3.4. The addition of a hydroxyl group to the adamantane structure (Figure 3.4 A) was found to improve compound solubility dramatically, however, reductions in CB2 agonist potency were observed. Only one compound having the amide linkage switched, such that the nitrogen component is linked to the adamantyl scaffold, was evaluated (Figure 3.4 B). Although the compound was found to have lesser solubility, its agonist potency at CB2 was high, with low agonist activity at CB1 [358].
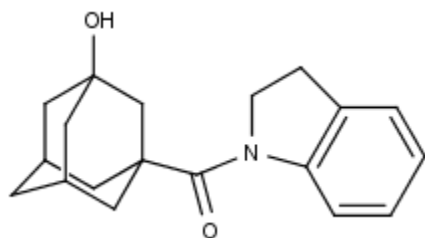
A   **B**
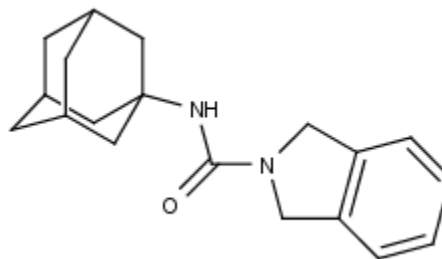
Figure 3.4. Adamantyl CB2-selective agonist compounds developed by Nettekoven and colleagues.
Agonist potencies (EC$_{50}$) at CB2, determined by cAMP assay in transfected CHO cells, were 0.49 µM (A)
and 0.022 µM (B). cAMP EC$_{50}$ at CB1 was > 10 µM for both compounds. LogP values reported were
2.77 and 4.26 for (A) and (B), respectively [358] .

3.1.1   Specific Aims

To design, model and synthesize novel small molecules which act as CB2R-selective

agonists and to evaluate their pharmacologic activity at human CB1 and CB2 cannabinoid

receptors.

3.2   Design and Modeling of CB2 Receptor Ligands

3.2.1   Development of a Mini-Library of Potential CB2 Agonists

Based on the previous work by Nettekoven and colleagues, compounds having an

adamantyl group linked via amide bond to a bi-cyclic structure could reasonably be expected to

have some degree of CB2 agonist activity [358]. Although specific receptor binding interactions

were not reported by the authors, it can be hypothesized that the adamantyl group of such

structures interacts with the hydrophobic pocket of the CB2 binding cavity, analogous to the C3

hydrophobic tail present on classical cannabinoids. The amide oxygen atom is likely binding

within the CB2 active site via polar H-bond interactions with K109, and possibly with other
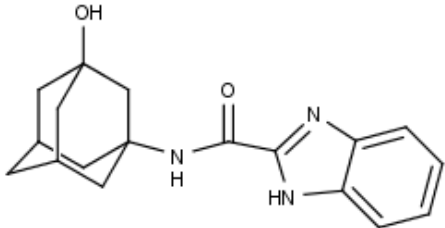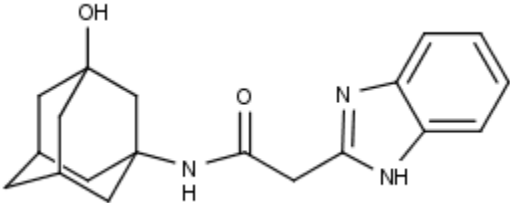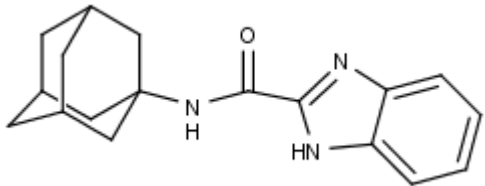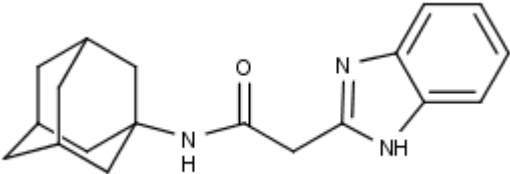
members of the hydrogen bonding cluster exclusive to CB2 (*i.e.,* S112) or other hydrophilic

residues previously identified to mediate CB2-ligand binding. The presence of the aromatic

benzene ring on the isoindoline group may also facilitate aromatic stacking interactions with

F197 and possibly several other aromatic residues in the CB2 binding pocket previously reported

to engage in π-π interactions with ligands. Although several variations of the final optimized

compounds shown in Figure 3.4 were included in the study, none included a benzimidazole

group as the bi-cyclic component. With the entire bi-cyclic structure of benzimidazole being

aromatic, compared to only a single benzene ring, we postulated that such a chemical

modification may enhance π-π interactions with the aromatic amino acid residues found

exclusively in the CB2 receptor. Specifically, these may include F197, F87, F94, F97, F117,

W258, W194 and H95, as discussed above in Section 3.1. Taking into account that the addition

of a hydroxyl group at the 3 position of the adamantyl scaffold (as in Figure 3.4 A) imparted an

increase in aqueous solubility, we hypothesized that such a modification may also confer

favorable solubility properties on benzimidazole-containing compounds. This rationale led us to

the design of four structures, shown in Table 3.2.

Surprisingly, modification of the bi-cyclic structure from the isoindoline (as in Figure 3.4

B) to a benzimidazole group (as in the Table 3.2 library) provided a considerable improvement to

the clogP value, even in case of DML-3 and DML-4 with no adamantyl hydroxyl group. That is,

a LogP value of 4.26 was reported for compound (B) in Figure 3.4, whereas the cLogP values for

DML-3 and DML-4 were found to be 2.80 and 2.78, respectively. These values are highly

similar to the reported LogP of 2.77 for the hydroxylated compound (A) in Figure 3.4 which was

found to have good aqueous solubility (> 318 µg/mL [358]). Since DML-3 and DML-4 would be

expected to have good aqueous solubility comparable to compound (B) based on the similarity in

LogP values, the addition of the adamantyl hydroxyl group was deemed to be unnecessary for imparting suitable solubility properties on the compounds. Furthermore, addition of the adamantyl hydroxyl in compound A (Figure 3.4) was found to reduce cAMP EC50 agonist potency at CB2 22-fold [358]. Therefore, we selected DML-3 and DML-4, along with β-caryophyllene (discussed in Chapter 1.8) for further investigation.

Table 3.1. Structure and calculated physicochemical parameters of test compounds
Molecular weight (MW) and topological polar surface area (TPSA) were calculated using Instant JChem v. 14.7.21.0 (IJC) software [359]. The logarithm of octanol-water partition co-efficient (LogP) has been estimated using the calculated log P (cLogP) from BioByte Corporation software [360].

Compound Name	Structure	MW (g/mol)	Formula	TPSA (Å^2)	cLogP
DML-1		311.37	C18H21N3O2	78.01	1.41
DML-2		325.40	C19H23N3O2	78.01	1.39
DML-3		295.38	C18H21N3O	57.78	2.80
DML-4		309.41	C19H23N3O	57.78	2.78

3.2.2   CB2 Receptor Homology Modelling

The use of CB2 homology modelling and ligand docking studies *in silico* have played an integral role in furthering our understanding of receptor-ligand interactions and structure-activity relationships and served as an important tool in the development of novel CB2-selective ligands. Early models of the CB2 receptor were developed based upon the x-ray crystallography structure of bovine rhodopsin GPCR [352,353,361]. Subsequent CB2 homology models were developed based upon the 3D crystal structure of the human β2 adrenergic receptor [354,362] and A2a adenosine receptor [363].

In the present investigation, a 3D homology model of the human CB2 receptor (UniProt accession number P34972) was established using the X-ray structure of the human adenosine A2a receptor (Protein Data Bank entry 3QAK) as a template. The sequence alignment was done using CLUSTALW, followed by the manual refinement of non-conserved regions. Based on the resulting alignment, the CB2 homology model was generated by Modeller v.9.10 software. The loops obtained from gaps in the sequence alignment were energy-optimized to obtain a refined, energetically favorable structure according to the dope-score. The resulting model was subjected to energy minimization to remove unfavorable contacts and optimize its geometry by the implemented AMBER89 force field using the default parameters. The quality of the protein was assessed by Ramanchandran plot analysis, PROCHECK, and PROSA. The ligand binding pocket was determined using SPACER [364].
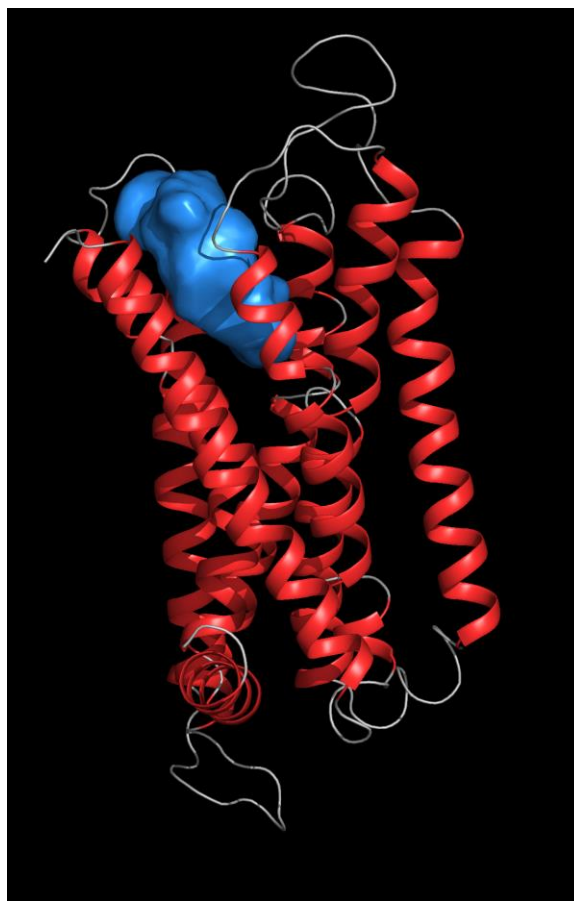
Figure 3.5. CB2 receptor homology model with the predicted ligand binding pocket.
The 3D structure of the CB2 receptor homology model is depicted in line and ribbon format. The seven transmembrane α-helix structures are shown in red. The estimated area of the binding pocket is 351.74 A^3 (blue).

3.2.3 Ligand Docking Experiments

The 3D structure of CB2 ligands were generated using Avogadro [365] and their molecular geometries were optimized using Gaussian 09 [366]. The MGL AutoDockTools package was employed to prepare the protein and the ligands for molecular docking. For each ligand, hydrogens were added and Gasteiger–Hückel partial charges plus proper atomic types were assigned. Autotors was then used to define rotatable bonds. The receptor was prepared adding hydrogen polar atoms to amino acid residues, and partial atomic charges were assigned to

all the atoms using the Kollman method. Docking experiments were carried out taking into account the flexibility of both ligand and receptor. Docking calculations were performed with AutoDock 4.2 [367], increasing default parameters to obtain 2.5 million Lamarkian Genetic Algorithm (LGA) evaluations, with a population of 150. A grid box was defined to cover the binding cavity of the protein with dimensions 126 Å x 126 Å x 126 Å placed on the center of mass of the gorge (3.55, 5.15, 2.30). Grid spacing 0.413 Å step and 100 docking runs were conducted. After clustering the resultant poses with a tolerance of 2 Å root mean square standard deviation (RMSD), docking results were classified in different groups taking into account scoring and population criteria for each analysis as well as the main interactions between the ligand and the binding site of the receptor. Conformations with the lowest overall binding energy were further analyzed in order to quantify individual amino acid-ligand binding energies (in kcal/mol).

3.2.3.1   Active Site Residues

Amino acid residues located within 3 angstroms of the ligand binding pocket (Figure 3.5) were identified. Of these 25 residues, 19 have been identified as lining the CB2 ligand binding pocket and/or participating in ligand binding interactions directly. Specifically, the amino acid residues we identified, which have been reported previously [351-355,362], include, in alphabetical order D189, C288, H95, L262, K109, M265, F87, F91, F94, F97, F117, F197, N188, P187, S112, S285, W194, W258 and V261.

Given that the majority of the amino acids found in the binding pocket matched those identified previously, it was concluded that our CB2 homology model should be capable of accurately identifying receptor-ligand interactions with our test compounds.

3.2.3.2   Ligand Docking
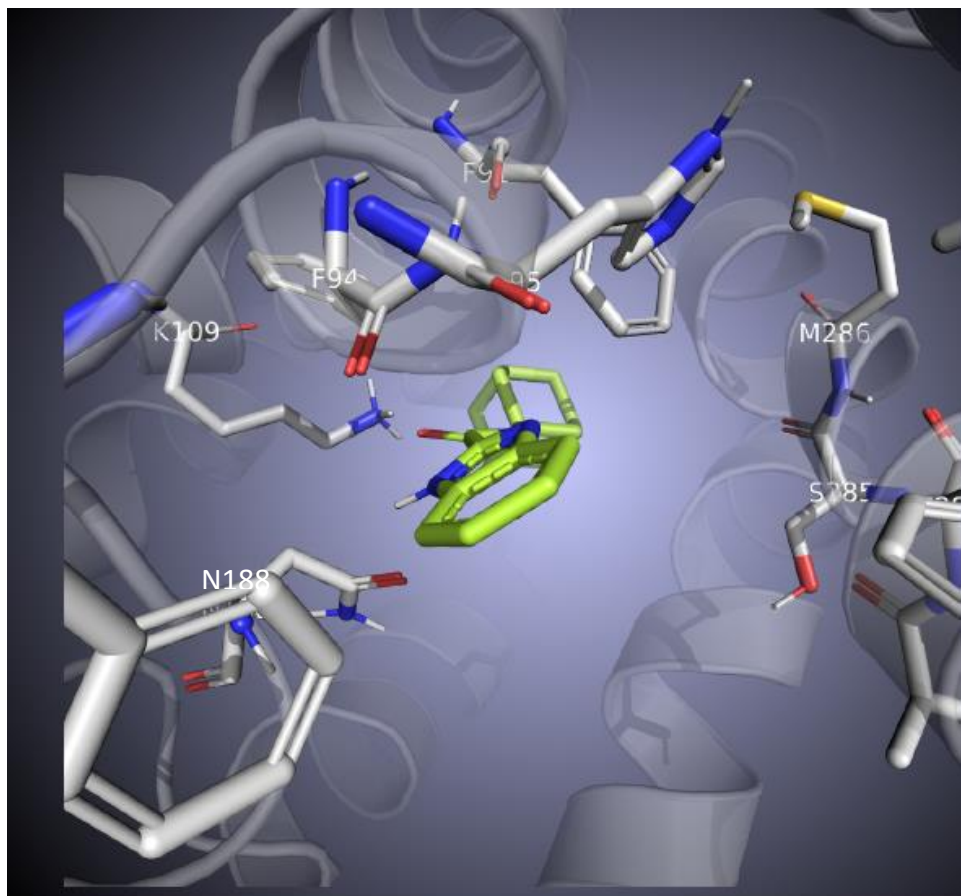
Figure 3.6. Molecular docking of DML-3 in CB2 homology model.
A 'top-down' view of the CB2 binding pocket (gray) with the most stable docking position of DML-3 (green) shown. Hydrophilic atoms, oxygen and nitrogen, are shown in red and blue, respectively. Amino acid residues located within 5 Å of the ligand are labelled (white) and include F94, F91, H95, K109, S285 and M286.

Table 3.2. Binding energies (kcal/mol) of CB2 active site residues with DML-3. The strongest detected interactions are shown, from left to right.

Active Site Residue Energy of Binding with DML-3 (kcal/mol)												
Residue	F	F	H	N	K	P	F	F	F	W	V	S	F
Position	94	91	95	188	109	187	87	117	97	258	261	112	197
Binding Energy	-19.5	-16.0	-12.4	-12.1	-9.5	-4.6	-4.2	-3.0	-2.9	-2.9	-2.7	-2.4	-1.6

As shown in Figure 3.6, DML-3 was found to bind stably within the CB2 active site. The adamantyl structure appears to penetrate furthest into the receptor binding cavity, interacting with residues of the hydrophobic pocket. As shown in Table 3.2, residues providing the strongest energetic interactions with DML-3 are the aromatic residues F94, F91 and H95. As predicted, the benzimidazole structure appears to be engaging in π-π stacking and/or aromatic T-stacking with several aromatic residues exclusive to the CB2 binding pocket. Important hydrophilic interactions also appear to take place between DML-3 and K109 as well as N188. Based on the spatial docking position shown in Figure 3.6, N188 and K109 are likely engaging in H-bond interactions with the DML-3 amide oxygen atom, as predicted. S112, another member of the CB2 hydrophilic cluster, was also found to contribute to energetically favorable interactions with DML-3, and, although not shown in Figure 3.6, is likely also interacting with the amide oxygen atom. P187 was also found to contribute energetically to DML-3 active site binding, likely through hydrophobic van der Waals interactions. Several other aromatic residues were found to engage in ligand interactions, including F87, F97, F117, F197 and W258. These residues likely contribute to energetically favorable π-π stacking and/or aromatic T-stacking with the DML-3 benzimidazole. Highly similar interactions were observed upon docking of DML-4 (not shown).

Previously, Gertsch *et al*. reported that β-caryophyllene docks within the hydrophobic cavity of the CB2 binding pocket, using a homology model based upon the bovine rhodopsin crystal structure, and engages in π-π stacking interactions with F177 and W258 [194]. Additional hydrophobic ligand-receptor interactions reported involved I198, M265 and V113 [194]. Here, for the first time in a CB2 homology model based upon the human A2a crystal structure, we report a variety of CB2 active site residue interactions with β-caryophyllene (Table 3.3) along with its most stable docking pose in the receptor binding cavity (Figure 3.7). As shown in Figure

3.7, β-caryophyllene docks most stably in closest proximity to H95, F283, F94, F91, F97, N188 and V36. The residues providing the strongest energetic interactions with β-caryophyllene, in descending order, are the aromatic residues H95, F283, F94 and F91 (see Table 3.3). These residues likely engage in π-π interactions with the two alkyl double bonds present in β-caryophyllene. N188 was also found to contribute considerably to stabilizing β-caryophyllene in the binding pocket. No hydrophilic oxygen or nitrogen atoms are present in the chemical structure of β-caryophyllene and therefore the typical H-bonding interactions between cannabinoid ligands and N188 would not be possible. However, based upon the most stable docking position of β-caryophyllene within the CB2 active site, shown in Figure 3.7, the nitrogen-bound hydrogen atom in N188 may be interacting with π electrons present in the β-caryophyllene C8 double bond. Although not depicted in Figure 3.7, S285 was also found to contribute to energetically favorable interactions with β-caryophyllene within the active site (Table 3.3). This may occur through similar hydrogen-π bond interactions with the β-caryophyllene double bonds. Additional CB2 receptor-ligand interactions found in the docking simulation involved F97, which likely interacts with β-caryophyllene via the same π-π interactions described above. Other hydrophobic interactions with A282 and P187 also contributed to the energetic docking stability of β-caryophyllene within the active site.

The total binding energy (kcal/mol) of the most stable docking pose found for each test compound (termed the minimum binding energy) is compared to that of two control CB2 agonists in Table 3.4. The control compounds, WIN-55,212 and SER-601 were found to have the strongest binding affinity to the CB2 active site (-105.15 and -103.20 kcal/mol, respectively). In rank order, DML-4, DML-3 and β-caryophyllene were found to have binding affinities of -92.73,
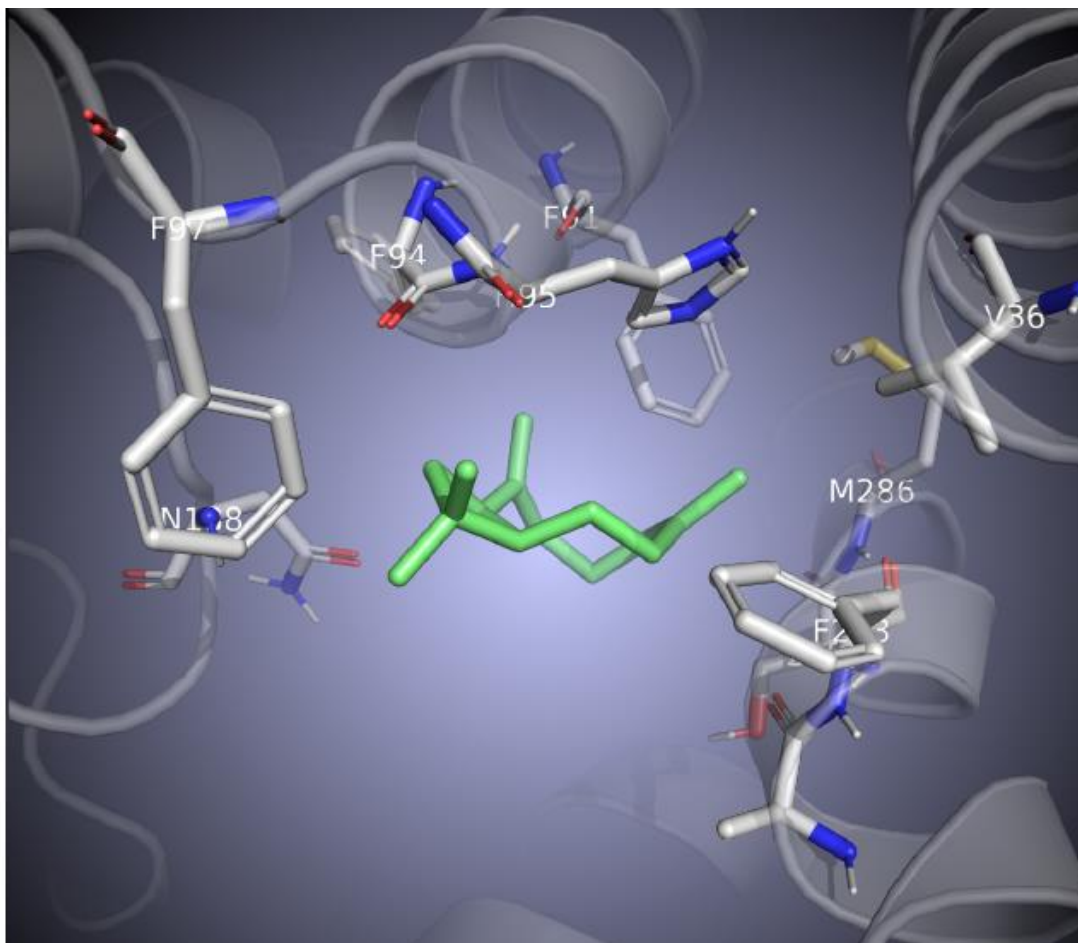
Figure 3.7. Molecular docking of β-caryophyllene in CB2 homology model.
The most stable binding position of β-caryophyllene (green) in the CB2 homology model binding pocket (gray) is shown. Hydrophilic atoms oxygen and nitrogen are shown in red and blue, respectively. Amino acid residues involved in the ligand binding interaction are labelled (white) and include H95, F283, F94, F91, F97, N188 and V36.

Table 3.3. Binding energies (kcal/mol) of CB2 active site residues with β-Caryophyllene. The strongest detected interactions are shown, from left to right.

Active Site Residue Energy of Binding with β-Caryophyllene (kcal/mol)												
Residue	H	F	F	F	N	F	A	P	S	M	D	I	V
Position	95	283	94	91	188	97	282	187	285	286	189	186	36
Binding Energy	-18.3	-11.6	-9.3	-9.2	-5.6	-3.6	-3.2	-3.2	-2.4	-1.4	-0.9	-0.8	-0.8

-71.16 and -63.95 kcal/mol, respectively. The predicted binding affinities of DML-3 and DML-4 fell within the range found for WIN-55,212, SER-601 and β-caryophyllene (*i.e.,* compounds with previously reported CB2 agonist activity). Therefore, it was inferred that DML-3 and DML-4 may potentially have CB2 agonist activity given their energetically favorable interactions within the active site, as shown in our homology model. DML-3 and DML-4 were synthesized for further characterization and pharmacologic testing.

Table 3.4. Minimum binding energies (kcal/mol) of control CB2 agonists (WIN-55,212, SER-601) and test compounds within the CB2 homology model active site.

Compound ID	Minimum Binding Energy (kcal/mol)
WIN-55,212	- 105.15
SER-601	- 103.20
DML-4	- 92.73
DML-3	- 71.16
β-Caryophyllene	- 63.95

3.3   Synthesis of Compounds DML-3 and DML-4

Both DML-3 and DML-4 were synthesized under identical conditions following the amide coupling reaction scheme depicted in Figure 3.8. The solid reactants consisted of 1-H-1-benzimidazole carboxylic acid, 1-adamantyl amine, 1-ethyl-3-(3-dimethylaminopropyl) carbodiimide hydrochloride (EDC) and hydroxybenzotriazole (HOBt), all from Sigma-Aldrich

(St. Louis, MO). The reaction was carried out in a dried round-bottom flask within a closed system under vacuum. The flask was filled with argon gas followed by the addition of dried dimethylformamide (DMF; Sigma-Aldrich, St. Louis, MO) and solid reactants. The reaction was stirred overnight at room temperature. Solvent was removed by rotoevaporation and the crude product was washed first with sodium bicarbonate (1.0 M) then with brine, then with water and finally dried over magnesium sulfate. The crude product was dissolved in dichloromethane and purified by column chromatography.
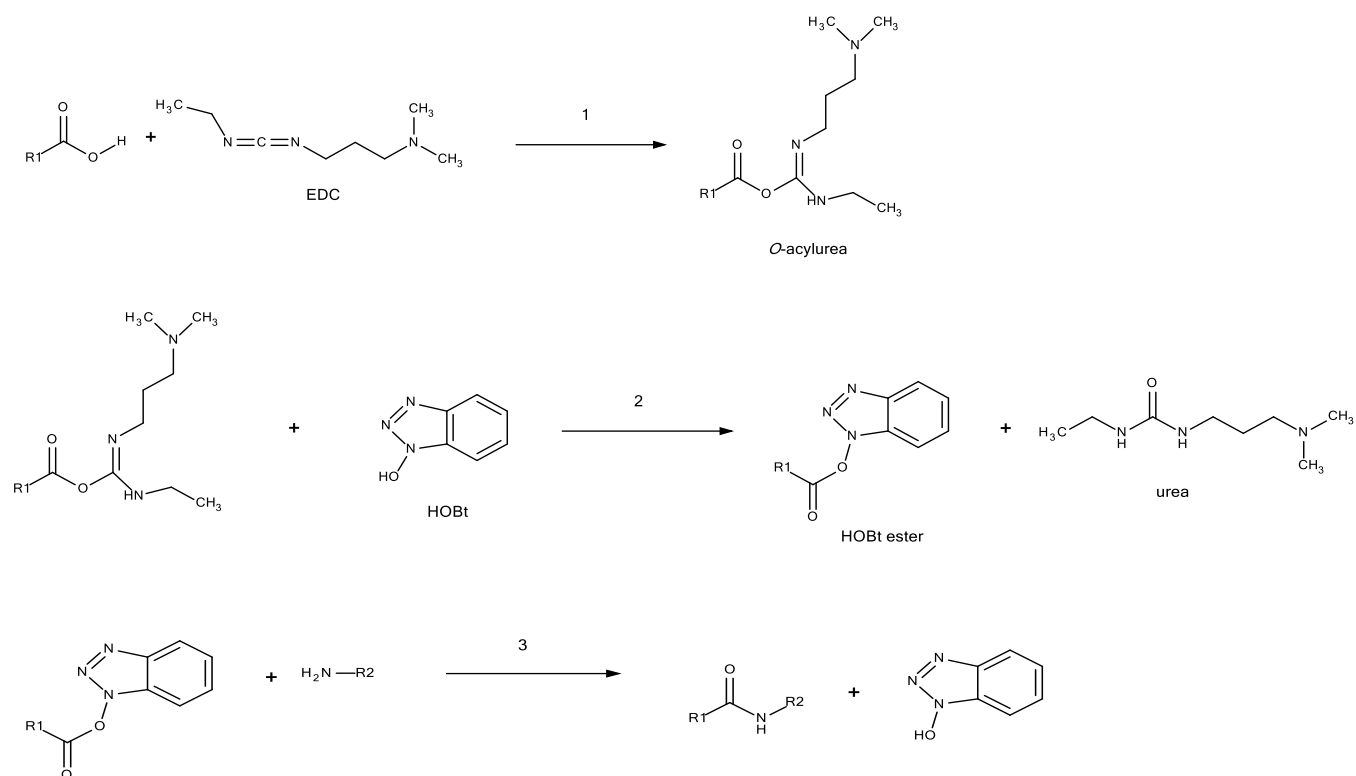
Figure 3.8. Amide coupling scheme using EDC and HOBt.
In reaction 1, R1-carboxylic acid reacts with 1-ethyl-3-(3-dimethylaminopropyl) carbodiimide hydrochloride (EDC), a water-soluble carbodiimide, to form an unstable O-acylurea intermediate which is susceptible to nucleophilic attack. In the presence of water, the O-acylurea may react and result in the formation of its urea derivative and regenerate the original R1-carboxylic acid. It is also possible for the O-acylurea to spontaneously re-arrange forming an undesirable N-acylurea product. Formation of this product is avoided by carrying out the reaction in the presence of HOBt. As shown in reaction 2, HOBt reacts with the R1-O-acylcurea to form HOBt ester along with a urea derivative. Subject to nucleophilic attack, the R2-amine reacts with the HOBt ester to form an amide bond with release of HOBt base (reaction 3). R1 = 1-H-benzimidazole; R2 = adamantane.

92

3.4 Chemical Analysis of DML-3 and DML-4

After synthesis, DML-3 and DML-4 were subjected to elemental, ^{1}H-NMR and mass spectrometry analyses. NMR spectra with shifts assigned to the compound structures are shown in Figures 3.9 and 3.10. Mass spectrometry analysis is listed in Appendix A.1. The ^{1}H-NMR spectra of both DML-3 and DML-4 revealed ppm shifts corresponding to each of the carbon-bound hydrogen atoms in the molecular structures, confirming the chemical synthesis was successful in producing both compounds. Some solvent contamination was observed in DML-3.
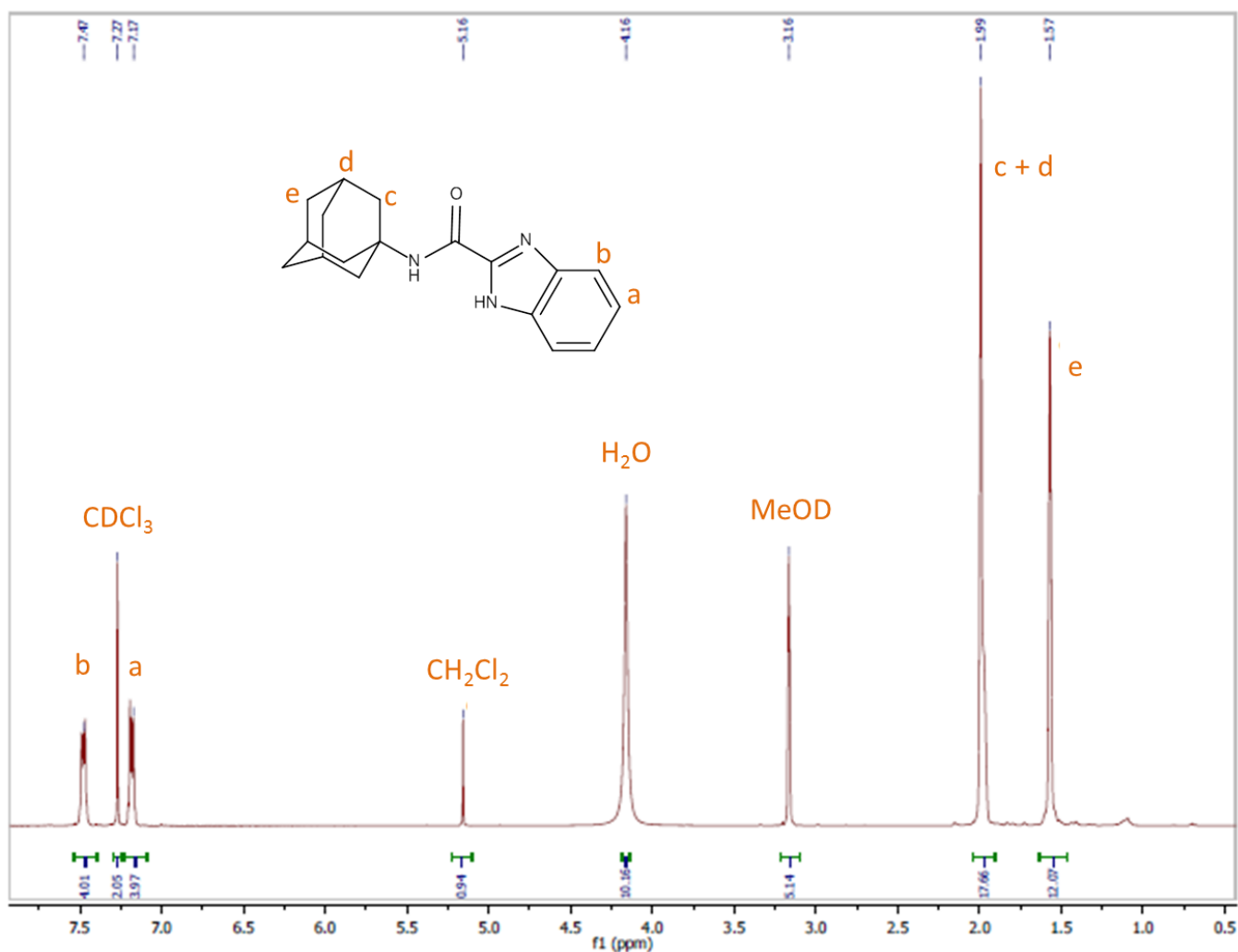
Figure 3.9. ^{1}H-NMR analysis of DML-3.
[1]H (CDCl$_3$, 400 MHz): δ 1.57 (e, CH$_2$), 1.99 (c+d, CH$_2$,CH), 7.17 (a, CH), 7.47 (b, CH).
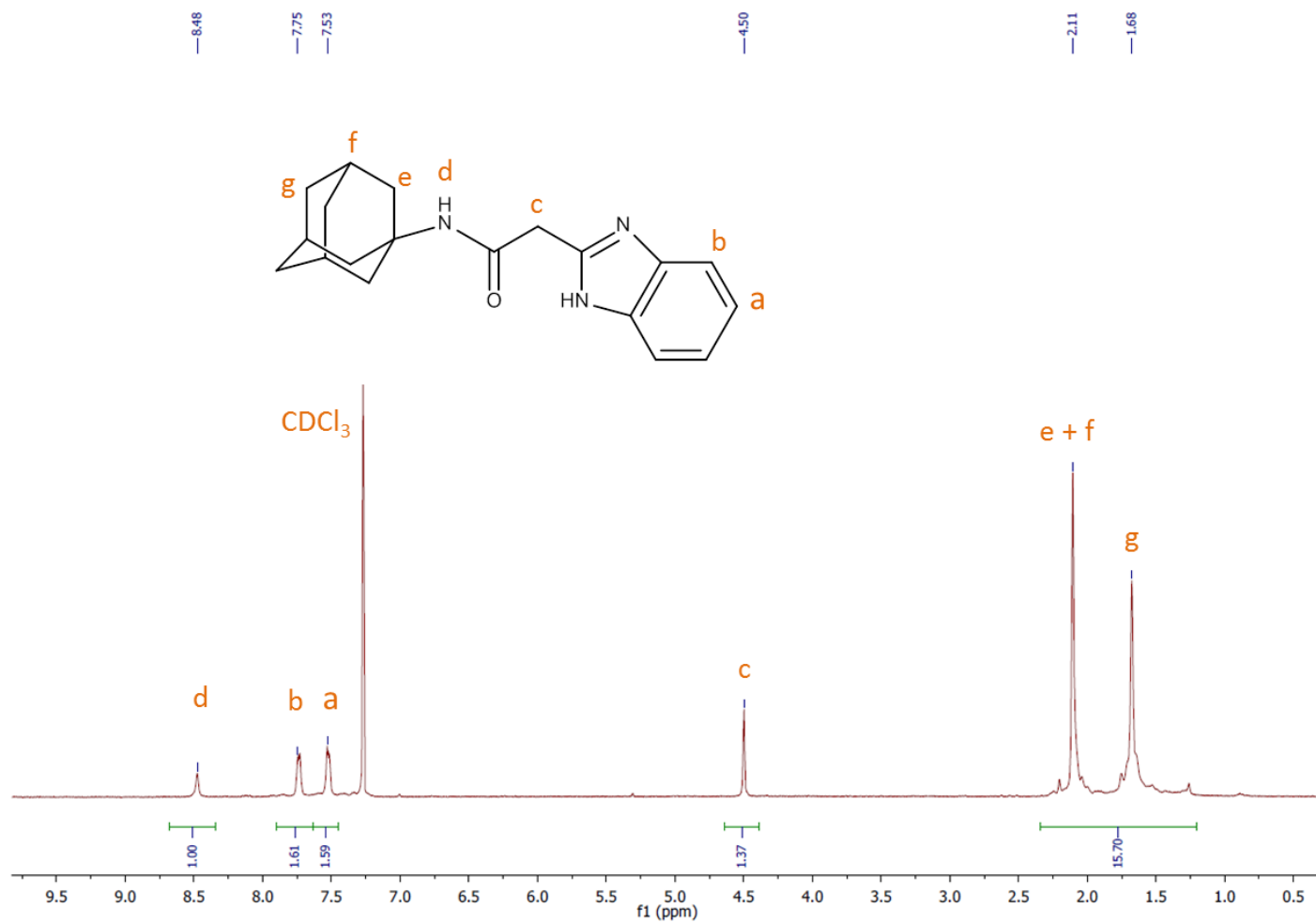
Figure 3.10. ¹H-NMR analysis of DML-4.
¹H (CDCl₃, 400 MHz): δ 1.68 (g, CH₂), 2.11 (e+f, CH₂,CH), 4.50 (c, CH₂), 7.53 (a, CH), 7.75 (b, CH), 8.48 (d, NH).

Table 3.5. Elemental Analysis of DML-3 and DML-4, with elemental content reported as percentage (%).

	DML-3		DML-4	
	Theoretical	Analysis Result	Theoretical	Analysis Result
Nitrogen	14.17	14.04	13.40	13.58
Carbon	73.16	73.23	74.06	73.73
Hydrogen	7.10	7.17	7.59	7.49

Elemental analysis (Table 3.5) revealed that an acceptably high level of purity was attained for both DML-3 and DML-4.

3.5   Determination of Solubility

Solubility of test compounds was determined in water, DMSO and cell culture media following the National Institute of Health (NIH) test method for determination of solubility [368] with some minor modifications. All dissolution tests were done using a stepwise mixing protocol (see Appendix A.2). Dissolution was initially attempted in distilled water at a 1 mg/mL concentration. If dissolution was not attained, an increased volume of distilled water was added to dilute the sample by 5 times. Dilution was repeated in subsequent steps if dissolution was not observed. The presence of dissolved compound in the aqueous solution was tested by centrifugation of the sample at 1000 x g for 5 min followed by measurement of absorbance at 292 nm.

Solubility in DMSO was tested by attempting to dissolve a quantity of test compound sufficient to produce a 50 mM solution. If solubility was not achieved, a dilution was performed and solubility was re-tested. If unsuccessful, dilution was repeated until solubility was achieved. The highest molarity solution produced in DMSO was used as a stock solution for subsequent testing of solubility in cell culture medium consisting of DMEM with 10% fetal bovine serum and 1% w/v penicillin/streptomycin (10,000 units/mL penicillin and 10 mg/mL streptomycin in sterile 0.9% NaCl). The maximum concentration of test compound soluble in cell culture medium using the DMSO stock solution was determined by first attempting to produce a 500 µM concentration. If precipitate or signs of cloudiness appeared, solutions of decreasing concentration were prepared.

Table 3.6. Aqueous solubility of DML-3 and DML-4.

Test Concentration (mg/mL)	1	0.2	0.1	0.01	0.002	0.001
DML-3	Insoluble	Insoluble	Insoluble	Insoluble	Insoluble	Insoluble
DML-4	Insoluble	Insoluble	Insoluble	Insoluble	Insoluble	Insoluble

Table 3.7. DMSO solubility of DML-3 and DML-4.

Test Concentration (mM)	50	25	10	5	2
DML-3	Insoluble	Insoluble	Insoluble	Insoluble	**Soluble**
DML-4	Insoluble	Insoluble	**Soluble**	**Soluble**	**Soluble**

As shown in Table 3.6, aqueous solubility of both compounds was extremely low (< 1 µg/mL). DML-3 was completely soluble in DMSO at a 2 mM concentration whereas DML-4 was increasingly soluble in DMSO and a 10 mM solution could be prepared (Table 3.7). The highest achievable concentration of DML-3 in cell culture media using the 2 mM DMSO stock solution was 100 µM. Using the 10 mM DMSO stock solution of DML-4, the highest achievable concentration in cell culture media was also 100 µM.

3.6   Pharmacologic Characterization of Test Compounds at Cannabinoid Receptors

3.6.1   Materials and Methods

All cell culture supplies were obtained from Thermo Fisher Scientific (Waltham, USA), unless otherwise specified.

3.6.1.1   Cell Culture and Stable Transfection

Human embryonic kidney (HEK-293) cells as well a HEK-293 cell line stably transfected with human CB1 cDNA (HEK-CB1) were generously donated by the Kumar Laboratory, UBC Faculty of Pharmaceutical Sciences. In order to create a HEK-293 cell line stably transfected with human CB2 cDNA, HEK-293 cells were cultured in DMEM with 10% fetal bovine serum and 1% w/v penicillin/streptomycin (10,000 units/mL penicillin and 10 mg/mL streptomycin in sterile 0.9% NaCl). Purified CB2 cDNA plasmid containing G418 resistance (OriGene, Rockville, MD) was mixed with HEKfectin transfection reagent in a 1:2 ratio and added to cell culture media such that 5 µg DNA was added per 28.2 cm^2 cell culture flask. Cells were incubated at 37°C and 5% CO_2 for 40 h, with addition of extra cell culture media at the 24 h time point. Cells were then incubated in selection media (above cell culture media containing 725 µg/mL G418), allowed to proliferate, and stored in liquid nitrogen in cryotubes containing 5 x 10^6 cells/mL with 10% DMSO as cryo-protectant.

3.6.1.2   Cannabinoid Receptor Radioligand Displacement Assay

3.6.1.2.1   Membrane Preparation

Cell pellets of cultured HEK-CB1 and HEK-CB2 cells were suspended in a homogenization buffer, pH 7.2, containing 250 mM sucrose, 10 mM Tris HCl and a protease inhibitor cocktail containing 2 mM 4-(2-aminoethyl)benzenesulfonyl fluoride, 0.3 µM aprotinin, 130 µM bestatin, 1 mM EDTA, 14 µM E-64 and 1 µM leupeptin. The suspension was transferred to a 20 mL Dounce glass homogenizer and subjected to 20 manual strokes. The homogenate was transferred to microcentrifuge tubes and sonicated, on ice, at 30% power for two 10 s pulses with 30 s in between pulses. Nuclei and cell debris were removed by centrifugation at 500 x g for 10 min at 4°C. The supernatant was collected and centrifuged at 100,000 x g for 60 min at 4°C. The supernatant was discarded and the pellet was washed in homogenization buffer and re-centrifuged at 100,000 x g for 60 min at 4°C. The supernatant was discarded and the pellet (containing the cell membrane fraction) was resuspended in buffer to achieve a concentration of approximately 4 mg/mL protein. Samples were aliquoted and stored at -80°C.

3.6.1.2.2   Cannabinoid Receptor Saturation Binding Studies

Binding was initiated by the addition of 50 µg membrane protein to silanized glass tubes containing [^{3}H]CP-55,940 and a sufficient volume of binding buffer (50 mM Tris HCl, 1 mM EDTA, 3 mM MgCl$_2$, and 0.5% fatty acid-free BSA, pH 7.4) to bring the total volume to 0.2 mL. Total binding of [^{3}H]CP-55,940 (164.9 Ci/mmol; Perkin Elmer, Waltham, USA) was determined at concentrations ranging from 0.01 – 5 nM. Non-specific binding at each test concentration was determined by the addition of 10 µM unlabeled CP-55,940 (BioTechne, Abingdon, UK).

Following incubation (1 h at 37°C with mild agitation), the reaction was terminated by addition of 0.8 mL ice cold wash buffer (50 mM Tris HCl and 0.1% fatty acid-free BSA, pH 7.4) to the incubation tube followed by rapid vacuum filtration through Whatman GF/C glass fiber filters (pre-treated with aqueous polyethyleneimine 0.1% for 1 h at 4°C) in 96 well harvest plates (Perkin Elmer, Waltham, USA). Wells were then washed twice under vacuum with ice cold wash buffer. Harvest plates were then back-sealed and filters were incubated in scintillation fluid for 30 min at room temperature. Radioactivity was quantified as CPM on a Microlux beta counter (Perkin Elmer, Waltham, USA) which was normalized to a known tritium standard. Specific binding of [^{3}H]CP-55,940 was calculated as total binding minus non-specific binding. Specific binding data was plotted and the saturation curve was used to determine the binding saturation constant (B_{max}) and the equilibrium dissociation constant (K_D) of [^{3}H]CP-55,940 using the saturation binding nonlinear regression function (one site, specific binding) in GraphPad Prism 6.0 software. Saturation binding curves are listed in Appendix A.3.

3.6.1.2.3   Competition Binding Studies of Test Compounds

Binding incubation, sample harvesting and radioactivity measurement was performed using the procedure described immediately above using the competitor ligands at varying test concentrations plus 0.5 nM [^{3}H]CP-55,940. IC_{50} values were determined using the competitive binding nonlinear regression function (one site, fit IC50) for sigmoidal data, and linear regression for Hill plot transform data, in GraphPad Prism 6.0 software. Binding affinity constants (K_i) of each competitor ligand for CB1 and CB2 receptors was then calculated using the method of Cheng and Prusoff ($K_i = IC_{50}/(1 + L/K_D)$) [369].

3.6.1.3   cAMP Assay for Agonist Activity

cAMP assays in CB1 and CB2-transfected HEK293 cells were conducted using the homogenous time-resolved fluorescence resonance energy transfer (HTRF) method with the cAMP dynamic 2 kit (Cisbio, Bedford, MA), following the manufacturer's protocol. An optimization experiment was conducted to determine the ideal assay parameters with our experimental cell line, as per the manufacturer's instructions. Optimization data is shown in Appendix A.4. Briefly, cells were suspended in cell culture media and plated in 384-well microplates (1,000 cells/well) followed by the addition of 0.5 mM IBMX, 20 µM forskolin, and test compounds at varying concentrations. Following a 30 min incubation, cAMP-d2 conjugate plus the anti-cAMP-cryptate conjugate were added to each well in lysis buffer. Fluorescence at 665 nM was analyzed on a PHERAstar microplate reader equipped with an HTRF optical module (BMG Lab technologies, Offenburg, Germany). EC_{50} values were determined using non-linear regression (log agonist versus response function) in Graphpad Prism 6.0 Software.

3.6.2   Results

As shown in Table 3.8, the equilibrium dissociation constant values (K_D) obtained for the radio-ligand [^{3}H]CP-55,940 were 1.25 ± 0.024 nM and 0.73 ± 0.09 nM at CB1 and CB2 receptors, respectively. β-caryophyllene, DML-3 and DML-4, bind to the cannabinoid binding site in CB2 with nanomolar affinity, as demonstrated by the concentration-dependent displacement of [^{3}H]CP-55,940 (Figure 3.11.A). In rank order, DML-3 showed the strongest affinity ($K_i = 95.1$ nM), followed by DML-4 ($K_i = 185.2$ nM) and β-caryophyllene ($K_i = 548.9$ nM; see Table 3.9). Neither DML-3 nor DML-4 showed considerable binding affinity for CB1

($K_i = >10~\mu M$), while β-caryophyllene bound with modest affinity ($K_i = 7.3~\mu M$; see Figure 3.11.B).

It was determined that all three test compounds acted as full agonists at the CB2 receptor (see Figure 3.13). DML-4 was found to inhibit cAMP production in CB2-HEK 293 cells with an EC_{50} value corresponding to 0.17 nM (Table 3.10). β-caryophyllene also had strong agonist activity at CB2 with an EC_{50} of 8.7 nM. DML-3 was also a full agonist at CB2 with an EC_{50} value of 223 nM. In contrast, at CB1, both DML-3 and DML-4 displayed very low activity (EC_{50} >10 μM), indicating >40- fold and >10,000-fold CB2 agonist selectivity for each compound, respectively. In comparison, β-caryophyllene was found to have weak agonist activity at CB1 ($EC_{50} = 0.95~\mu M$). Nonetheless, it displayed strong CB2 selectivity, with the agonist potency at CB2 being 109-fold higher than at CB1.

Table 3.8. Calculated Equilibrium Dissociation Constants (K_D) ± SE for [^{3}H]CP-55,940 at cannabinoid receptors.

Constant	CB1	CB2
K_D	1.25 ± 0.24 nM	0.73 ± 0.09 nM

A

CB2 [³H]CP-55,940 Displacement

■ CP-55,940
□ β-Caryophyllene
▲ DML-3
○ DML-4

B

CB1 [³H]CP-55,940 Displacement

■ CP-55,940
□ β-Caryophyllene
▲ DML-3
○ DML-4
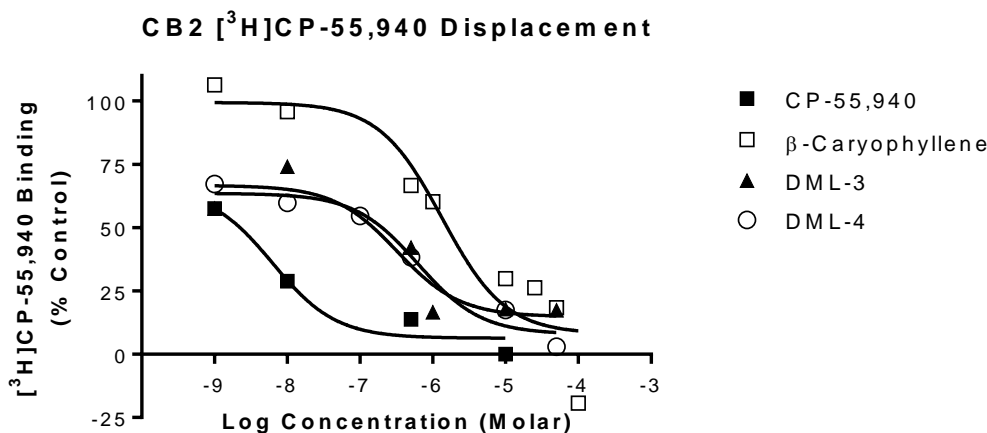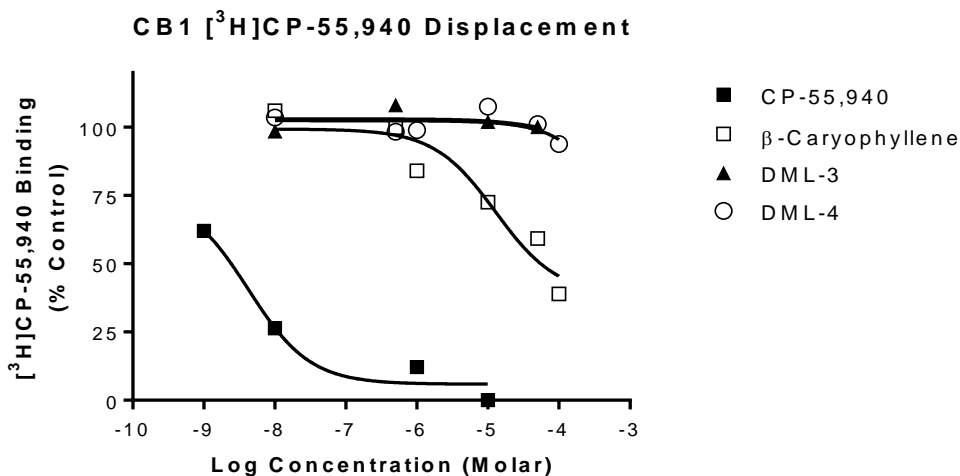
Figure 3.11. [³H]CP-55,940 displacement following cannabinoid treatment of membranes isolated from HEK293 cells stably transfected with either CB2 (A) or CB1 (B).
The specific binding of 0.5 nM [³H]CP-55,940 in competition with non-labeled CP-55,940 (■), β-caryophyllene (□), DML-3 (▲) and DML-4 (○) is displayed, as a percent of control. The specific binding of 0.5 nM [³H]CP-55,940 measured in the absence of competitor was taken as 100% [³H]CP-55,940 binding and the specific binding of 0.5 nM [³H]CP-55,940 in the presence of 10 µM non-labeled CP-55,940 was taken as 0% [³H]CP-55,940 binding. Data points represent the mean of three independent experiments.

A

C B 2 [^{3}H]C P-55,940 Displacement Hill Plot

■ C P-55,940
□ β-Caryophyllene
▲ D M L-3
○ D M L-4

B

C B 1 [^{3}H]C P-55,940 Displacement Hill Plot

■ C P-55,940
□ β-Caryophyllene
▲ D M L-3
○ D M L-4
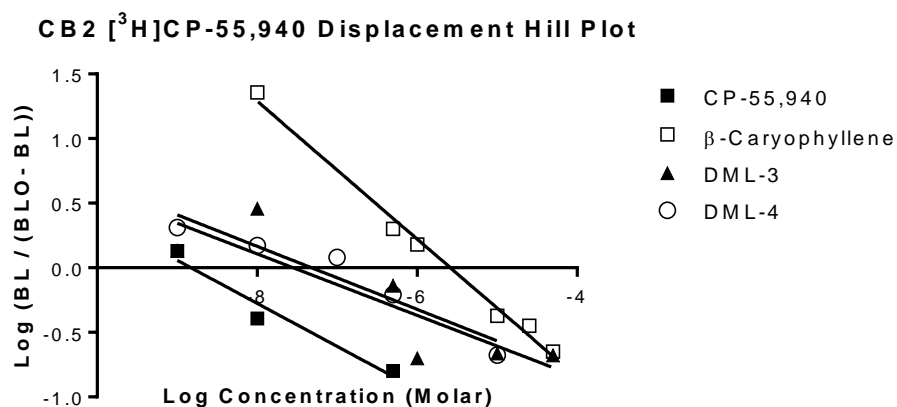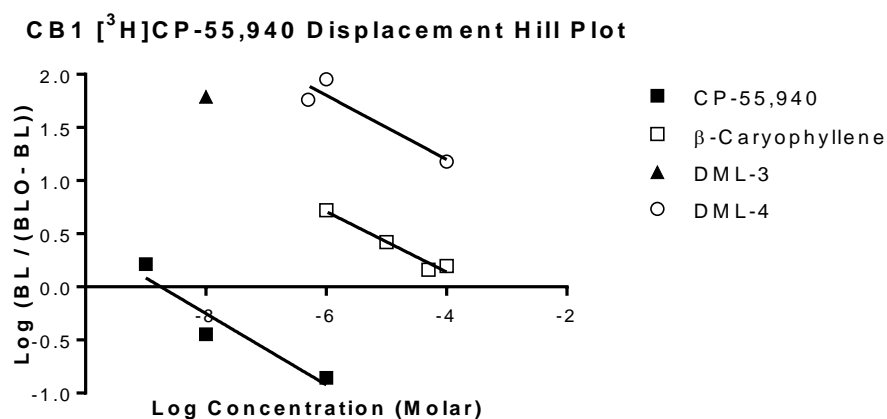
Figure 3.12. Hill Plot transformation of Figure 3.11 data showing linearized [^{3}H]CP-55,940 displacement in HEK293 cells stably transfected with either CB2 (A) or CB1 (B).
The linearized specific binding of 0.5 nM [^{3}H]CP-55,940 in competition with non-labeled CP-55,940 (■), β-caryophyllene (□), DML-3 (▲) and DML-4 (○) is displayed, in Hill Plot transform.

103
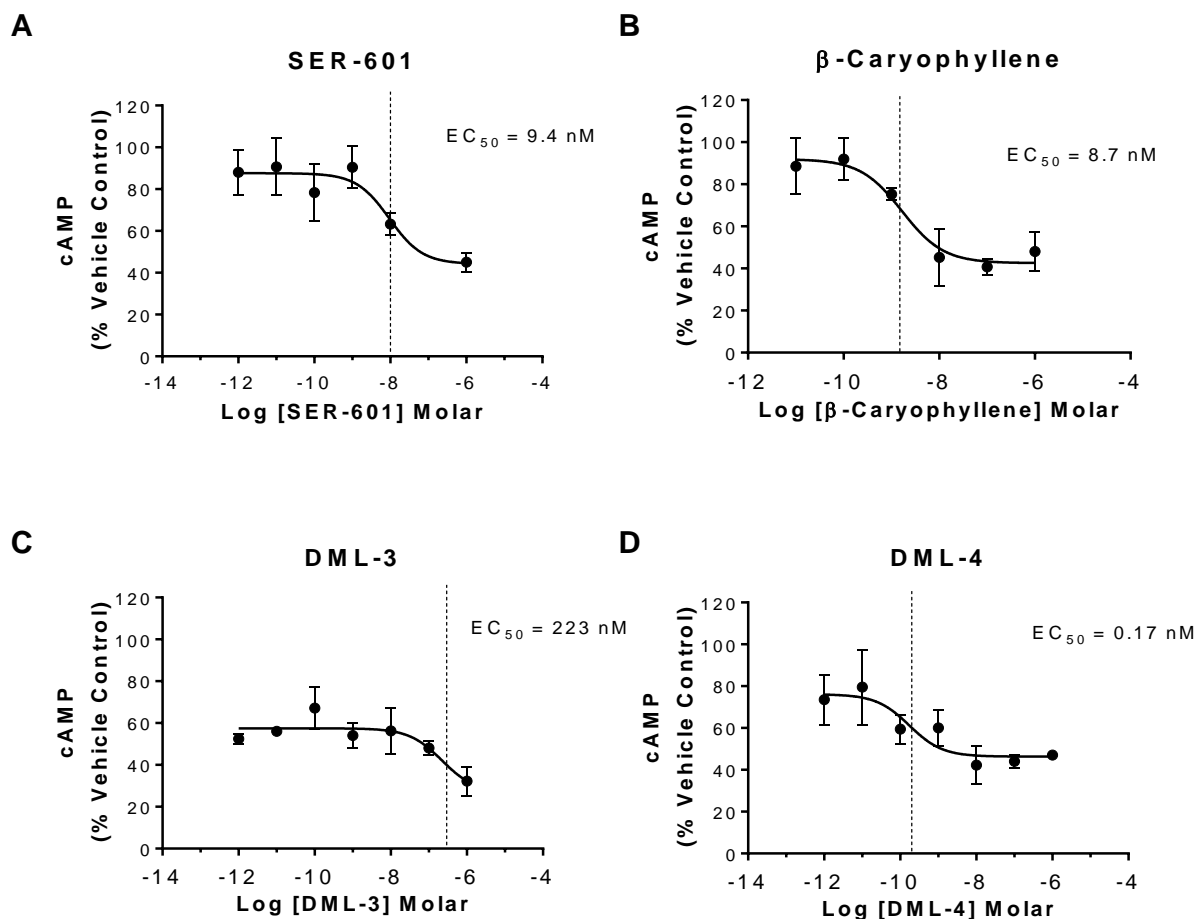
Figure 3.13. Inhibition of cAMP in CB2-HEK293 cells treated with cannabinoid test compounds.
Inhibition of cAMP production in CB2-tranfected HEK293 cells following treatment with SER-601 (A), β-caryophyllene (B), DML-3 (C) and DML-4 (D), expressed as a percent of control. The cAMP concentration following vehicle treatment with 20 μM forskolin was taken as 100% whereas the cAMP concentration following vehicle treatment in the absence of forskolin was taken as 0%. Data represents the mean ± SD of three independent experiments.
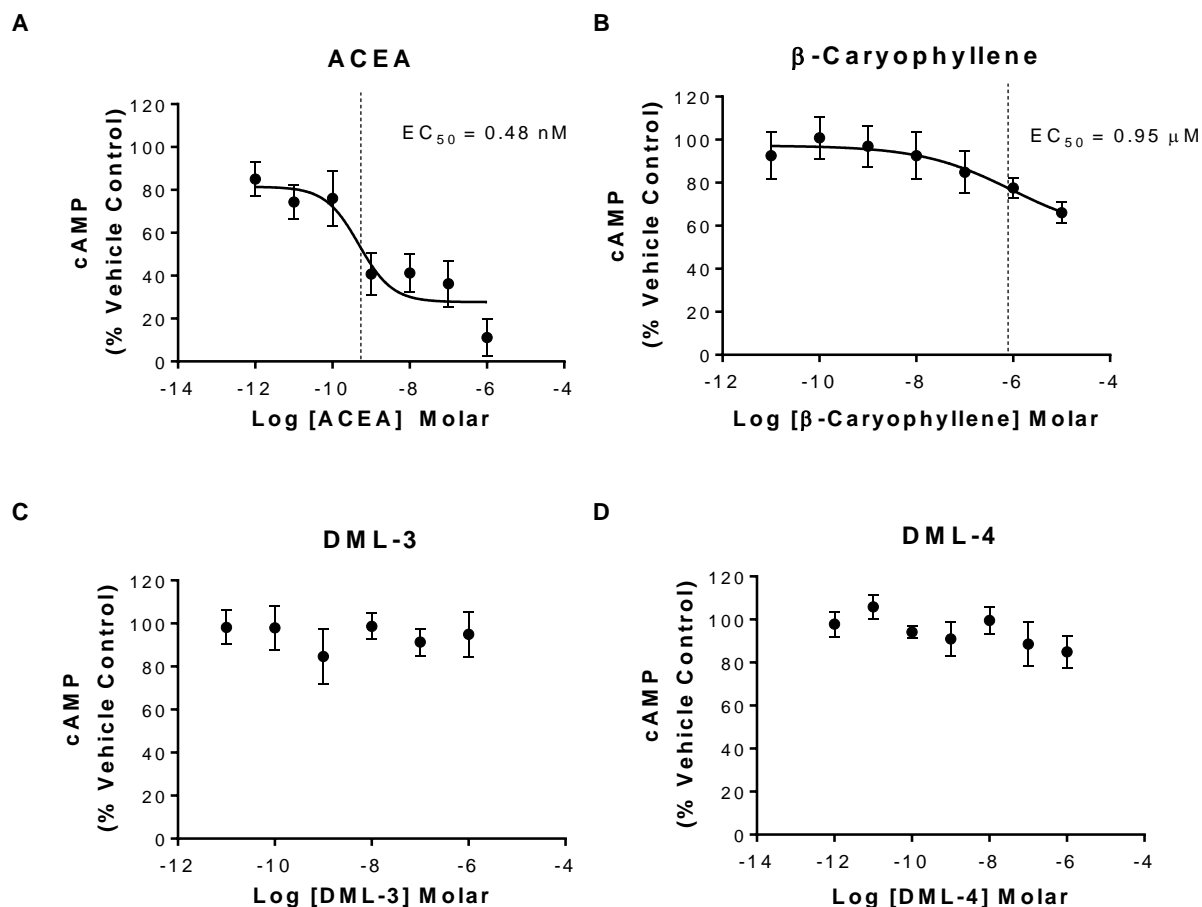
Figure 3.14. Inhibition of cAMP in CB1-HEK293 cells treated with cannabinoid test compounds.
Inhibition of cAMP production in CB1-tranfected HEK293 cells following treatment with ACEA (A), β-caryophyllene (B), DML-3 (C) and DML-4 (D), expressed as a percent of control. The cAMP concentration following vehicle treatment with 20 µM forskolin was taken as 100% whereas the cAMP concentration following vehicle treatment in the absence of forskolin was taken as 0%. Data represents the mean ± SD of three independent experiments.

Table 3.9. Binding Affinities (K$_i$) of test compounds at cannabinoid receptors.

Test Compound	CB1			CB2		
	Sigmoidal	Hill	**Mean**	Sigmoidal	Hill	**Mean**
β-Caryophyllene	9.16 μM	5.44 μM	**7.30 μM**	797 nM	301 nM	**548.9 nM**
DML-3	> 10 μM	> 10 μM	**> 10 μM**	190 nM	0.22 nM	**95.1 nM**
DML-4	> 10 μM	> 10 μM	**> 10 μM**	370 nM	0.42 nM	**185.2 nM**

Table 3.10. Agonist activity (cAMP, EC$_{50}$) of test compounds at cannabinoid receptors.

Test Compound	CB1	CB2
β-Caryophyllene	0.95 μM	8.7 nM
DML-3	> 10 μM	223 nM
DML-4	> 10 μM	0.17 nM

3.7   Discussion

Based on the published literature describing cannabinoid receptor-ligand interactions, it was possible to design, model and synthesize two novel compounds, DML-3 and DML-4, having strong binding affinity and potent agonist activity at CB2 with limited interactions at CB1. Furthermore, new information regarding the specific CB2 active site interactions of the natural sesquiterpene β-caryophyllene has been generated, and additionally, the degree of selectivity of the compound for the CB2 receptor over CB1 has been established.

The *in silico* CB2 homology model accurately predicted the ability of the test compounds to stably bind within the CB2 active site, as confirmed *in vitro* via radio-ligand displacement

106

assay. The CB2 binding pocket residues found to be chiefly responsible for providing energetically favorable interactions with of each of our test compounds *in silico* have all been previously reported to mediate CB2 ligand binding (as discussed in Section 3.1 and 3.2.3.1). As predicted, increasing the aromaticity of the bicyclic component of the adamantyl derivatives reported previously by Nettekoven and colleagues [358] resulted in improved CB2 agonist potency in the present investigation in the case of DML-4. As demonstrated by receptor docking studies *in silico*, the aromatic benzimidazole group engages with several aromatic binding cavity residues exclusive to the CB2 receptor, likely accounting for the strong binding affinity at CB2 and the low affinity for CB1.

The rank order of compound binding affinities calculated *in silico* (*i.e.*, DML-4 > DML-3 > β-caryophyllene) was semi-predictive of the relative corresponding CB2 agonist potencies determined *in vitro* via cAMP assay (*i.e.*, DML-4 > β-caryophyllene > DML-3). Surprisingly, the agonist potency of DML-4 was considerably greater than DML-3 (*i.e.*, EC_{50} of 0.17 nM versus 223 nM), which was not reflective of the relative CB2 binding affinity estimated via radio-ligand displacement assay (*i.e.*, K_i = 185.2 nM and 95.1 nM for DML-4 and DML-3, respectively). This difference may be explained, at least partially, by the inherent variability present in both assays. This may also exemplify a case in which receptor functionality (*i.e.*, G-protein-mediated intracellular signaling) is generated in a manner which is independent of ligand binding affinity. This scenario also appears to be true in the case of β-caryophyllene. Given that it scored lowest, relative to DML-3 and DML-4, in terms of its CB2 binding affinity *in silico* and actual binding affinity *in vitro*, the EC_{50} agonist potency of 8.7 nM was somewhat unexpected. Comparatively, however, both the CB2 agonist potency and binding affinity (*i.e.*, K_i = 548.9 nM) values

determined for β-caryophyllene in the present investigation are highly similar to those reported previously by Gertsch and colleagues [194].

The residue interactions found to stabilize β-caryophyllene within the CB2 active site are distinctly different than those reported previously by Gertsch and colleagues [194]. The CB2 homology model developed in the present investigation is based upon the known crystal structure of the human A2a receptor with bound ligand, whereas the previously reported CB2 binding interactions of β-caryophyllene were generated from a homology model based upon the bovine rhodopsin GPCR structure. Therefore, the disparity between the findings is likely owing to small differences in the crystal structure of the bovine versus human GPCR and possibly to differences in alignment of the peptide sequence to the 3D receptor structure. In both reports, however, it was determined that aromatic residues stabilize β-caryophyllene within the hydrophobic pocket of the active site, likely through π-π interactions with the two alkyl double bonds present in the ligand. These findings are therefore consistent, overall, in terms of the binding site location and mechanism of ligand stabilization.

The finding that β-caryophyllene has mild CB1 binding affinity and weak agonist activity is novel. The 109-fold selectivity at CB2 versus CB1 is consistent with the observation that folk medicines containing β-caryophyllene as the principal active constituent (*i.e.*, copaiba oil) are not considered to be psychotropic [195]. Given the agonist potency of the compound at CB2 (*i.e.*, EC_{50} of 8.7 nM) versus CB1 (*i.e.*, EC_{50} of 0.95 μM), it would be expected that therapeutic effects of β-caryophyllene would be observed at concentrations well below those which have activity at CB1. Furthermore, the magnitude of cAMP inhibition in CB1-transfected HEK293 cells upon treatment with β-caryophyllene was relatively low (i.e., cAMP was ~80% of the vehicle control at 1 μM). Therefore, mild intracellular reductions in cAMP may not be sufficient to evoke

downstream intracellular responses classically associated with agonist treatment, given that cells will be receiving multiple competing inputs from other ligands present *in vivo*. Future studies could evaluate the ability of β-caryophyllene to signal through CB1 by investigating, for example, inhibitory effects on neuronal firing.

The cLogP values for both DML-3 and DML-4 were not predictive of the actual aqueous solubility determined for both compounds (*i.e.*, < 1 µg/mL for both compounds). Given that aqueous solubility of 318 µg/mL was reported by Nettekoven and colleagues for an adamantyl amine derivative with a LogP of 2.77 [358] (see Figure 3.4), it was anticipated that DML-3 and DML-4 would have reasonable aqueous solubility given their virtually identical cLogP values (i.e., 2.80 and 2.78 for DML-3 and DML-4, respectively). Given that the chemical analysis data presented for DML-3 and DML-4 confirms structural integrity and compound purity, this is a case in which cLogP is not predictive of aqueous solubility. This is not an uncommon phenomenon, as the LogP coefficient indicates the preference of a compound to partition into water within a *two phase octanol-water system*, and does not necessarily reflect the ability of a compound to dissolve in water alone.

Finally, the lower degree of DMSO solubility of DML-3 relative to DML-4 may be explained by greater conformational freedom DML-4 imparted by the added 1-carbon akyl spacer between the amide and benzimidazole. Given that it was possible to prepare both compounds as treatment solutions in cell culture media with the use of DMSO as a co-solvent, at concentrations up to 100 µM, both compounds were considered to be suitable for further investigation *in vitro*.

Chapter 4: Investigation of the Safety and Potential Therapeutic Activity of the CB2 Agonist Compounds *In Vitro*

4.1   Specific Aim

The specific aim of the research described in this chapter is to evaluate the safety and potential therapeutic activity of the novel CB2 receptor ligands developed (Chapter 3) by testing their effect on human cell proliferation, death, and mitochondrial respiration, by assessing their ability to modulate key intracellular pathways that mediate glial cell proliferation and inflammation, and by assessing their ability to exert anti-inflammatory effects on human glial cells.

4.2   Introduction

The data presented in the previous chapter confirm the ability of our test compounds to bind and act as selective agonists at the CB2 receptor with limited activity at CB1. We postulate that by targeting CB2-expressing CNS glial cells with these compounds, a therapeutic benefit may be conferred for chronic pain mediated by gliosis. Therefore, further investigations were conducted to evaluate the potential utility of these molecules as therapeutic agents within the context of gliosis. The first component of this process included assessment of the compounds' safety. Studies were therefore conducted to examine each compound's effect of mitochondrial respiration, cell proliferation, and cell death in a variety of cell lines. This was achieved using a combination of MTT assays, cell confluence imaging, and YOYO®-1-based cell death detection.

Based on existing data suggesting that certain CB2 ligands are capable of reducing behavioral pain measures and ameliorating pro-inflammatory glial cell activity *in vivo* (see

110

Chapter 1, Section 1.9), we may expect our test compounds to achieve similar results. However, cannabinoid receptor-mediated modulation of intracellular signaling appears to vary across cell types and differ depending on the specific CB2 agonist involved. For example, cannabinoid receptor activation by anandamide was found to inhibit the activity of ERK1/2 in neuronal cells [370]. In contrast to this finding, Shoemaker and colleagues demonstrated that cannabinoid agonists CP-55,940, noladin ether and 2AG increase intracellular activation of ERK1/2 in CB2-transfected CHO cells at substantially different EC_{50} concentrations (2.6 nM, 240 nM and 12.4 nM, respectively) [371]. It has also been discovered that cannabinoid treatment increased the activity of ERK1/2 in PC-3 cells transfected with either CB1 or CB2. This action appeared to be driven by activation of phosphatidylinositol-3-kinase (PI3K). While inhibition of ERK1/2 activity by cannabinoids may confer therapeutic benefits in gliosis (mechanisms are discussed in Section 4.1.1), activation of ERK1/2 may promote increases in cell growth and proliferation and may therefore be detrimental. Therefore, elucidating the specific effects of our cannabinoid compounds on relevant intracellular signaling cascades within our target cell type is crucial for determining their potential utility in gliosis. Using U87-MG cells, a malignant astrocyte cell line (astroglioma) as an *in vitro* model for our investigation, the effects of our test compounds on key intracellular signaling pathways were probed using Western blot techniques. The relevance of the biochemical effectors we investigated in this study, including those identified above, is discussed below in Section 4.1.1.

Finally, we tested the ability of our CB2 ligands to exert anti-inflammatory effects *in vitro* within U87-MG astrocytes. This cell line is an ideal model system for this investigation since previous studies indicate that U87-MG are a pro-inflammatory cell phenotype which secrete cytokines IL6 and IL8 under normal cell culture conditions [372,373], mimicking the

pro-inflammatory glial cell activity present in gliosis. Therefore, noxious stimulation or pre-treatment to induce an inflammatory response was not necessary. The effect of our test compounds on pro-inflammatory cytokine secretion by U87-MG cells was investigated using ELISA techniques.

4.2.1 Relevant Biochemical Signaling Cascades

4.2.1.1 NF-κB

As discussed in Section 1.9 (Chapter 1), the NF-κB complex is a nuclear transcription factor, which, when activated by phosphorylation of its IκBα subunit, translocates to the cell nucleus where it binds to several different DNA response elements. With binding of further co-activators and RNA-polymerase, phosphorylated NF-κB (p-NF-κB) facilitates transcription of cytokines and other proteins involved in immune responses, inflammation, and cell survival. For example, NF-kB binding sites are located on the promoter region of the IL6 and IL8 genes, and expression of both IL6 and IL8 has been found to increase in response to NF-κB activation [374]. NF-κB is an important intracellular driver of biochemical processes associated with gliosis. Increased NF-κB activity in the spinal cord dorsal horn is associated with central pain sensitization via up-regulation of cytokines and pro-nociceptive peptides [258,375] while suppression of NF-κB has been shown to significantly reduce hyperalgesia and cytokine production in chronic pain models [259,376]. Since activation of NF-κB occurs via phosphorylation by PKA, cannabinoids may therefore be capable of down-regulating this process through $G_{i/o}$-mediated inhibition of cAMP synthesis and subsequent PKA activity.

In U87-MG astrocytes, NF-kB plays an important role in regulating cell survival and proliferation. For example, Bao *et al.* found that inhibition of the NF-κB pathway in U87-MG

impaired cell proliferation [256]. Additionally, pharmacologic inhibition of NF-κB resulted in apoptosis, reduced mRNA expression of survivin, c-Myc and hTERT, and diminished expression of down-stream targets involved in cell proliferation and invasion, including cathepsin B, matrix metalloprotease (MMP) -2, MMP-9 and MMP-14 in this cell line [377]. Further data published by Xia *et al.* demonstrated that angiogenin treatment activated NF-κB in U87-MG and increased cell proliferation, whereas knockdown of the NK-κB pathway suppressed angiogenin-induced cell proliferation [257]. Therefore, determining the effect of our cannabinoid test compounds on NF-κB activity is critical due to the important role played by this effector in driving both glial cell proliferation and pro-inflammatory activity.

4.2.1.2   ERK1/2

ERK1/2 (also known as ERK42/44) is part of a complex intracellular signaling cascade which regulates cell proliferation and cell survival. ERK1/2 is converted into its active form upon phosphorylation. Phosphorylated ERK1/2 (p-ERK1/2) translocates to the nucleus where it ultimately works to enhance transcription of growth-related proteins, including c-Fos. Translocation of p-ERK1/2 to the nucleus is required for the G_0 to G_1 cell cycle transition [378] and is also involved in driving the transition from G_1 to S phase during cell proliferation [379,380]. Furthermore, CB2 receptor activation has been shown previously to reduce pro-inflammatory activity and cell migration in microglia specifically via inhibition of ERK1/2 phosphorylation [381]. The ability of the test compounds to reduce p-ERK1/2 levels may therefore confer a possible therapeutic benefit by limiting glial cell differentiation, proliferation and pro-inflammatory activity within the context of gliosis. On the other hand, some CB2 receptor agonists have been found to increase the activity of ERK1/2, as noted above. Such

113

actions of our test compounds may therefore promote glial cell proliferation and inflammation. Therefore, discerning the specific effect of each of the CB2 test compounds on ERK1/2 activation in glial cells is critical.

4.2.1.3   PI3K

Activated PI3K (*i.e.*, phosphorylated PI3K or p-PI3K) is involved in driving cell proliferation, survival, as well as tumorigenesis and cell invasion in several cell types, including U87-MG astrocytes [382,383]. Given the literature discussed above implicating cannabinoids in driving PI3K activation and increased activity of ERK1/2 in PC-3 cells, it is critical to screen our compounds for the presence of this undesired effect. *I.e.*, activation of p-PI3K in response to treatment with our test compounds may drive gliosis by enhancement of proliferation in concert with ERK1/2. Reduction in p-PI3K concentrations, on the other hand, would suggest that the test compounds may be capable of limiting cell proliferation.

4.3   Materials and Methods

All experimental reagents and cell culture supplies were obtained from Thermo Fisher Scientific (Waltham, USA), unless otherwise specified. HEK-293 cells were generously donated from the Kumar Laboratory in UBC Pharmaceutical Sciences. THP-1 cells were generously shared by the Dutz Laboratory at BC Children's Hospital Research Institute. U87-MG cells were kindly shared by Dr. Guillaume Amouroux at the BC Cancer Research Centre.

HEK-293 and U87-MG cells were cultured in DMEM with 10% fetal bovine serum and 1% w/v penicillin/streptomycin (10,000 units/mL penicillin and 10 mg/mL streptomycin in sterile 0.9% NaCl). THP-1 cells were cultured in suspension in RPMI with 10% fetal bovine

serum and 1% w/v penicillin/streptomycin. Prior to assays, THP-1 cells were incubated in media containing 100 nM phorbol 12-myristate 13-acetate (Abcam, Cambridge, UK) for 72 h to induce cell differentiation into the adherent macrophage phenotype.

4.3.1 MTT, Cell Proliferation and Cell Death Assays

4.3.1.1 MTT Assay

Mitochondrial respiration was assessed via MTT assay in HEK-293, THP-1 and U87-MG cells. In order to perform the assay, an optimized number of cells were seeded in 96-well cell culture plates in 200 µL media per well. Cells were incubated at 37°C in 5% CO_2 for a 24 h growth period. Media was then aspirated and replaced with serum-free media followed by another 24 h incubation period. Media was then aspirated and replaced with treatment-containing media with full serum. Cells were then incubated for another 24 h (treatment period). Twenty µL of 5 mg/mL sterile-filtered methylthiazolyldiphenyl-tetrazolium bromide (Millipore-Sigma, Oakville, Canada) in PBS was then added to each well and cells were then incubated for 3 h. All wells were aspirated and replaced with 100 µL DMSO for formazan dissolution. Absorbance at 570 nm was read in a Pherastar™ spectrophotometer. All absorbance data was normalized to control (vehicle treatment) wells. Each experimental treatment was assayed in triplicate and data shown represent the average of three independent experiments. IC_{50} values were calculated using non-linear regression to a three parameter sigmoidal dose-response curve using GraphPad Prism® software.

4.3.1.2 Cell Proliferation

To measure cell proliferation, cells were seeded in 96 well plates and incubated in 200 µL media for a 24 h growth period. Media was then aspirated and replaced with serum-free media followed by another 24 h incubation period. Media was then aspirated and replaced with treatment-containing media with full serum. Cells were then incubated for another 24 h (treatment period). At the end of the treatment period, cell confluence was determined using Incucyte® imaging software. Cell proliferation was defined as the mean cell confluence of the treatment group divided by the mean cell confluence with vehicle treatment. Each experimental treatment was assayed in triplicate and data shown represent the average of three independent experiments.

4.3.1.3 Cell Death

To measure cell death, cells were seeded in 96 well plates and incubated in 200 µL media for a 24 h growth period. Media was then aspirated and replaced with serum-free media followed by another 24 h incubation period. Media was then aspirated and replaced with treatment-containing media with full serum as well as 100 nM YOYO®-1 (Life Technologies, Carlsbad, USA), followed by incubation for another 24 h (treatment period). At the end of the treatment period, cell death was determined using Incucyte® with phase microscopy combined with fluorescence imaging. Cell death was calculated as the percent YOYO®-1 fluorescence area divided by overall cell confluence area. Overall cell death was defined as mean cell death with treatment divided by mean cell death with vehicle treatment. Treatments were assayed in triplicate and data presented represent the average of three independent experiments.

4.3.2   Western Blot Intracellular Marker Probing

4.3.2.1   Cell Culture, Treatment, Sample Preparation

U87-MG cells were seeded into 6-well plates at a density of 750,000 cells/well in DMEM supplemented with 10% fetal bovine serum, and 1% w/v penicillin/streptomycin. Following 20 h of incubation at 37°C and 5% CO_2, media was aspirated, cells were washed once with PBS and 1 mL of treatment-containing media was added to each well. N=3 wells per treatment group. The treatment concentration of each test compound was 50 µM and the treatment period was 16 h at 37°C and 5% CO_2. The vehicle for β-caryophyllene and DML-4 was 0.5% v/v DMSO, while the vehicle for DML-3 was 1.5% v/v DMSO. At the end of the treatment period, media was aspirated and the cells were washed twice in PBS. The cells in each well were then lysed using 150 µL RIPA with protease and phosphatase inhibitors (New England Biolabs, product number 9806) on ice for 10 min. The lysate was collected and homogenized via sonication, and then centrifuged to remove cell debris and nuclei (500 x g for 10 min). The sample protein concentration was then determined via fluorescamine assay, as described by Udenfriend *et al.* [384] and adapted to 96-well plate format by Lorenzen *et al.* [385] (fluorescamine assay protocol listed in Appendix B.1).

4.3.2.2   SDS-PAGE Electrophoresis

Samples were mixed with an equal volume of Laemmli buffer 2X (BioRad, Hercules, USA) and boiled at 100 °C for five min for protein denaturing. Samples were loaded, 30 µg protein per lane, into 1.5 mm thick 8% polyacrylamide gel and run at 100 V for 80 min under constant voltage. Protein in the gel was then transferred to a PVDF membrane using electrophoresis, 100 V for 90 min.

4.3.2.3 Immunoblotting and Imaging

Membranes were blocked in tris-buffered saline, pH 7.4, with 0.1% v/v Tween-20

(TBST) containing 5% w/v skim milk powder at room temperature for 1 h with mild agitation.

Blocking buffer was removed and fresh blocking buffer containing all three primary antibodies

was added to the membranes followed by overnight incubation at 4°C with gentle rocking. The

following primary antibodies and optimized dilutions were used: New England Biolabs® rabbit

anti-phospho NF-κB (Product number 3033), 1:1000 dilution; rabbit anti-phospho-p44/42

MAPK (ERK1/2) (Product number 9101), 1:700 dilution; and Sigma® rabbit anti-phospho-PI3-

kinase p85 (SAB4504315), 1:500 dilution. The membrane was then washed in TBST 3 times, for

5 min each with mild agitation at room temperature. Blocking buffer containing Jackson® goat

anti-rabbit-HRP-conjugated secondary antibody, 1:1000 dilution, was then added to the

membranes and incubated for 1 h at room temperature with mild agitation. After 3 washes in

TBST, 5 min each, ECL solution (Cell Signaling, Danvers, USA) was then added to the

membrane for HRP development (approximately 5 min development time) and the membranes

were imaged using a chemiluminescence imaging system. Densitometry analysis was performed

using Image Pro® software and data were normalized to β-actin.

4.3.2.4 Membrane Stripping and Re-probing for Beta-Actin

Membranes were then washed four times, 5 min each, in TBST, then stripped of

antibodies by incubation at 50°C for 30 min with mild agitation in stripping buffer. Following 6

washes in TBST, 5 min each, the membranes were blocked in TBST-5% milk blocking buffer at

room temperature for 1 h with mild agitation. The buffer was removed and mouse HRP-

118

conjugated anti-beta-actin (BioLegend product number 643807), 1:1000 dilution, in blocking buffer was added. Following an overnight incubation at 4°C with mild agitation and three subsequent washes in TBST, 5 min each, the membrane was developed with ECL solution an imaged, as per the procedure described above.

4.3.3   Cytokine Secretion Assays

U87-MG cells were seeded at 750,000 cells per well in 6 well cell culture plates in 2 mL media and were incubated for an 18 h growth period at 37°C and 5% CO_2. Following the growth period, the media was aspirated and each well was washed twice with PBS. One mL of fresh, treatment-containing media was added to each well followed by a 2 h treatment incubation period. Optimization experiments justifying the use of these parameters are presented in Appendix B.2. Following the treatment period, the cell culture supernatant was collected and immediately frozen at -80°C until the assay was performed.

IL-6 and IL-8 supernatant concentrations were determined using ELISA (R&D Systems Human IL-6 and IL-8 Quantikine ELISA Kits; respective product numbers 6050 and 8000C) following the manufacturer's protocol. One sample was obtained per cell culture well and each treatment group consisted of n=3 wells. All samples were assayed in duplicate. Absorbance was read at both 450 nm and 540 nm. The signal at 540 nm has been subtracted from the OD 450 nm value reported (as per the manufacturer's protocol). Cell culture media was used as the assay blank. Cytokine concentrations were interpolated from the assay standard curves (shown in Appendix B.2) using GraphPad Prism® software.

4.3.4 Statistical Analysis

For both Western blot intracellular marker experiments and cytokine secretion assays, statistical analysis was performed using one-way ANOVA followed by Dunnett's post-hoc analysis to test for differences between treatment and vehicle control. A p-value of less than 0.05 was considered statistically significant.

4.4 Results

4.4.1 Effects of CB2 Ligands on Mitochondrial Respiration, Cell Proliferation and Cell Death

In vitro experiments to measure cell proliferation and mitochondrial respiration in response to CB2 ligand treatment were initially conducted in an endothelial cell line (HEK-293 cells) and immune cell line (THP-1 monocytes). Subsequently, the effect of the test compounds on proliferation, mitochondrial respiration and cell death was studied in U87-MG astrocytes using Triton X-100® as a cytotoxic comparator.

4.4.1.1 HEK-293 and THP-1 Cell Proliferation and Mitochondrial Respiration

Upon cannabinoid treatment of HEK-293 cells, concentration-dependent anti-proliferative effects were observed. Specifically, β-caryophyllene treatment resulted in the strongest anti-proliferative effect out the three CB2 ligands (Figure 4.1). Cell proliferation was reduced to 53% of the vehicle control at the 25 µM treatment concentration. Although higher data variability was observed at the highest three β-caryophyllene treatment concentrations, cell proliferation was reduced to 40.4% of the control group as a maximal effect of the treatment. The estimated IC_{50} value was 0.64 µM (Table 4.1). In contrast, only a minor anti-proliferative effect

was observed with DML-3 treatment at concentrations above 10 µM, with considerable

variability in the data. The maximal effect was a reduction in cell proliferation to 79.6% of the

vehicle control. The estimated IC_{50} value was 5.7 µM (Table 4.1). More robust anti-proliferative

effects were, however, observed with DML-4 treatment at concentrations above 1 µM. The

strongest anti-proliferative effect observed with DML-4 treatment was 58% of vehicle control at

the 100 µM concentration. The estimated IC_{50} value was 24.7 µM (Table 4.1).
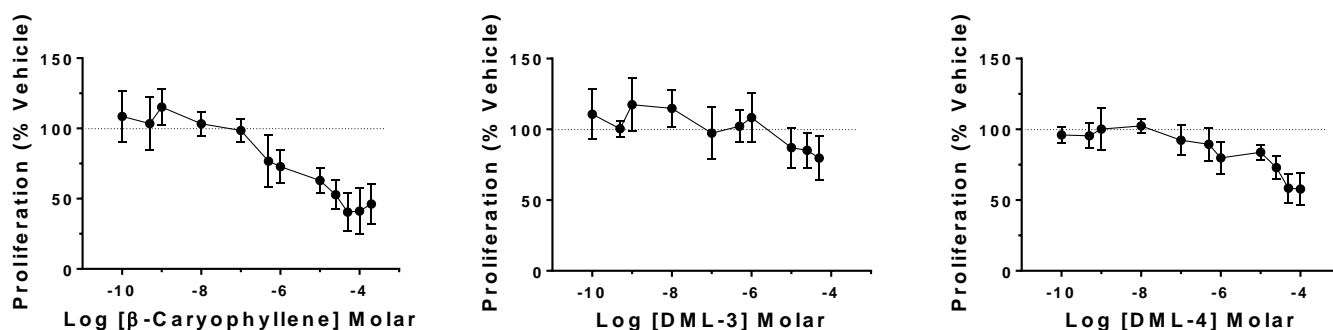
Figure 4.1. HEK-293 cell proliferation in response to cannabinoid treatment. Data points represent
the average of three independent experiments ± SD.
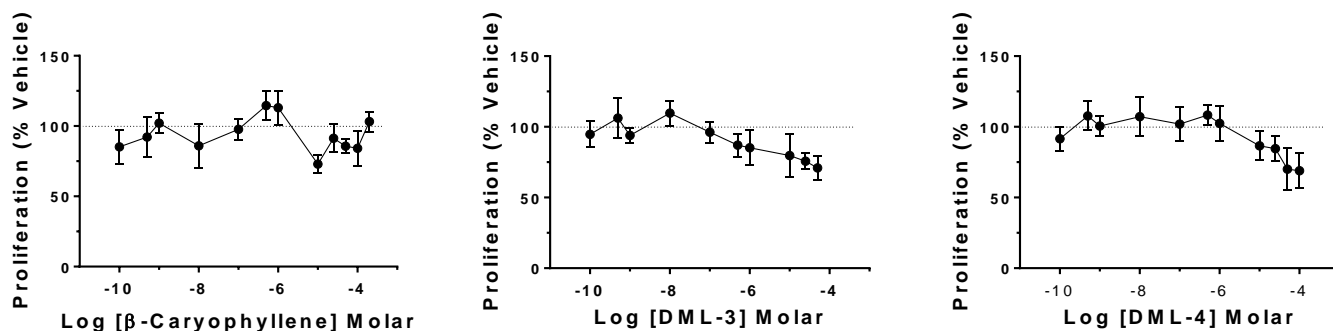
Figure 4.2. THP-1 cell proliferation in response to cannabinoid treatment. Data points represent the
average of three independent experiments ± SD.

In contrast to HEK-293 cells, anti-proliferative effects were not apparent in THP-1 cells with β-caryophyllene treatment (Figure 4.2). DML-3 treatment did, however result in reduced cell proliferation with a maximum reduction of 74.6% of the vehicle control and an estimated IC_{50} of 0.59 µM (Table 4.1). Modest anti-proliferative effects were also observed with DML-4 treatment in THP-1 cells. The inhibition of proliferation was strongest (70.1% of the control) at the highest concentration of 100 µM and the estimated IC_{50} was 22.4 µM (Table 4.1).

Figure 4.3. HEK-293 mitochondrial respiration in response to cannabinoid treatment.
Data points represent the average of three independent experiments ± SD.

Figure 4.4. THP-1 mitochondrial respiration in response to cannabinoid treatment.
Data points represent the average of three independent experiments ± SD.

122

In HEK-293 cells, mitochondrial respiration was profoundly impacted by treatment with both β-caryophyllene and DML-4 (Figure 4.3). The maximum reduction in mitochondrial respiration (21.2% of vehicle) occurred with 100 µM β-caryophyllene treatment while the top concentration of DML-4 tested (100 µM) resulted in a reduction of mitochondrial respiration to 27.5% of vehicle control (Table 4.2). In contrast, DML-3 treatment had considerably less impact on HEK-293 mitochondrial respiration. The maximal effect of DML-3 treatment was 85% of the vehicle control at 50 µM treatment while the estimated IC_{50} value was 6.2 µM (Table 4.2).

In THP-1 cells, treatment with each of the CB2 ligands resulted in only minor effects on mitochondrial respiration (Figure 4.4). β-caryophyllene produced the greatest effect (84.8% of vehicle control) at 100 µM while dose-response effects on mitochondrial respiration were not observed with DML-3 and DML-4 treatment (Table 4.2).

4.4.1.1.1   Cell Death Observations

The considerable decline in cell proliferation and mitochondrial respiration observed in HEK-293 cells in response to β-caryophyllene and DML-4 treatment (Figures 4.1 and 4.3, respectively) prompted a visual inspection of the phase microscopy images captured by the Incucyte® system (see Figures 4.5 and 4.6 below).

A	**B**	**C**	**D**
25 µM	50 µM	100 µM	200 µM

E	**F**	**G**	**H**
0.25% DMSO	0.5% DMSO	1% DMSO	2% DMSO
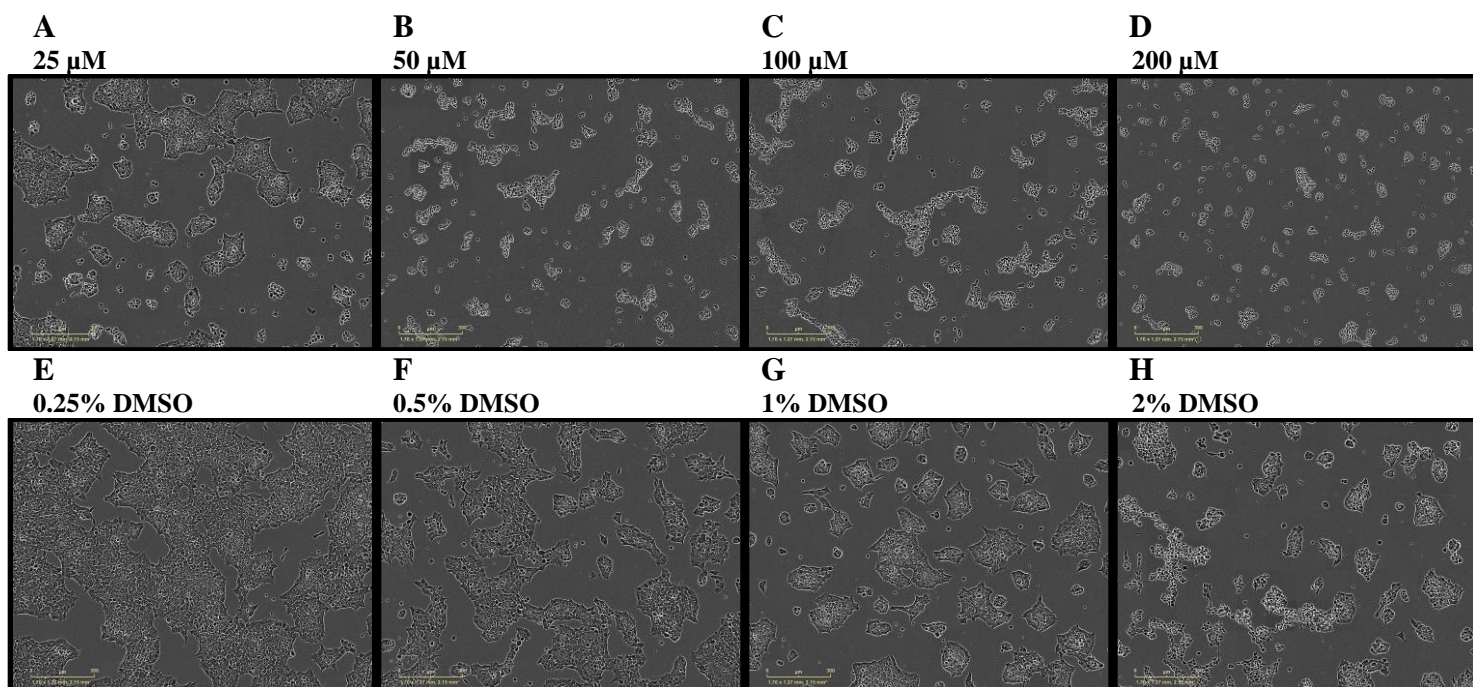
Figure 4.5. Phase microscopy images of HEK-293 cells following 24 h treatment with β-caryophyllene (top row) and the corresponding DMSO vehicle (bottom row) at the specified concentrations

A	**B**	**C**	**D**
10 µM	25 µM	50 µM	100 µM

E	**F**	**G**	**H**
0.1% DMSO	0.25% DMSO	0.5% DMSO	1% DMSO
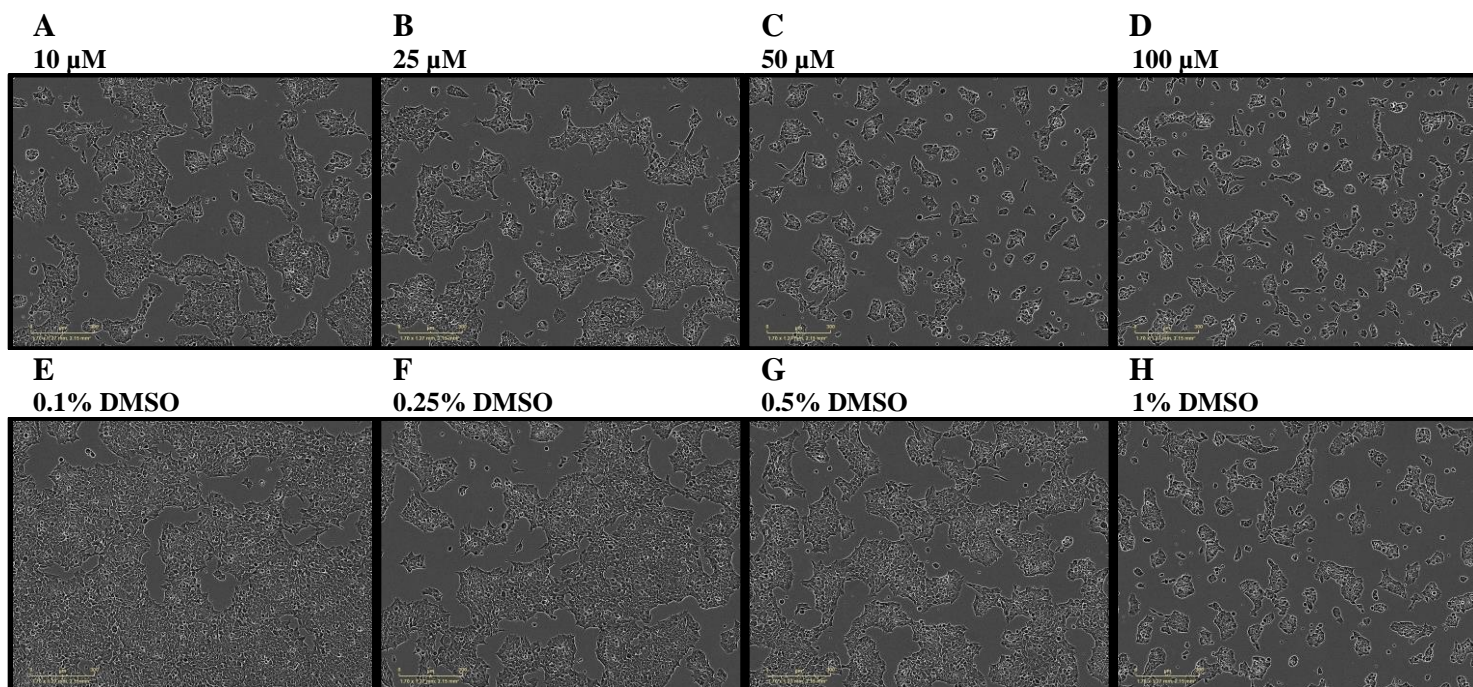
Figure 4.6. Phase microscopy images of HEK-293 cells following 24 h treatment with DML-4 (top row) and the corresponding DMSO vehicle (bottom row) at the concentrations specified.

As seen in Figure 4.5, the uniformly different morphology of the cells treated with 50 to 200 µM β-caryophyllene (*i.e*., smaller size, round shape, non-adherence) suggests widespread cell death. Cell death also appeared to be present, based on morphological appearance, in the 25 µM treatment group in a lesser proportion of cells. Although the morphological changes suggesting cell death with β-caryophyllene treatment may be attributable to the presence of the DMSO vehicle, the same morphological changes are not present in the majority of vehicle-treated cells (Figure 4.5, bottom row), suggesting that β-caryophyllene, and not the vehicle, is responsible for the effect. Although a portion of the cells appear dead in the 2% DMSO vehicle group, much of the cell population appears to be adherent with typical HEK-293 cell morphology. In contrast, DML-4 treatment did not seem to induce the same widespread morphological changes, suggestive of cell death, as β-caryophyllene (Figure 4.6). The effect of DML-4 in limiting cell proliferation, relative to the vehicle, was apparent in a dose-dependent manner.

Based on these observations, it was suspected that β-caryophyllene may cause cell death at concentrations above 25 µM, rather than exerting a true anti-proliferative effect in living cells. YOYO®-1 (Life Technologies, Carlsbad, USA), a fluorescent cyanine dimer nucleic acid stain impermeable to living cells, was therefore utilized to quantify cell death in subsequent studies in U87-MG astrocytes.

4.4.1.2 U87-MG Cell Proliferation, Mitochondrial Respiration and Death

4.4.1.2.1 β-caryophyllene

In U87-MG cells, reductions in cell proliferation were observable only at the top two concentrations of β-caryophyllene tested (100 and 200 µM; Figure 4.7). The magnitude of the

maximal effect was high (14.7% of vehicle control; Table 4.1). Importantly though, signs of

cytotoxicity were apparent within this concentration range. Specifically, reductions in

mitochondrial respiration became apparent at 25 µM and markedly increased upon treatment

with higher concentrations (Figure 4.8). Mitochondrial respiration was maximally reduced with

200 µM β-caryophyllene treatment (13.7% of vehicle; Table 4.2). Furthermore, considerable cell

death was observed with 100 µM and 200 µM treatments (334.9% and 3818.0% death of the

vehicle control, respectively; Figure 4.9). The cell death observed with 200 µM β-caryophyllene

treatment was roughly equivalent to that produced by 0.5% v/v Triton X-100® (Figure 4.9).

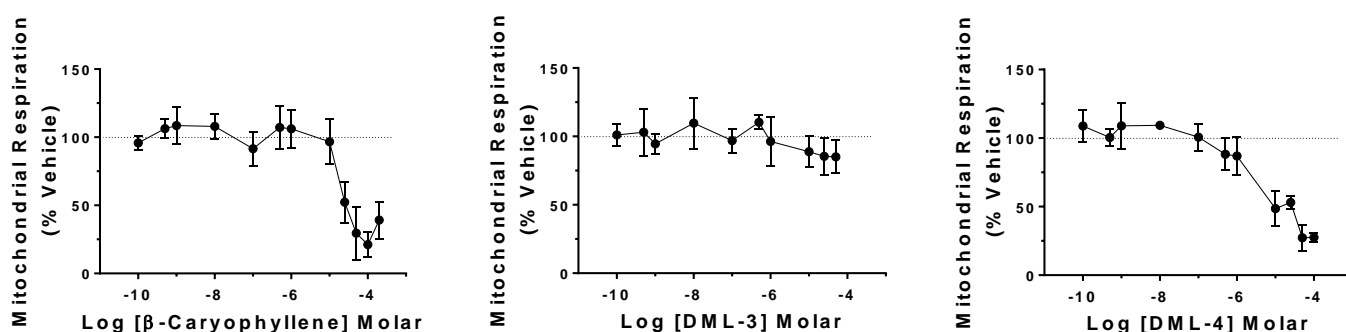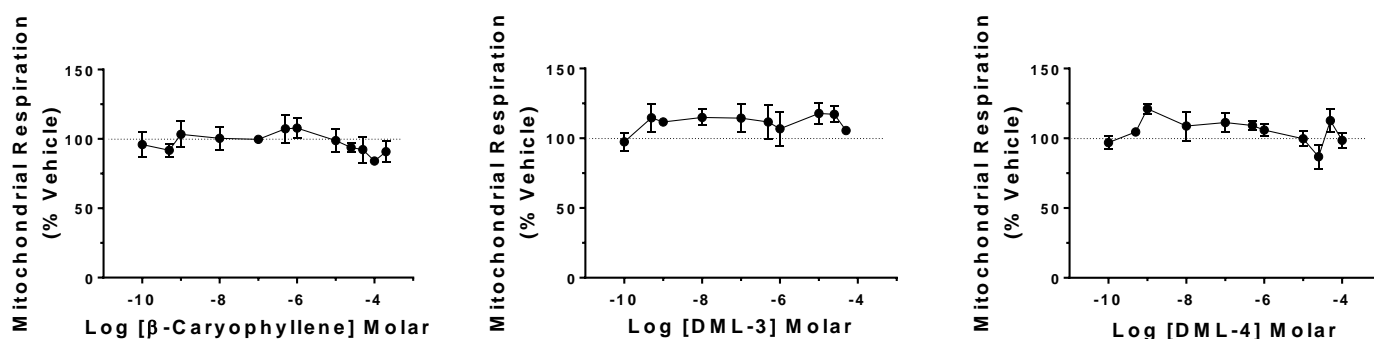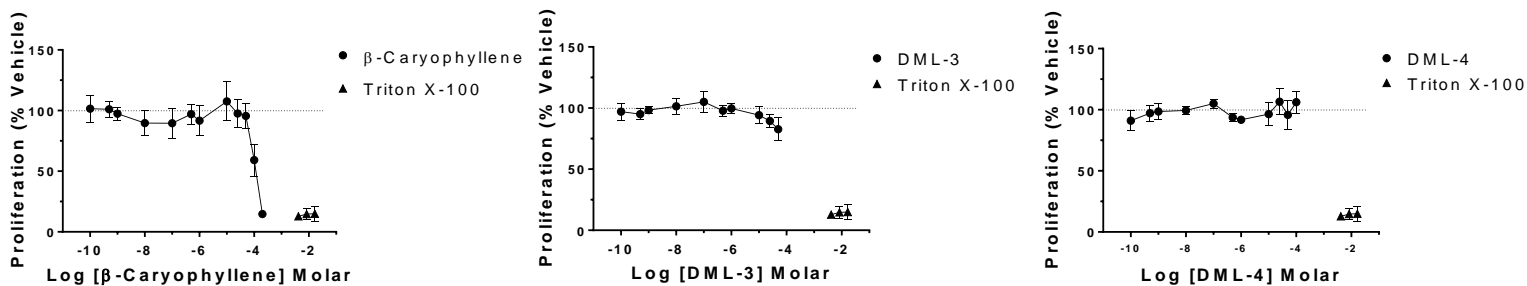**Figure 4.7. U87-MG proliferation in response to cannabinoid treatment.**
Data points represent the average of three independent experiments ± SD.
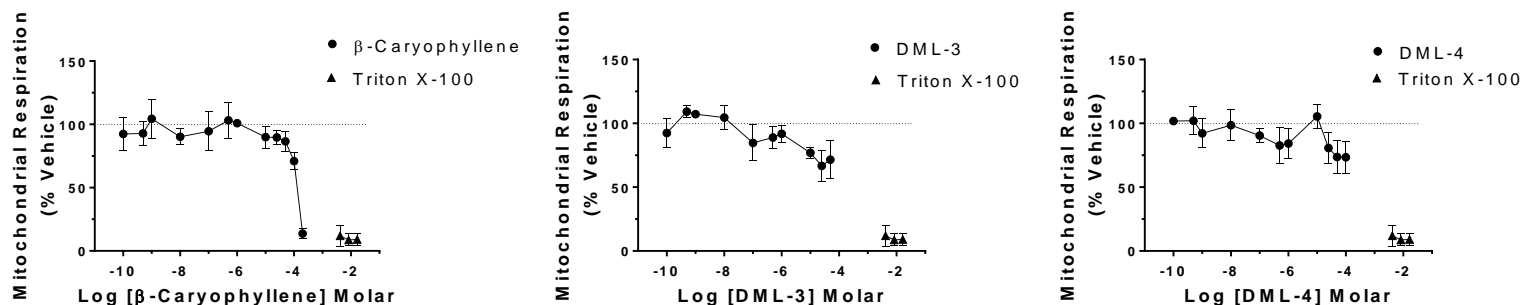
Figure 4.8. U87-MG mitochondrial respiration in response to cannabinoid treatment.
Data points represent the average of three independent experiments ± SD.

126
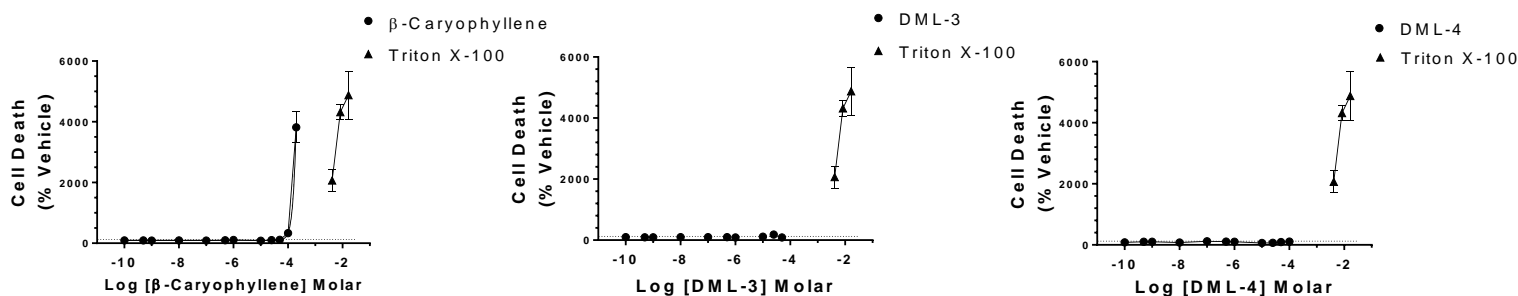
Figure 4.9. U87-MG cell death in response to cannabinoid treatment.
Data points represent the average of three independent experiments ± SD.

4.4.1.2.2   DML-3

In U87-MG, a minor anti-proliferative effect was observed with DML-3 treatment

(Figure 4.7). The maximum response was 82.7% of vehicle proliferation with 50 µM treatment

and the estimated IC_{50} was 89.5 µM (Table 4.1). In terms of cell toxicity, DML-3 produced

modest reductions in mitochondrial respiration (Figure 4.8), and no indication of cell death, at

concentrations up to 50 µM (Figure 4.9). Mitochondrial respiration was maximally reduced to

70.1% of vehicle control with 50 µM DML-3 treatment and the estimated IC_{50} value was 1.2 µM

(Table 4.2).

Table 4.1. Maximal inhibition of cell proliferation and IC_{50} values in response to CB2 ligand treatment.
Table values represent the average from three independent experiments.
[a]Data did not converge to fit the non-linear regression model or fit was poor ($R^2 < 0.25$).

Test Compound	Cell Proliferation Maximal Inhibition (% Vehicle Proliferation)			IC_{50} (µM)		
	HEK293	THP-1	U87-MG	HEK293	THP-1	U87-MG
β-Caryophyllene	40.4	88.4	14.7	0.64	47.6	
DML-3	79.7	74.6	82.7	5.7	0.59	89.5
DML-4	57.8	70.5	99.4	24.7	22.4	-[a]

Table 4.2. Maximal inhibition of mitochondrial respiration and IC_{50} values in response to CB2 ligand treatment.
Table values represent the average from three independent experiments.
[a]Data did not converge to fit the non-linear regression model or fit was poor ($R^2 < 0.25$).

Test Compound	Mitochondrial Respiration Maximal Inhibition (% Vehicle Respiration)			IC_{50} (µM)		
	HEK293	THP-1	U87-MG	HEK293	THP-1	U87-MG
β-Caryophyllene	21.2	84.8	13.7	22.8	35.9	4.9
DML-3	85.0	97.4	70.1	6.2	-[a]	3.6
DML-4	30.2	86.8	73.5	3.2	-[a]	-[a]

Table 4.3. Maximal U87-MG cell death and EC_{50} values in response to CB2 ligand treatment.
Table values represent the average from three independent experiments.
[a]Data did not converge to fit the non-linear regression model or fit was poor ($R^2 < 0.25$).

Test Compound	Maximal Death (% Vehicle)	EC_{50} (µM)
β-Caryophyllene	3818.0	291
DML-3	132.8	4.0
DML-4	117.4	-[a]

4.4.1.2.3   DML-4

Reductions in U87-MG cell proliferation were not detected with DML-4 treatment at concentrations up to 100 µM (Figure 4.7). With respect to cell toxicity, DML-4 treatment caused modest reductions in mitochondrial respiration at concentrations of 25 µM and above (Figure 4.8). The maximum effect of DML-4 on mitochondrial respiration was 73.5% of the vehicle control (Table 4.2). DML-4 did not appear to be cytotoxic to U87-MG cells as very low rates of cell death were observed across all treatment concentrations tested (Figure 4.9).

4.4.2   Effects of CB2 Agonists on Intracellular Pathways Modulated by CB2 in Astrocytes

Using western blot experiments, the effect of our investigational CB2 agonists on expression of p-PI3K, p-NF-κB and p-ERK1/2 was tested in U87-MG astrocytes (Figure 4.10). Densitometry data in Tables 4.4, 4.5 and 4.6 show reasonably good agreement between the two experimental replicates performed. The average data plotted in Figure 4.11 indicate that β-caryophyllene, DML-3 and DML-4 all significantly reduced the expression of each active biomarker.

A
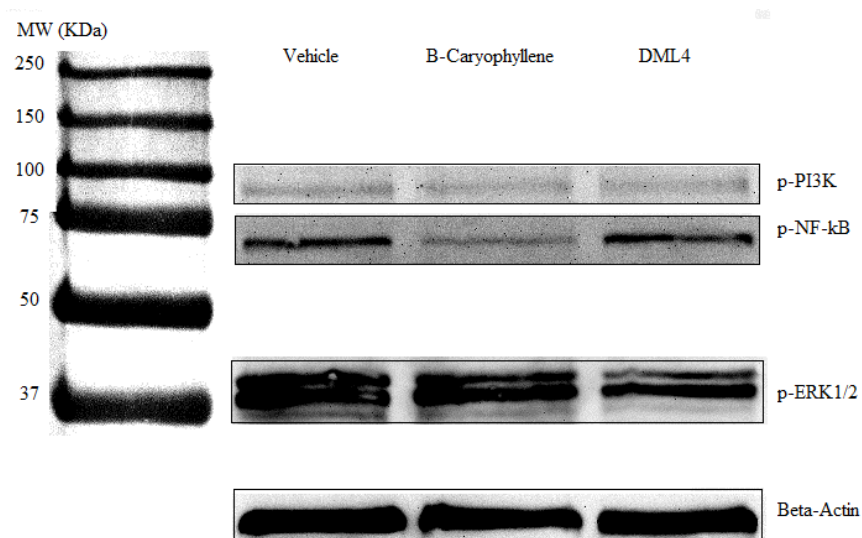
B
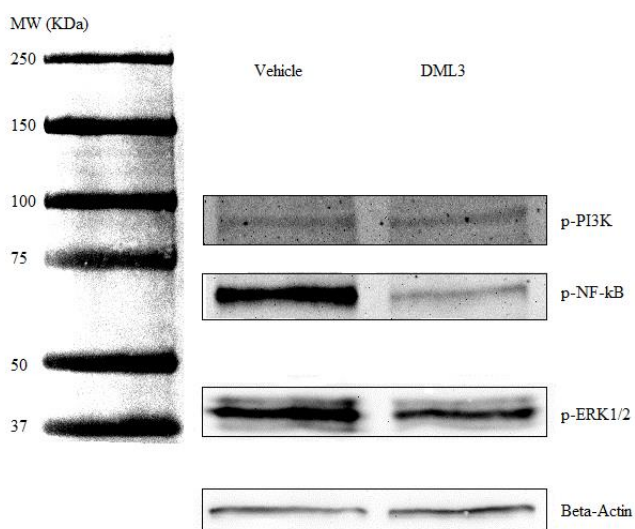
Figure 4.10. Western blots showing expression of phosphorylated PI3K, NF-κB and ERK1/2 in response to cannabinoid treatment.
U87-MG cell lysates were probed for expression of biomarkers following treatment with 50 µM β-caryophyllene, DML-4 (A) and DML-3 (B) and the corresponding vehicle treatment.

Table 4.4. Mean densitometry of p-PI3K following CB2 ligand treatment, expressed as percent of vehicle, as calculated from western blot replicates 1 and 2.

Test Compound	Rep 1	Rep 2	Mean	SD
β-Caryophyllene	74.02	52.16	63.12	15.50
DML-3	58.31	77.02	67.66	13.23
DML-4	80.37	60.41	70.39	14.11

Table 4.5. Mean densitometry of p-NF-κB following CB2 ligand treatment, expressed as percent of vehicle, as calculated from western blot replicates 1 and 2.

Test Compound	Rep 1	Rep 2	Mean	SD
β-Caryophyllene	27.52	30.00	28.76	1.75
DML-3	33.92	26.16	30.04	5.48
DML-4	78.69	61.32	70.00	12.29

Table 4.6. Mean densitometry of p-ERK1/2 following CB2 ligand treatment, expressed as percent of vehicle, as calculated from western blot replicates 1 and 2.

Test Compound	Rep 1	Rep 2	Mean	SD
β-Caryophyllene	71.21	50.81	61.01	14.42
DML-3	55.47	75.98	65.72	14.51
DML-4	38.94	45.72	42.33	4.79
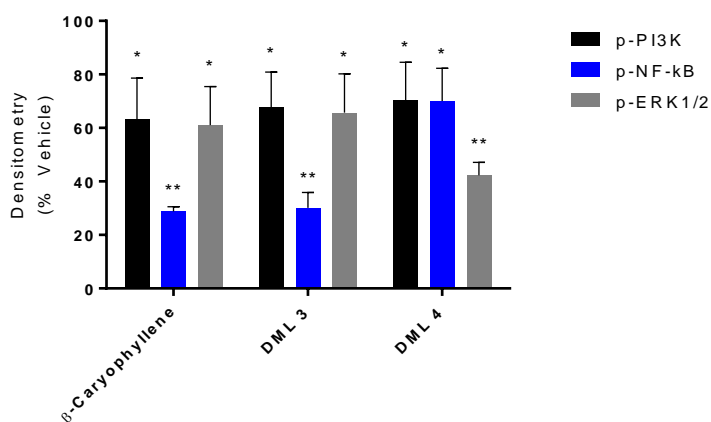
Figure 4.11. Intracellular expression of phosphorylated PI3K, NF-κB and ERK1/2 in response to cannabinoid treatment.
Mean band densitometry, normalized to beta-actin, shows the expression of phosphorylated biomarkers in U87-MG cell lysates in response to treatment with 50 µM β-caryophyllene, DML-3 and DML-4, expressed as percent of vehicle. The mean of 2 independent experimental replicates is shown ± SD. * $p < 0.05$; ** $p < 0.01$.

All three CB2 agonist compounds lowered the expression of p-PI3K to a similar extent, ranging from 63 – 70% of vehicle control (Figure 4.11). Reductions in p-ERK1/2 expression were also observed in response to treatment with each CB2 agonist, with the greatest effect observed with DML-4 treatment (42% of the vehicle control; Figure 4.11). Based on the reductions in both p-PI3K and p-ERK1/2, each of the CB2 agonists may be capable of limiting glial cell growth and proliferation by limiting the activation of downstream molecular targets involved in cell cycle regulation.

With respect to NF-κB regulation, both β-caryophyllene and DML-3 showed a strong ability to reduce its activation (29 and 30% p-NF-κB expression of the vehicle control, respectively). DML-4 treatment also significantly reduced p-NF-κB expression (70% of the vehicle; Figure 4.11). This data suggests that each of the CB2 ligand compounds may be capable of limiting the expression of downstream transcription targets of NF-κB including cytokines and other pro-inflammatory mediators.

4.4.3   Effects of CB2 Ligands on Pro-Inflammatory Cytokine Secretion in Astrocytes

As shown in Figure 4.12, 1 µM β-caryophyllene treatment significantly reduced secretion of IL-6 and IL-8 in U87-MG astrocytes in a CB2 antagonist (AM630)-dependent manner. The magnitude of the effect was comparable to the positive control cannabinoid WIN-55,212-2. In contrast, neither DML-3 nor DML-4 reduced cytokine secretion at 1 µM treatment concentrations, although a non-significant trend suggesting lower cytokine levels was observed (Figure 4.12).

A
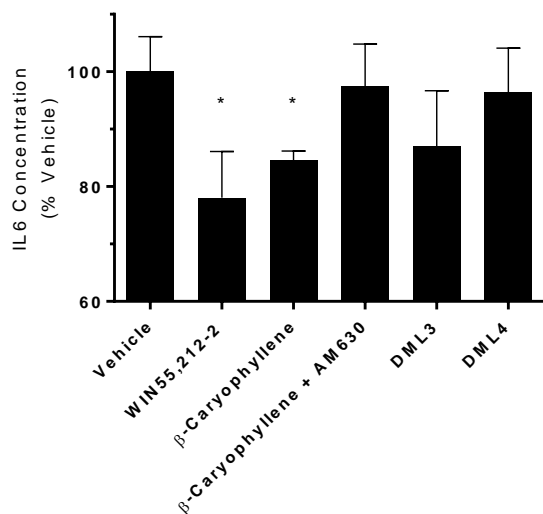
B
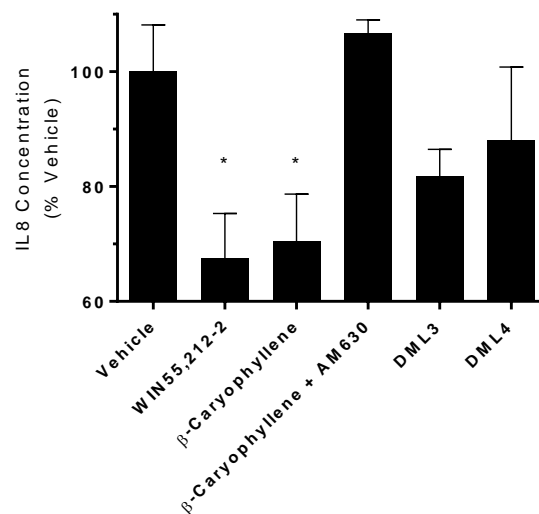
Figure 4.12. Changes in pro-inflammatory cytokine secretion in U87-MG astrocytes in response to 1 μM cannabinoid treatment.
IL-6 (A) and IL-8 (B) concentrations measured in U87-MG culture supernatant following 2 h treatment with cannabinoid test compounds. The mean of n=3 culture supernatants is shown $\pm$ SD. * $p<0.05$.

C
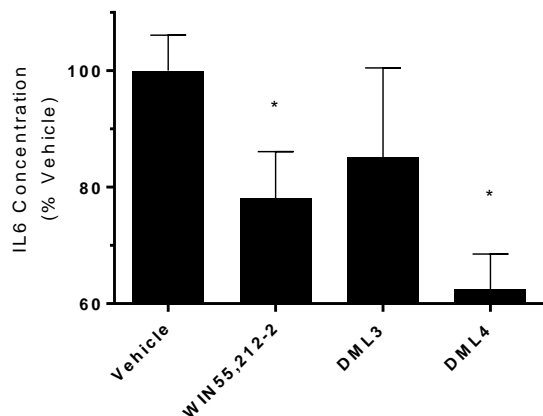
D
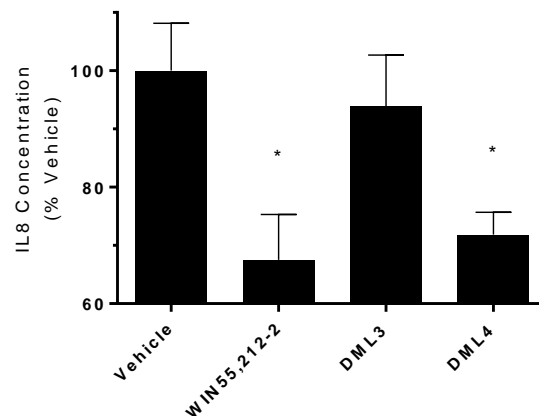
Figure 4.13. Changes in pro-inflammatory cytokine secretion in U87-MG astrocytes in response to 25 μM cannabinoid treatment.
IL-6 (A) and IL-8 (B) concentrations measured in U87-MG culture supernatant following 2 h treatment with cannabinoid test compounds. The mean of n=3 culture supernatants is shown $\pm$ SD. * $p<0.05$.

At a 25 µM treatment concentration, DML-4 significantly reduced IL-6 and IL-8 secretion in U87-MG cells (Figure 4.13). Although marginal reductions in cytokine secretion were observed with DML-3 treatment, the effects at 25 µM were not statistically significant.

4.5   Discussion

4.5.1   Toxicity

Several assays are commonly used to evaluate end-point parameters indicative of cytotoxicity during screening of investigational compounds. These include the use of MTT for evaluation of mitochondrial respiration (also considered an evaluation of cell viability), sulphorhodamine B (SRB) for evaluation of cell proliferation, measurement of lactate dehydrogenase (LDH) and glutathione (GSH) which become released when the cell membrane loses integrity, as well as the use of cell impermeable fluorescent nuclear stains to determine membrane integrity loss and cell death, such as YOYO®-1. In the present study, cytotoxicity of our three CB2 agonist test compounds, β-caryophyllene, DML-3 and DML-4 was evaluated using MTT and YOYO®-1 assays to measure mitochondrial respiration and cell death, respectively. We also employed the use of Incucyte® imaging software to measure cell confluence as a means of quantifying cell proliferation.

As a general rule when assessing toxicity small molecules, assay IC_{50} values of less than 20 µg/mL are considered indicative of cytotoxicity. With respect to our test compounds, 20 µg/mL is equivalent to 97.9 µM, 67.7 µM and 64.6 µM for β-caryophyllene, DML-3 and DML-4, respectively. Considering only the assay IC_{50} value for a compound is not, however, sufficient to gauge the compound's cytotoxicity since the IC_{50} does not give an indication of the magnitude of the cytotoxic effect observed in the assay. IC_{50} simply indicates the drug concentration at

which the half-maximal response was observed. Therefore, a compound with an IC_{50} of, for example, 1 µg/mL may not in fact be cytotoxic if the maximal response observed in the assay was of low magnitude (*ex.* 90% cell viability, relative to the control). Therefore, both the magnitude of the maximal effect, relative to the vehicle control, and the IC_{50} value should be taken into account when gauging the cytotoxicity of a compound.

Out of the three investigational CB2 agonists, DML-3 appeared to be the least cytotoxic, with modest reductions in mitochondrial respiration in HEK-293 and U87-MG observed (maximal effects were 85.0 and 70.1% of the vehicle control, respectively), no apparent effect on mitochondrial respiration in THP-1 cells and no considerable ability to induce cell death. Similarly, minor, dose-dependent reductions in mitochondrial respiration were observed with DML-4 treatment in U87-MG (maximal reduction in respiration was 73.5% of the vehicle control at 100 µM) and no apparent effect on mitochondrial respiration observed in THP-1 cells. DML-4 did, however cause a considerable dose-dependent decrease in mitochondrial respiration in HEK-293 cells (maximal decline in respiration was 30.2% of the vehicle control and IC_{50} was 3.2 µM). This effect did not appear to be associated with cell death, however (Figure 4.6). Data from the YOYO®-1 cell death assay in U87-MG cells indicated that DML-4 treatment was not associated with cell death, at concentrations of up to 100 µM. In contrast, β-caryophyllene was associated with dose-dependent decreases in mitochondrial respiration in both HEK-293 and U87-MG (maximal decreases in respiration were 21.2 and 13.7% of vehicle control, respectively). Furthermore, concentrations at and above 50 µM appeared to cause considerable cell death in HEK-293 cells (Figure 4.5). The YOYO®-1 cell death assay in U87-MG cells revealed 335% and 3818% cell death relative to vehicle control at 100 and 200 µM β-caryophyllene concentrations, respectively.

The cytotoxic effects of β-caryophyllene in HEK293 and U87-MG cells were surprising, given that the compound is generally considered safe and the oral and acute dermal LD_{50} values both exceed 5 g/kg in rats and rabbits, respectively [176,386]. Furthermore, β-caryophyllene has been found to display low cytotoxicity upon MTT assay in cervical carcinoma (HeLa), hepatocarcinoma (Hep-G2), and fibroblast cells [387,388]. Some studies have, however, found cytotoxic effects of β-caryophyllene in certain cancer cell lines. For example, Kubo *et al.* reported IC_{50} values ranging from 19.0 – 23.8 µM β-caryophyllene in cervical carcinoma (HeLa), breast (BT-20) and melanoma (B-16 and HTB) cell lines using MTT assay [389]; Tundis *et al.* report IC_{50} values of 98.4 and 106.7 µM in treatment of melanoma (C32) and renal adenocarcinoma (ACHN) cell lines, respectively, using SRB assay [390]; Costa *et al.* found β-caryophyllene had an IC_{50} of 63.5 and 66.9 µM in hepatocarcinoma (Hep-G2) and promyelocytic leukemia (HL-60) cells, respectively, using the Alamar blue cytotoxicity assay [391]. However, in some cases, a botanically-derived essential oil containing β-caryophyllene as principal constituent, but not β-caryophyllene itself has produced cytotoxicity in cancer cells. These examples include the essential oil of *Guatteria pogonopus*, but not β-caryophyllene alone, having an IC_{50} < 20 µg/mL in ovarian adenocarcinoma (OVCAR-8), bronchoalveolar lung carcinoma (NCI-H358M) and metastatic prostate cancer (PC-3M) cell lines and the essential oil of *Zornia brasiliensis* but not β-caryophyllene alone having an IC_{50} < 20 µg/mL in melanoma (B16-F10) and chronic myelocytic leukemia (K562) cells [391,392]. β-caryophyllene was found to have low cytotoxicity in non-cancerous human peripheral macrophages (PBMC; IC_{50} > 25 µg/mL) [391]. Because our data demonstrate cytotoxicity of β-caryophyllene in both cancerous (U87-MG) and non-malignant (HEK-293) human cells, producing considerable cell death and reductions in mitochondrial respiration (with IC_{50} values well below < 20 µg/mL), there is reason to suspect

that the compound may not be selectively toxic to malignant cells and potentially harmful to healthy human cells above certain concentration thresholds. The cytotoxic effects observed in the present investigation were clearly dose-dependent, however, it is unknown whether the therapeutic doses of β-caryophyllene (*i.e.,* those ingested within the context of traditional herbal medicine) would result in potentially toxic concentrations in humans. Although pharmacokinetic data in humans is lacking, a single 50 mg/kg dose of β-caryophyllene administered orally to rats in complex with an absorption enhancer, β-cyclodextran, resulted in peak serum concentrations of 2.7 µM and no signs of toxicity [393]. It is, however, conceivable that through higher acute oral doses or via repeated administration, concentrations may be attained *in vivo* which have potentially cytotoxic effects.

4.5.2   Anti-proliferative Effects

With respect to β-caryophyllene, the anti-proliferative effects observed in HEK-293 occurred at concentrations of 1 µM and above while those observed in U87-MG occurred at only the 100 and 200 µM concentrations. In HEK-293 cells, β-caryophyllene treatment was not associated with declines in mitochondrial respiration at concentrations up to 10 µM. However, concentrations of 25 µM and above were associated with marked declines in mitochondrial respiration and the appearance of cell death. Therefore, treatment concentrations of β-caryophyllene between 1 – 10 µM may limit cell proliferation in the absence of cytotoxic effects in HEK-293 cells. In the case of U87-MG, the reduced cell proliferation observed at 100 µM and 200 µM concentrations was directly associated with reduced mitochondrial respiration and cell death. Therefore, the anti-proliferative effect in U87-MG astroglia with 100 – 200 µM β-caryophyllene may be due to the appearance of cell death. Although the western blot

137

investigations revealed that 50 µM β-caryophyllene strongly inhibits NF-κB activation, and, to a lesser extent ERK1/2 and PI3K activation, this treatment concentration was not associated with a significant decline in cell proliferation in U87-MG, and, higher concentrations were associated with considerable cytotoxicity.

Anti-proliferative effects were observed consistently at 25 µM and 50 µM concentrations of DML-3 in all three human cell lines tested. Although the magnitude of the effect was modest, treatment with DML-3 at these concentrations was not associated with reductions in mitochondrial respiration in HEK-293 and THP-1 cells and signs of cell death were not apparent. Although declines in mitochondrial respiration were observed at these treatment concentrations in U87-MG, cell death was not visible and the YOYO®-1 assay indicated no considerable cell death occurred. Since 50 µM DML-3 treatment also significantly reduced NF-κB and ERK1/2 activation, the reductions in cell proliferation observed with DML-3 treatment, particularly those in U87-MG astrocytes, may be mediated by the these intracellular transcription factors. DML-3 may therefore be capable of limiting cell proliferation within the context of gliosis.

DML-4 treatment was associated with concentration-dependent anti-proliferative effects in both HEK-293 and THP-1 cells, at concentrations starting at 1µM and 10 µM, respectively. No anti-proliferative effects were observed, however, in U87-MG cells. Although reductions in cell viability were observed upon MTT assay in both HEK-293 and U87-MG cells with an IC_{50} of approximately 3 µM, DML-4 treatment was not associated with reductions in cell viability in THP-1 cells, nor was any considerable cell death observed or measured in the YOYO®-1 assay. Therefore, anti-proliferative effects of DML-4 are not expected to coincide with any significant cytotoxicity. The western blot results indicating reduced activity of ERK1/2 and NF-κB with

DML-4 treatment were not, however, correlated with an observable reduction in U87-MG cell proliferation. DML-4 therefore may not be able to limit glial cell proliferation.

4.5.3   Anti-inflammatory Effects

While all three CB2 agonist compounds significantly reduced activation of NF-κB and ERK1/2 at 50 µM in U87-MG, suggesting the ability to mitigate pro-inflammatory effects in glia, β-caryophyllene was the only compound found to inhibit cytokine IL-6 and IL-8 secretion at 1 µM in a CB2-dependent manner. Although both β-caryophyllene and DML-3 reduced NF-κB and ERK1/2 activation with virtually identical magnitude, the expression of these intracellular markers did not correlate with reduced cytokine secretion upon DML-3 treatment as IL-6 and IL-8 production was not lowered to a significant extent at both 1 µM and 25 µM treatment concentrations. Although DML-3 treatment did produce an observable decline in cytokine levels at both 1 µM and 25 µM concentrations, there was considerable variation in the data and the effects were non-significant. An increased sample size and/or further experimental replicates may therefore be required to detect a reduction in cytokine secretion at these treatment concentrations if an effect truly exists. The results of the present investigation may also suggest that if DML-3 does possess anti-inflammatory effects, a longer treatment duration may be required in order for the effects to be observed, since the treatment period for the western blot of intracellular markers was 16 h, versus 2 h for the cytokine secretion assay. Therefore, a longer treatment period and/or an increased treatment concentration may have produced a detectable effect on cytokine secretion.

Although DML-4 did significantly reduce NF-κB activation, the magnitude of the effect and statistical significance were not as high compared to β-caryophyllene and DML-3. DML-4

139

was, however, the compound which exerted the strongest ability to reduce ERK1/2 activation. The effects of DML-4 on U87-MG cytokine secretion were non-significant at 1 µM, however a non-significant trend in reduced IL-8 concentrations were observed. At 25 µM, however a significant reductions in both IL-6 and IL-8 secretion were observed. Based on the intracellular marker data, these actions may be mediated by reductions in both ERK1/2 and NF-κB activity.

Chapter 5: Conclusions

The research described in the preceding chapters aimed firstly, to determine whether gliosis may contribute to the pathophysiology of chronic widespread musculoskeletal pain, and secondly, to develop and evaluate novel and existing CB2 agonist compounds for potential therapeutic application in centrally-mediated chronic pain.

5.1   Significance and Contribution of the Research

The findings presented in Chapter 2 provide evidence that chronic widespread musculoskeletal pain, such as that present in fibromyalgia syndrome, may indeed be centrally-mediated by gliosis. This is the first report demonstrating that glial cell activation develops in the lumbar spinal cord within a research model of chronic widespread musculoskeletal pain *in vivo*. The data suggest specifically that lumbar spinal cord astrocytes become activated in response to repeated peripheral skeletal muscle insults of reduced pH regardless of whether a behavioral pain response (*i.e.,* mechanical hyperalgesia) develops, implying sensitivity of this cell type to noxious peripheral input. These findings also suggest that astrocyte activation alone is insufficient for the development of bilateral hyperalgesia in this research model. The data furthermore point to microglia activation as a specific indicator of hyperalgesia development. This research provides the first specific evidence that spinal cord glial cell activation may be present in chronic widespread musculoskeletal pain. These findings also suggest that targeting gliosis may be a potentially viable pharmacotherapeutic strategy for addressing chronic widespread musculoskeletal pain.

Taking into account the research evidence suggesting that pharmacologic targeting of the endocannabinoid system, specifically, the CB2 cannabinoid receptor, may be beneficial for the

141

treatment of centrally-mediated chronic pain in the absence of adverse CNS effects, two novel compounds having such pharmacologic activity were developed and evaluated, as presented in Chapter 3. This work resulted in further optimization of previously identified adamantyl chemical compounds for the selective activation of the human CB2 receptor. Specifically, the novel compound DML-4 was found to act more potently as a CB2 agonist than the previous adamantyl compounds, with a cAMP EC_{50} value in the sub-nanomolar range. DML-3, a second novel compound, also had potent CB2 agonist activity in the low nanomolar range. Furthermore, DML-3 and DML-4 retained CB2-selectivity, with the fold-selectivity over CB1 being > 40 and > 10,000, respectively. This research investigation also led to the first full characterization of the binding affinity and agonist activity of the naturally occurring sesquiterpene compound, β-caryophyllene, at both cannabinoid receptors. As per the data presented in Chapter 3, β-caryophyllene is a full agonist at the human CB2 receptor with weak agonist activity at CB1, the selectivity toward CB2 being approximately 109-fold. Furthermore, this was the first investigation into the CB2 receptor binding interactions of β-caryophyllene within a CB2 homology model based on a human GPCR structure. Analogous to the previous homology model report, β-caryophyllene was found to adopt the most stable binding interaction within the hydrophobic pocket region of the CB2 active site. However, the strongest interactions in our model took place with aromatic residues distinct from those reported previously, likely owing to the minor conformational differences between the human and bovine GPCR crystal structure.

As demonstrated in Chapter 4, the novel compounds DML-3 and DML-4 have reasonably good *in vitro* cell toxicity profiles, although a great deal of further safety data would be required in order to determine the compounds' suitability for clinical study. This would need to include characterization of biodistribution, organ-specific toxicity, toxicokinetics, genotoxicity

142

and potential, reproductive toxicity, as well as LD_{50} values. Although β-caryophyllene has a previous history of safe use in humans, including LD_{50} values in excess of 5 g/kg in two mammalian species (as described in Section 1.8), the research data presented in Chapter 4 demonstrate considerable concentration-dependent cytotoxic effects both in malignant and non-malignant human cell types. Specifically, concentrations above 50 µM were associated with pronounced cell death. Based on previous pharmacokinetic data, the likelihood of reaching serum concentrations within this range following a single oral dose of 5 mg/kg is low. Typical dosages administered may therefore exert therapeutic CB2-mediated effects without toxicity, given the low nanomolar CB2 agonist potency of the compound. However, the organ-specific biodistribution of β-caryophyllene has not been evaluated and it may therefore be possible for exposure to concentrations at or above 50 µM to occur, particularly following higher oral doses and/or repeated doses. The present research points to the need for further studies in human cells to determine the mechanism of cell death (*i.e.*, necrosis versus apoptosis) as well as *in vivo* toxicokinetic studies examining biodistribution and organ-specific toxicity.

With the aim of targeting cannabinoid receptors expressed by glia for application in chronic pain mediated by gliosis, the effects of the CB2 test compounds on intracellular signaling pathways involved in glial cell inflammatory responses, which may be influenced by CB2 activation, were studied *in vitro* in a pro-inflammatory astrocyte cell line (U87MG). All three CB2 agonist compounds appeared to have pharmacologic properties relevant to the treatment of gliosis. Specifically, DML-3 strongly reduced intracellular activation of NF-κB and also limited the activation of ERK1/2 and PI3K. DML-4 strongly reduced the activation of ERK1/2 with lesser reductions in NF-kB and PI3K activity observed. β-caryophyllene showed a pattern analogous to DML-3, with a comparable ability to reduce activation of NF-κB, and, to a

143

lesser extent, ERK1/2 and PI3K. In terms of direct anti-inflammatory activity, β-caryophyllene

significantly inhibited U87MG secretion of IL-6 and IL-8 at 1 µM. The anti-inflammatory effect

reached statistical significance following 25 µM DML-4 treatment, while non-significant

reductions in cytokine secretion were observed following the same concentration of DML-3

treatment. Together, the data indicate that each compound may have the potential to limit cell

proliferation, migration and pro-inflammatory activity such as cytokine secretion within the

context of gliosis. Therefore, all three compounds are considered to be candidates for further

investigation in the treatment of centrally-mediated chronic pain.

5.2   Limitations of the Research

Given the scope and limitations of the *in vivo* study in the acidic saline model, there is a

need for further investigation both in research models and clinically in diagnosed individuals

before firm conclusions can be drawn around the involvement of gliosis in chronic widespread

musculoskeletal pain. Despite the fact that our research findings were statistically significant, the

limited number of animals which developed bilateral hyperalgesia in our experimental cohorts

precluded a complete estimation of the specific time course of glial cell activation in the acidic

saline model. Furthermore, the data demonstrated up-regulation of glial cell activation markers

only. No specific markers of neuro-inflammation were tested and therefore it cannot be

concluded that the glial cell activation observed was indeed pro-inflammatory in nature. For

example, it has been previously reported that microglia activation in response to minor injury

may be associated with surveillance and regenerative functions which are protective, rather than

pro-inflammatory [394]. Additionally, this study examined differences between acidic saline

model animals and healthy controls. The effect of pH could have been more specifically studied

through the use of a control group which received neutral pH saline injections. Finally, this research may not hold relevance to females with chronic widespread musculoskeletal pain disorders since the experiments described herein were conducted in male animals only, whereas the majority of individuals affected by CWP are female. Importantly, sex differences in neuro-inflammatory responses have been found within various models of chronic pain and CNS pathology. For example, in a cortical stab wound model of brain injury, males showed increased Iba-1 immunoreactivity in the wound proximity, increased microglia expression of arginase-1 and neuroglobin, increased astrocyte expression of CCL2, and increased neuronal density in the lesion edge, relative to females [395]. Therefore, the observations of the present research may only carry relevance to male subjects.

The drug discovery research was limited to the synthesis and pharmacologic characterization of two novel CB2 agonist compounds. Further structure-activity relationship studies using the methods and tools described in Chapter 3 could have allowed for development of a greater number of compounds, possibly having enhanced agonist potency and improved solubility properties. Although the use of a co-solvent was sufficient to facilitate biological testing of our compounds, enhanced aqueous solubility may be preferred from the future perspective of human drug delivery (*i.e*., to ensure proper drug dissolution in order to facilitate oral absorption). Nonetheless, many options exist in the field of pharmaceutics to mitigate poor aqueous drug solubility. Examples of these include the use of surfactants, co-solvents, emulsifying agents, as well as vesicle-forming lipids (liposomes) and polymers (polymersomes).

The investigation of the pharmacologic properties of the CB2 agonist compounds for potential application in gliosis was limited to an *in vitro* model. Although the U87MG cell line aptly models glial cells in a pro-inflammatory state, this cell line is derived from a malignant

145

glioma, and therefore, fundamental differences between malignant and normal cells may limit the applicability of the research findings to non-malignant glia. Furthermore, as the findings from the *in vivo* study suggest, microglia activation may have a stronger influence on hyperalgesia in chronic widespread musculoskeletal pain than astrocytes. The effect of the CB2 agonist compounds on microglia was not evaluated in the present investigation; therefore it is unknown whether this glial cell type would respond favorably (*i.e.*, reduced inflammatory activity and reduced proliferation/migration) to treatment with the compounds within the context of gliosis. In addition, it cannot be concluded that the CB2 agonist compounds may have the ability to treat pain mediated by gliosis without further investigation within an *in vivo* system, since pain perception is a multi-factorial phenomenon, as discussed in the Introduction, which is influenced by more components than gliosis alone. Should the CB2 agonist test compounds have the ability to mitigate gliosis *in vivo*, the ultimate effect on pain perception may not be of significance. Although CB2 agonists may work to mediate pain perception through other mechanisms, in addition to those involving glial cells (i.e., as described in the Introduction, peripheral anti-inflammatory effects, actions at vanilloid receptors, CB2-evoked release of endorphins, etc.), the true effect of the CB2 agonist compounds described here on pain perception can only be discerned through careful study *in vivo*, and, specifically within the target patient population in a clinical setting.

5.3 Future Perspectives

During the course of this research investigation, several other independently developed CB2 agonist compounds were investigated through commercial development programs, with examples shown in Table 5.1. As indicated in the table, the development of clinically useful CB2

146

agonist compounds has proven to be challenging. The first two drug candidates failed phase II

clinical trials for the treatment of osteoarthritis pain and pain following dental tooth extraction

surgery. To date, no CB2 agonist compound has successfully completed the phase II clinical trial

stage for a pain-related indication. A CB2 agonist known as olorinab is, however, currently

undergoing phase II trials for pain in Crohn's disease. Interestingly, several commercial CB2

agonist compounds have successfully completed phase II clinical trials for treatment of cystic

fibrosis as well as atopic dermatitis, with further phase II trials underway for several other

autoimmune conditions, including SLE. One CB2 agonist compound which previously failed for

osteoarthritis pain, LY2828360, is being re-investigated for potential application in neuropathic

pain, while another is undergoing pre-clinical study for treatment of pain in endometriosis.

Table 5.1. Commercial development status of CB2-selective agonists.

Compound Name	Chemical Class	Therapeutic Indication	Stage of Development
GW142866X	Pyrimidine	Pain following third molar tooth extraction surgery; osteoarthritis pain	Phase II – failure [396,397]
LY2828360	Purine	Osteoarthritis pain	Phase II – failure [398,399]
LY2828360	Purine	Neuropathic pain	Pre-clinical [398]
S-777469	Dihydropyridine	Atopic dermatitis	Phase II – complete [400]
JBT-101	THC-11-oic acid analogue	Cystic fibrosis	Phase II – complete [401]
JBT-101	THC-11-oic acid analogue	Systemic Lupus Erythematosis (SLE); Sermatomyositis; Scleroderma	Phase II – in progress [402,403]
Olorinab (APD37D)	Cyclopentapyrazole	Pain associated with Crohn's disease	Phase II – in progress [356,404]
rel-(5aR, 9aR)-3-(1,1-Dimethyl-heptyl)-7,7-dimethyl-5a, 6,7,8, 9,9a-hexahydro-dibenzo-[b, d]-furan-1-ol	Dimethylheptyl bezofuran	Endometriosis	Pre-clinical [405]

Reasons for the early failures of CB2 agonists for pain treatment are thought to be several-fold. Poor translatability of pre-clinical animal model efficacy to the clinical setting is a likely contributing factor. Clinical studies typically involve a heterogenous patient population, including both males and females, with varying ages, medical backgrounds and pain severities. In contrast, pre-clinical studies are usually conducted in a highly uniform group of animals (*i.e.*, animals of the same sex, age and weight) with the same artificially-induced disease pathology. It is therefore unrealistic to expect that the conditions of an animal model study will be faithfully recapitulated within a clinical study population. Furthermore, species differences are present between rodent and human cannabinoid receptors which can affect the specific pharmacologic action of the test compound. For example, the compound AM1241 acts as an agonist at human CB2 receptors, whereas in mouse and rat CB2 receptors, it acts as an inverse agonist [146]. Although the activity of a candidate drug compound is likely to be studied *in vitro* in human receptors, subtle differences in the pharmacologic action of the compound in rodent receptors in pre-clinical models may produce misleading results. Receptor coupling and downstream intracellular effects elicited by a given compound may be species-dependent. Therefore, positive results in pre-clinical rodent models may not predict the same pharmacologic effects and efficacy in humans. In addition, fundamental differences in the underlying pain mechanism between research models and the actual human disease may preclude the translatability of pre-clinical efficacy to patients.

Another concept thought to be of crucial importance for the development of clinically effective CB2 agonists is the functional selectivity of the given compound at the receptor [406,407]. Functional selectivity refers to the specific intracellular effects a compound elicits through action at a receptor. With previous data to suggest that different CB2 agonists are

capable of eliciting varying intracellular responses (discussed in Section 4.1), the CB2 agonist compounds in the present research investigation were tested for their effects on various intracellular signaling pathways in the target cell type. However, recent literature has highlighted the concept of biased agonism, that is, a compound may signal at a GPCR by activating either a g-protein-mediated response or a β-arrestin-mediated response (biased agonism) or the compound may elicit a mixture of both responses (unbiased agonism). Since β-arrestin is known to mediate receptor de-sensitization, and promote receptor removal from the cell membrane, such activity is expected to limit the potentially beneficial effects mediated by g-protein signaling. It is therefore important that CB2 agonist compounds undergo careful evaluation for functional selectivity, in order to ensure that the ligand is not biased toward β-arrestin activation. This may include *in vitro* screening for β-arrestin recruitment as well as examination of membrane receptor expression following treatment. Overall, the lessons learned from the current commercial development of CB2 agonists suggest that thorough pre-clinical testing and pharmacologic characterization is essential.

The research described here supports the potential of the CB2 agonist compounds studied to have possible therapeutic effects, specifically for chronic pain disorders associated with neuro-inflammation and gliosis. There are, however, several further investigations recommended prior to testing the compounds in patients. In addition to the toxicology work described above, the functional selectivity of each compound must be assessed by screening for β-arrestin-mediated activity. Next, the affinity of the compounds for additional receptor targets and the potential for off-target effects must be investigated. Should positive results be attained from *in vivo* studies in suitable research models, pharmacokinetic investigations should then be conducted in order to help guide the drug delivery and formulation strategy.

In conclusion, this research has produced important data suggesting gliosis may be a pathophysiologic component of chronic widespread musculoskeletal pain disorders, prompting further investigation. This work has also added to the current body of knowledge on the pharmacologic activity of β-caryophyllene at human cannabinoid receptors. In addition, this work has laid the foundation to support further study of β-caryophyllene as well as two novel adamantyl derivative compounds, DML-3 and DML-4, for application in centrally-mediated chronic pain.

Bibliography

[1] International Association for the Study of Pain, Task Force on Taxonomy (1994). *Part III: Pain Terms, A Current List with Definitions and Notes on Usage*. In: Merskey H, Bogduk N (eds) Classification of Chronic Pain, 2nd edn. IASP Press, Seattle, 209 - 214.

[2] Melzack R, Katz J (2013). *Pain*. Wiley interdisciplinary reviews Cognitive science **4**, 1-15.

[3] Melzack R (2001). *Pain and the neuromatrix in the brain*. Journal of dental education **65**, 1378-82.

[4] Bonica JJ (1953). *The management of pain*. Lea & Febiger, Philadelphia.

[5] Merskey H, Bogduk N (1994). *Classification of chronic pain*, 2nd edn. IASP Press, Seattle.

[6] Goldberg DS, McGee SJ (2011). *Pain as a global public health priority*. BMC public health **11**, 770.

[7] Gureje O, Von Korff M, Kola L, Demyttenaere K, et al. (2008). *The relation between multiple pains and mental disorders: results from the World Mental Health Surveys*. Pain **135**, 82-91.

[8] IOM (Institute of Medicine) Committee on Advancing Pain Research, Care, and Education (2011). *Relieving Pain in America: A Blueprint for Transforming Prevention, Care, Education and Research*. The National Acadamies Press, Washington, D.C.

[9] Mantyselka P, Kumpusalo E, Ahonen R, Kumpusalo A, et al. (2001). *Pain as a reason to visit the doctor: a study in Finnish primary health care*. Pain **89**, 175-80.

[10] Handwerker HO (2007). *[From Descartes to fMRI. Pain theories and pain concepts]*. Schmerz (Berlin, Germany) **21**, 307-10, 312-7.

[11] Melzack R (1991). *The gate control theory 25 years later: New perspectives on phantom limb pain*. In: Bond MR, Charlton JE, Woolf CJ (eds) Pain Research and Therapy: Proceedings of the VIth World Congress on Pain Elsevier, 9-21.

[12] Goldscheider A (1894). *Uber den schmerzes in physiologischer and lkinicher hinsicht*. Hirschwald, Berlin.

[13] Livingston WK (1943). *Pain Mechanisms*. Macmillan, New York.

[14] Noorenbos W (1959). *Pain*. Elsevier, Amsterdam.

[15] Melzack R, Wall PD (1965). *Pain mechanisms: a new theory*. Science **150**, 971-9.

[16] Melzack R, Casey KL (1968). *Sensory, motivational, and central control determinants of pain*. In: Kenshaldo D (ed) The Skin Senses. Charles C. Thomas, Springfield, IL., 423-443.

[17] Melzack R, Loeser JD (1978). *Phantom body pain in paraplegics: evidence for a central "pattern generating mechanism" for pain*. Pain **4**, 195-210.

[18] Cairns BE, Prateepavanich P (2009). *Role of Peripheral Mechanisms in Spinal Pain Conditions*. In: Cairns BE (ed) Peripheral Receptor Targets for Analgesia. John Wiley & Sons, Hoboken, New Jersey, 21-40.

[19] Erlanger J, Bishop GH, Gasser HS (1926). *The action potential waves transmitted between the sciatic nerve and its spinal roots*. The American Journal of Physiology **78**, 574-591.

[20] Erlanger J, Gasser HS (1930). *The action potential in fibers of slow conduction in spinal roots and somatic nerves*. The American Journal of Physiology **92**, 43-82.

[21]   Gasser HS (1941). *The Classification of Nerve Fibers*. The Ohio Journal of Science **41**, 145-159.

[22]   Hunt SP, Mantyh PW (2001). *The molecular dynamics of pain control*. Nat Rev Neurosci **2**, 83-91.

[23]   Spinothalamic Tract; https://www.physio-pedia.com/index.php?title=Spinothalamic_tract&oldid=194379 (accessed 19 August 2018).

[24]   Scholz J, Woolf CJ (2002). *Can we conquer pain?* Nature neuroscience **5 Suppl**, 1062-7.

[25]   Milligan ED, Watkins LR (2009). *Pathological and protective roles of glia in chronic pain*. Nat Rev Neurosci **10**, 23-36.

[26]   Murphy JA, Stein IS, Lau CG, Peixoto RT, et al. (2014). *Phosphorylation of Ser1166 on GluN2B by PKA is critical to synaptic NMDA receptor function and Ca2+ signaling in spines*. J Neurosci **34**, 869-79.

[27]   Gao YJ, Ji RR (2010). *Chemokines, neuronal-glial interactions, and central processing of neuropathic pain*. Pharmacology & therapeutics **126**, 56-68.

[28]   Abbadie C (2005). *Chemokines, chemokine receptors and pain*. Trends in immunology **26**, 529-34.

[29]   Abbadie C, Bhangoo S, De Koninck Y, Malcangio M, et al. (2009). *Chemokines and pain mechanisms*. Brain research reviews **60**, 125-34.

[30]   Araque A, Parpura V, Sanzgiri RP, Haydon PG (1999). *Tripartite synapses: glia, the unacknowledged partner*. Trends in neurosciences **22**, 208-15.

[31]   Carmignoto G (2000). *Reciprocal communication systems between astrocytes and neurones*. Progress in neurobiology **62**, 561-81.

[32]   Stoll G, Jander S (1999). *The role of microglia and macrophages in the pathophysiology of the CNS*. Progress in neurobiology **58**, 233-47.

[33]   Ji RR, Berta T, Nedergaard M (2013). *Glia and pain: is chronic pain a gliopathy?* Pain **154 Suppl 1**, S10-28.

[34]   Chiang CY, Sessle BJ, Dostrovsky JO (2012). *Role of astrocytes in pain*. Neurochemical research **37**, 2419-31.

[35]   Xanthos DN, Sandkuhler J (2014). *Neurogenic neuroinflammation: inflammatory CNS reactions in response to neuronal activity*. Nat Rev Neurosci **15**, 43-53.

[36]   Zhu GQ, Liu S, He DD, Liu YP, et al. (2014). *Activation of the cAMP-PKA signaling pathway in rat dorsal root ganglion and spinal cord contributes toward induction and maintenance of bone cancer pain*. Behavioural pharmacology **25**, 267-76.

[37]   Tumati S, Roeske WR, Largent-Milnes TM, Vanderah TW, et al. (2011). *Intrathecal PKA-selective siRNA treatment blocks sustained morphine-mediated pain sensitization and antinociceptive tolerance in rats*. Journal of neuroscience methods **199**, 62-8.

[38]   Sun R-Q, Tu Y-J, Lawand NB, Yan J-Y, et al. (2004). *Calcitonin Gene-Related Peptide Receptor Activation Produces PKA- and PKC-Dependent Mechanical Hyperalgesia and Central Sensitization*. J Neurophysiol **92**, 2859-66.

[39]   Bird G, Han J, Fu Y, Adwanikar H, et al. (2006). *Pain-related synaptic plasticity in spinal dorsal horn neurons: role of CGRP*. Molecular pain **2**, 31.

[40]   Ebersberger A, Charbel Issa P, Vanegas H, Schaible HG (2000). *Differential effects of calcitonin gene-related peptide and calcitonin gene-related peptide 8-37 upon responses to N-methyl-D-aspartate or (R, S)-alpha-amino-3-hydroxy-5-methylisoxazole-4-*

propionate in spinal nociceptive neurons with knee joint input in the rat. Neuroscience **99**, 171-8.

[41] Beggs S, Trang T, Salter MW (2012). *P2X4R+ microglia drive neuropathic pain*. Nature neuroscience **15**, 1068-73.

[42] Coull JA, Beggs S, Boudreau D, Boivin D, et al. (2005). *BDNF from microglia causes the shift in neuronal anion gradient underlying neuropathic pain*. Nature **438**, 1017-21.

[43] Zhang J, De Koninck Y (2006). *Spatial and temporal relationship between monocyte chemoattractant protein-1 expression and spinal glial activation following peripheral nerve injury*. J Neurochem **97**, 772-83.

[44] Abbadie C, Lindia JA, Cumiskey AM, Peterson LB, et al. (2003). *Impaired neuropathic pain responses in mice lacking the chemokine receptor CCR2*. Proceedings of the National Academy of Sciences of the United States of America **100**, 7947-52.

[45] Gao YJ, Zhang L, Samad OA, Suter MR, et al. (2009). *JNK-induced MCP-1 production in spinal cord astrocytes contributes to central sensitization and neuropathic pain*. J Neurosci **29**, 4096-108.

[46] Ulmann L, Hatcher JP, Hughes JP, Chaumont S, et al. (2008). *Up-regulation of P2X4 receptors in spinal microglia after peripheral nerve injury mediates BDNF release and neuropathic pain*. J Neurosci **28**, 11263-8.

[47] Tominaga M, Caterina MJ (2004). *Thermosensation and pain*. Journal of neurobiology **61**, 3-12.

[48] Yao X, Kwan HY, Huang Y (2005). *Regulation of TRP channels by phosphorylation*. Neuro-Signals **14**, 273-80.

[49] Akopian AN, Ruparel NB, Jeske NA, Patwardhan A, et al. (2009). *Role of ionotropic cannabinoid receptors in peripheral antinociception and antihyperalgesia*. Trends in pharmacological sciences **30**, 79-84.

[50] Vellani V, Mapplebeck S, Moriondo A, Davis JB, et al. (2001). *Protein kinase C activation potentiates gating of the vanilloid receptor VR1 by capsaicin, protons, heat and anandamide*. The Journal of physiology **534**, 813-25.

[51] Bhave G, Hu HJ, Glauner KS, Zhu W, et al. (2003). *Protein kinase C phosphorylation sensitizes but does not activate the capsaicin receptor transient receptor potential vanilloid 1 (TRPV1)*. Proceedings of the National Academy of Sciences of the United States of America **100**, 12480-5.

[52] Premkumar LS, Ahern GP (2000). *Induction of vanilloid receptor channel activity by protein kinase C*. Nature **408**, 985-90.

[53] Numazaki M, Tominaga T, Toyooka H, Tominaga M (2002). *Direct phosphorylation of capsaicin receptor VR1 by protein kinase Cepsilon and identification of two target serine residues*. The Journal of biological chemistry **277**, 13375-8.

[54] Rathee PK, Distler C, Obreja O, Neuhuber W, et al. (2002). *PKA/AKAP/VR-1 module: A common link of Gs-mediated signaling to thermal hyperalgesia*. J Neurosci **22**, 4740-5.

[55] Lopshire JC, Nicol GD (1998). *The cAMP transduction cascade mediates the prostaglandin E2 enhancement of the capsaicin-elicited current in rat sensory neurons: whole-cell and single-channel studies*. J Neurosci **18**, 6081-92.

[56] Canadian Pharmacists Association (2018). *RxTx*. Canadian Pharmacists Association, Ottawa.

[57]   Finnerup NB, Attal N, Haroutounian S, McNicol E, et al. (2015). *Pharmacotherapy for neuropathic pain in adults: a systematic review and meta-analysis*. The Lancet Neurology **14**, 162-73.

[58]   Kean W, Kean CA, Hogan MG (2018). *Osteoarthritis*. In: Gray J (ed) Compendium of Therapeutic Choices. Canadian Pharmacists Association, Ottawa.

[59]   Hauser W, Urrutia G, Tort S, Uceyler N, et al. (2013). *Serotonin and noradrenaline reuptake inhibitors (SNRIs) for fibromyalgia syndrome*. The Cochrane database of systematic reviews **1**, CD010292.

[60]   Wiffen PJ, Derry S, Moore RA, Aldington D, et al. (2013). *Antiepileptic drugs for neuropathic pain and fibromyalgia - an overview of Cochrane reviews*. The Cochrane database of systematic reviews **11**, CD010567.

[61]   Wiffen PJ, Derry S, Bell RF, Rice AS, et al. (2017). *Gabapentin for chronic neuropathic pain in adults*. The Cochrane database of systematic reviews **6**, CD007938.

[62]   Gaskell H, Moore RA, Derry S, Stannard C (2014). *Oxycodone for neuropathic pain and fibromyalgia in adults*. The Cochrane database of systematic reviews, CD010692.

[63]   Wolfe F, Clauw DJ, Fitzcharles MA, Goldenberg DL, et al. (2010). *The American College of Rheumatology preliminary diagnostic criteria for fibromyalgia and measurement of symptom severity*. Arthritis care & research **62**, 600-10.

[64]   Bennett RM, Jones J, Turk DC, Russell IJ, et al. (2007). *An internet survey of 2,596 people with fibromyalgia*. BMC musculoskeletal disorders **8**, 27.

[65]   Ge HY, Fernandez-de-Las-Penas C, Yue SW (2011). *Myofascial trigger points: spontaneous electrical activity and its consequences for pain induction and propagation*. Chinese medicine **6**, 13.

[66]   Alonso-Blanco C, Fernandez-de-las-Penas C, Morales-Cabezas M, Zarco-Moreno P, et al. (2011). *Multiple active myofascial trigger points reproduce the overall spontaneous pain pattern in women with fibromyalgia and are related to widespread mechanical hypersensitivity*. Clin J Pain **27**, 405-13.

[67]   Ge HY, Nie H, Madeleine P, Danneskiold-Samsoe B, et al. (2009). *Contribution of the local and referred pain from active myofascial trigger points in fibromyalgia syndrome*. Pain **147**, 233-40.

[68]   White KP, Speechley M, Harth M, Ostbye T (1999). *The London Fibromyalgia Epidemiology Study: the prevalence of fibromyalgia syndrome in London, Ontario*. The Journal of rheumatology **26**, 1570-6.

[69]   Queiroz LP (2013). *Worldwide epidemiology of fibromyalgia*. Curr Pain Headache Rep **17**, 356.

[70]   Skaer TL (2014). *Fibromyalgia: disease synopsis, medication cost effectiveness and economic burden*. PharmacoEconomics **32**, 457-66.

[71]   Fibromyalgia Tender Points; https://www.ineedpeakpt.com/2012/01/physical-therapy-helping-those-who-are-in-pain/cure-fibromyalgia-tender-points/ (accessed 21 August 2018).

[72]   Sluka KA, Clauw DJ (2016). *Neurobiology of fibromyalgia and chronic widespread pain*. Neuroscience **338**, 114-129.

[73]   Staud R (2011). *Peripheral pain mechanisms in chronic widespread pain*. Best practice & research Clinical rheumatology **25**, 155-64.

[74]   Staud R, Robinson ME, Price DD (2007). *Temporal summation of second pain and its maintenance are useful for characterizing widespread central sensitization of fibromyalgia patients*. The journal of pain : official journal of the American Pain Society **8**, 893-901.

[75]   Ge HY, Wang Y, Danneskiold-Samsoe B, Graven-Nielsen T, et al. (2010). *The predetermined sites of examination for tender points in fibromyalgia syndrome are frequently associated with myofascial trigger points*. The journal of pain : official journal of the American Pain Society **11**, 644-51.

[76]   Giamberardino MA, Affaitati G, Fabrizio A, Costantini R (2011). *Effects of treatment of myofascial trigger points on the pain of fibromyalgia*. Current pain and headache reports **15**, 393-9.

[77]   Staud R, Nagel S, Robinson ME, Price DD (2009). *Enhanced central pain processing of fibromyalgia patients is maintained by muscle afferent input: a randomized, double-blind, placebo-controlled study*. Pain **145**, 96-104.

[78]   Kuan TS, Hsieh YL, Chen SM, Chen JT, et al. (2007). *The myofascial trigger point region: correlation between the degree of irritability and the prevalence of endplate noise*. American journal of physical medicine & rehabilitation / Association of Academic Physiatrists **86**, 183-9.

[79]   Simons DG, Hong CZ, Simons LS (2002). *Endplate potentials are common to midfiber myofacial trigger points*. American journal of physical medicine & rehabilitation **81**, 212-22.

[80]   Shah JP, Danoff JV, Desai MJ, Parikh S, et al. (2008). *Biochemicals associated with pain and inflammation are elevated in sites near to and remote from active myofascial trigger points*. Archives of physical medicine and rehabilitation **89**, 16-23.

[81]   Gerwin RD, Dommerholt J, Shah JP (2004). *An expansion of Simons' integrated hypothesis of trigger point formation*. Curr Pain Headache Rep **8**, 468-75.

[82]   Harris RE, Clauw DJ, Scott DJ, McLean SA, et al. (2007). *Decreased central mu-opioid receptor availability in fibromyalgia*. J Neurosci **27**, 10000-6.

[83]   Russell IJ, Vaeroy H, Javors M, Nyberg F (1992). *Cerebrospinal fluid biogenic amine metabolites in fibromyalgia/fibrositis syndrome and rheumatoid arthritis*. Arthritis and rheumatism **35**, 550-6.

[84]   Yunus MB, Dailey JW, Aldag JC, Masi AT, et al. (1992). *Plasma tryptophan and other amino acids in primary fibromyalgia: a controlled study*. The Journal of rheumatology **19**, 90-4.

[85]   Sarchielli P, Mancini ML, Floridi A, Coppola F, et al. (2007). *Increased levels of neurotrophins are not specific for chronic migraine: evidence from primary fibromyalgia syndrome*. The journal of pain : official journal of the American Pain Society **8**, 737-45.

[86]   Russell IJ, Orr MD, Littman B, Vipraio GA, et al. (1994). *Elevated cerebrospinal fluid levels of substance P in patients with the fibromyalgia syndrome*. Arthritis and rheumatism **37**, 1593-601.

[87]   Giovengo SL, Russell IJ, Larson AA (1999). *Increased concentrations of nerve growth factor in cerebrospinal fluid of patients with fibromyalgia*. The Journal of rheumatology **26**, 1564-9.

[88]   Kadetoff D, Lampa J, Westman M, Andersson M, et al. (2012). *Evidence of central inflammation in fibromyalgia-increased cerebrospinal fluid interleukin-8 levels*. Journal of neuroimmunology **242**, 33-8.

[89]   Pernambuco AP, Schetino LP, Alvim CC, Murad CM, et al. (2013). *Increased levels of IL-17A in patients with fibromyalgia*. Clinical and experimental rheumatology **31**, S60-3.

[90]   Garcia JJ, Cidoncha A, Bote ME, Hinchado MD, et al. (2013). *Altered profile of chemokines in fibromyalgia patients*. Annals of clinical biochemistry.

[91]   Wang H, Moser M, Schiltenwolf M, Buchner M (2008). *Circulating cytokine levels compared to pain in patients with fibromyalgia -- a prospective longitudinal study over 6 months*. The Journal of rheumatology **35**, 1366-70.

[92]   Zhang Z, Cherryholmes G, Mao A, Marek C, et al. (2008). *High plasma levels of MCP-1 and eotaxin provide evidence for an immunological basis of fibromyalgia*. Experimental biology and medicine (Maywood, NJ) **233**, 1171-80.

[93]   Zhang L, Li YG, Li YH, Qi L, et al. (2012). *Increased frequencies of Th22 cells as well as Th17 cells in the peripheral blood of patients with ankylosing spondylitis and rheumatoid arthritis*. PloS one **7**, e31000.

[94]   Romero-Sanchez C, Jaimes DA, Londono J, De Avila J, et al. (2011). *Association between Th-17 cytokine profile and clinical features in patients with spondyloarthritis*. Clinical and experimental rheumatology **29**, 828-34.

[95]   Liu Y, Ho RC, Mak A (2012). *The role of interleukin (IL)-17 in anxiety and depression of patients with rheumatoid arthritis*. International journal of rheumatic diseases **15**, 183-7.

[96]   Chen Y, Jiang T, Chen P, Ouyang J, et al. (2011). *Emerging tendency towards autoimmune process in major depressive patients: a novel insight from Th17 cells*. Psychiatry research **188**, 224-30.

[97]   Meng X, Zhang Y, Lao L, Saito R, et al. (2013). *Spinal interleukin-17 promotes thermal hyperalgesia and NMDA NR1 phosphorylation in an inflammatory pain rat model*. Pain **154**, 294-305.

[98]   Brederson JD, Jarvis MF, Honore P, Surowy CS (2011). *Fibromyalgia: mechanisms, current treatment and animal models*. Current pharmaceutical biotechnology **12**, 1613-26.

[99]   Finestone HM (2013). *Musculoskeletal Disorders: Fibromyalgia*. In: McLeod PJea (ed) Therapeutic Choices. Canadian Pharmacists Association, Ottawa.

[100]   Painter JT, Crofford LJ (2013). *Chronic opioid use in fibromyalgia syndrome: a clinical review*. Journal of clinical rheumatology : practical reports on rheumatic & musculoskeletal diseases **19**, 72-7.

[101]   Carville SF, Arendt-Nielsen S, Bliddal H, Blotman F, et al. (2008). *EULAR evidence-based recommendations for the management of fibromyalgia syndrome*. Annals of the rheumatic diseases **67**, 536-41.

[102]   Hutchinson MR, Shavit Y, Grace PM, Rice KC, et al. (2011). *Exploring the neuroimmunopharmacology of opioids: an integrative review of mechanisms of central immune signaling and their implications for opioid analgesia*. Pharmacological reviews **63**, 772-810.

[103]   Watkins LR, Hutchinson MR, Johnston IN, Maier SF (2005). *Glia: novel counter-regulators of opioid analgesia*. Trends in neurosciences **28**, 661-9.

[104]   Clauw DJ (2014). *Fibromyalgia: a clinical review*. JAMA : the journal of the American Medical Association **311**, 1547-55.

[105]   Pertwee RG (2005). *Pharmacological actions of cannabinoids*. Handbook of experimental pharmacology, 1-51.

[106]   Howlett AC, Barth F, Bonner TI, Cabral G, et al. (2002). *International Union of Pharmacology. XXVII. Classification of cannabinoid receptors*. Pharmacological reviews **54**, 161-202.

[107]   Di Marzo V (2008). *Endocannabinoids: synthesis and degradation*. Reviews of physiology, biochemistry and pharmacology **160**, 1-24.

[108]   Ueda N, Tsuboi K, Uyama T, Ohnishi T (2011). *Biosynthesis and degradation of the endocannabinoid 2-arachidonoylglycerol*. BioFactors (Oxford, England) **37**, 1-7.

[109]   Ryberg E, Larsson N, Sjogren S, Hjorth S, et al. (2007). *The orphan receptor GPR55 is a novel cannabinoid receptor*. British journal of pharmacology **152**, 1092-101.

[110]   Pistis M, O'Sullivan SE (2017). *Chapter Nine - The Role of Nuclear Hormone Receptors in Cannabinoid Function*. In: Kendall D, Alexander SPH (eds) Advances in Pharmacology, vol 80. Academic Press, 291-328.

[111]   Fawley JA, Hofmann ME, Andresen MC (2014). *Cannabinoid 1 and transient receptor potential vanilloid 1 receptors discretely modulate evoked glutamate separately from spontaneous glutamate transmission*. J Neurosci **34**, 8324-32.

[112]   Jeske NA, Patwardhan AM, Gamper N, Price TJ, et al. (2006). *Cannabinoid WIN 55,212-2 regulates TRPV1 phosphorylation in sensory neurons*. The Journal of biological chemistry **281**, 32879-90.

[113]   Zygmunt PM, Petersson J, Andersson DA, Chuang H, et al. (1999). *Vanilloid receptors on sensory nerves mediate the vasodilator action of anandamide*. Nature **400**, 452-7.

[114]   Felder CC, Joyce KE, Briley EM, Mansouri J, et al. (1995). *Comparison of the pharmacology and signal transduction of the human cannabinoid CB1 and CB2 receptors*. Molecular Pharmacology **48**, 443-450.

[115]   Mackie K (2008). *Cannabinoid receptors: where they are and what they do*. Journal of neuroendocrinology **20 Suppl 1**, 10-4.

[116]   Pertwee RG (2008). *The diverse CB1 and CB2 receptor pharmacology of three plant cannabinoids: delta9-tetrahydrocannabinol, cannabidiol and delta9-tetrahydrocannabivarin*. British journal of pharmacology **153**, 199-215.

[117]   Caulfield MP, Brown DA (1992). *Cannabinoid receptor agonists inhibit Ca current in NG108-15 neuroblastoma cells via a pertussis toxin-sensitive mechanism*. British journal of pharmacology **106**, 231-2.

[118]   Mackie K, Hille B (1992). *Cannabinoids inhibit N-type calcium channels in neuroblastoma-glioma cells*. Proceedings of the National Academy of Sciences of the United States of America **89**, 3825-9.

[119]   Sugiura T, Kodaka T, Kondo S, Tonegawa T, et al. (1997). *Inhibition by 2-arachidonoylglycerol, a novel type of possible neuromodulator, of the depolarization-induced increase in intracellular free calcium in neuroblastoma x glioma hybrid NG108-15 cells*. Biochemical and biophysical research communications **233**, 207-10.

[120]   Kreitzer AC (2005). *Neurotransmission: emerging roles of endocannabinoids*. Current biology : CB **15**, R549-51.

[121] Vaughan CW, Christie MJ (2005). *Retrograde signalling by endocannabinoids*. In: Pertwee RG (ed) Cannabinoids Handbook of Experimental Pharmacology, vol 168. Springer-Verlag, Heidelbert, 367-383.

[122] Guo J, Ikeda SR (2004). *Endocannabinoids modulate N-type calcium channels and G-protein-coupled inwardly rectifying potassium channels via CB1 cannabinoid receptors heterologously expressed in mammalian neurons*. Mol Pharmacol **65**, 665-74.

[123] Diana MA, Marty A (2004). *Endocannabinoid-mediated short-term synaptic plasticity: depolarization-induced suppression of inhibition (DSI) and depolarization-induced suppression of excitation (DSE)*. British journal of pharmacology **142**, 9-19.

[124] Kodirov SA, Jasiewicz J, Amirmahani P, Psyrakis D, et al. (2010). *Endogenous cannabinoids trigger the depolarization-induced suppression of excitation in the lateral amygdala*. Learning & memory (Cold Spring Harbor, NY) **17**, 43-9.

[125] Mato S, Chevaleyre V, Robbe D, Pazos A, et al. (2004). *A single in-vivo exposure to delta 9THC blocks endocannabinoid-mediated synaptic plasticity*. Nature neuroscience **7**, 585-6.

[126] Jamshidi N, Taylor DA (2001). *Anandamide administration into the ventromedial hypothalamus stimulates appetite in rats*. British journal of pharmacology **134**, 1151-4.

[127] Williams CM, Kirkham TC (1999). *Anandamide induces overeating: mediation by central cannabinoid (CB1) receptors*. Psychopharmacology **143**, 315-7.

[128] Kirkham TC, Williams CM, Fezza F, Di Marzo V (2002). *Endocannabinoid levels in rat limbic forebrain and hypothalamus in relation to fasting, feeding and satiation: stimulation of eating by 2-arachidonoyl glycerol*. British journal of pharmacology **136**, 550-7.

[129] Pertwee RG (2005). *The therapeutic potential of drugs that target cannabinoid receptors or modulate the tissue levels or actions of endocannabinoids*. The AAPS journal **7**, E625-54.

[130] Zimmer A, Zimmer AM, Hohmann AG, Herkenham M, et al. (1999). *Increased mortality, hypoactivity, and hypoalgesia in cannabinoid CB1 receptor knockout mice*. Proceedings of the National Academy of Sciences of the United States of America **96**, 5780-5.

[131] Ledent C, Valverde O, Cossu G, Petitet F, et al. (1999). *Unresponsiveness to cannabinoids and reduced addictive effects of opiates in CB1 receptor knockout mice*. Science **283**, 401-4.

[132] Klein TW, Newton C, Larsen K, Lu L, et al. (2003). *The cannabinoid system and immune modulation*. Journal of leukocyte biology **74**, 486-96.

[133] Atwood BK, Mackie K (2010). *CB2: a cannabinoid receptor with an identity crisis*. British journal of pharmacology **160**, 467-79.

[134] Pacher P, Mechoulam R (2011). *Is lipid signaling through cannabinoid 2 receptors part of a protective system?* Progress in lipid research **50**, 193-211.

[135] Docagne F, Mestre L, Loria F, Hernangomez M, et al. (2008). *Therapeutic potential of CB2 targeting in multiple sclerosis*. Expert opinion on therapeutic targets **12**, 185-95.

[136] Rajesh M, Pan H, Mukhopadhyay P, Batkai S, et al. (2007). *Cannabinoid-2 receptor agonist HU-308 protects against hepatic ischemia/reperfusion injury by attenuating oxidative stress, inflammatory response, and apoptosis*. Journal of leukocyte biology **82**, 1382-9.

[137]   Gui H, Liu X, Wang ZW, He DY, et al. (2014). *Expression of cannabinoid receptor 2 and its inhibitory effects on synovial fibroblasts in rheumatoid arthritis*. Rheumatology (Oxford, England) **53**, 802-9.

[138]   Ke P, Shao BZ, Xu ZQ, Wei W, et al. (2016). *Activation of Cannabinoid Receptor 2 Ameliorates DSS-Induced Colitis through Inhibiting NLRP3 Inflammasome in Macrophages*. PloS one **11**, e0155076.

[139]   Ofek O, Karsak M, Leclerc N, Fogel M, et al. (2006). *Peripheral cannabinoid receptor, CB2, regulates bone mass*. Proceedings of the National Academy of Sciences of the United States of America **103**, 696-701.

[140]   Zhao Y, Yuan Z, Liu Y, Xue J, et al. (2010). *Activation of cannabinoid CB2 receptor ameliorates atherosclerosis associated with suppression of adhesion molecules*. Journal of cardiovascular pharmacology **55**, 292-8.

[141]   Steffens S, Veillard NR, Arnaud C, Pelli G, et al. (2005). *Low dose oral cannabinoid therapy reduces progression of atherosclerosis in mice*. Nature **434**, 782-6.

[142]   Yoshihara S, Morimoto H, Ohori M, Yamada Y, et al. (2005). *Endogenous cannabinoid receptor agonists inhibit neurogenic inflammations in guinea pig airways*. International archives of allergy and immunology **138**, 80-7.

[143]   Hanus L, Breuer A, Tchilibon S, Shiloah S, et al. (1999). *HU-308: a specific agonist for CB(2), a peripheral cannabinoid receptor*. Proceedings of the National Academy of Sciences of the United States of America **96**, 14228-33.

[144]   Malan TP, Jr., Ibrahim MM, Deng H, Liu Q, et al. (2001). *CB2 cannabinoid receptor-mediated peripheral antinociception*. Pain **93**, 239-45.

[145]   Ibrahim MM, Porreca F, Lai J, Albrecht PJ, et al. (2005). *CB2 cannabinoid receptor activation produces antinociception by stimulating peripheral release of endogenous opioids*. Proceedings of the National Academy of Sciences of the United States of America **102**, 3093-8.

[146]   Bingham B, Jones PG, Uveges AJ, Kotnis S, et al. (2007). *Species-specific in vitro pharmacological effects of the cannabinoid receptor 2 (CB2) selective ligand AM1241 and its resolved enantiomers*. British journal of pharmacology **151**, 1061-70.

[147]   Nackley AG, Makriyannis A, Hohmann AG (2003). *Selective activation of cannabinoid CB(2) receptors suppresses spinal fos protein expression and pain behavior in a rat model of inflammation*. Neuroscience **119**, 747-57.

[148]   Quartilho A, Mata HP, Ibrahim MM, Vanderah TW, et al. (2003). *Inhibition of inflammatory hyperalgesia by activation of peripheral CB2 cannabinoid receptors*. Anesthesiology **99**, 955-60.

[149]   Elmes SJ, Winyard LA, Medhurst SJ, Clayton NM, et al. (2005). *Activation of CB1 and CB2 receptors attenuates the induction and maintenance of inflammatory pain in the rat*. Pain **118**, 327-35.

[150]   Gutierrez T, Farthing JN, Zvonok AM, Makriyannis A, et al. (2007). *Activation of peripheral cannabinoid CB1 and CB2 receptors suppresses the maintenance of inflammatory nociception: a comparative analysis*. British journal of pharmacology **150**, 153-63.

[151]   Valenzano KJ, Tafesse L, Lee G, Harrison JE, et al. (2005). *Pharmacological and pharmacokinetic characterization of the cannabinoid receptor 2 agonist, GW405833,*

utilizing rodent models of acute and chronic pain, anxiety, ataxia and catalepsy. Neuropharmacology **48**, 658-72.

[152]   Elmes SJ, Jhaveri MD, Smart D, Kendall DA, et al. (2004). *Cannabinoid CB2 receptor activation inhibits mechanically evoked responses of wide dynamic range dorsal horn neurons in naive rats and in rat models of inflammatory and neuropathic pain*. The European journal of neuroscience **20**, 2311-20.

[153]   Ibrahim MM, Deng H, Zvonok A, Cockayne DA, et al. (2003). *Activation of CB2 cannabinoid receptors by AM1241 inhibits experimental neuropathic pain: pain inhibition by receptors not present in the CNS*. Proceedings of the National Academy of Sciences of the United States of America **100**, 10529-33.

[154]   Sagar DR, Kelly S, Millns PJ, O'Shaughnessey CT, et al. (2005). *Inhibitory effects of CB1 and CB2 receptor agonists on responses of DRG neurons and dorsal horn neurons in neuropathic rats*. The European journal of neuroscience **22**, 371-9.

[155]   Rahn EJ, Makriyannis A, Hohmann AG (2007). *Activation of cannabinoid CB1 and CB2 receptors suppresses neuropathic nociception evoked by the chemotherapeutic agent vincristine in rats*. British journal of pharmacology **152**, 765-77.

[156]   ElSohly MA, Gul W (2014). *Constituents of Cannabis Sativa*. In: Pertwee RG (ed) Handbook of Cannabis. Oxford University Press,

[157]   Turner SE, Williams CM, Iversen L, Whalley BJ (2017). *Molecular Pharmacology of Phytocannabinoids*. Progress in the chemistry of organic natural products **103**, 61-101.

[158]   Maresz K, Carrier EJ, Ponomarev ED, Hillard CJ, et al. (2005). *Modulation of the cannabinoid CB2 receptor in microglial cells in response to inflammatory stimuli*. J Neurochem **95**, 437-45.

[159]   Gaoni Y, Mechoulam R (1964). *Hashish III. Isolation, structure, and partial synthesis of an active constituent of hashish*. Journal of the American Chemical Society **86**, 1646-1647.

[160]   Iwamura H, Suzuki H, Ueda Y, Kaya T, et al. (2001). *In vitro and in vivo pharmacological characterization of JTE-907, a novel selective ligand for cannabinoid CB2 receptor*. The Journal of pharmacology and experimental therapeutics **296**, 420-5.

[161]   Maida V, Ennis M, Irani S, Corbo M, et al. (2008). *Adjunctive nabilone in cancer pain and symptom management: a prospective observational study using propensity scoring*. The journal of supportive oncology **6**, 119-24.

[162]   Skrabek RQ, Galimova L, Ethans K, Perry D (2008). *Nabilone for the treatment of pain in fibromyalgia*. The journal of pain : official journal of the American Pain Society **9**, 164-73.

[163]   Berlach DM, Shir Y, Ware MA (2006). *Experience with the synthetic cannabinoid nabilone in chronic noncancer pain*. Pain medicine (Malden, Mass) **7**, 25-9.

[164]   Narang S, Gibson D, Wasan AD, Ross EL, et al. (2008). *Efficacy of dronabinol as an adjuvant treatment for chronic pain patients on opioid therapy*. The journal of pain : official journal of the American Pain Society **9**, 254-64.

[165]   Schimrigk S, Marziniak M, Neubauer C, Kugler EM, et al. (2017). *Dronabinol Is a Safe Long-Term Treatment Option for Neuropathic Pain Patients*. European neurology **78**, 320-329.

[166] Issa MA, Narang S, Jamison RN, Michna E, et al. (2014). *The subjective psychoactive effects of oral dronabinol studied in a randomized, controlled crossover clinical trial for pain*. Clin J Pain **30**, 472-8.

[167] Valeant (2008). *Cesamet (nabilone)*. RxTx. Canadian Pharmacists Association, Ottawa

[168] Thomas A, Baillie GL, Phillips AM, Razdan RK, et al. (2007). *Cannabidiol displays unexpectedly high potency as an antagonist of CB1 and CB2 receptor agonists in vitro*. British journal of pharmacology **150**, 613-23.

[169] Bow EW, Rimoldi JM (2016). *The Structure-Function Relationships of Classical Cannabinoids: CB1/CB2 Modulation*. Perspectives in medicinal chemistry **8**, 17-39.

[170] Laprairie RB, Bagher AM, Kelly ME, Denovan-Wright EM (2015). *Cannabidiol is a negative allosteric modulator of the cannabinoid CB1 receptor*. British journal of pharmacology **172**, 4790-805.

[171] Martinez-Pinilla E, Varani K, Reyes-Resina I, Angelats E, et al. (2017). *Cannabidiol acts as an allosteric modulator of cannabinoid CB2 receptors*. International Cannabinoid Research Symposium, Montreal.

[172] Pertwee RG, Ross RA, Craib SJ, Thomas A (2002). *(-)-Cannabidiol antagonizes cannabinoid receptor agonists and noradrenaline in the mouse vas deferens*. Eur J Pharmacol **456**, 99-106.

[173] Pertwee RG (2005). *Pharmacologic actions of cannabinoids*. In: Pertwee RG (ed) Cannabinoids Handbook of Experimental Pharmacology. Springer-Verlag, Heidelberg,

[174] O'Sullivan SE, Tarling EJ, Bennett AJ, Kendall DA, et al. (2005). *Novel time-dependent vascular actions of Delta9-tetrahydrocannabinol mediated by peroxisome proliferator-activated receptor gamma*. Biochemical and biophysical research communications **337**, 824-31.

[175] Bisogno T, Hanus L, De Petrocellis L, et al. (2001). *Molecular targets for cannabidiol and its synthetic analogues: effect on vanilloid VR1 receptors and on the cellular uptake and enzymatic hydrolysis of anadamide.* British journal of pharmacology **134**, 845-852.

[176] Russo EB (2011). *Taming THC: potential cannabis synergy and phytocannabinoid-terpenoid entourage effects*. British journal of pharmacology **163**, 1344-64.

[177] Government of Canada (2018). *Health effects of cannabis*. Health Canada, https://www.canada.ca/en/health-canada/services/drugs-medication/cannabis/health-effects/effects.html.

[178] GW Pharma (2014). *Sativex (delta-9-tetrahydrocannabinol-cannabidiol)*. RxTx. Canadian Pharmacists Association, Ottawa.

[179] McNeil Consumer Healthcare (2016). *Tylenol*. RxTx. Canadian Pharmacists Association (CPhA), Ottawa.

[180] Morse HN (1878). *Ueber eine neue Darstellungsmethode der Acetylamidophenole*. Ber Deutscher Chem Ges **11**, 232-233.

[181] Mattia A, Coluzzi F (2009). *What anesthesiologists should know about paracetamol (acetaminophen)*. Minerva Anestesiol **75**, 644-53.

[182] Aronoff DM, Oates JA, Boutaud O (2006). *New insights into the mechanism of action of acetaminophen: Its clinical pharmacologic characteristics reflect its inhibition of the two prostaglandin H2 synthases*. Clinical pharmacology and therapeutics **79**, 9-19.

[183] Hogestatt ED, Jonsson BAG, Ermund A, al. E (2005). *Conversion of Acetaminophen to the Bioactive N-Acylphenolamine AM404 via Fatty Acid Amide Hydrolase-dependent*

Arachadonic Acid Conjugation in the Nervous System. Journal of Biological Chemistry **280**, 31405-31412.

[184] Beltramo M, Stella N, Calignano A, Lin S, et al. (1997). *Functional role of high-affinity anandamide transport, as revealed by selective inhibition*. Science **277**, 1094-1097.

[185] Ottani A, Leone S, Sandrini M, Ferrari A, et al. (2006). *The analgesic activity of paracetamol is prevented by the blockade of cannabinoid CB1 receptors*. European Journal of Pharmacology **531**, 280-281.

[186] Zygmunt PM, Chuang H, Movahed P, Julius D, et al. (2000). *The anandamide transport inhibitor AM404 activates vanilloid receptors*. Eur J Pharmacol **396**, 39-42.

[187] De Petrocellis L, Bisogno T, Davis JB, Pertwee RG, et al. (2000). *Overlap between the ligand recognition properties of the anandamide transporter and the VR1 vanilloid receptor: inhibitors of anandamide uptake with negligible capsaicin-like activity*. FEBS letters **483**, 52-56.

[188] Price TJ, Patwardhan AM, Flores CM, Hargreaves KM (2005). *A role for the anandamide membrane transporter in TRPV1-mediated neurosecretion from trigeminal sensory neurons*. Neuropharmacology **49**, 25-39.

[189] Veiga VF, Zunino L, Calixto JB, Patitucci ML, et al. (2001). *Phytochemical and antioedematogenic studies of commercial copaiba oils available in Brazil*. Phytotherapy Research **15**, 476-480.

[190] Zheng G-Q, Kenney PM, Lam LKT (1992). *Sesquiterpenes from Clove (Eugenia caryophyllata) as Potential Anticarcinogenic Agents*. Journal of Natural Products **55**, 999-1003.

[191] Jirovetz L, Buchbauer G, Ngassoum MB, Geissler M (2002). *Aroma compound analysis of Piper nigrum and Piper guineense essential oils from Cameroon using solid-phase microextraction–gas chromatography, solid-phase microextraction–gas chromatography–mass spectrometry and olfactometry*. Journal of Chromatography A **976**, 265-275.

[192] Mockute D, Bernotiene G, Judzentiene A (2001). *The essential oil of Origanum vulgare L. ssp. vulgare growing wild in Vilnius district (Lithuania)*. Phytochemistry **57**, 65-69.

[193] Paranagama PA, Wimalasena S, Jayatilake GS, Jayawardena AL, et al. (2001). *A comparison of essential oil constituents of bark, leaf, root and fruit of cinnamon (Cinnamomum zeylanicum Blum) grown in Sri Lanka*. Journal of the National Science Foundation of Sri Lanka **29**, 147-53.

[194] Gertsch J, Leonti M, Raduner S, Racz I, et al. (2008). *Beta-caryophyllene is a dietary cannabinoid*. Proceedings of the National Academy of Sciences of the United States of America **105**, 9099-104.

[195] Veiga Junior VF, Pinto AC (2002). *O Genero Copaifera L.* Quimica Nova **25**, 273-286.

[196] Rodrigues F, Oliveira L, Rodrigues F, Saraiva M, et al. (2012). *Chemical composition, antibacterial and antifungal activities of essential oil from Cordia verbenacea DC leaves*. Pharmacognosy Research **4**, 161.

[197] de Almeida TS, Rocha JBT, Rodrigues FFG, Campos AR, et al. (2013). *Chemical composition, antibacterial and antibiotic modulatory effect of Croton campestris essential oils*. Industrial Crops and Products **44**, 630-633.

[198] Larayetan RA, Okoh OO, Sadimenko A, Okoh AI (2017). *Terpene constituents of the aerial parts, phenolic content, antibacterial potential, free radical scavenging and*

antioxidant activity of Callistemon citrinus (Curtis) Skeels (Myrtaceae) from Eastern Cape Province of South Africa. BMC complementary and alternative medicine **17**, 292.

[199]   Basholli-Salihu M, Schuster R, Hajdari A, Mulla D, et al. (2017). *Phytochemical composition, anti-inflammatory activity and cytotoxic effects of essential oils from three Pinus spp.* Pharmaceutical biology **55**, 1553-1560.

[200]   Pinheiro BG, Silva AS, Souza GE, Figueiredo JG, et al. (2011). *Chemical composition, antinociceptive and anti-inflammatory effects in rodents of the essential oil of Peperomia serpens (Sw.) Loud.* J Ethnopharmacol **138**, 479-86.

[201]   de Pinho JPM, Silva ASB, Pinheiro BG, Sombra I, et al. (2012). *Antinociceptive and Antispasmodic Effects of the Essential Oil of Ocimum micranthum: Potential Anti-inflammatory Properties.* Planta Med **78**, 681-685.

[202]   Wu QF, Wang W, Dai XY, Wang ZY, et al. (2012). *Chemical compositions and anti-influenza activities of essential oils from Mosla dianthera.* J Ethnopharmacol **139**, 668-71.

[203]   Khalilzadeh E, Vafaei Saiah G, Hasannejad H, Ghaderi A, et al. (2015). *Antinociceptive effects, acute toxicity and chemical composition of Vitex agnus-castus essential oil.* Avicenna journal of phytomedicine **5**, 218-30.

[204]   Xiao KJ, Wang WX, Dai JL, Zhu L (2014). *Anti-inflammatory activity and chemical composition of the essential oils from Senecio flammeus.* EXCLI journal **13**, 782-91.

[205]   Sousa OV, Silverio MS, Del-Vechio-Vieira G, Matheus FC, et al. (2008). *Antinociceptive and anti-inflammatory effects of the essential oil from Eremanthus erythropappus leaves.* The Journal of pharmacy and pharmacology **60**, 771-7.

[206]   Yoon WJ, Moon JY, Song G, Lee YK, et al. (2010). *Artemisia fukudo essential oil attenuates LPS-induced inflammation by suppressing NF-kappaB and MAPK activation in RAW 264.7 macrophages.* Food and chemical toxicology : an international journal published for the British Industrial Biological Research Association **48**, 1222-9.

[207]   Lim HS, Jin SE, Kim OS, Shin HK, et al. (2015). *Alantolactone from Saussurea lappa Exerts Antiinflammatory Effects by Inhibiting Chemokine Production and STAT1 Phosphorylation in TNF-alpha and IFN-gamma-induced in HaCaT cells.* Phytotherapy research : PTR **29**, 1088-96.

[208]   de Carvalho PM, Jr., Rodrigues RF, Sawaya AC, Marques MO, et al. (2004). *Chemical composition and antimicrobial activity of the essential oil of Cordiaverbenacea D.C.* J Ethnopharmacol **95**, 297-301.

[209]   Akisue MK, Oliveira F, Maraes MS, Akisue G, et al. (1983). *Caracterização farmacognóstica da droga e da tintura de Cordia verbenacea D.C. — Boraginacea.* Rev Cienc Farm **5**, 69-82.

[210]   Oliveira-Tintino CDdM, Pessoa RT, Fernandes MNM, Alcântara IS, et al. (2018). *Anti-inflammatory and anti-edematogenic action of the Croton campestris A. St.-Hil (Euphorbiaceae) essential oil and the compound β-caryophyllene in in vivo models.* Phytomedicine : international journal of phytotherapy and phytopharmacology **41**, 82-95.

[211]   Fernandes ES, Passos GF, Medeiros R, da Cunha FM, et al. (2007). *Anti-inflammatory effects of compounds alpha-humulene and (−)-trans-caryophyllene isolated from the essential oil of Cordia verbenacea.* European Journal of Pharmacology **569**, 228-236.

[212] Medeiros R, Passos GF, Vitor CE, Koepp J, et al. (2007). *Effect of two active compounds obtained from the essential oil of Cordia verbenacea on the acute inflammatory responses elicited by LPS in the rat paw*. British journal of pharmacology **151**, 618-27.

[213] Vijayalaxmi A, Bakshi V, Begum N (2015). *Anti-Arthritic and Anti-Inflammatory Activity of Beta Caryophyllene Against Freund's Complete Adjuvant Induced Arthritis in Wistar Rats*. Journal of Bone Research and Report **1**

[214] Alvarez-Gonzalez I, Madrigal-Bujaidar E, Castro-Garcia S (2014). *Antigenotoxic capacity of beta-caryophyllene in mouse, and evaluation of its antioxidant and GST induction activities*. The Journal of toxicological sciences **39**, 849-59.

[215] Di Sotto A, Mazzanti G, Carbone F, Hrelia P, et al. (2010). *Inhibition by β-caryophyllene of ethyl methanesulfonate-induced clastogenicity in cultured human lymphocytes*. Mutation Research/Genetic Toxicology and Environmental Mutagenesis **699**, 23-28.

[216] Di Sotto A, Evandri MG, Mazzanti G (2008). *Antimutagenic and mutagenic activities of some terpenes in the bacterial reverse mutation assay*. Mutation Research/Genetic Toxicology and Environmental Mutagenesis **653**, 130-133.

[217] Legault J, Pichette A (2007). *Potentiating effect of β-caryophyllene on anticancer activity of α-humulene, isocaryophyllene and paclitaxel*. Journal of Pharmacy and Pharmacology **59**, 1643-1647.

[218] Loizzo MR, Tundis R, Menichini F, Saab AM, et al. (2008). *Antiproliferative effects of essential oils and their major constituents in human renal adenocarcinoma and amelanotic melanoma cells*. Cell Proliferation **41**, 1002-1012.

[219] Cho HI, Hong JM, Choi JW, Choi HS, et al. (2015). *beta-Caryophyllene alleviates D-galactosamine and lipopolysaccharide-induced hepatic injury through suppression of the TLR4 and RAGE signaling pathways*. Eur J Pharmacol **764**, 613-21.

[220] Kelany ME, Abdallah MA (2016). *Protective effects of combined beta-caryophyllene and silymarin against ketoprofen-induced hepatotoxicity in rats*. Canadian journal of physiology and pharmacology **94**, 739-44.

[221] Varga ZV, Matyas C, Erdelyi K, Cinar R, et al. (2018). *beta-Caryophyllene protects against alcoholic steatohepatitis by attenuating inflammation and metabolic dysregulation in mice*. British journal of pharmacology **175**, 320-334.

[222] Horvath B, Mukhopadhyay P, Kechrid M, Patel V, et al. (2012). *beta-Caryophyllene ameliorates cisplatin-induced nephrotoxicity in a cannabinoid 2 receptor-dependent manner*. Free radical biology & medicine **52**, 1325-33.

[223] Yang M, Lv Y, Tian X, Lou J, et al. (2017). *Neuroprotective Effect of beta-Caryophyllene on Cerebral Ischemia-Reperfusion Injury via Regulation of Necroptotic Neuronal Death and Inflammation: In Vivo and in Vitro*. Frontiers in neuroscience **11**, 583.

[224] Guo K, Mou X, Huang J, Xiong N, et al. (2014). *Trans-caryophyllene suppresses hypoxia-induced neuroinflammatory responses by inhibiting NF-kappaB activation in microglia*. Journal of molecular neuroscience : MN **54**, 41-8.

[225] Lou J, Cao G, Li R, Liu J, et al. (2016). *beta-Caryophyllene Attenuates Focal Cerebral Ischemia-Reperfusion Injury by Nrf2/HO-1 Pathway in Rats*. Neurochemical research **41**, 1291-304.

[226]   Liu H, Song Z, Liao D, Zhang T, et al. (2015). *Neuroprotective effects of trans-caryophyllene against kainic acid induced seizure activity and oxidative stress in mice*. Neurochemical research **40**, 118-23.

[227]   Bento AF, Marcon R, Dutra RC, Claudino RF, et al. (2011). *beta-Caryophyllene inhibits dextran sulfate sodium-induced colitis in mice through CB2 receptor activation and PPARgamma pathway*. Am J Pathol **178**, 1153-66.

[228]   Viveros-Paredes JM, Gonzalez-Castaneda RE, Gertsch J, Chaparro-Huerta V, et al. (2017). *Neuroprotective Effects of beta-Caryophyllene against Dopaminergic Neuron Injury in a Murine Model of Parkinson's Disease Induced by MPTP*. Pharmaceuticals (Basel, Switzerland) **10**.

[229]   Ojha S, Javed H, Azimullah S, Haque ME (2016). *beta-Caryophyllene, a phytocannabinoid attenuates oxidative stress, neuroinflammation, glial activation, and salvages dopaminergic neurons in a rat model of Parkinson disease*. Molecular and cellular biochemistry **418**, 59-70.

[230]   Basha RH, Sankaranarayanan C (2016). *beta-Caryophyllene, a natural sesquiterpene lactone attenuates hyperglycemia mediated oxidative and inflammatory stress in experimental diabetic rats*. Chemico-biological interactions **245**, 50-8.

[231]   Basha RH, Sankaranarayanan C (2014). *beta-Caryophyllene, a natural sesquiterpene, modulates carbohydrate metabolism in streptozotocin-induced diabetic rats*. Acta histochemica **116**, 1469-79.

[232]   Cheng Y, Dong Z, Liu S (2014). *beta-Caryophyllene ameliorates the Alzheimer-like phenotype in APP/PS1 Mice through CB2 receptor activation and the PPARgamma pathway*. Pharmacology **94**, 1-12.

[233]   Alberti TB, Barbosa WL, Vieira JL, Raposo NR, et al. (2017). *(-)-beta-Caryophyllene, a CB2 Receptor-Selective Phytocannabinoid, Suppresses Motor Paralysis and Neuroinflammation in a Murine Model of Multiple Sclerosis*. International journal of molecular sciences **18.**

[234]   Fontes LBA, Dias DDS, Aarestrup BJV, Aarestrup FM, et al. (2017). *beta-Caryophyllene ameliorates the development of experimental autoimmune encephalomyelitis in C57BL/6 mice*. Biomedicine & pharmacotherapy = Biomedecine & pharmacotherapie **91**, 257-264.

[235]   Bahi A, Al Mansouri S, Al Memari E, Al Ameri M, et al. (2014). *beta-Caryophyllene, a CB2 receptor agonist produces multiple behavioral changes relevant to anxiety and depression in mice*. Physiology & behavior **135**, 119-24.

[236]   Al Mansouri S, Ojha S, Al Maamari E, Al Ameri M, et al. (2014). *The cannabinoid receptor 2 agonist, beta-caryophyllene, reduced voluntary alcohol intake and attenuated ethanol-induced place preference and sensitivity in mice*. Pharmacology, biochemistry, and behavior **124**, 260-8.

[237]   Abbas MA, Taha MO, Zihlif MA, Disi AM (2013). *beta-Caryophyllene causes regression of endometrial implants in a rat model of endometriosis without affecting fertility*. Eur J Pharmacol **702**, 12-9.

[238]   Ghelardini C, Galeotti N, Di Cesare Mannelli L, Mazzanti G, et al. (2001). *Local anaesthetic activity of beta-caryophyllene*. Farmaco (Societa chimica italiana : 1989) **56**, 387-9.

[239] Katsuyama S, Mizoguchi H, Kuwahata H, Komatsu T, et al. (2013). *Involvement of peripheral cannabinoid and opioid receptors in beta-caryophyllene-induced antinociception*. Eur J Pain **17**, 664-75.

[240] Kuwahata H KS, Komatsu T, et al. (2012). *Local Peripheral Effects of beta-Caryophyllene through CB2 Receptors in Neuropathic Pain in Mice*. Pharmacology & Pharmacy **3**, 397-403.

[241] Klauke AL, Racz I, Pradier B, Markert A, et al. (2014). *The cannabinoid CB(2) receptor-selective phytocannabinoid beta-caryophyllene exerts analgesic effects in mouse models of inflammatory and neuropathic pain*. European neuropsychopharmacology : the journal of the European College of Neuropsychopharmacology **24**, 608-20.

[242] Paula-Freire LI, Andersen ML, Gama VS, Molska GR, et al. (2014). *The oral administration of trans-caryophyllene attenuates acute and chronic pain in mice*. Phytomedicine : international journal of phytotherapy and phytopharmacology **21**, 356-62.

[243] Quintans-Junior LJ, Araujo AA, Brito RG, Santos PL, et al. (2016). *beta-caryophyllene, a dietary cannabinoid, complexed with beta-cyclodextrin produced anti-hyperalgesic effect involving the inhibition of Fos expression in superficial dorsal horn*. Life sciences **149**, 34-41.

[244] Burston JJ, Sagar DR, Shao P, Bai M, et al. (2013). *Cannabinoid CB2 receptors regulate central sensitization and pain responses associated with osteoarthritis of the knee joint*. PloS one **8**, e80440.

[245] Wotherspoon G, Fox A, McIntyre P, Colley S, et al. (2005). *Peripheral nerve injury induces cannabinoid receptor 2 protein expression in rat sensory neurons*. Neuroscience **135**, 235-45.

[246] Van Sickle MD, Duncan M, Kingsley PJ, Mouihate A, et al. (2005). *Identification and functional characterization of brainstem cannabinoid CB2 receptors*. Science **310**, 329-32.

[247] Palazuelos J, Aguado T, Pazos MR, Julien B, et al. (2009). *Microglial CB2 cannabinoid receptors are neuroprotective in Huntington's disease excitotoxicity*. Brain : a journal of neurology **132**, 3152-64.

[248] Solas M, Francis PT, Franco R, Ramirez MJ (2013). *CB2 receptor and amyloid pathology in frontal cortex of Alzheimer's disease patients*. Neurobiology of aging **34**, 805-8.

[249] Ramirez BG, Blazquez C, Gomez del Pulgar T, Guzman M, et al. (2005). *Prevention of Alzheimer's disease pathology by cannabinoids: neuroprotection mediated by blockade of microglial activation*. J Neurosci **25**, 1904-13.

[250] Benito C, Nunez E, Tolon RM, Carrier EJ, et al. (2003). *Cannabinoid CB2 receptors and fatty acid amide hydrolase are selectively overexpressed in neuritic plaque-associated glia in Alzheimer's disease brains*. J Neurosci **23**, 11136-41.

[251] Benito C, Romero JP, Tolon RM, Clemente D, et al. (2007). *Cannabinoid CB1 and CB2 receptors and fatty acid amide hydrolase are specific markers of plaque cell subtypes in human multiple sclerosis*. J Neurosci **27**, 2396-402.

[252] Mukhopadhyay S, Das S, Williams EA, Moore D, et al. (2006). *Lipopolysaccharide and cyclic AMP regulation of CB(2) cannabinoid receptor levels in rat brain and mouse RAW 264.7 macrophages*. Journal of neuroimmunology **181**, 82-92.

[253] Ashton JC, Rahman RM, Nair SM, Sutherland BA, et al. (2007). *Cerebral hypoxia-ischemia and middle cerebral artery occlusion induce expression of the cannabinoid CB2 receptor in the brain*. Neurosci Lett **412**, 114-7.

[254] Sun Y, Zhang W, Liu Y, Liu X, et al. (2014). *Intrathecal injection of JWH015 attenuates remifentanil-induced postoperative hyperalgesia by inhibiting activation of spinal glia in a rat model*. Anesthesia and analgesia **118**, 841-53.

[255] Beltramo M, Bernardini N, Bertorelli R, Campanella M, et al. (2006). *CB2 receptor-mediated antihyperalgesia: possible direct involvement of neural mechanisms*. The European journal of neuroscience **23**, 1530-8.

[256] Bao Z, Duan C, Gong C, Wang L, et al. (2016). *Protein phosphatase 1gamma regulates the proliferation of human glioma via the NF-kappaB pathway*. Oncology reports **35**, 2916-26.

[257] Xia W, Fu W, Cai X, Wang M, et al. (2015). *Angiogenin promotes U87MG cell proliferation by activating NF-kappaB signaling pathway and downregulating its binding partner FHL3*. PloS one **10**, e0116983.

[258] Luo JG, Zhao XL, Xu WC, Zhao XJ, et al. (2014). *Activation of spinal NF-kappaB/p65 contributes to peripheral inflammation and hyperalgesia in rat adjuvant-induced arthritis*. Arthritis & rheumatology (Hoboken, NJ) **66**, 896-906.

[259] Meunier A, Latremoliere A, Dominguez E, Mauborgne A, et al. (2007). *Lentiviral-mediated targeted NF-kappaB blockade in dorsal spinal cord glia attenuates sciatic nerve injury-induced neuropathic pain in the rat*. Molecular therapy : the journal of the American Society of Gene Therapy **15**, 687-97.

[260] Klegeris A, Bissonnette CJ, McGeer PL (2003). *Reduction of human monocytic cell neurotoxicity and cytokine secretion by ligands of the cannabinoid-type CB2 receptor*. British journal of pharmacology **139**, 775-86.

[261] Ortega-Gutierrez S, Molina-Holgado E, Arevalo-Martin A, Correa F, et al. (2005). *Activation of the endocannabinoid system as therapeutic approach in a murine model of multiple sclerosis*. FASEB journal : official publication of the Federation of American Societies for Experimental Biology **19**, 1338-40.

[262] Ehrhart J, Obregon D, Mori T, Hou H, et al. (2005). *Stimulation of cannabinoid receptor 2 (CB2) suppresses microglial activation*. Journal of neuroinflammation **2**, 29.

[263] Sheng WS, Hu S, Min X, Cabral GA, et al. (2005). *Synthetic cannabinoid WIN55,212-2 inhibits generation of inflammatory mediators by IL-1beta-stimulated human astrocytes*. Glia **49**, 211-9.

[264] Toth CC, Jedrzejewski NM, Ellis CL, Frey WH, 2nd (2010). *Cannabinoid-mediated modulation of neuropathic pain and microglial accumulation in a model of murine type I diabetic peripheral neuropathic pain*. Molecular pain **6**, 16.

[265] Gu X, Mei F, Liu Y, Zhang R, et al. (2011). *Intrathecal administration of the cannabinoid 2 receptor agonist JWH015 can attenuate cancer pain and decrease mRNA expression of the 2B subunit of N-methyl-D-aspartic acid*. Anesthesia and analgesia **113**, 405-11.

[266] Patwardhan AM, Jeske NA, Price TJ, Gamper N, et al. (2006). *The cannabinoid WIN 55,212-2 inhibits transient receptor potential vanilloid 1 (TRPV1) and evokes peripheral antihyperalgesia via calcineurin*. Proceedings of the National Academy of Sciences of the United States of America **103**, 11393-8.

[267]   Akopian AN, Ruparel NB, Patwardhan A, Hargreaves KM (2008). *Cannabinoids desensitize capsaicin and mustard oil responses in sensory neurons via TRPA1 activation*. J Neurosci **28**, 1064-75.

[268]   Cesare P, McNaughton P (1996). *A novel heat-activated current in nociceptive neurons and its sensitization by bradykinin*. Proceedings of the National Academy of Sciences of the United States of America **93**, 15435-9.

[269]   Davis JB, Gray J, Gunthorpe MJ, Hatcher JP, et al. (2000). *Vanilloid receptor-1 is essential for inflammatory thermal hyperalgesia*. Nature **405**, 183-7.

[270]   Suter MR (2016). *Microglial role in the development of chronic pain*. Current opinion in anaesthesiology **29**, 584-9.

[271]   Farina C, Aloisi F, Meinl E (2007). *Astrocytes are active players in cerebral innate immunity*. Trends in immunology **28**, 138-45.

[272]   Lu C, Liu Y, Sun B, Sun Y, et al. (2015). *Intrathecal Injection of JWH-015 Attenuates Bone Cancer Pain Via Time-Dependent Modification of Pro-inflammatory Cytokines Expression and Astrocytes Activity in Spinal Cord*. Inflammation **38**, 1880-90.

[273]   Sun R, Zhang W, Bo J, Zhang Z, et al. (2017). *Spinal activation of alpha7-nicotinic acetylcholine receptor attenuates posttraumatic stress disorder-related chronic pain via suppression of glial activation*. Neuroscience **344**, 243-254.

[274]   Chen JJ, Lue JH, Lin LH, Huang CT, et al. (2010). *Effects of pre-emptive drug treatment on astrocyte activation in the cuneate nucleus following rat median nerve injury*. Pain **148**, 158-66.

[275]   Chen J, Zhang J, Zhao Y, Yuan L, et al. (2007). *Hyperalgesia in response to traumatic occlusion and GFAP expression in rat parabrachial [correction of parabranchial] nucleus: modulation with fluorocitrate*. Cell and tissue research **329**, 231-7.

[276]   Yan X, Maixner DW, Li F, Weng HR (2017). *Chronic pain and impaired glial glutamate transporter function in lupus-prone mice are ameliorated by blocking CSF-1 receptors*. J Neurochem **140**, 963-76.

[277]   Syngle A, Verma I, Krishan P, Garg N, et al. (2014). *Minocycline improves peripheral and autonomic neuropathy in type 2 diabetes: MIND study*. Neurological sciences : official journal of the Italian Neurological Society and of the Italian Society of Clinical Neurophysiology **35**, 1067-73.

[278]   Vanelderen P, Van Zundert J, Kozicz T, Puylaert M, et al. (2015). *Effect of minocycline on lumbar radicular neuropathic pain: a randomized, placebo-controlled, double-blind clinical trial with amitriptyline as a comparator*. Anesthesiology **122**, 399-406.

[279]   Martinez V, Szekely B, Lemarié J, Martin F, et al. (2013). *The efficacy of a glial inhibitor, minocycline, for preventing persistent pain after lumbar discectomy: A randomized, double-blind, controlled study*. PAIN® **154**, 1197-1203.

[280]   Kwok YH, Swift JE, Gazerani P, Rolan P (2016). *A double-blind, randomized, placebo-controlled pilot trial to determine the efficacy and safety of ibudilast, a potential glial attenuator, in chronic migraine*. Journal of pain research **9**, 899-907.

[281]   Johnson JL, Kwok YH, Sumracki NM, Swift JE, et al. (2015). *Glial Attenuation With Ibudilast in the Treatment of Medication Overuse Headache: A Double-Blind, Randomized, Placebo-Controlled Pilot Trial of Efficacy and Safety*. Headache **55**, 1192-208.

[282]   Anand P, Shenoy R, Palmer JE, Baines AJ, et al. (2011). *Clinical trial of the p38 MAP kinase inhibitor dilmapimod in neuropathic pain following nerve injury*. Eur J Pain **15**, 1040-8.

[283]   Ostenfeld T, Krishen A, Lai RY, Bullman J, et al. (2015). *A randomized, placebo-controlled trial of the analgesic efficacy and safety of the p38 MAP kinase inhibitor, losmapimod, in patients with neuropathic pain from lumbosacral radiculopathy*. Clin J Pain **31**, 283-93.

[284]   Sluka KA, Kalra A, Moore SA (2001). *Unilateral intramuscular injections of acidic saline produce a bilateral, long-lasting hyperalgesia*. Muscle & nerve **24**, 37-46.

[285]   Nielsen AN, Mathiesen C, Blackburn-Munro G (2004). *Pharmacological characterisation of acid-induced muscle allodynia in rats*. Eur J Pharmacol **487**, 93-103.

[286]   Jasper LL, MacNeil BJ (2012). *Diverse sensory inputs permit priming in the acidic saline model of hyperalgesia*. Eur J Pain **16**, 966-73.

[287]   Radhakrishnan R, Bement MKH, Skyba D, Sluka KA, et al. (2004). *Models of Muscle Pain: Carrageenan Model and Acidic Saline Model*. Current Protocols in Pharmacology **25**, 5.35.1-5.35.28.

[288]   Tillu DV, Gebhart GF, Sluka KA (2008). *Descending facilitatory pathways from the RVM initiate and maintain bilateral hyperalgesia after muscle insult*. Pain **136**, 331-9.

[289]   Da Silva LF, Desantana JM, Sluka KA (2010). *Activation of NMDA receptors in the brainstem, rostral ventromedial medulla, and nucleus reticularis gigantocellularis mediates mechanical hyperalgesia produced by repeated intramuscular injections of acidic saline in rats*. The journal of pain : official journal of the American Pain Society **11**, 378-87.

[290]   Da Silva LF, Walder RY, Davidson BL, Wilson SP, et al. (2010). *Changes in expression of NMDA-NR1 receptor subunits in the rostral ventromedial medulla modulate pain behaviors*. Pain **151**, 155-61.

[291]   Radhakrishnan R, Sluka KA (2009). *Increased glutamate and decreased glycine release in the rostral ventromedial medulla during induction of a pre-clinical model of chronic widespread muscle pain*. Neurosci Lett **457**, 141-5.

[292]   Skyba DA, Lisi TL, Sluka KA (2005). *Excitatory amino acid concentrations increase in the spinal cord dorsal horn after repeated intramuscular injection of acidic saline*. Pain **119**, 142-9.

[293]   Skyba DA, King EW, Sluka KA (2002). *Effects of NMDA and non-NMDA ionotropic glutamate receptor antagonists on the development and maintenance of hyperalgesia induced by repeated intramuscular injection of acidic saline*. Pain **98**, 69-78.

[294]   Hoeger-Bement MK, Sluka KA (2003). *Phosphorylation of CREB and mechanical hyperalgesia is reversed by blockade of the cAMP pathway in a time-dependent manner after repeated intramuscular acid injections*. J Neurosci **23**, 5437-45.

[295]   Ledeboer A, Mahoney JH, Milligan ED, Martin D, et al. (2006). *Spinal cord glia and interleukin-1 do not appear to mediate persistent allodynia induced by intramuscular acidic saline in rats*. The journal of pain : official journal of the American Pain Society **7**, 757-67.

[296]   Norton WT, Aquino DA, Hozumi I, Chiu F-C, et al. (1992). *Quantitative aspects of reactive gliosis: A review*. Neurochemical research **17**, 877-885.

[297] Ito D, Imai Y, Ohsawa K, Nakajima K, et al. (1998). *Microglia-specific localisation of a novel calcium binding protein, Iba1*. Brain research Molecular brain research **57**, 1-9.

[298] Ito D, Tanaka K, Suzuki S, Dembo T, et al. (2001). *Enhanced expression of Iba1, ionized calcium-binding adapter molecule 1, after transient focal cerebral ischemia in rat brain*. Stroke **32**, 1208-15.

[299] Hirayama A, Okoshi Y, Hachiya Y, Ozawa Y, et al. (2001). *Early immunohistochemical detection of axonal damage and glial activation in extremely immature brains with periventricular leukomalacia*. Clinical neuropathology **20**, 87-91.

[300] Kim DS, Figueroa KW, Li KW, Boroujerdi A, et al. (2009). *Profiling of dynamically changed gene expression in dorsal root ganglia post peripheral nerve injury and a critical role of injury-induced glial fibrillary acidic protein in maintenance of pain behaviors [corrected]*. Pain **143**, 114-22.

[301] Alexander JK, DeVries AC, Kigerl KA, Dahlman JM, et al. (2009). *Stress exacerbates neuropathic pain via glucocorticoid and NMDA receptor activation*. Brain, behavior, and immunity **23**, 851-860.

[302] Perea G, Navarrete M, Araque A (2009). *Tripartite synapses: astrocytes process and control synaptic information*. Trends in neurosciences **32**, 421-31.

[303] Zou JY, Crews FT (2005). *TNF alpha potentiates glutamate neurotoxicity by inhibiting glutamate uptake in organotypic brain slice cultures: neuroprotection by NF kappa B inhibition*. Brain research **1034**, 11-24.

[304] Hu S, Sheng WS, Ehrlich LC, Peterson PK, et al. (2000). *Cytokine effects on glutamate uptake by human astrocytes*. Neuroimmunomodulation **7**, 153-9.

[305] Ye ZC, Sontheimer H (1996). *Cytokine modulation of glial glutamate uptake: a possible involvement of nitric oxide*. Neuroreport **7**, 2181-5.

[306] Liaw WJ, Stephens RL, Jr., Binns BC, Chu Y, et al. (2005). *Spinal glutamate uptake is critical for maintaining normal sensory transmission in rat spinal cord*. Pain **115**, 60-70.

[307] Bezzi P, Gundersen V, Galbete JL, Seifert G, et al. (2004). *Astrocytes contain a vesicular compartment that is competent for regulated exocytosis of glutamate*. Nature neuroscience **7**, 613-20.

[308] Pasti L, Zonta M, Pozzan T, Vicini S, et al. (2001). *Cytosolic calcium oscillations in astrocytes may regulate exocytotic release of glutamate*. J Neurosci **21**, 477-84.

[309] Araque A, Li N, Doyle RT, Haydon PG (2000). *SNARE protein-dependent glutamate release from astrocytes*. J Neurosci **20**, 666-73.

[310] Brand-Schieber E, Lowery SL, Werner P (2004). *Select ionotropic glutamate AMPA/kainate receptors are expressed at the astrocyte-vessel interface*. Brain research **1007**, 178-82.

[311] Brand-Schieber E, Werner P (2003). *AMPA/kainate receptors in mouse spinal cord cell-specific display of receptor subunits by oligodendrocytes and astrocytes and at the nodes of Ranvier*. Glia **42**, 12-24.

[312] Fellin T, Pascual O, Gobbo S, Pozzan T, et al. (2004). *Neuronal synchrony mediated by astrocytic glutamate through activation of extrasynaptic NMDA receptors*. Neuron **43**, 729-43.

[313] Pasti L, Volterra A, Pozzan T, Carmignoto G (1997). *Intracellular calcium oscillations in astrocytes: a highly plastic, bidirectional form of communication between neurons and astrocytes in situ*. J Neurosci **17**, 7817-30.

[314] D'Ascenzo M, Fellin T, Terunuma M, Revilla-Sanchez R, et al. (2007). *mGluR5 stimulates gliotransmission in the nucleus accumbens*. Proceedings of the National Academy of Sciences of the United States of America **104**, 1995-2000.

[315] Parri HR, Gould TM, Crunelli V (2001). *Spontaneous astrocytic Ca2+ oscillations in situ drive NMDAR-mediated neuronal excitation*. Nature neuroscience **4**, 803.

[316] Parpura V, Basarsky TA, Liu F, Jeftinija K, et al. (1994). *Glutamate-mediated astrocyte-neuron signalling*. Nature **369**, 744-7.

[317] Gwak YS, Hulsebosch CE (2009). *Remote astrocytic and microglial activation modulates neuronal hyperexcitability and below-level neuropathic pain after spinal injury in rat*. Neuroscience **161**, 895-903.

[318] Ji RR, Suter MR (2007). *p38 MAPK, microglial signaling, and neuropathic pain*. Molecular pain **3**, 33.

[319] Khasar SG, Green PG, Levine JD (2005). *Repeated sound stress enhances inflammatory pain in the rat*. Pain **116**, 79-86.

[320] Loggia ML, Chonde DB, Akeju O, Arabasz G, et al. (2015). *Evidence for brain glial activation in chronic pain patients*. Brain : a journal of neurology **138**, 604-15.

[321] Albrecht DS, Ahmed SU, Kettner NW, Borra RJ, et al. (2018). *Neuroinflammation of the spinal cord and nerve roots in chronic radicular pain patients*. Pain **159**, 968-977.

[322] Fox MS, Gaudet JM, Foster PJ (2015). *Fluorine-19 MRI Contrast Agents for Cell Tracking and Lung Imaging*. Magnetic resonance insights **8**, 53-67.

[323] Temme S, Bonner F, Schrader J, Flogel U (2012). *19F magnetic resonance imaging of endogenous macrophages in inflammation*. Wiley Interdisciplinary Reviews: Nanomedicine and Nanobiotechnology **4**, 329-43.

[324] Fujimura Y, Ikoma Y, Yasuno F, Suhara T, et al. (2006). *Quantitative analyses of 18F-FEDAA1106 binding to peripheral benzodiazepine receptors in living human brain*. Journal of nuclear medicine : official publication, Society of Nuclear Medicine **47**, 43-50.

[325] Babbini M, Torrielli MV, Gaiardi M, Bartoletti M, et al. (1974). *Central effects of three fluorinated benzodiazepines in comparison with diazepam*. Pharmacology **12**, 74-83.

[326] Matsuda LA, Lolait SJ, Brownstein MJ, Young AC, et al. (1990). *Structure of a cannabinoid receptor and functional expression of the cloned cDNA*. Nature **346**, 561-4.

[327] Munro S, Thomas KL, Abu-Shaar M (1993). *Molecular characterization of a peripheral receptor for cannabinoids*. Nature **365**, 61-5.

[328] Dixon H, Cornish-Bowden A, Liebecq C, Loening K, et al. (1984). *IUPAC-IUB Joint Commission on Biochemical Nomenclature (JCBN) Nomenclature and Symbolism for Amino Acids and Peptides. Recommendations 1983.* European journal of biochemistry / FEBS **138**, 9-37.

[329] Abadji V, Lucas-Lenard JM, Chin C, Kendall DA (1999). *Involvement of the carboxyl terminus of the third intracellular loop of the cannabinoid CB1 receptor in constitutive activation of Gs*. J Neurochem **72**, 2032-8.

[330] Felder CC, Joyce KE, Briley EM, Glass M, et al. (1998). *LY320135, a Novel Cannabinoid CB1 Receptor Antagonist, Unmasks Coupling of the CB1 Receptor to Stimulation of cAMP Accumulation*. Journal of Pharmacology and Experimental Therapeutics **284**, 291-297.

[331] Glass M, Felder CC (1997). *Concurrent stimulation of cannabinoid CB1 and dopamine D2 receptors augments cAMP accumulation in striatal neurons: evidence for a Gs linkage to the CB1 receptor*. J Neurosci **17**, 5327-33.

[332] Bash R, Rubovitch V, Gafni M, Sarne Y (2003). *The Stimulatory Effect of Cannabinoids on Calcium Uptake Is Mediated by G_s GTP-Binding Proteins and cAMP Formation*. Neuro-Signals **12**, 39-44.

[333] Abood ME (2009). *Molecular Biology of Cannabinoid Receptors: Mutational Analyses of the CB Receptors*. In: Reggio PH (ed) The Cannabinoid Receptors. Humana Press, New York, USA, pp 203-234.

[334] Devane WA, Hanus L, Breuer A, Pertwee RG, et al. (1992). *Isolation and structure of a brain constituent that binds to the cannabinoid receptor*. Science **258**, 1946-9.

[335] Mechoulam R, Ben-Shabat S, Hanus L, Ligumsky M, et al. (1995). *Identification of an endogenous 2-monoglyceride, present in canine gut, that binds to cannabinoid receptors*. Biochemical pharmacology **50**, 83-90.

[336] Eissenstat MA, Bell MR, D'Ambra TE, Alexander EJ, et al. (1995). *Aminoalkylindoles: structure-activity relationships of novel cannabinoid mimetics*. Journal of medicinal chemistry **38**, 3094-105.

[337] Xie XQ, Melvin LS, Makriyannis A (1996). *The conformational properties of the highly selective cannabinoid receptor ligand CP-55,940*. The Journal of biological chemistry **271**, 10640-7.

[338] Rinaldi-Carmona M, Barth F, Heaulme M, Shire D, et al. (1994). *SR141716A, a potent and selective antagonist of the brain cannabinoid receptor*. FEBS letters **350**, 240-4.

[339] Rinaldi-Carmona M, Barth F, Millan J, Derocq JM, et al. (1998). *SR 144528, the first potent and selective antagonist of the CB2 cannabinoid receptor*. The Journal of pharmacology and experimental therapeutics **284**, 644-50.

[340] Melvin LS, Johnson MR, Harbert CA, Milne GM, et al. (1984). *A cannabinoid derived prototypical analgesic*. Journal of medicinal chemistry **27**, 67-71.

[341] Johnson MR, Melvin LS, Milne GM (1982). *Prototype cannabinoid analgetics, prostaglandins and opiates--a search for points of mechanistic interaction*. Life sciences **31**, 1703-6.

[342] Howlett AC, Johnson MR, Melvin LS, Milne GM (1988). *Nonclassical cannabinoid analgetics inhibit adenylate cyclase: development of a cannabinoid receptor model*. Mol Pharmacol **33**, 297-302.

[343] Huffman JW, Yu S, Showalter V, Abood ME, et al. (1996). *Synthesis and pharmacology of a very potent cannabinoid lacking a phenolic hydroxyl with high affinity for the CB2 receptor*. Journal of medicinal chemistry **39**, 3875-7.

[344] Tao Q, McAllister SD, Andreassi J, Nowell KW, et al. (1999). *Role of a conserved lysine residue in the peripheral cannabinoid receptor (CB2): evidence for subtype specificity*. Mol Pharmacol **55**, 605-13.

[345] Bell MR, D'Ambra TE, Kumar V, Eissenstat MA, et al. (1991). *Antinociceptive (aminoalkyl)indoles*. Journal of medicinal chemistry **34**, 1099-110.

[346] D'Ambra TE, Estep KG, Bell MR, Eissenstat MA, et al. (1992). *Conformationally restrained analogues of pravadoline: nanomolar potent, enantioselective, (aminoalkyl)indole agonists of the cannabinoid receptor*. Journal of medicinal chemistry **35**, 124-35.

[347]   Song ZH, Bonner TI (1996). *A lysine residue of the cannabinoid receptor is critical for receptor recognition by several agonists but not WIN55212-2*. Mol Pharmacol **49**, 891-6.

[348]   Chin CN, Lucas-Lenard J, Abadji V, Kendall DA (1998). *Ligand binding and modulation of cyclic AMP levels depend on the chemical nature of residue 192 of the human cannabinoid receptor 1*. J Neurochem **70**, 366-73.

[349]   Showalter VM, Compton DR, Martin BR, Abood ME (1996). *Evaluation of binding in a transfected cell line expressing a peripheral cannabinoid receptor (CB2): identification of cannabinoid receptor subtype selective ligands*. The Journal of pharmacology and experimental therapeutics **278**, 989-99.

[350]   Song Z, Slowey, C-A, Hurst, D, Reggio, P (1999). *The difference between the CB1 and CB2 cannabinoid receptors at position 5.46 is crucial for the selectivity of WIN55212-2 for CB2*. Mol Pharmacol **56**, 834-40.

[351]   Chin CN, Murphy JW, Huffman JW, Kendall DA (1999). *The third transmembrane helix of the cannabinoid receptor plays a role in the selectivity of aminoalkylindoles for CB2, peripheral cannabinoid receptor*. The Journal of pharmacology and experimental therapeutics **291**, 837-44.

[352]   Salo O, Raitio, KH, Savinainen, JR, et al (2005). *Virtual screening of novel CB2 ligands using a comparative model of the human cannabinoid CB2 receptor*. Journal of medicinal chemistry **48**, 7166-71.

[353]   Stern E, Muccioli GG, Millet R, Goossens JF, et al. (2006). *Novel 4-oxo-1,4-dihydroquinoline-3-carboxamide derivatives as new CB2 cannabinoid receptors agonists: synthesis, pharmacological properties and molecular modeling*. Journal of medicinal chemistry **49**, 70-9.

[354]   Kusakabe K, Tada Y, Iso Y, Sakagami M, et al. (2013). *Design, synthesis, and binding mode prediction of 2-pyridone-based selective CB2 receptor agonists*. Bioorganic & medicinal chemistry **21**, 2045-55.

[355]   Alqarni M, Myint KZ, Tong Q, Yang P, et al. (2014). *Examining the critical roles of human CB2 receptor residues Valine 3.32 (113) and Leucine 5.41 (192) in ligand recognition and downstream signaling activities*. Biochemical and biophysical research communications **452**, 334-9.

[356]   Morales P, Hernandez-Folgado L, Goya P, Jagerovic N (2016). *Cannabinoid receptor 2 (CB2) agonists and antagonists: a patent update*. Expert Opinion on Therapeutic Patents **26**, 843-856.

[357]   Navarro G, Morales P, Rodríguez-Cueto C, Fernández-Ruiz J, et al. (2016). *Targeting Cannabinoid CB(2) Receptors in the Central Nervous System. Medicinal Chemistry Approaches with Focus on Neurodegenerative Disorders*. Frontiers in neuroscience **10**, 406.

[358]   Nettekoven M, Fingerle J, Grether U, Gruner S, et al. (2013). *Highly potent and selective cannabinoid receptor 2 agonists: initial hit optimization of an adamantyl hit series identified from high-through-put screening*. Bioorganic & medicinal chemistry letters **23**, 1177-81.

[359]   ChemAxon Kft. (2014). *Instant JChem*. 14.7.21.0 edn, Budapest.

[360]   BioByte Corporation (1999). *clog P*. 4.0 edn, Claremont, CA.

[361] Tuccinardi T, Ferrarini PL; Manera C; Ortore G; Saccomanni G; Martinelli A (2006). *Cannabinoid CB2/CB1 Selectivity. Receptor Modeling and Automated Docking Analysis*. Journal of medicinal chemistry **49**, 984-994.

[362] Cichero E, Ligresti A, Allara M, di Marzo V, et al. (2011). *Homology modeling in tandem with 3D-QSAR analyses: a computational approach to depict the agonist binding site of the human CB2 receptor*. European journal of medicinal chemistry **46**, 4489-505.

[363] Rühl T, Deuther-Conrad W, Fischer S, Günther R, Hennig L, Krautscheid H, Burst P (2012). *Cannabinoid receptor type 2 (CB2)-selective N-aryl-oxadiazolyl-propionamides: synthesis, radiolabelling, molecular modelling and biological evaluation*. Organic and Medicinal Chemistry Letters **2**, 32.

[364] Goncearenco A, Mitternacht S, Yong T, Eisenhaber B, et al. (2013). *SPACER: server for predicting allosteric communication and effects of regulation*. Nucleic acids research **41**, W266-W272.

[365] Hanwell MD, Curtis DE, Lonie DC, Vandermeersch T, et al. (2012). *Avogadro: An advanced semantic chemical editor, visualization, and analysis platform*. Journal of Cheminformatics **4**, 17.

[366] Frisch MJ, Trucks GW, Schlegel HB, Scuseria GE, et al. (2009). *Gaussian 09*. Gaussian Inc., Wallingford CT.

[367] Morris GM, Huey R, Lindstrom W, Sanner MF, et al. (2009). *AutoDock 4 and AutoDockTools4: automated docking with selective receptor flexibility*. Journal of Computational Chemistry **16**, 2785-91.

[368] National Institute of Health (NIH) (2003). *Test Method Protocol for Solubility Determination*. U.S. Public Health Service. https://ntp.niehs.nih.gov/iccvam/methods/acutetox/invidocs/phiiiprot/solphiii.pdf

[369] Cheng Y, Prussoff, W.J. (1973). *Relationship between the inhibition constant (Ki) and the concentration of inhibitor which causes 50% inhibition (I50) of an enzymatic reaction*. Biochem Pharmacol **22**, 3099-3108.

[370] Rueda D, Navarro B, Martinez-Serrano A, Guzman M, et al. (2002). *The endocannabinoid anandamide inhibits neuronal progenitor cell differentiation through attenuation of the Rap1/B-Raf/ERK pathway*. The Journal of biological chemistry **277**, 46645-50.

[371] Shoemaker JL, Ruckle MB, Mayeux PR, Prather PL (2005). *Agonist-directed trafficking of response by endocannabinoids acting at CB2 receptors*. The Journal of pharmacology and experimental therapeutics **315**, 828-38.

[372] He W, Luistro L, Carvajal D, Smith M, et al. (2011). *High tumor levels of IL6 and IL8 abrogate preclinical efficacy of the gamma-secretase inhibitor, RO4929097*. Molecular oncology **5**, 292-301.

[373] Wei L, Sheng H, Chen L, Hao B, et al. (2016). *Effect of pannexin-1 on the release of glutamate and cytokines in astrocytes*. Journal of clinical neuroscience : official journal of the Neurosurgical Society of Australasia **23**, 135-41.

[374] Matsusaka T, Fujikawa K, Nishio Y, Mukaida N, et al. (1993). *Transcription factors NF-IL6 and NF-kappa B synergistically activate transcription of the inflammatory cytokines, interleukin 6 and interleukin 8*. Proceedings of the National Academy of Sciences **90**, 10193-10197.

[375] Xu J, Zhu MD, Zhang X, Tian H, et al. (2014). *NFkappaB-mediated CXCL1 production in spinal cord astrocytes contributes to the maintenance of bone cancer pain in mice*. Journal of neuroinflammation **11**, 38.

[376] Song ZP, Xiong BR, Guan XH, Cao F, et al. (2016). *Minocycline attenuates bone cancer pain in rats by inhibiting NF-kappaB in spinal astrocytes*. Acta pharmacologica Sinica **37**, 753-62.

[377] Ghaffari SH, Yousefi M, Dizaji MZ, Momeny M, et al. (2016). *Arsenic Trioxide Induces Apoptosis and Incapacitates Proliferation and Invasive Properties of U87MG Glioblastoma Cells through a Possible NF-kappaB-Mediated Mechanism*. Asian Pacific journal of cancer prevention : APJCP **17**, 1553-64.

[378] Lenormand P, Sardet C, Pages G, L'Allemain G, et al. (1993). *Growth factors induce nuclear translocation of MAP kinases (p42mapk and p44mapk) but not of their activator MAP kinase kinase (p45mapkk) in fibroblasts*. The Journal of cell biology **122**, 1079-88.

[379] Yamamoto T, Ebisuya M, Ashida F, Okamoto K, et al. (2006). *Continuous ERK activation downregulates antiproliferative genes throughout G1 phase to allow cell-cycle progression*. Current biology : CB **16**, 1171-82.

[380] Brunet A, Roux D, Lenormand P, Dowd S, et al. (1999). *Nuclear translocation of p42/p44 mitogen-activated protein kinase is required for growth factor-induced gene expression and cell cycle entry*. The EMBO journal **18**, 664-74.

[381] Romero-Sandoval EA, Horvath R, Landry RP, DeLeo JA (2009). *Cannabinoid receptor type 2 activation induces a microglial anti-inflammatory phenotype and reduces migration via MKP induction and ERK dephosphorylation*. Molecular pain **5**, 25.

[382] Tang SL, Gao YL, Wen-Zhong H (2018). *Knockdown of TRIM37 suppresses the proliferation, migration and invasion of glioma cells through the inactivation of PI3K/Akt signaling pathway*. Biomedicine & pharmacotherapy = Biomedecine & pharmacotherapie **99**, 59-64.

[383] Zhao HF, Wang J, Jiang HR, Chen ZP, et al. (2016). *PI3K p110beta isoform synergizes with JNK in the regulation of glioblastoma cell proliferation and migration through Akt and FAK inhibition*. Journal of experimental & clinical cancer research : CR **35**, 78.

[384] Udenfriend S, Stein S, Bohlen P, Dairman W, et al. (1972). *Fluorescamine: a reagent for assay of amino acids, peptides, proteins, and primary amines in the picomole range*. Science **178**, 871-2.

[385] Lorenzen A, Kennedy SW (1993). *A fluorescence-based protein assay for use with a microplate reader*. Analytical biochemistry **214**, 346-8.

[386] Opdyke DLJ (1973). *Monographs on fragrance raw materials: Caryophyllene*. Food and Cosmetics Toxicology **11**, 1059-1060.

[387] Selestino Neta MC, Vittorazzi C, Guimaraes AC, Martins JD, et al. (2017). *Effects of beta-caryophyllene and Murraya paniculata essential oil in the murine hepatoma cells and in the bacteria and fungi 24-h time-kill curve studies*. Pharmaceutical biology **55**, 190-197.

[388] Kamaraj C, Rahuman AA, Roopan SM, Bagavan A, et al. (2014). *Bioassay-guided isolation and characterization of active antiplasmodial compounds from Murraya koenigii extracts against Plasmodium falciparum and Plasmodium berghei*. Parasitology Research **113**, 1657-1672.

[389]   Kubo I, Chaudhuri SK, Kubo Y, Sanchez Y, et al. (1996). *Cytotoxic and antioxidative sesquiterpenoids from Heterotheca inuloides*. Planta Medica **62**, 427-430.

[390]   Tundis R, Loizzo MR, Bonesi M, Menichini F, et al. (2009). *In vitro cytotoxic effects of Senecio stabianus Lacaita (Asteraceae) on human cancer cell lines*. Natural product research **23**, 1707-18.

[391]   Costa EV, Menezes LR, Rocha SL, Baliza IR, et al. (2015). *Antitumor Properties of the leaf essential oil of Zornia brasiliensis*. Planta Med **81**, 563-7.

[392]   do NFJE, Ferraz RP, Britto AC, Carvalho AA, et al. (2013). *Antitumor effect of the essential oil from leaves of Guatteria pogonopus (Annonaceae)*. Chemistry & biodiversity **10**, 722-9.

[393]   Liu H, Yang G, Tang Y, Cao D, et al. (2013). *Physicochemical characterization and pharmacokinetics evaluation of β-caryophyllene/β-cyclodextrin inclusion complex*. International journal of pharmaceutics **450**, 304-310.

[394]   Kreutzberg GW (1996). *Microglia: a sensor for pathological events in the CNS*. Trends in neurosciences **19**, 312-318.

[395]   Acaz-Fonseca E, Duran JC, Carrero P, Garcia-Segura LM, et al. (2015). *Sex differences in glia reactivity after cortical brain injury*. Glia **63**, 1966-1981.

[396]   GlaxoSmithKline (2007). *Dental Pain 3rd Molar Tooth Extraction GW842166*. National Institute of Health (NIH), clinicaltrials.gov.

[397]   GlaxoSmithKline (2007). *A Study of GW842166 in Adults with Osteoarthritis Pain*. National Institute of Health (NIH), clinicaltrials.gov.

[398]   Lin X, Dhopeshwarkar AS, Huibregtse M, Mackie K, et al. (2018). *Slowly Signaling G Protein–Biased CB2 Cannabinoid Receptor Agonist LY2828360 Suppresses Neuropathic Pain with Sustained Efficacy and Attenuates Morphine Tolerance and Dependence*. Molecular Pharmacology **93**, 49-62.

[399]   Eli Lilly and Company (2012). *A Study of LY2828360 in Patients with Osteoarthritic Knee Pain*. National Institute of Health (NIH), clinicaltrials.gov.

[400]   Shionogi I (2009). *A Randomized, Double-Blind Study to Evaluate the Safety and Efficacy of 2 Doses of S-777469 in Patients with Atopic Dermatitis*. National Institute of Health (NIH), clinicaltrials.gov.

[401]   Corbus Pharmaceuticals Inc (2018). *Safety, Tolerability, Pharmacokinetics, and Efficacy of JBT-101 (Lenabasum) in Cystic Fibrosis*. National Institute of Health (NIH), clinicaltrials.gov.

[402]   Corbus Pharmaceuticals Inc (2015). *Safety, Tolerability, and Efficacy of JBT-101 in Subjects with Dermatomyositis*. National Institute of Health (NIH), clinicaltrials.gov.

[403]   National Institute of Allergy and Infectious Diseases (NIAID) (2017). *JBT-101 in Systemic Lupus Erythematosus (SLE)*. National Institute of Health (NIH), clinicaltrials.gov.

[404]   Internal Programs Pipeline; www.arenapharm.com/pipeline/ (accessed July 18, 2018).

[405]   Koch M, Wolf S, Buchmann B, Fuhrmann U, et al. (2012). *CB2 for the Treatment and Prevention of Endometriosis*. Patent No. WO2012098090A1.

[406]   Dhopeshwarkar A, Mackie K (2014). *CB2 Cannabinoid receptors as a therapeutic target-what does the future hold?* Mol Pharmacol **86**, 430-7.

[407]   Morales P, Goya P, Jagerovic N (2018). *Emerging strategies targeting CB2 cannabinoid receptor: Biased agonism and allosterism*. Biochemical pharmacology **157**, 8-17.
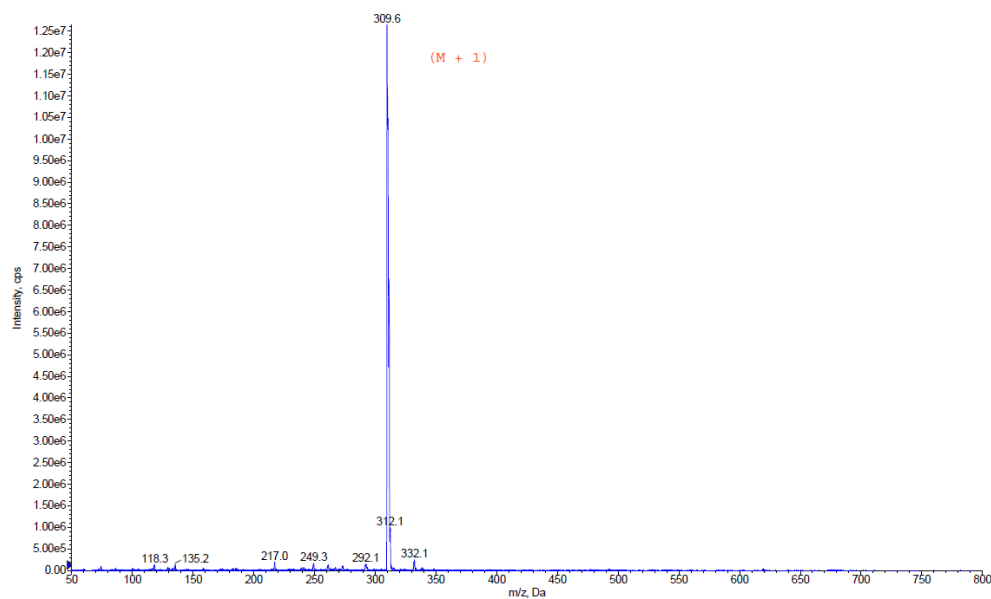
Appendix A

A.1 Mass Spectrometry Analysis
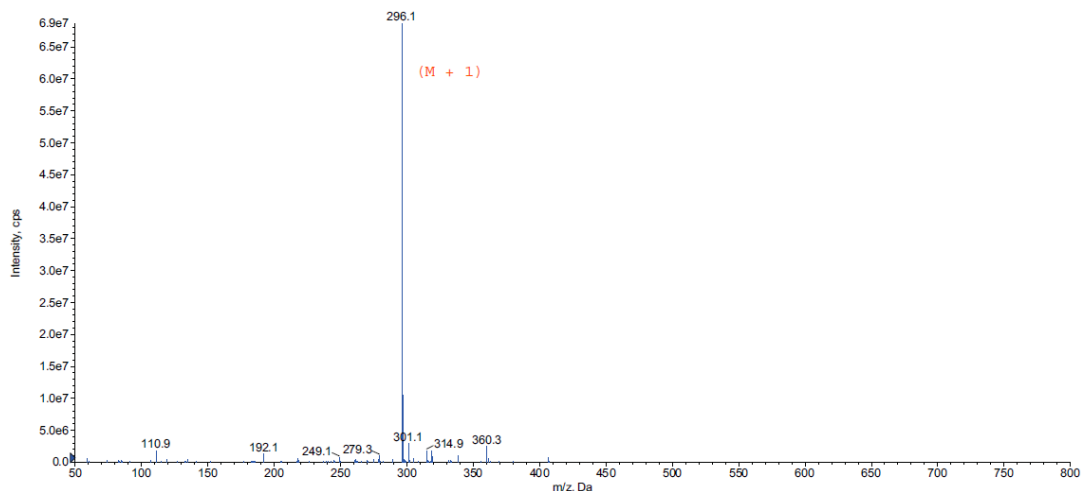
Figure A.1. Mass spectrometry analysis of DML-3
Measurement was conducted in electrospray positive ionization mode in an AB Sciex mass spectrometer. The mass to charge ratio (m/z) peak at 296.1 Da corresponds to the theoretical molecular mass plus proton (M + 1) of DML-3. Theoretical mass (M) = 295.38 Da.


Figure A.2. Mass spectrometry analysis of DML-4
Measurement was conducted in electrospray positive ionization mode in an AB Sciex mass spectrometer. The mass to charge ratio (m/z) peak at 309.6 Da corresponds to the theoretical molecular mass plus proton (M + 1) of DML-4. Theoretical mass (M) = 309.41 Da.

A.2   Dissolution Test Mixing Protocol

The protocol was stopped at the end of each step listed below if dissolution was observed. Test compounds were considered to be dissolved if the solution was found to be clear with no signs of cloudiness or precipitation.

1. Vortexing of the sample tube for 1 min at high intensity. Up to three vortexing attempts of 1 min each.

2. Waterbath sonication for 5 min.

3. Heated waterbath sonication at 37°C for up to 60 min.

A.3   [^{3}H]CP-55,940 Saturation Binding

A   **B**
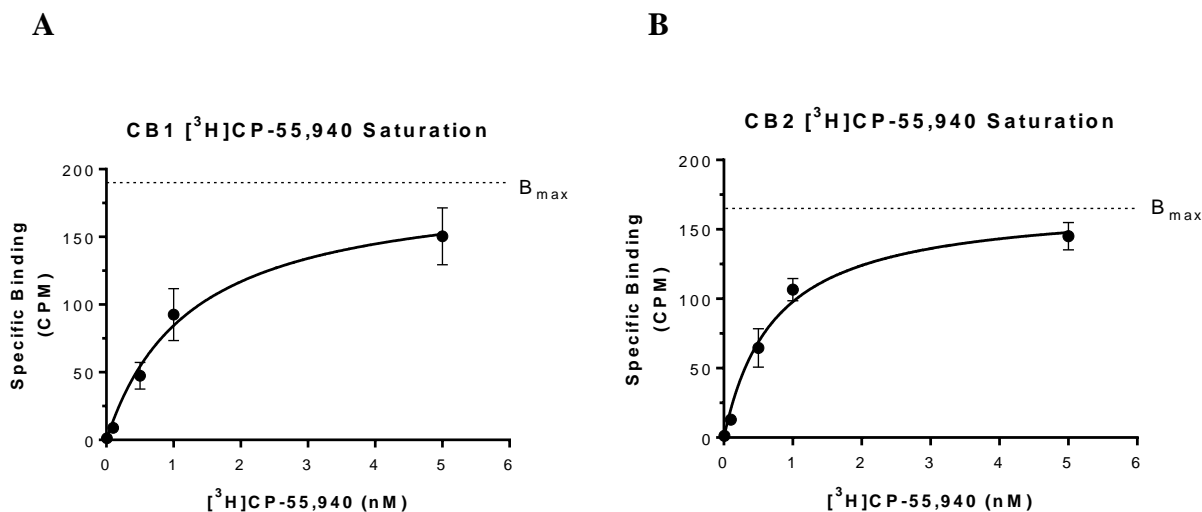
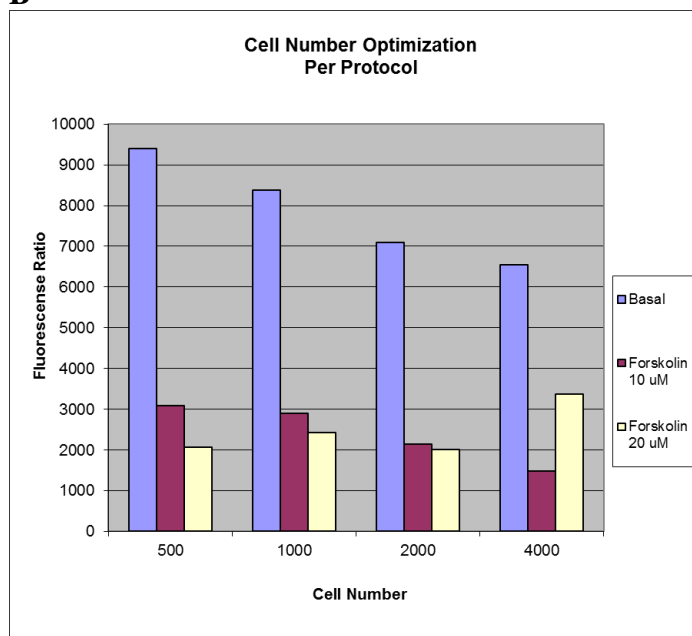**Figure A.3. CB1 (A) and CB2 (B) saturation binding curves.**
Specific binding at each concentration [^{3}H]CP-55,940 was calculated as total binding minus non-specific binding measured with the addition of 10 µM nonlabeled CP-55,940. Each data point represents the mean of 3 independent experiments ± SEM.

A.4   cAMP Assay Parameter Optimization

A
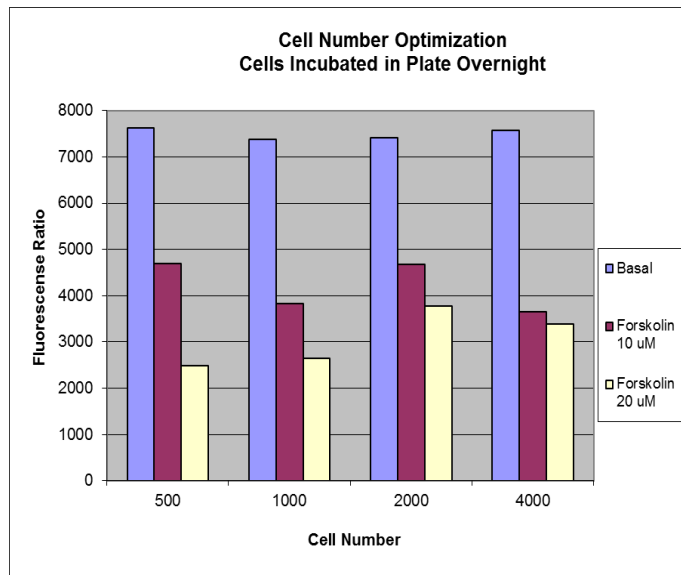
B

Figure A.4. Differences in fluorescence ratio between basal and forskolin-treated cells under varying assay conditions using the HTRF cAMP dynamic 2 kit (Cisbio, Bedford, MA).
The assay was conducted following a 12 h cell incubation (A) or immediately following cell plating as per the manufacturer's protocol (B). The effects of varying cells plated per well were examined as well as two different forskolin treatment concentrations. Data represent the mean from a single experimental replicate.

179

Appendix B

B.1   Fluorescamine Protein Quantification Assay

The method utilized for determining total protein concentration in biological samples is as follows:

1. Protein standard solution was prepared by dissolving 1 mg ovalbumin (Milipore-Sigma, Oakville, Canada) in 1 mL Milli-Q® water. Standard solutions were prepared by serial dilution of the 1 mg/mL ovalbumin solution such that seven standard concentrations ranging from 7.8 to 500 µg/mL were obtained.

2. 100 µL of each standard solution and samples were loaded into 96 well plates. Both standards and samples were assayed in triplicate.

3. 20 µL of 3 mg/mL fluorescamine (Milipore-Sigma) in acetone was added to each well.

4. Fluorescence emission at 470 nm was read upon 390 nm excitation using a fluorescence spectrophotometer.

5. Sample protein concentrations were interpolated from the assay standard curve. Standard curves were generated with each experiment.

B.2   Cytokine Secretion Assay Optimization

Cell proliferation rates and confluence at varying cell seeding densities along with supernatant cytokine concentrations after various incubation periods were studied in order to select appropriate experimental parameters for the cytokine secretion assay in U87-MG astrocytes presented in Chapter 4.

Based on the data shown in Figures B.1 and B.2 below, 18 h of incubation was selected as the initial cell culture growth period following seeding. At this time point, the cell culture was

180

established and into a steady growth phase without nearing the time of growth rate decline. Since

cell crowding and decline in growth rate appeared in the 1,000,000 cell seeding density group

after approximately 45 h (Figure B.1), only the lower 3 seeding density groups were carried

forward into the next round of optimization studies. Figure B.2 demonstrates that 18 h of

incubation allows for proper establishment and growth of U87-MG cells in the 250, 500 and 750

thousand seeding density groups, with room for further, uncrowded growth to occur during the

subsequent experimental treatment period.
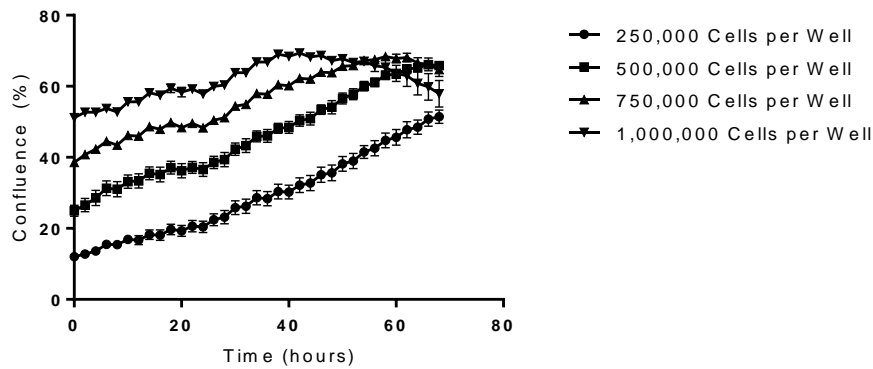
Figure B.5. Mean cell confluence over time of U87-MG cells at varying seeding densities in 6 well cell culture plates.
Each data point represents the mean of 3 wells ± SD. The confluence in each well at every time point was determined from the average six phase microscopy images by the Incucyte system.
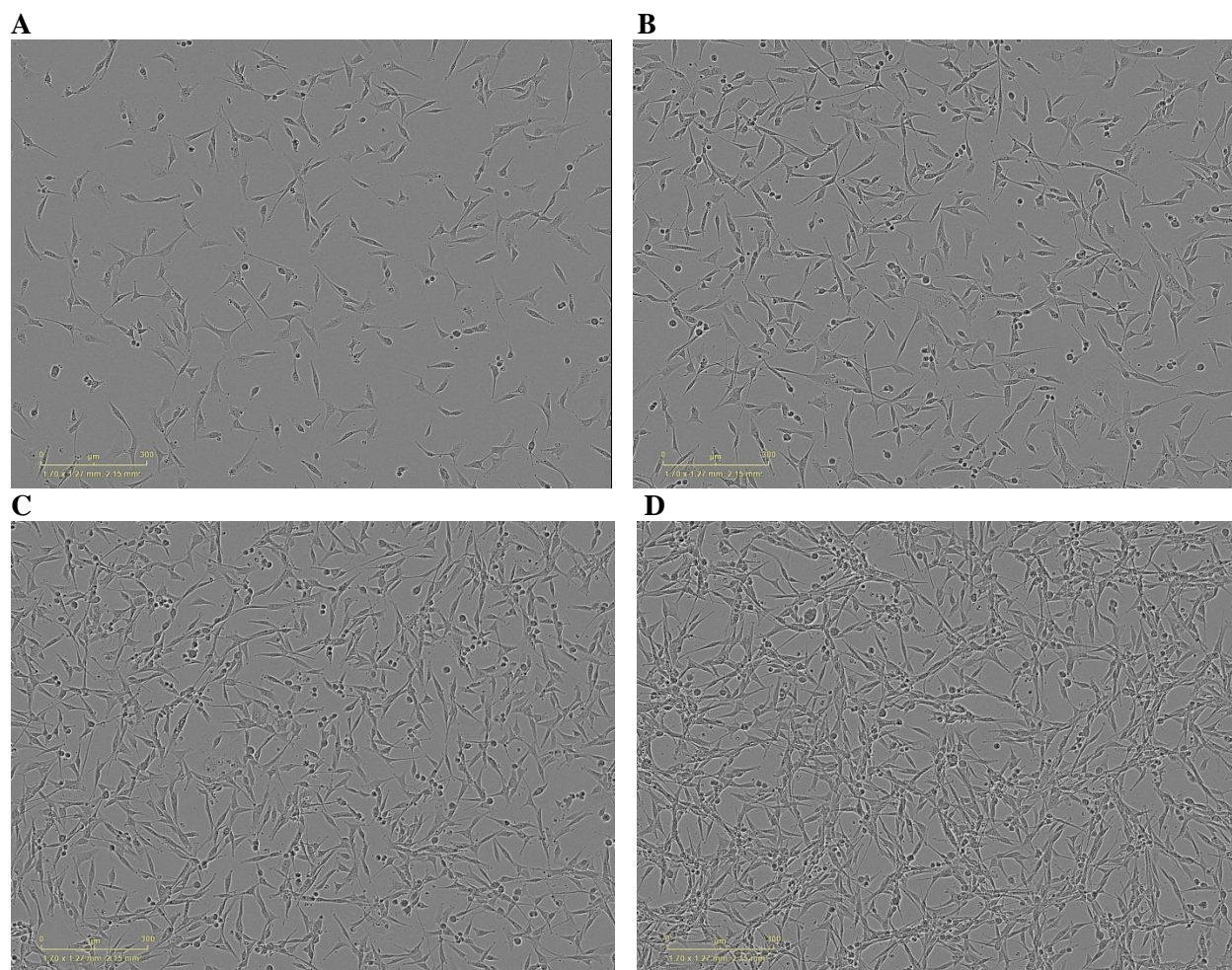
Figure B.6. Representative phase microscopy images of U87-MG cells in six-well culture plates at varying seeding densities.
U87-MG cells seeded at 250,000 (A), 500,000 (B), 750,000 (C) and 1,000,000 cells per well following 18 h incubation.

In order to determine the best cell seeding number and a suitable treatment time period, cytokine concentrations were measured from differing cell seeding density groups (250,000, 500,000 and 750,000 cells per well) after varying time durations (mock treatment periods) using the ELISA system. The assay standard curves generated from IL6 and IL8 standards (R&D Systems, Minneapolis, USA) are shown below in Figure B.3. As determined by the

manufacturer, the assay detection limits of human IL-6 and IL-8 are 0.7 pg/mL and 3.5 pg/mL, respectively.

A　　　　　　　　　　　　　　　　　　　　　　　　　　**B**
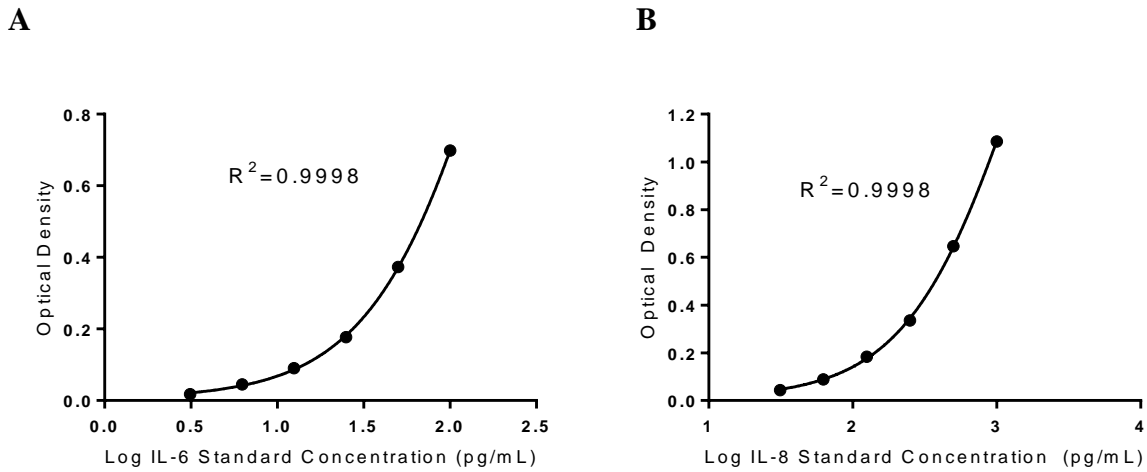
Figure B.7. IL-6 (A) and IL-8 (B) standard curves generated using standard cytokine solutions.
Optical density was read at 450 nm and corrected for background signal at 540 nm, as per the manufacturer's protocol. The standard curve was generated, as per the manufacturer's recommendation, using non-linear regression and four parametric logistic (4-PL) curve fit with GraphPad Prism® software. Each standard concentration was assayed in triplicate with the mean value plotted.

Using trial experiments, the study parameters which allowed our ELISA systems to detect IL-6 and IL-8 from the culture supernatant at concentrations which fell within the assay dynamic range were determined. An optimum result was obtained from 750,000 cells per well grown for 18 h, with the media aspirated then replaced with fresh media followed by a 2 h incubation period as the treatment duration for the experiment (data shown below in Tables B.1 and B.2).

Table B.1. Determination of the mean U87-MG culture supernatant IL-6 concentration following a 2 h mock treatment period.

Supernatant samples were obtained from independent culture wells of U87-MG cells incubated for 2 h in fresh media. Cells were grown in 6-well culture plates at a seeding density of 750,000 cells per well and an initial growth period of 18 h. Samples were assayed in duplicate and the IL-6 concentration was interpolated from the assay standard curve using GraphPad Prism® software.

Sample	Mean Optical Density (450 nm)	Corrected Optical Density	Interpolated IL6 Concentration (pg/mL)	Mean IL6 Concentration (pg/mL)	Standard Deviation (pg/mL)	C.V. (%)
Blank	0.017					
Supernatant 1	1.0375	1.0205	165.6	178.7	12.3	6.9
Supernatant 2	1.133	1.116	190.1			
Supernatant 3	1.0965	1.0795	180.4			

Table B.2. Determination of the mean U87-MG culture supernatant IL-8 concentration following a 2 h mock treatment period.

Supernatant samples were obtained from independent culture wells of U87-MG cells incubated for 2 h in fresh media. Cells were grown in 6-well culture plates at a seeding density of 750,000 cells per well and an initial growth period of 18 h. Samples were assayed in duplicate and the IL-8 concentration was interpolated from the assay standard curve using GraphPad Prism® software.

Sample	Mean Optical Density (450 nm)	Corrected Optical Density	Interpolated IL8 Concentration (pg/mL)	Mean IL8 Concentration (pg/mL)	Standard Deviation (pg/mL)	C.V. (%)
Blank	0.0185					
Supernatant 1	0.484	0.4655	345.4	361.6	18.4	5.1
Supernatant 2	0.499	0.4805	357.8			
Supernatant 3	0.5275	0.509	381.6			